Effective Field Theory Methods Applied to Two-Body and Three-Body Systems

Dissertation
zur
Erlangung des Doktorgrades (Dr. rer. nat.)
der
Mathematisch-Naturwissenschaftlichen Fakultät
der
Rheinischen Friedrich-Wilhelms-Universität Bonn

vorgelegt von
Rishabh Bubna
aus
Patna, Indien

Bonn 2025

Angefertigt mit Genehmigung der Mathematisch-Naturwissenschaftlichen Fakultät der Rheinischen Friedrich-Wilhelms-Universität Bonn

Gutachter/Betreuer:	PD Dr. Akaki Rusetsky
Gutachter:	Prof. Dr. Dr. h. c. Ulf-G. Meißner
Tag der Promotion:	17.12.2025
Erscheinungsjahr:	2026

Abstract

Quantum Chromodynamics is the fundamental theory of strong interactions. However, at low energies QCD strong coupling becomes very large and perturbative techniques are no more applicable. Lattice QCD offers an ab-initio non-perturbative method of solving QCD in this region. Since LQCD simulations are performed on finite dimensional Euclidean lattice, the result is contaminated with finite-volume effects. Moreover, establishing the relation between the finite-volume energy levels obtained from simulations and the continuum physical observables is highly non-trivial.

In this thesis, methods for extraction of two-body and three-body observables from lattice data are developed with the help of the non-relativistic effective field theory approach. The basic principles of LQCD are outlined while also detailing the methods used for extraction of two-body parameters from lattice data. The NREFT formalism is introduced and its application to both two-body and three-body sector are discussed, with special focus on methods for analysis of lattice data.

A formalism, the modified Lüscher equation, is developed and derived for extraction of physical scattering parameters in the presence of short- plus long-range interaction in the two-body case based on the modified effective-range expansion. This method allows one to analyze finite-volume energy levels that lie in the left-hand cut region while also addressing the issue of slow convergence of partial-wave expansion in the presence of long-range interactions.

Moreover, an efficient numerical algorithm is detailed for working with the modified Lüscher equation. Analysis of synthetic data generated from a toy model is carried out to test the accuracy of the approach. Various numerical and technical issues are described in detail.

In the three-body sector, result from the perturbative calculation of the three-nucleon ground state energy shift up to and including $O(L^{-6})$, where L is the size of the finite-volume box, is presented. The convergence of the calculation for physical nucleon scattering lengths is discussed. The box size L required for convergence is very large and highly impractical.

Finally, The Lellouch-Lüscher factor for $K \to 3\pi$ decay is evaluated numerically and its sensitivity to the three-pion amplitude is studied. It is found that the LL factor shows negligible dependence on the three-pion amplitude and hence one can use a rough estimate of this amplitude from ChPT instead of extracting it from LQCD.

Contents

CHAPTER 1

Introduction

Quantum Chromodynamics

The birth of strong interactions can be traced back to 1911, when Rutherford [1] proposed his atomic model consisting of a positively charged center with electrons going around this center in orbits like planets. This positively charged center was termed as the *atomic nucleus* and was built with positively charged building blocks called *protons*. This model hinted towards a new kind of force stronger than the electromagnetic force capable of holding the protons together in the nucleus. The discovery of the *neutron* in 1932 [2] further indicated that electrically neutral particle interacted via this new force as well. Following this isospin was introduced as a symmetry of the strong interaction by Heisenberg [3] to explain the approximate same masses of the proton and neutron and their similar behavior in strong interactions. In 1935, Yukawa proposed that the nuclear force was mediated by a spinless particle, *meson* [4]. Throughout the 1930s and 1940s considerable progress was made in understanding the nuclear interactions.

In 1950s, a plethora of new particles were discovered that interacted via the strong force. These particles were named *hadrons*. It seemed unlikely that all of these new particles were fundamental. In 1961-1962 using the *Eightfold Way*, Gell-Mann and Ne'eman were able to organize the hadrons into groups having similar properties such as the mass [5, 6]. These groups formed representation of an underlying approximate SU(3) symmetry. The mass splitting in the multiplets could be understood by perturbative breaking of this symmetry leading to the Gell-Mann-Okubo formula [6, 7]. This formula was successful in predicting masses up-to the then unknown Ω^- particle, which was experimentally discovered [8] in 1964.

The existence of *quarks* was postulated in 1964 by Gell-Mann [9] and Zweig [10]. They proposed baryons to be bound states built of three quarks, whereas mesons were made up of quark and anti-quark pairs. Quarks were postulated to be spin-1/2 particles which came in three *flavors*. This quark model, however, was incompatible with the spin statistic theorem. It was pointed out by Bogolyubov, Struminsky and Tavkhelidze [11], Han and Nambu [12] and Miyamoto [13] independently, that this problem could be solved by introducing an additional quantum number for each flavor quark. This led to the introduction of an additional SU(3) symmetry termed as *color*.

Even-though quarks cannot be directly observed, Bjorken had pointed out that the electron-proton cross section should obey scaling laws in the deep inelastic region if the nucleons are made up of constituent point-like particles [14]. This was experimentally confirmed by scattering experiments

that were carried out by MIT-SLAC collaboration [15]. The spin and fractional charges of these constituent particles were confirmed to match with that of the quarks in [16] and [17] respectively. More elaborate models were developed, see e.g. [18], which were consistent with experiments.

Gross and Wilczek [19] and Politzer [20] independently showed that a gauge theory becomes weaker at higher energies, i.e. obey *asymptotic freedom*. This was consistent with the approximate scaling behavior observed in deep-inelastic scattering experiments. These development enabled Fritzsch, Leutwyler and Gell-Mann to argue in favor of promoting the SU(3)-color group to a non-abelian gauge symmetry [21], with the strong force being mediated by a gauge boson termed as *gluon*. This theory became known as *Quantum Chromodynamics* (QCD), an essential part of the Standard Model of particle physics as we know it today. QCD has some special characteristics which make it fundamentally different from the electroweak theory. The degrees of freedom in QCD obey *color confinement*, i.e. color-charged particles cannot be observed independently. However, since the strong coupling constant α_s becomes small at high energies, perturbative techniques can be readily applied. A plethora of experiments provide quantitative support to QCD as a theory of strong interactions [22].

As one moves towards the infrared regime, the strength of the coupling constant increases and at the hadronic scale perturbation theory breaks down. Hence, at lower energies alternative techniques need to be employed to probe the strong interaction. Two such methods lie at the center of this thesis, namely, *Lattice QCD* (LQCD) and *Effective Field Theories* (EFTs). This thesis aims to employ existing Formalism to show how one can relate three-body decay amplitudes from LQCD to experiments. Moreover, a formalism to extract effective-range parameters for short-range potential in the presence of long-range potential will be derived.

Lattice Quantum Chromodynamics and Finite Volume

The birth of lattice gauge theory can be traced to formulation of gauge theory on a space-time lattice by Kenneth Wilson in Ref. [23] in 1974. This work laid the foundation for understanding quark confinement conceptually. The timing of this work was indeed optimal as the CRAY-1 supercomputer was developed in 1976 and had changed the scientific computing landscape. Moreover, Monte Carlo methods, which had been well known since the late 40's and early 50's with the Metropolis algorithm being formulated in 1953 [24], become increasingly applied to spin systems in 60's and 70's. In 1979 Creutz, Jacobs and Rebbi in Ref. [25], Wilson in Ref. [26] showed the possibility of performing such calculations on the computer. Furthermore, in 1981-82 hadron masses were calculated by Weingarten [27] and Hamber and Parisi [28]. By 1980's lattice QCD computations could be performed quickly using supercomputers. In the last four decades, lattice QCD has progressed a great deal enhancing understanding of the strong interactions. Nowadays, one can perform simulations with the physical values of quark masses, sufficiently large lattice sizes and small enough lattice spacings.

Lattice QCD (LQCD) is an *ab initio*, non-perturbative approach that formulates QCD on a finite, discrete Euclidean space-time grid. It employs the path integral formulation of QCD. The discretization of space-time onto a four-dimensional hypercube of length L and lattice spacing a, serves as a natural ultraviolet cutoff $\sim 1/a$. Moreover, the momenta are quantized in a finite volume which leads to finite, but high-dimensional path integral. These integrals are impossible to evaluate analytically. Hence, in LQCD, ensembles of field configurations are generated according to a probability distribution ascertained by the path integral. Then correlation functions are evaluated using *Monte Carlo* methods.

To relate the correlators calculated in LQCD to infinite-volume QCD observables, three limits

have to be taken. These limits are namely, the continuum limit ($a \to 0$), the thermodynamic limit ($L \to \infty$) and the extrapolation to physical quark masses. Even-though performing LQCD calculations at physical quark masses has become possible [29, 30], computational cost can be significantly reduced by performing such calculations at higher quark masses.

An interesting problem arises when one tries to relate the correlation functions calculated on the Euclidean space-time lattice to the scattering amplitude evaluated in the continuum. Above threshold, the continuum scattering amplitude is complex where as the lattice correlator is purely real and hence, establishing a relation between the two is a highly non-trivial task. In general, it is not possible to straightforwardly extract on-shell scattering matrix elements from Euclidean correlation functions defined in the infinite volume as they are dominated by off-shell contributions. This statement is the well-known Maiani-Testa no-go theorem [31]. However, Lüscher demonstrated in Ref. [32, 33], that in the two-particle sector, it is possible to directly extract the scattering phase shift from the finite-volume energy spectrum. Lüscher's method has become the go-to procedure for analysis of lattice data in the two-body sector, with the approach being generalized to moving frames [34, 35], non-identical particles with spin [36–38] and coupled channel interactions [39–42]. Furthermore, the two-particle weak decay amplitude was related to the corresponding finite-volume transition matrix elements by Lüscher and Lellouch [43]. Further generalization of this method can be found in the Refs. [35, 41, 44–46]. The inclusion of external currents was carried out in [45–52]. A more extensive list of applications to various systems can be found in the following reviews [53, 54].

In certain physical system such as the NN system, exchange of a light particle (long-range potential) such as the pion leads to a branch cut lying close to the threshold. This branch cut is known as the left-hand cut or the t-channel cut. Some energy levels can lie in this left-hand cut region, which results in the K-matrix becoming complex and hence the standard Lüscher approach is no more valid [55]. Another consequence of this interaction, which is mediated by a long-range force, is the slow convergence of the partial-wave expansion. Several proposals have been made to counter this problem of the left-hand cut. The plane-wave basis can be used to solve the two-body Lippmann-Schwinger equation in a finite volume and then the parameters of the effective Hamiltonian can be extracted from fitting the resulting levels to the lattice data as shown in Refs. [56–58]. In Refs. [59, 60], the long- and short-range part are isolated and then treated separately. In Refs. [61, 62], the D^*D scattering was studied for different quark masses using the three-body formalism. A detailed comparison between these three approaches was carried out in Ref. [63]. Yet another alternative approach to this problem has been developed in this research project. This approach is similar to the original Lüscher equation and is based on the use of the modified effective-range expansion derived in [64].

With most of the two-body sector well understood, efforts were made to generalize Lüscher's method to the three-body sector. However, the three-body sector had some challenges of its own. The first question that needed to be answered was whether the three-body finite-volume spectra is completely determined by the S-matrix elements. This was shown to be the case in Refs. [65, 66]. Over the next few years great progress was made in developing a counterpart to Lüscher's method in the three-body sector.

There are three different but conceptually *equivalent* approaches for studying the three-body sector on lattice, namely, the *Relativistic Field Theory* (RFT) [67, 68], the *Finite Volume Unitarity* (FVU) [69] and the *Non-relativistic Field Theory* (NREFT) [70, 71] approaches. The equivalence between these approaches was shown in Refs. [71–74] under specific setups. All the three methods mentioned involve, solving a *quantization condition* to fix parameters by fitting to the three-body finite-volume spectrum. The fixed parameters can then be used to calculate infinite-volume observables.

The RFT approach has been applied to $\pi^+\pi^+\pi^+$-system [29, 75], $\pi\pi K$- and $KK\pi$-systems [76], whereas the FVU approach has been applied to $\pi^+\pi^+\pi^+$-system [77], KKK-system [30], to determine the pole position and branching ratio of $a_1(1260)$ resonance [78] and the pole position of the ω meson [79]. In Ref. [80], it was shown that both the RFT and FVU approaches exhibited good agreement for lattice φ^4-theory. A manifestly relativistic invariant formulation of the NREFT approach was derived in Ref. [81] making it readily usable for global analysis of lattice spectra. Moreover, the RFT approach was generalized for $2 \leftrightarrow 3$ channels [82], resonant sub-channels [83], scattering of three-pions in different isospin-channels [84], non-degenerate scalars [85, 86], and inclusion of fermions [87].

An alternative but restrictive approach to the three-particle problem exists, that focuses on the perturbative shift of the free three-particle energy levels. In this approach a perturbative expansion is carried out in $1/L$, where L corresponds to the box size. Different parameters can be then fixed by calculating the energy shift up-to different orders in perturbation theory. The first attempt to calculate the finite-volume energy shift using perturbation theory was carried out in Refs. [88–90]. The ground state energy shift was given up to $O(L^{-6})$ and $O(L^{-7})$ in Refs. [91–93] and [94], respectively. The expression for the energy shift of the ground state and first excited states were derived using threshold expansion in the non-relativistic limit in Ref. [95] at $O(L^{-6})$. Further, the threshold expansion of the relativistic quantization condition results in the relativistic expression of the ground state energy at the same order was shown in Ref. [96]. Finally, the relativistic corrections to the ground state and first excited states energy level, in the NREFT framework, were calculated in Ref. [97]. Using these results, the finite-volume ground state energy shift for three pions and three nucleons system in the non-relativistic framework were calculated in Refs. [98] and [99], respectively. One aim of this thesis is to present the results obtained in [99].

The three-body equivalent to the two-body Lellouch-Lüscher (LL) formula was derived independently by two groups in Refs. [100–102]. The main difference between the two-body and three-body sector lies in the fact that in the two-body case, the LL factor is a single function whereas it is a (truncated) matrix in three-body sector. One of the goals of the research project was to explicitly calculate the LL factor for the decay of the kaon into three pions.

Effective Field Theory

When studying any physical system, only a limited amount of information is available. Hence, the phenomenon of separation of scales, by virtue of which relevant degrees of freedom can be separated from the irrelevant ones, becomes an important asset. Effective field theories (EFTs) exploit this scale separation to provide an approximation of a underlying theory in a specific energy-regime. By utilizing the *decoupling theorem*, which states that physics at low-energies (*large distances*) is insensitive to the dynamics at high-energies (*short distances*), EFTs explicitly consider only the relevant degrees of freedom at a given scale and encode all the short distance behavior in the parameters of the EFT. These parameters are aptly called *Low-Energy Constants* (LECs). The construction of any EFT involves writing down all possible operators using the relevant degrees of freedom that obey the symmetries of the underlying theory. This leads to an infinite tower of operators. These operators are then ordered according to their individual contribution using an ordering scheme known as *power counting*. With this a perturbative expansion can be employed in terms of a small parameter of the theory such as the typical momenta of particles involved, that improves as more and more operators are considered. Lastly, the LECs appearing in the EFT are matched to physical parameters. A thorough

and instructional introduction to EFTs can be found in Ref [103].

Chiral perturbation theory (ChPT) [104–106], is one of the most well-known EFT for low-energy hadron dynamics. It is based on the fact that massless QCD is invariant under global $\mathrm{SU}(N_f)_L \times \mathrm{SU}(N_f)_R$ chiral transformations, where N_f is the number of quark flavors. This global chiral symmetry is however spontaneously broken, $\mathrm{SU}(N_f)_L \times \mathrm{SU}(N_f)_R \longrightarrow \mathrm{SU}(N_f)_V$. The observed spectrum of hadrons show that the $\mathrm{SU}(N_f)_A$ axial vector symmetry is not respected by the QCD vacuum, whereas the Vafa-Witten theorem [107] proves that the $\mathrm{SU}(N_f)_V$ symmetry is protected. Moreover, the $U(1)$ axial-vector symmetry is broken due to the axial-vector anomaly. Hence, in the case of massless quarks, eight massless pseudoscalar particles should be present according to Goldstone's theorem [108, 109]. These can be identified with the pseudoscalar meson octet. Note that due to the $U(1)$ axial anomaly the η' meson is not massless and hence not a Goldstone boson. However, quarks are not massless and hence chiral symmetry is explicitly broken. This leads to the Goldstone bosons gaining mass in accordance with the Gell-Mann-Oakes-Renner relation [110]. Callan, Coleman, Wess and Zumino (CCWZ) [111, 112] formulated a general effective Lagrangian grounded in group theory, taking spontaneous symmetry breaking into account. The power counting scheme established, enables an expansion of the observables in $p/\Lambda_{\mathrm{Chpt}}$. Here, p ($\approx M_\pi \approx 140\,\mathrm{MeV}$) is the momenta of the order of the low lying octet mesons and Λ_{ChPT} ($\approx 1\,\mathrm{GeV}$) is the scale corresponding to the set of next heavier hadrons.

Naive inclusion of nucleons in the CCWZ framework leads to the breakdown of counting rules. This is because the nucleon mass is of the order of the heavy scale (Λ_{ChPt}) and appears explicitly in the Lagrangian. Multiple methods have been developed to impose a consistent power counting scheme in the nucleon sector, such as the *infrared regularization* [113], the *extended on-mass-shell scheme* [114, 115] and *heavy baryon ChPT* [116, 117].

Since the pion mass is an input parameter in ChPT, it serves as an effective way to study the dependence of observables on the pion mass. This property of ChPT is very useful for analysis of LQCD data as large quark masses are used to render the finite-volume computations cheaper. Hence, the chiral extrapolation of physical quark masses in LQCD can be studied using ChPT. To account for non-zero lattice spacing effects certain modifications can be made to ChPT as shown in Refs. [118–120]. The effects of finite volume were studied in Refs. [121–123]. Moreover, Lattice data can be fit to extract parameters of ChPT Lagrangian, Ref. [124] provides a review of recent results.

Non-Relativistic Effective Field Theory

Non-relativistic effective field theory (NREFT) is a powerful tool which can be employed to describe systems in which the typical scale of momenta is much smaller than the mass of particles involved. This framework was developed for bound-state calculation by Caswell and Lepage in Ref. [125]. Further, Non-relativistic QCD (NRQCD) was developed by Bodwin, Braaten and Lepage in 1995 [126], where an expansion in the quark velocity was employed to include interactions involving heavy quarks. In 1999, the NREFT framework was applied to the study of hadronic atoms by Gall, Gasser, Lyubovitskij and Rusetsky in Ref. [127]. In Refs. [128–130] nucleon-nucleon scattering was described using non-relativistic pionless EFTs, based on the proposal of extracting nuclear forces from chiral Lagrangian [131, 132]. Here, the external momenta involved are way below the pion mass and hence pions can be integrated out. Since, a closed form of the two-body scattering amplitude (summed up to all orders) can be obtained in the NREFT framework, the LECs can be directly matched to the

effective-range expansion parameters. Thus using NREFT to study nucleon-nucleon scattering can be very advantageous.

This non-relativistic treatment of nucleon-nucleon scattering was further extended to the three-nucleon and three-boson systems in Refs. [133–136] enabling the study of neutron-deutron scattering. The volume dependence of the three-body bound state spectrum was studied in Refs. [137–140]. These developments acted as catalyst for the three-particle quantization condition being developed in the NREFT approach.

NREFTs have become an essential tool in particle physics, enabling accurate calculations of physical observables such as scattering length in a consistent manner while accounting for the underlying symmetries of the Standard Model. A detailed review of NREFT framework can be found in Ref. [141].

Outline: This thesis is aimed at developing further understanding of two-body and three-body systems in both infinite- and finite volume using the NREFT approach. The extraction of physical observables from lattice data in the presence of long-range interaction is addressed in the two-body sector, while in the three-body sector already existing approaches are applied to physical systems. This includes the application of the perturbative calculation of ground state energy shift in the three-nucleon system and evaluation of the Lellouch-Lüscher factor for kaon decay into three-pions.

The thesis is arranged as follows: Chap. 2 briefly introduces the core concepts and methods used in LQCD, whereas Chap. 3 introduces the NREFT approach and discusses in detail the two-body and three-body systems within this approach. In Chap. 4, an approach for extracting physical observables from lattice data in the presence of the long-range force is detailed, giving rise to the modified Lüscher equation. Chap. 5 details the numerical implementation of approach derived in the previous chapter. In Chap. 6, a perturbative calculation of three-nucleon ground state energy shift is carried out and the box size for a convergent result is estimated. Finally in Chap. 7, the Lellouch-Lüscher factor for kaon decay into three-pions is evaluated numerically and the sensitivity of the calculated factor to the three-pion amplitude is studied.

CHAPTER 2

Quantum Chromodynamics in a Finite Volume

This chapter aims to introduce the basic concepts of Quantum Chromodynamics and Lattice QCD. After outlining the setup of LQCD, hadron spectroscopy is discussed in detail. Special emphasis is given on the discussion relating to Lüscher equation and symmetries in a finite volume. Finally, the chapter ends with a discussion on the situation involving long- plus short-range interactions and its consequence on the extraction of physical observables from lattice data.

2.1 Quantum Chromodynamics

Quantum Chromodynamics, as stated in the introduction is the theory of strong interaction. The Lagrangian of QCD can be stated in a single line,

$$\mathcal{L}_{\text{QCD}} = -\frac{1}{2g^2}\text{Tr}\Big[F_{\mu\nu}F^{\mu\nu}\Big] + \sum_f \overline{\Psi}_f\Big(i\gamma^\mu D_\mu - m_f\Big)\Psi_f\,, \tag{2.1}$$

where g is the flavor-independent strong coupling constant, each quark field is represented by a Dirac-spinor Ψ_f having mass corresponding to m_f (Note: $f = 1, \ldots N$) , $F_{\mu\nu}$ is the field strength tensor of the gluon field defined as

$$F_{\mu\nu} = \partial_\mu G_\nu - \partial_\nu G_\mu + i\big[G_\mu, G_\nu\big]\,, \tag{2.2}$$

with G_μ representing the massless gluon field. D_μ is the gauge-covariant derivative and it is defined as follows:

$$D_\mu = \partial_\mu - iG_\mu\,. \tag{2.3}$$

QCD is a SU(3) gauge theory and hence each Ψ_f transforms as a vector of the fundamental representation of the SU(3) color gauge group, whereas the gluon field transforms according to the adjoint representation. Furthermore, the QCD Lagrangian is invariant under local SU(3) gauge

transformations

$$\begin{aligned}
&\Psi_f(x) \to \Psi'_f(x) = \mathcal{U}(x)\Psi_f(x)\,,\\
&\overline{\Psi}_f(x) \to \overline{\Psi'}_f(x) = \overline{\Psi}_f(x)\mathcal{U}^\dagger(x)\,,\\
&G_\mu(x) \to G'_\mu(x) = \mathcal{U}(x)G_\mu(x)\mathcal{U}^\dagger(x) + i\big(\partial_\mu \mathcal{U}(x)\big)\mathcal{U}^\dagger(x)\,,
\end{aligned} \tag{2.4}$$

where $\mathcal{U}(x) \in \mathrm{SU}(3)$.

In addition to the above mentioned components, the QCD Lagrangian also includes a CP violation term given by,

$$\mathcal{L}_\theta = -\frac{\theta}{32\pi^2}\epsilon^{\mu\nu\alpha\beta}\mathrm{Tr}\Big[F_{\mu\nu}F_{\alpha\beta}\Big]\,, \tag{2.5}$$

and gauge-fixing terms. However, these are not relevant for this thesis.

In contrast to Quantum Electrodynamics (QED), QCD exhibits additional interesting properties. Gluons are self-interacting, unlike photons, and hence, in addition to quark-gluon vertex, QCD also includes triple and quartic gluon vertices. All physical observables of the theory are parameterized in terms of the quark masses m_f and the strong coupling constant g (or equivalently $\alpha_s = g^2/4\pi$). Similar to QED, to render the observables finite, these bare parameters have to be *renormalized*. Renormalization procedure leads to the inclusion of an arbitrary scale μ, which could lead to the physical observables becoming scale dependent. This is however not the case as the parameters of the theory are also scale dependent and cancel any explicit μ dependence in the observables.

The running of the QCD coupling with the arbitrary scale μ is given by the renormalization group (RG) equation. At one-loop this is given by [142],

$$\mu\frac{d\alpha_s(\mu)}{d\mu} = \beta(\alpha_s(\mu)) = -\beta_0\frac{\alpha_s^2(\mu)}{2\pi}\,,\ \ \beta_0 = \Big(\frac{11}{3}N_c - \frac{2}{3}N\Big)\,. \tag{2.6}$$

Here, $N_c = 3$ is the number of color and $N = 6$ is the number of quark flavors. The β-function being negative has important consequence. As $\mu \to \infty$, the renormalized coupling $\alpha_s(\mu)$ decreases. This leads to asymptotic freedom in QCD at high energies. As μ becomes smaller, α_s becomes larger, ultimately leading to QCD becoming non-perturbative at small energies. This phenomenon is called color-confinement as, quarks and gluons become confined by the strong force and only color-neutral bound states exist freely. The energy at which the coupling diverges and the non-perturbative nature of QCD takes over is called Λ_{QCD} and it can be obtained by solving the differential equation mentioned above,

$$\Lambda_{\mathrm{QCD}} = \mu\exp\Big(-\frac{1}{\beta_0}\frac{2\pi}{\alpha_s(\mu)}\Big)\,. \tag{2.7}$$

Note that Λ_{QCD} is not dependent on μ, however it does depend on the renormalization scheme and number of quarks present in the theory. This phenomenon of spontaneous emergence of a mass scale via the renormalization procedure is called *dimensional transmutation*.

Another interesting aspect of QCD is that, the Lagrangian possesses a global flavor symmetry. If the masses of N_q quarks are the same, then the Lagrangian is invariant under $\mathrm{SU}(N_q)$ group transformations, given by,

$$\Phi_q = (\Psi_1, \ldots, \Psi_{N_q})^{\mathrm{T}}\,,\ \ \Phi_q \to U\Phi_q\,, \tag{2.8}$$

where $U \in \mathrm{SU}(N_q)$.

However, this is an approximate symmetry as the masses of the quarks are not exactly the same in nature. As compared to the typical hadronic scale ($\approx$ 1 GeV), the masses of the u and d quarks are almost negligible. Hence, QCD exhibits approximate SU(2) symmetry known as the *isospin* symmetry. Including the s quark[1] into the mix, the symmetry group can be extended to the SU(3) group. Hadrons inherit this approximate symmetry from the quarks and can be classified into multiplets of the SU(3) group as mentioned in the introduction. These symmetry arguments are not only useful for classification of hadrons but also for predicting ratios of cross sections, ratio of masses and scattering properties.

Moreover, QCD is invariant under global *Chiral* symmetry when massless quarks are considered. The quark field can be decomposed into left-handed and right-handed components using the projection operators $P_{L/R} = \left(1 \mp \gamma_5\right)/2$,

$$\Psi = (\Psi_1, \ldots, \Psi_{N_q})^{\mathrm{T}}, \;\; \Psi_{L/R} = P_{L/R}\Psi \,. \tag{2.9}$$

Here, $P_{L/R}$ obey the following properties:

$$\begin{aligned} P_{L/R}^2 &= P_{L/R} \,, \\ P_L + P_R &= 1 \,. \end{aligned} \tag{2.10}$$

With this, the fermionic Lagrangian can be written in terms of $\Psi_{L/R}$ as

$$\mathcal{L}_f = \overline{\Psi}_L\Big(i\gamma_\mu D_\mu\Big)\Psi_L + \overline{\Psi}_R\Big(i\gamma_\mu D_\mu\Big)\Psi_R - \overline{\Psi}_L\mathcal{M}\Psi_R - \overline{\Psi}_R\mathcal{M}\Psi_L \,. \tag{2.11}$$

Here, $\mathcal{M} = diag(m_1, \ldots, m_N)$ represents the mass matrix for the quarks. Clearly, if $\mathcal{M} = 0$ the Lagrangian would be invariant under the following transformations,

$$\Psi_{L/R} \rightarrow \Psi'_{L/R} = g_{L/R}\Psi_{L/R} \,, \;\; \text{with} \;\; g_{L/R} \in \mathrm{U}(N)_{L/R} \,. \tag{2.12}$$

This leads to the Lagrangian being invariant under global $\mathrm{U}(N)_L \times \mathrm{U}(N)_R$ symmetry. As stated above, the masses of u,d and s quark is well below the hadronic scale and hence this symmetry is good for $N = 3$. Furthermore, the left-handed and right-handed components can be combined into vector- and axial-vector components. The axial anomaly leads to the violation of the singlet axial-vector current, whereas the conservation of the singlet vector current leads to the conservation of baryon number density. It can be further shown that the non-singlet axial-vector current is violated by quark masses themselves. Hence, in QCD, $\mathrm{SU}(N)_L \times \mathrm{SU}(N)_R$ is spontaneously broken to $\mathrm{SU}(N)_V$, resulting in hadrons not forming opposite parity multiplets. The remaining $\mathrm{SU}(N)_V$ symmetry corresponds to the flavor symmetry mentioned above. The spontaneous symmetry breaking results in $N^2 - 1$ Goldstone bosons. However, since chiral symmetry is explicitly broken due to the non-zero quark masses, the Goldstone bosons acquire masses proportional to the quark masses. These Goldstone bosons can be identified with the particles of the pseudoscalar meson octet, namely, pions, kaons and eta. The EFT that treats these particle as the fundamental degree of freedom and describes their dynamics in the low-energy regime is called chiral perturbation theory.

[1] The mass of the s quark is still smaller than the typical hadronic scale.

2.2 Path Integral Formalism

An effective way to calculate the expectation values of operators in any Quantum Field Theory (QFT) is the *path integral formalism*. Vacuum expectation values in QCD can be calculated as shown below,

$$\begin{aligned} \langle O \rangle &= \frac{1}{Z} \int D\Psi\, D\overline{\Psi} \int DG\, O[\Psi, \overline{\Psi}, G] e^{iS_{\mathrm{QCD}}[\Psi,\overline{\Psi},G]}\,, \\ Z &= \int D\Psi\, D\overline{\Psi} \int DG\, e^{iS_{\mathrm{QCD}}[\Psi,\overline{\Psi},G]}\,. \end{aligned} \tag{2.13}$$

Here, $\int D\Psi\, D\overline{\Psi} \int DG$ refers to the integration over all possible field configurations, $O[\Psi, \overline{\Psi}, G]$ represents the observable made up of quarks and gluon fields and S_{QCD} is the QCD action. Each possible integral configuration is *weighted* with the factor $e^{iS_{\mathrm{QCD}}[\Psi,\overline{\Psi},G]}/Z$. At high energies QCD is perturbative and hence the exponential appearing in the path integral can be expanded in the powers of the coupling constants. However, a regularization scheme needs to be imposed to render the path integrals well defined such as *dimensional regularization*.

As stated above, at low energies (the scale defined by Λ_{QCD}) perturbation theory cannot be applied. In this low-energy region one has to turn to Lattice QCD, which is a non-perturbative, ab-initio method of studying QCD. Moreover, discretization on a finite-dimensional Euclidean lattice acts as a natural regularization method and permits numerical techniques such as *Monte Carlo methods* to be applied.

2.3 Lattice QCD

The following section introduces in brief the relevant concepts of LQCD. A more detailed introduction can be found in any Lattice QCD book (cf. e.g. [143]).

2.3.1 Euclidean Path Integral

The first step involved in defining QCD on a finite-dimensional Euclidean lattice is to analytically continue the path integral from Minkowski space-time to Euclidean space-time via the Wick's rotation. This results in Eq. (2.13) taking the form,

$$\begin{aligned} \langle O \rangle_E &= \frac{1}{Z_E} \int D\Psi\, D\overline{\Psi} \int DG\, O[\Psi, \overline{\Psi}, G] e^{-S_{\mathrm{E}}[\Psi,\overline{\Psi},G]}\,, \\ Z_E &= \int D\Psi\, D\overline{\Psi} \int DG\, e^{-S_{\mathrm{E}}[\Psi,\overline{\Psi},G]}\,. \end{aligned} \tag{2.14}$$

Here, S_{E} is the Euclidean QCD action[2]. The time-independent observables can be expressed in terms of Euclidean path integrals. Moreover, the Euclidean correlators can be analytically continued to Minkowski space [144, 145]. The exponential appearing in the Eq. (2.14) can be interpreted as the Boltzmann weight and hence stochastic methods can be employed to numerically evaluate such

[2] $S_{\mathrm{E}} = \int d^4x \left(\frac{1}{2g^2} \mathrm{Tr}\left[F_{\mu\nu}(x) F_{\mu\nu}(x) \right] + \sum_f \overline{\Psi}_f(x) (\gamma_\mu D_\mu + m_f) \Psi_f(x) \right)$, where all the quantities are defined in the Euclidean space-time.

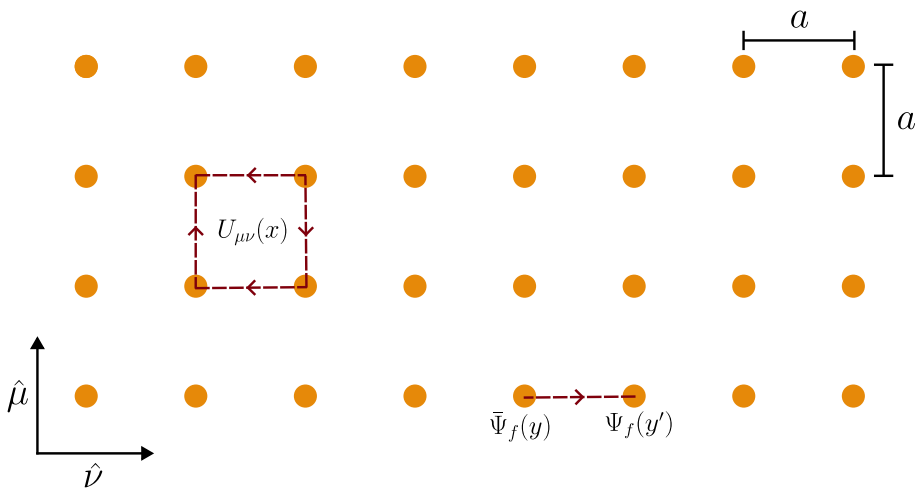

Figure 2.1: Euclidean Lattice with orange dots representing the lattice points with spacing a. The red arrows represent the link fields. The Plaquette operator $U_{\mu\nu}(x)$ and the parallel transporter connecting fermion fields are also depicted above.

integrals. Before applying stochastic methods, one has to perform discretization of the space-time lattice. This step will be discussed in the following section.

2.3.2 Discretization

This step entails discretizing the Euclidean space-time on a 4-dimensional Lattice Λ, schematically shown in Fig. 2.1, defined as

$$\Lambda = \left\{ x_\mu \in \mathbb{R}^4 \,\middle|\, x_\mu = a \times n_\mu, \quad n_\mu = 0, 1, \ldots, N_\mu - 1, \;\; \text{with} \;\; \mu = 1, 2, 3, 4 \right\}. \tag{2.15}$$

Here, a is the lattice spacing between two consecutive lattice sites, which are defined by x_μ. The spatial extents of the lattice are given by $L_1 = aN_1$, $L_2 = aN_2$ and $L_3 = aN_3$ and the temporal extent is given by $L_4 = L_T = aN_4$. For simplicity, $L_1 = L_2 = L_3 = L$ will be considered for rest of the discussion. Note that the lattice spacing a can be chosen to be different for each of the space-time directions. This discretized space-time is subjected to a boundary condition. Periodic boundary conditions are a popular choice, i.e. $x_\mu \equiv x_\mu + L\hat{\mu}$ with $\hat{\mu}$ denoting a unit-vector which leads to the lattice taking the shape of a 4D-torus. However this is not the only choice. A more general class of boundary condition is known as the twisted boundary condition, where the fields on the lattice gain an additional phase at the boundary. If this phase is equal to 1, one ends up with the periodic boundary condition whereas if this phase is equal to -1, one ends up with the anti-periodic boundary condition which are useful in the case of fermions on the lattice.

The quark fields, Ψ_f and $\overline{\Psi}_f$ are then placed on the lattice sites. These fields carry the same charge and color and transform in the same way as in the continuum theory. To discretize fermions on the lattice, the derivative has to be defined. This definition is not unique on the lattice and can be done in

multiple ways. The following definition of the derivative is used in rest of this chapter

$$\partial_\mu \Psi_f(x) \to \partial_\mu^{\mathrm{Lat}} \Psi_f(x) = \frac{\Psi_f(x + a\hat{\mu}) - \Psi_f(x - a\hat{\mu})}{2a} \,. \tag{2.16}$$

In the infinite volume, invariance of the Lagrangian under local SU(3) color gauge group leads to the introduction of the gauge fields. Imposing gauge invariance on the lattice is a non-trivial task. If one naively chooses a $\Omega(x) \in \mathrm{SU}(3)$ similar to the continuum theory for each lattice site, then the bilinear $\overline{\Psi}(x)\Psi(x + a\hat{\mu})$, arising due to the derivative, is no more gauge invariant. Therefore, $U_\mu(x)$ is introduced as a gauge field which transforms as follows,

$$U_\mu(x) \to U'_\mu(x) = \Omega(x) U_\mu(x) \Omega(x + a\hat{\mu})^\dagger \,. \tag{2.17}$$

Hence, the gauge invariance of the Lagrangian is restored. $U_\mu(x)$ is an element of the SU(3) group and is called a *link variable* as it forms a link between two subsequent lattice sites. Note that these link variables have orientation and can be defined for both negative and positive μ directions. $U_\mu(x)$ can be identified with the so-called *gauge transporter* or *parallel transporter* in the continuum. A parallel transporter is defined as the path-ordered exponential integral of a gauge field G_μ, connecting two points along a curve. With this definition, one gets

$$U_\mu(x) = P \exp\left(i \int_0^a G(x + z\hat{\mu})\, dz \right), \tag{2.18}$$

which at $O(a)$ can be written as

$$U_\mu(x) = \exp\left(iaG_\mu(x) \right). \tag{2.19}$$

The finite-dimensional lattice path integral is then defined with the following measure,

$$\int D\Psi\, D\overline{\Psi} \int DG \to \int \prod_{x \in \Lambda} d\Psi(x)\, d\overline{\Psi}(x) \int \prod_\mu dU_\mu(x) \,. \tag{2.20}$$

Note that dU represents the invariant Haar-measure of SU(3).

At the next step, the gauge invariant Euclidean action has to be constructed with the discretized quark and gauge fields mentioned above. Only two possible building blocks exist that are invariant under gauge transformation on the lattice. The first term is

$$\overline{\Psi}_f(x) \mathcal{P}_C[U] \Psi_f(y) = \overline{\Psi}_f(x) \Big[\prod_{(z,\mu) \in C} U_\mu(z) \Big] \Psi_f(y) \,, \tag{2.21}$$

where the operator $\mathcal{P}_C[U]$ forms a link connecting quark fields at x and y via the path C and transforms like $U_\mu(x)$. Therefore the whole structure is gauge invariant. The other building block consists of a trace of link variables taken over a closed loop l as follows,

$$L_l[U] = \mathrm{Tr} \Big[\prod_{(z,\mu) \in l} U_\mu(z) \Big] \,. \tag{2.22}$$

The *plaquette* is an example of such a structure, defined as:

$$U_{\mu\nu}(x) = U_\mu(x)U_\nu(x + a\hat{\mu})U_\mu^\dagger(x + a\hat{\nu})U_\nu^\dagger(x) \,. \tag{2.23}$$

The euclidean gauge action can then be written down as follows:

$$S_G = -\frac{2}{g^2}\sum_{x\in\Lambda}\sum_{\mu<\nu}\mathrm{Re}\,\mathrm{Tr}\big[U_{\mu\nu}(x)\big] \,. \tag{2.24}$$

Expanding the exponential in Eq. (2.19) up to $O(a)$ and dropping irrelevant constants, the gauge action becomes

$$S_G = \frac{a^4}{2g^2}\sum_{x\in\Lambda}\sum_{\mu,\nu}\mathrm{Tr}\big[F_{\mu\nu}(x)^2\big] + O(a^2) \,. \tag{2.25}$$

Taking the limit $a \to 0$ results in the continuum action.

2.3.3 Fermions on Lattice

To write down the fermionic action, the covariant derivative can be written in terms of the link variables and the derivative defined in Eq. (2.16) as follows:

$$D_\mu\Psi_f(x) \to D_\mu[U]\Psi_f(x) = \frac{U_\mu(x)\Psi_f(x + a\hat{\mu}) - U_\mu^\dagger(x - a\hat{\mu})\Psi_f(x - a\hat{\mu})}{2a} \,. \tag{2.26}$$

With this, the naive fermion action can be written as

$$S_F = a^4\sum_{x\in\Lambda}\sum_f \overline{\Psi}_f(x)\Big(\gamma_\mu D_\mu[U] + m_f\Big)\Psi_f(x) \,. \tag{2.27}$$

Even though this action reproduces the correct continuum action up to $O(a^2)$, it leads to what is called the *fermion doubling problem*. Each Dirac field discretized on the lattice describes 16 identical fermion fields, as the free fermion propagator has 15 additional poles in addition to the physical one due to periodicity. Moreover, the Nielsen–Ninomiya theorem [146] states that the imposition of locality, hermiticty and translational invariance on chiral fermions will necessarily lead to fermion doubling on the lattice. Various methods exist to overcome this problem.

One of the possible ways to deal with the doublers is to add the so-called *Wilson term* [147] to the action. This term breaks chiral symmetry explicitly and is given by

$$D_w[U] = -a\frac{r}{2}D_\mu[U]D_\mu[U] \,. \tag{2.28}$$

Here, r is called the Wilson parameter. This addition leads to all the unphysical doublers gaining an additional mass of $2r/a$, causing them to decouple in the continuum limit leaving behind only the physical fermion. However, Wilson term leads to discretization effects[3] of $O(a)$.

In contrast to Wilson fermions, the method with staggered fermions [148, 149] involves placing the

[3] Any discretization procedure for the Euclidean action will lead to discretization effects (proportional to some positive power of a) which vanishes in the limit $a \to 0$.

components of the Dirac field on different lattice points. This reduces the number of fermions to 4. Many other approaches such as the overlap fermion [150, 151] and domain-wall discretization [152, 153], which are types of Ginsparg-Wilson fermions[4] have been developed and are used in different situations.

2.3.4 Symanzik Improvement of the Action

Performing the continuum limit is highly non-trivial. In the continuum one has infinite volume and no concept of lattice spacing. On the other hand, the lattice spacing a also plays the role of UV regulator. Hence taking the limit a going to 0 is not a simple task. The lattice spacing a has to be systematically decreased while increasing the number of lattice points in order to ensure the volume remains constant. Setting a to 0 implies making the number of lattice points infinite, thus in any real world lattice simulation a should be finite. Hence, this leads to physical observables having lattice artifacts that may start at leading order, i.e. $O(a)$. This dependence on a is one of the sources of discretization effect. By adding terms, that vanish in the continuum, to the action this dependence can be shifted to higher order terms leading to a smoother limit in observables corresponding to the renormalized quantities when considering $a \to 0$. This procedure goes by the name of *Symanzik improvement program* [155, 156]. Note that, for the full improvement of the correlator, the interpolators also need to be improved in addition to the action.

Symanzik improvement program involves the following, first a continuum EFT of the lattice action is considered. The terms appearing in the effective action are organized according to their mass dimensions and then multiplied with appropriate powers of a. Then, suitable counter terms are added such that the correction terms cancel out explicitly up to the required order in a. In case of the Wilson lattice action one adds the Pauli term to achieve $O(a)$ improvement [157],

$$S_I = S_{\text{Wilson}} + c_{sw} a^5 \sum_{x\in\Lambda} \sum_{\mu<\nu} \sum_f \overline{\Psi}_f(x) \frac{1}{2} \sigma_{\mu\nu} \hat{F}_{\mu\nu}(x) \Psi_f(x) \,. \tag{2.29}$$

Where c_{sw} is called the *Sheikholeslami–Wohlert coefficient* whose value can be found in Refs. [158–160], $\sigma_{\mu\nu} = -i[\gamma_\mu, \gamma_\nu]/2$ and $\hat{F}_{\mu\nu}(x)$ is defined as follows,

$$\begin{aligned} \hat{F}_{\mu\nu}(x) &= \frac{-i}{8a^2} \left(Q_{\mu\nu}(x) - Q_{\nu\mu}(x) \right) , \\ Q_{\mu\nu}(x) &= U_{\mu\nu}(x) + U_{\nu,-\mu}(x) + U_{-\mu,-\nu}(x) + U_{-\nu,\mu}(x) \,. \end{aligned} \tag{2.30}$$

The purely gauge action can also be improved up to $O(a^2)$ by including the following term in the action [161–163],

$$S_{G'} = -\frac{2}{g^2} \sum_{x\in\Lambda} \left(\beta_0 \sum_{\mu<\nu} \text{Re Tr}[U_{\mu\nu}(x)] + \beta_1 \sum_{\mu\neq\nu} \text{Re Tr}[U^{1\times2}_{\mu\nu}(x)] \right) , \tag{2.31}$$

where $U^{1\times2}_{\mu\nu}(x)$ represents a 1×2 rectangular loop similar to the plaquette, the values of β_0 and β_1 are given in Refs. [161, 164]. The improved action is then called the *Lüscher–Weisz gauge action*.

[4] Although Ginsparg-Wilson fermions break chiral symmetry explicitly, the symmetry is restored in the continuum limit [154].

2.3.5 Euclidean Path Integral on Lattice

Substituting the discretized Euclidean action in Eq. (2.14) and applying the Wick's theorem, one gets

$$\langle O \rangle = \frac{1}{Z} \int \mathcal{D}U \, \langle O \rangle_F \, e^{-S_G[U]} \mathrm{det} D[U] \,, \quad Z = \int \mathcal{D}U \, e^{-S_G[U]} \mathrm{det} D[U] \,. \tag{2.32}$$

Here, $\prod_{x \in \Lambda} \prod_{\mu} dU_\mu(x)$ is abbreviated to $\mathcal{D}U$, $\mathrm{det}D[u]$ is the determinant of the lattice Dirac operator and $\langle O \rangle_F$ is the Wick contracted operator. A probability measure can be defined if $\mathrm{det}D[U]$ is positive definite given by

$$DP[U] = \frac{1}{Z} \mathcal{D}U \, e^{-S_G[U]} \mathrm{det} D[U] \,. \tag{2.33}$$

With this definition the path integral can be solved numerically using Monte Carlo methods. Different gauge configurations are selected based on this probability distribution via *importance sampling* and then expectation values of the operators are calculated by averaging over N such independent samples. The expectation value is hence given by

$$\langle O \rangle = \frac{1}{N} \sum_{i}^{N} \langle O \rangle_F^i + O(N^{-\frac{1}{2}}) \,, \tag{2.34}$$

where $\langle O \rangle_F^i$ denotes Wick contracted operator for different gauge configurations. A popular Monte Carlo method used in LQCD goes by the name of Hybrid Monte Carlo (HMC) [165]. It is a sampling algorithm which couples Hamiltonian dynamics with Metropolis-Hastings algorithm [24, 166] to investigate probability distributions.

2.4 Hadron Spectroscopy

Hadron spectroscopy refers to the extraction and study of physical properties such as masses of the hadrons from LQCD. After having setup the Euclidean action for LQCD, *interpolating operators* have to be identified that build up the necessary correlators for performing spectroscopic calculation on the lattice. An interpolator is a functional of the lattice fields which carries the quantum numbers of the hadronic state of interest. The typical form of a meson interpolator is given by

$$O_M(x) = \overline{\Psi}_f(x) \, \Gamma \, \Psi_{f'}(x) \,, \tag{2.35}$$

where Γ is some combination of gamma matrices in accordance with the symmetric properties of the meson. For example, the interpolators for the pion fields are given by,

$$\begin{aligned} O_{\pi^+}(x) &= \bar{d}(x) \gamma_5 u(x) \,, \\ O_{\pi^-}(x) &= \bar{u}(x) \gamma_5 d(x) \,, \\ O_{\pi^0}(x) &= \frac{1}{\sqrt{2}} \big(\bar{u}(x) \gamma_5 u(x) - \bar{d}(x) \gamma_5 d(x) \big) \,. \end{aligned} \tag{2.36}$$

where $q(x)$ and $\bar{q}(x)$ represent $f = q$ component of $\Psi_f(x)$ and $\overline{\Psi}_f(x)$ respectively. The conjugate interpolator $\overline{O}_M(x)$ is defined as $O^\dagger_M(x)$, with which the meson correlators can be defined as follows:

$$\langle O_M(x,y)\rangle = \langle O_M(x)\overline{O}_M(y)\rangle\,. \tag{2.37}$$

Therefore, the pion correlators as given by

$$\begin{aligned}
\langle O_{\pi^+}(x,y)\rangle &= \langle O_{\pi^+}(x)O_{\pi^-}(y)\rangle\,,\\
\langle O_{\pi^-}(x,y)\rangle &= \langle O_{\pi^-}(x)O_{\pi^+}(y)\rangle\,,\\
\langle O_{\pi^0}(x,y)\rangle &= \langle O_{\pi^0}(x)\overline{O}_{\pi^0}(y)\rangle\,.
\end{aligned} \tag{2.38}$$

Note that $\overline{O}_{\pi^+}(x) = O^\dagger_{\pi^+}(x) = O_{\pi^-}(x)$. After Wick's contraction, the correlators become

$$\begin{aligned}
\langle O_{\pi^+}(x,y)\rangle_F &= -\mathrm{Tr}\big[\gamma_5 D_u^{-1}(x,y)\gamma_5 D_d^{-1}(y,x)\big]\,,\\
\langle O_{\pi^-}(x,y)\rangle_F &= -\mathrm{Tr}\big[\gamma_5 D_d^{-1}(x,y)\gamma_5 D_u^{-1}(y,x)\big]\,,\\
\langle O_{\pi^0}(x,y)\rangle_F &= -\frac{1}{2}\mathrm{Tr}\big[\gamma_5 D_u^{-1}(x,y)\gamma_5 D_u^{-1}(y,x)\big]\\
&\quad+\frac{1}{2}\mathrm{Tr}\big[\gamma_5 D_u^{-1}(x,x)\big]\mathrm{Tr}\big[\gamma_5 D_u^{-1}(y,y)\big]\\
&\quad-\frac{1}{2}\mathrm{Tr}\big[\gamma_5 D_u^{-1}(x,x)\big]\mathrm{Tr}\big[\gamma_5 D_d^{-1}(y,y)\big] + u \leftrightarrow d\,.
\end{aligned} \tag{2.39}$$

Here, $D_q^{-1}(x,y)$ denotes the quark propagator for the flavor $f = q$. The correlators defined above contain two types of terms. The traces that include two quark propagators represent *connected diagrams* whereas traces with a single quark propagator are referred to as *disconnected diagrams*, schematically shown in Fig. 2.2. Note that in the limit of exact isospin symmetry, i.e. $m_u = m_d$, the neutral pion correlator simplifies to the correlators of the charged pion, implying that the masses of all the three pions will be the same. This exhibits clearly, the inheritance of symmetric properties of the quarks to the hadrons[5].

2.4.1 Masses of stable Hadrons

Out of the huge number of hadrons, only a few do not decay via the strong interaction. In the case of 3 quark flavors, the particles in the pseudoscalar octet mesons (π , K and η) and the baryon decuplet (N , Λ , Σ , Ξ and Ω) are the only stable particles in pure QCD. The masses of such particles can be extracted by using the two-point correlation functions described in the previous section,

$$C_h(t) = \frac{1}{L^3}\sum_{\mathbf{x}}\langle 0|O_h(t,\mathbf{x})\overline{O}_h(0,\mathbf{0})|0\rangle\,. \tag{2.40}$$

Where O_h is the appropriate interpolator for the hadron h. The temporal extent of the lattice is considered to be infinite for simplicity. A complete set of Hamiltonian eigenstates can be introduced

[5] The small difference in the masses of u and d quarks in addition to the electroweak corrections causes the mass of neutral pion being different from that of the charged pion.

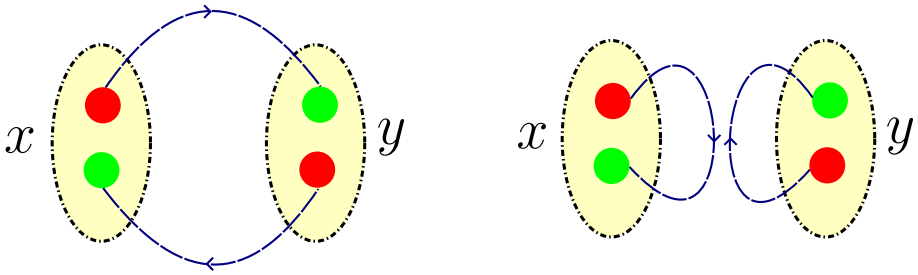

Figure 2.2: Schematic representation of the connected diagrams and disconnected diagrams in the meson correlator.

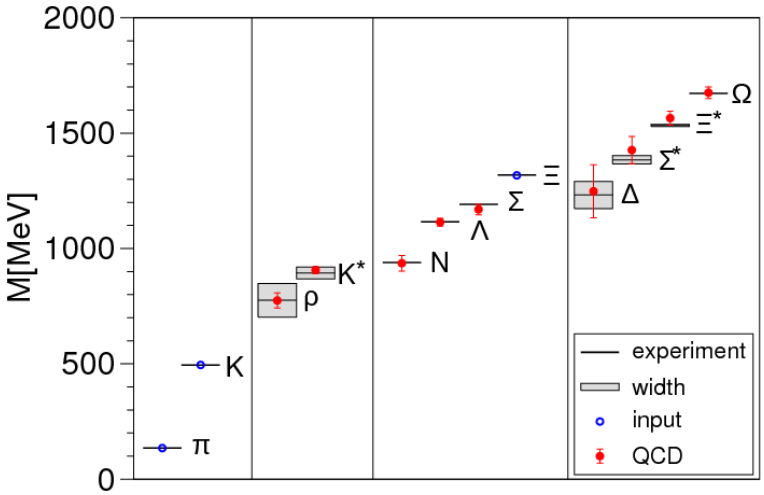

Figure 2.3: Comparison between the masses of light hadron from LQCD and corresponding experimental values, figure taken from Ref. [167]. The solid red dots represent the LQCD data whereas the horizontal lines and bands denote the experimental values along with their decay widths. Combined statistical and systematic error estimates are denoted by the vertical error bars. The blue circles represent the input used to set the light quark mass, the strange quark mass and the overall scale. Different multiplets are separated by the vertical gray lines.

in Eq. (2.40) and then translational invariance can be used to simplify the correlation function as follows:

$$C_h(t) = \sum_n \frac{|Z_n|^2}{2E_n} e^{-E_n t} . \tag{2.41}$$

Here, the probability of a state $|n\rangle$ with energy E_n being created by the interpolating operator O_h is given by $|Z_n|^2 = |\langle 0|O_h(0,\mathbf{0})|n\rangle|^2$. The state with $n = 0$ corresponds to the stable hadron and states with $n > 0$ denotes excited state. Due to the negative exponential in the equation above, the contribution of higher excited states are suppressed and eventually dies out for large t. The hadron

mass can be determined by defining the quantity known as the *effective mass*,

$$m_{\text{eff},h}(t) = \frac{1}{a} \log\left(\frac{C_h(t)}{C_h(t+a)}\right). \tag{2.42}$$

For $t \to \infty$ the effective mass becomes a constant and is equal to E_0. One can then plot $m_{\text{eff},h}(t)$ as a function of t and perform a constant fit for large t. Note that these equations are accurate only for the temporal extent of lattice being infinite. These expressions need modification in the case of finite periodic temporal extent (cf. e.g. Ref. [168]). Determination of the fitting interval depends on the signal-to-noise ratio at large t and contamination of the correlation function due to excited states at small t.

The overlap of the interpolators with the ground state can be optimized by using *smeared* quark fields instead of the simple ones defined in the previous section. Smearing is the process of averaging the quark field over a small region of space-time which results in a more natural wave function. Several smearing techniques have been developed such as Gaussian or Jacobi smearing technique [169–171], APE [172], HYP [173], and stout smearing [174].

The masses of excited state, in principle could be extracted from the same correlator at smaller time by disentangling the ground state and then performing a fit to a hypothesis function. However, since the data is generated via Monte Carlo simulation and has errors, this could lead to unreliable results. Multiple approaches exist in literature for extraction of excited state masses such as *Bayesian analysis*, *Maximum entropy method* and *Variational analysis* (cf. e.g. Ref [143]). In the variational approach, different interpolators for the same hadron is used to form a basis and the correlator matrix is calculated. Then the energies of the excited states can be determined by solving the generalized eigenvalue problem (GEVP) [175]:

$$\begin{aligned} C(t)\,\mathbf{u}_n &= \lambda_n(t) C(t_0)\,\mathbf{u}_n\,, \\ \lambda_n(t) &= e^{-E_n t}\left(1 + O(e^{-\Delta E_n t})\right), \end{aligned} \tag{2.43}$$

where $C(t)$ is the correlator matrix and $\Delta E_n = \text{Min}(|E_n - E_m|)_{n\neq m}$.

The light hadron spectrum as obtained by the BMW collaboration [167] for $N_f = 2+1$ is shown in Fig. 2.3. The mass of the strange quark is set to (approximately) its physical value whereas the masses of the light quarks are extrapolated to the physical point, given by $M_\pi \simeq 135$ MeV. Stout averaged, Symanzik improved gauge action along with Wilson fermions were used in the simulations.

2.4.2 The Lüscher Equation

The energy levels obtained in the previous section display regular dependence on the lattice size L and hence corresponds to continuum hadron mass in the limit $L \to \infty$ [32] modulo exponentially suppressed corrections. Moreover, the same method can be generalized to determine other quantities involving single particle in- and out-states such as, the electromagnetic form factor of hadrons. However, as stated in the introduction, this method fails when one considers more than one incoming and outgoing particles, as in the case of the timelike form factor or processes involving scattering. This is a consequence of the well-known Maiani-Testa no-go theorem [31]. The essential argument is the fact that intermediate state with energy smaller than the required out-state can dominate the

correlator[6]. Hence, a different method needs to be employed to extract scattering parameters from lattice simulations.

The three-momentum of a free particle in a finite dimensional box of length L with periodic boundary condition is quantized,

$$\mathbf{P} = \frac{2\pi \mathbf{n}}{L}, \quad \text{with } \mathbf{n} \in \mathbb{Z}^3 . \tag{2.44}$$

This leads to the spectrum being discrete with non-interacting two-particle energy levels in the rest frame given by

$$E_n = 2\sqrt{M_h^2 + \mathbf{p}^2}\,, \tag{2.45}$$

where M_h denotes the mass of the hadron. When interactions are turned on these free energy levels shift. The on-shell scattering amplitude can then be extracted from the correlation functions utilizing these discrete energy levels.

In Refs. [88, 90] it was shown that the scattering length, and hence in principle other scattering parameters, could be extracted from the discrete spectrum of the n-boson ground state using perturbation theory. Further in Refs [32, 33], Lüscher was able to show that the infinite volume S-matrix elements determine the two-particle finite-volume energy spectrum completely modulo exponentially suppressed corrections. The Lüscher equation or the *two-body quantization condition* relates the infinite volume S-matrix elements parameterized in terms of the scattering phase shifts $\delta_l(s)$ to the finite-volume energy levels E_n. In the case of two identical bosons, the two-body quantization condition is given by

$$\begin{aligned} &\det \mathscr{A} = 0\,, \\ &\mathscr{A}_{lm,l'm'} = \delta_{ll'}\delta_{mm'} \cot\delta_l(s) - \mathscr{M}_{lm,l'm'}(s,\mathbf{P})\,, \quad \text{with } s = E^2 - \mathbf{P}^2\,, \end{aligned} \tag{2.46}$$

where the determinant is taken over the angular momentum space coordinates $lm, l'm'$, $\mathbf{P}$ is the total momentum of the center of mass system (CMS) and E is the energy. $\mathscr{M}_{lm,l'm'}(s,\mathbf{P})$ is defined as follows:

$$\mathscr{M}_{lm,l'm'}(s,\mathbf{P}) = \frac{(-1)^l}{\pi^{3/2}\gamma} \sum_{j=|l-l'|}^{l+l'} \sum_{s=-j}^{j} \frac{i^j}{\eta^{j+1}} C_{lm,js,l'm'} \frac{i^j}{\eta^{j+1}} Z^{\mathbf{d}}_{js}(1;s)\,, \tag{2.47}$$

$$C_{lm,js,l'm'} = (-1)^{m'} i^{l-j+l'} \sqrt{(2l+1)(2j+1)(2l'+1)} \begin{pmatrix} l & j & l' \\ m & s & m' \end{pmatrix} \begin{pmatrix} l & j & l' \\ 0 & 0 & 0 \end{pmatrix}, \tag{2.48}$$

with

$$\mathbf{d} = \frac{L\mathbf{P}}{2\pi}\,, \quad \eta = \frac{Lq^*}{2\pi}\,, \quad \gamma = \frac{E}{\sqrt{s}}\,, \tag{2.49}$$

where $q^* = \sqrt{s/4 - m^2}$ is the CMS relative momentum, m is the mass of the boson and the Lüscher

[6] Note that this statement is strictly true when $L \to \infty$, for finite L situation is different and serves an important role in the Lüscher equation.

zeta-function is defined by

$$Z^{\mathbf{d}}_{lm}(1;s) = \sum_{\mathbf{r}\in P_{\mathbf{d}}} \frac{\mathcal{Y}_{lm}(\mathbf{r})}{r^2-\eta^2}\,,$$
$$P_{\mathbf{d}} = \left\{\mathbf{r}\in\mathbb{R}^3 \middle| r_{\parallel} = \gamma^{-1}(n_{\parallel} - \frac{|\mathbf{d}|}{2})\,, \mathbf{r}_{\perp} = \mathbf{n}_{\perp}\,, \mathbf{n}\in\mathbb{Z}^3\right\}. \tag{2.50}$$

Here, $\mathcal{Y}_{lm}(\mathbf{p}) = |\mathbf{p}|^l Y_{lm}(\hat{\mathbf{p}})$ denotes the solid harmonics with $Y_{lm}(\hat{\mathbf{p}})$ being the regular spherical harmonic function. The sum over the perpendicular and parallel components are taken w.r.t the CMS momentum. Some remarks are in order. First, the $\mathscr{M}_{lm,l'm'}(s,\mathbf{P})$ depends only on the geometry of the box and is independent of the interaction. Second, validity of the Lüscher equation, in the form stated above, is restricted to the elastic scattering region only. However, it was generalized to the case of two-particle coupled channel in Refs. [37, 39–42], extending its applicability to multi-particle threshold. Third, in a finite volume the rotational symmetry is broken and hence different partial-waves mix. This results in the Eq. 2.46 being non-diagonal in the angular momentum space. A cut-off has to be imposed on the orbital angular momentum $l = l_{\max}$. For all $l > l_{\max}$, the phase shift is assumed to be 0.

Starting from the infinite-volume scattering amplitude finite-volume energy levels can be determined in the following way. First, the partial-wave projected infinite-volume scattering amplitude $T_l(s)$ is related to scattering phase shift via unitarity as follows:

$$T_l(s) = \frac{16\pi\sqrt{s}}{q^*\cot\delta_l(s) - iq^*}\,. \tag{2.51}$$

Using the phase shift $\delta_l(s)$, the Lüscher equation is solved to obtain the finite-volume energy spectrum where $E = E_n$.

Proceeding in the opposite direction, the infinite-volume scattering amplitude can also be determined from the discrete energy spectrum of the finite volume. To do this, first lattice energy spectra is determined from LQCD. Then the Lüscher equation is used to fit these energy levels in order to determine the phase shift. Once the phase shift is determined, it can be parameterized in terms of scattering parameters. For this, one uses the fact that the function $(q^*)^{2l+1}\cot\delta_l(s)$, in the vicinity of $(q^*)^2 = 0$, is analytic and real above threshold and can hence be expanded as follows:

$$(q^*)^{2l+1}\cot\delta_l(s) = -\frac{1}{a_l} + \frac{1}{2}r_l(q^*)^2 + \dots\,. \tag{2.52}$$

This expansion is known as the *effective-range expansion* (ERE) [176]. Here, the scattering parameters a_l and r_l represents the *scattering length* and *effective range* respectively. The dots represent higher order term in $(p^*)^2$ and the parameters associated with these terms are called *shape parameters*. An important point should be noted, the ERE is valid in the case of short-range interactions[7] only. When long-range interactions[8] are included in addition to the short-range one, the convergence of the ERE is not very good and hence modification needs to be done. The *modified effective-range function*

[7] These are interactions in which observables are independent (or approximately independent) of the short-range details of the system under consideration.

[8] These are interactions which act over long distances and where observables are dependent the details of the system under consideration.

(MERF) was developed in Ref. [64] and is briefly discussed in Sec. 2.4.7.

2.4.3 Symmetries in a Finite Volume

As stated above, rotational symmetry is broken in a finite cubic box. This leads to the Eq. (2.46) being non-diagonal in angular momentum space. However, a finite cubic box still posses some residual rotational symmetry which help in partial diagonalization of the Lüscher equation and will be detailed in the following paragraphs.

In the infinite volume, rotational symmetry is described by the SO(3) group. In addition to this, space inversion is also a good symmetry and hence the total symmetry group becomes O(3) = SO(3) $\otimes$ $\{E, I\}$ with I representing the space inversion elements and E is the identity element. O(3) group has infinitely many irreducible representations (irreps) which are described by angular momentum l and parity p as l^p.

In the finite-volume rotational symmetry is partially broken down to finite-dimensional group that leaves the lattice invariant under spacial transformations. In the case of bosons for $\mathbf{d} = (0, 0, 0)$, where $\mathbf{d}$ is defined in Eq. 2.49, this group is called the octahedral group O_h whereas for fermions the double cover of the octahedral group ${}^2O_h$ has to be considered. The O_h group consists of 48 group elements which are constructed out of 24 rotations and space inversion. The elements that are combinations of the rotation transformations and identity element are called *proper rotations* whereas the elements formed by combining rotation transformations with space inversions are called *improper rotations*. The O_h group forms a subgroup of the O(3) group and hence, the basis vectors of the infinitely many irreps of the O(3) group can be expressed in terms of the basis vectors of the irreps of the octahedral group. O_h group has a total of 10 irreps, namely $\Gamma = A_1^{\pm}, A_2^{\pm}, E^{\pm}, T_1^{\pm}, T_2^{\pm}$ with dimensionality $d_\Gamma = 1, 1, 2, 3, 3$ respectively[9]. The matrices in the irrep Γ is represented by

$$T^{\Gamma}(g) \,\forall\, g \in O_h \,. \tag{2.53}$$

For example, in case of the trivial representation A_1^+, $T^{A_1} = 1 \,\forall\, g \in O_h$. The explicit form of $T^{\Gamma}(g)$ for all the irreps can be found in Refs. [177, 178].

As mentioned above, the basis vector of the various irreps l^p of O(3) can be represented as a linear combination of the basis vectors of the irreps Γ of O_h. This is shown for $l \leq 4$ in Tab. (2.1). Moreover, the contribution of individual irreps to various angular momenta is shown in Tab. (2.2). Both of these table make it pretty evident that different partial-waves mix in a finite volume.

Table 2.1: Decomposition of the angular momenta into the irreps of the O_h group.

l^p	decomposition of irreps of O_h
$0^{\pm}$	$A_1^{\pm}$
$1^{\pm}$	$T_1^{\pm}$
$2^{\pm}$	$E^{\pm} \oplus T_2^{\pm}$
$3^{\pm}$	$A_2^{\pm} \oplus T_1^{\pm} \oplus T_2^{\pm}$
$4^{\pm}$	$A_1^{\pm} \oplus E^{\pm} \oplus T_1^{\pm} \oplus T_2^{\pm}$

[9] The superscript of the irreps represents the parity of the irrep.

Table 2.2: Contribution of the irreps of O_h group to various angular momenta

Γ	Contribution to l^p
$A_1^{\pm}$	$0^{\pm}, 4^{\pm}, \ldots$
$A_2^{\pm}$	$3^{\pm}, 6^{\pm}, \ldots$
$E^{\pm}$	$2^{\pm}, 4^{\pm}, \ldots$
$T_1^{\pm}$	$1^{\pm}, 3^{\pm}, \ldots$
$T_2^{\pm}$	$2^{\pm}, 3^{\pm}, \ldots$

For moving frames, i.e. $\mathbf{d} \neq (0,0,0)$, the symmetry group becomes even smaller. These smaller groups, known as *little groups*, pick up those group elements of O_h whose action leaves $\mathbf{d}$ invariant, in other words, the little group $\mathcal{G}$ is defined as

$$\mathcal{G} = \left\{ g \in O_h \middle| \, g\mathbf{d} = \mathbf{d} \right\} . \tag{2.54}$$

The little groups[10] for different $\mathbf{d}$ with the number of elements and irreps are given in Tab. (2.3). Further details on the irreps of these groups can be found in Refs. [36, 179].

Table 2.3: Little groups and their irreps for different $\mathbf{d}$ with $n_{\mathcal{G}}$ representing the number of elements in the group

$\mathbf{d}$	$\mathcal{G}$	$n_{\mathcal{G}}$	Irreps
$(0,0,a)$	C_{4v}	8	A_1, A_2, B_1, B_2, E
$(a,a,0)$	C_{2v}	4	A_1, A_2, B_1, B_2
(a,a,a)	C_{3v}	6	A_1, A_2, E

To partially diagonalize the quantization condition, it needs to be expanded in a basis of the irreps of the group $\mathcal{G}$. These basis vectors are represented by $|\Gamma_t, \alpha, l\rangle$ for a given irrep Γ with dimensionality d_Γ and angular momentum l. Here, $\alpha = 1, \ldots, d_\Gamma$ and $t = 1, \ldots, N_\Gamma$ with N_Γ denoting the multiplicity of the irrep Γ. Since the little groups are subgroups of the O(3) group, the irreps of these little groups can be represented in the space spanned by the basis vectors $|l, m\rangle$, where l is the orbital angular momentum quantum number and m is the magnetic quantum number. The action of element g of $\mathcal{G}$ on these basis vectors are given by

$$g|l,m\rangle = \sum_{m'=-l}^{l} \mathscr{D}^{l}_{m'm}(g)|l,m'\rangle \, , \tag{2.55}$$

where $\mathscr{D}^{l}_{m'm}(g)$ are the Wigner-matrices. Moreover, a projector can be defined

$$\Pi^{\Gamma}_{\alpha} = \frac{d_\Gamma}{n_{\mathcal{G}}} \sum_{g \in \mathcal{G}} (T^{\Gamma}_{\alpha\rho}(g))^* g \, , \tag{2.56}$$

[10] Note that in equal mass case, the above mentioned condition becomes $g\mathbf{d} = \pm\mathbf{d}$.

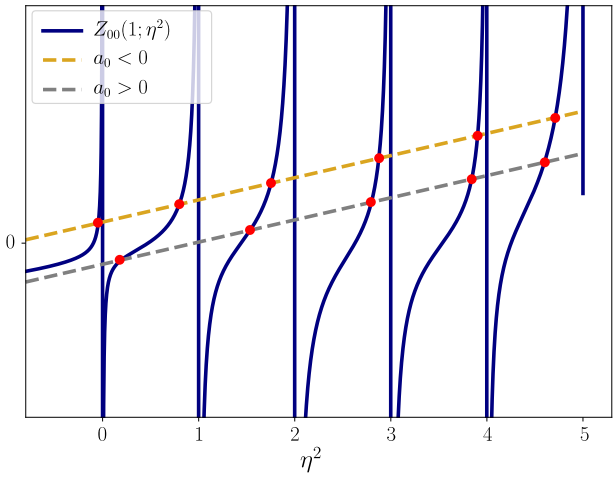

Figure 2.4: Schematic representation of the quantization condition given in Eq. (2.63). The blue line represents the Lüscher zeta-function in the S-wave, with $L = 2\pi$. This function has poles at integer values of η^2 which corresponds to the free energy levels. The dashed lines represent the cotangent of the phase shift parameterized in terms of the ERE. The yellow line represents attractive potential ($a_0 < 0$) whereas the gray line represents repulsive potential ($a_0 > 0$). The intersection of the blue line with the dashed lines, denoted by red dots, represents the interacting energy levels.

whose matrix elements[11] $\langle l, m'|\Pi^{\Gamma}_{\alpha}|l, m\rangle$ gives the basis vector $|\Gamma_t, \alpha, l\rangle$ as a linear combination of $|l, m\rangle$. Note, here the index ρ is fixed and $n_{\mathcal{G}}$ is the number of elements in the group $\mathcal{G}$. $T^{\Gamma}_{\alpha\rho}(g)$ is the matrix representation of the element g in a given irrep Γ. Hence, the basis vectors of the irreps of $\mathcal{G}$ are given by,

$$|\Gamma_t, \alpha, l\rangle = \sum_{m=-l}^{l} c^{\Gamma_t \alpha}_{lm} |l, m\rangle \,, \tag{2.57}$$

where the coefficient $c^{\Gamma_t \alpha}_{lm}$ results from the action of Π^{Γ}_{α} on the states $|l, m\rangle$. A list of these coefficients for some values of l can be found in Refs. [36, 178, 179].

The operator $\mathscr{A}$ in Eq. (2.46) takes the following form in the new basis,

$$\mathscr{A}^{\Gamma_t \Gamma'_{t'}}_{l\alpha, l'\alpha'} = \langle \Gamma_t, \alpha, l|\mathscr{A}|\Gamma'_{t'}, \alpha', l'\rangle = \sum_{m=-l}^{l} \sum_{m'=-l'}^{l'} \left(c^{\Gamma_t \alpha}_{lm}\right)^* \left(c^{\Gamma'_{t'} \alpha'}_{l'm'}\right) \mathscr{A}_{lm, l'm'} \,, \tag{2.58}$$

This expression can be simplified using Schur's first lemma,

$$\mathscr{A}^{\Gamma_t \Gamma'_{t'}}_{l\alpha, l'\alpha'} = \langle \Gamma_t, \alpha, l|\mathscr{A}|\Gamma'_{t'}, \alpha', l'\rangle = \delta_{\Gamma\Gamma'} \delta_{\alpha\alpha'} \mathscr{A}^{\Gamma}_{lt, l't'} \,. \tag{2.59}$$

[11] Note that the dimensionality of this matrix corresponds to the multiplicity N_{Γ} of the irrep Γ

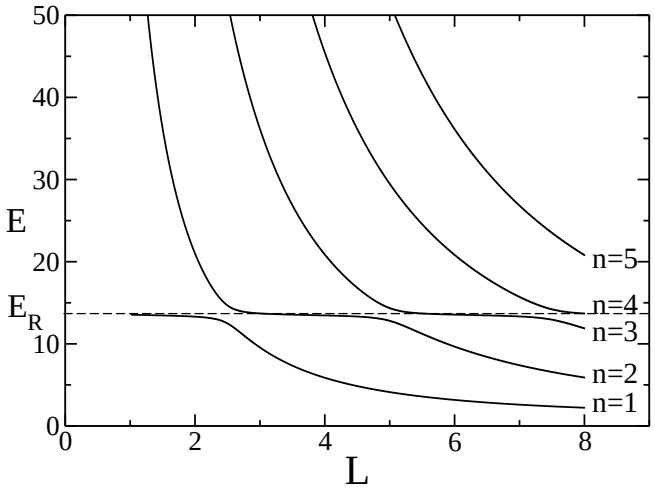

Figure 2.5: Two-particle finite-volume energy spectrum in a box of size L in the presence of a resonance. The energy levels exhibit the avoided level crossing represented by the plateau at resonance energy E_R. Figure taken from [180]

With this the quantization condition of Eq. (2.46) becomes

$$\det \mathscr{A}^{\Gamma} = 0\,, \tag{2.60}$$

$$\mathscr{A}^{\Gamma}_{lt,l't'} = \delta_{ll'}\delta_{tt'}\cot\delta_l(s) - \mathscr{M}^{\Gamma}_{lt,l't'}(s,\mathbf{P}) \tag{2.61}$$

$$\mathscr{M}^{\Gamma}_{lt,l't'}(s,\mathbf{P}) = \sum_{m=-l}^{l}\sum_{m'=-l'}^{l'}\left(c^{\Gamma_t\alpha}_{lm}\right)^*\left(c^{\Gamma_{t'}\alpha}_{l'm'}\right)\mathscr{M}_{lm,l'm'}(s,\mathbf{P})\,. \tag{2.62}$$

This partial diagonalization splits the quantization condition into separate conditions for each irrep Γ and greatly reduces the dimensions of the matrices involved.

In the S-wave, for $\mathbf{d} = (0,0,0)$ only the A_1^+ contributes. This leads to the Lüscher equation simplifying to

$$\cot\delta_0(s) = \frac{1}{\pi^{3/2}\gamma\eta}Z_{00}(1;s)\,. \tag{2.63}$$

The left side of the above equation is a function of the phase shift whereas the right side of the equation contains the Lüscher-zeta function which has poles corresponding to the free energy levels. The point of intersection of these two curves corresponds to the energy levels on the lattice for a given L. In the absence of bound states, if the potential is attractive ($a_0 < 0$), the energy levels shift below the free-energy levels whereas if the potential is repulsive ($a_0 > 0$), then the energy levels shift above the free-energy levels, this is shown schematically in Fig. 2.4. Note that if bound states are present, the energy levels corresponding to these states will shift below the bound state energy irrespective of the sign of the scattering length.

Another interesting situation to consider is the presence of a narrow resonance. Resonances show up as distinct features in the scattering phase shift. This distinct behavior is also transferred to the finite-volume energy spectrum. In the case of presence of a narrow resonance the phase shift can be parametrized using the Breit-Wigner formula as follows,

$$q^* \cot \delta_0(s) = \frac{6\pi\sqrt{s}}{m_R^2}(m_R^2 - s)\,, \tag{2.64}$$

where m_R represents the mass of the resonance. The energy levels in this case go along with the free-energy levels as usual. However in the vicinity of $\sqrt{s} = m_R \equiv E_R$, energy of the resonance, the levels tend to bend away. This is schematically shown in Fig. 2.5. This special feature of the spectrum in case of a narrow resonance is called *avoided level crossing* [181].

Lastly, some energy levels can lie in the middle of consecutive narrowly spaced free-energy levels in the case of moving frames. These narrow free-energy levels are degenerate in the non-relativistic limit and hence the energy levels pinched in between them should also vanish in the non-relativistic limit. This was discussed briefly in Refs. [182, 183].

2.4.4 Threshold Expansion

Threshold expansion offers another useful method that can be employed to extract scattering parameters from the ground state energy of hadrons. This method was outlined in Ref. [32] for lattice calculations. In the following paragraphs this method will be described in brief.

The two-particle free-energy levels in a finite volume as given in Eq. (2.45) can be expanded for large L as follows:

$$E_n = 2M_h + O(L^{-2})\,. \tag{2.65}$$

When interactions are turned on, these levels undergo $O(L^{-3})$ shifts. This enables one to employ perturbation theory to calculate this energy shift.

As stated above, the Lüscher-zeta function has poles corresponding to the free-energy levels. However, if one subtracts the pole at $\eta^2 = 0$, then rest of the function can be expanded around threshold. This is valid even though there are more poles corresponding to other free-energy levels as the typical separation between the interacting and non-interacting level is negligible compared to the separation between two successive free-energy levels. Hence the Taylor-expanded zeta function for S-wave takes the form,

$$Z_{00}(1;s) = \frac{1}{\sqrt{4\pi}}\left(\frac{-1}{\eta^2} + I + \eta^2 J + O(\eta^4)\right), \tag{2.66}$$

where I[12] and J are numbers given by,

[12] Note, the sum in the quantity I is formally UV-infinite and has to be regularized. This is done by rewriting I as follows,

$$I = \sum_{\mathbf{n}\in\mathbb{Z}^3\setminus 0}\left(\frac{1}{\mathbf{n}^2} - \frac{1}{\mathbf{n}^2+\mu^2}\right) + \sum_{\mathbf{n}\in\mathbb{Z}^3}\int d^3\mathbf{k}\,\frac{e^{2\pi i\mathbf{n}\mathbf{k}}}{\mathbf{k}^2+\mu^2} - \frac{1}{\mu^2}\,.$$

Here, the first term is convergent and the integral in the second term is calculated using dimensional regularization.

$$I = \sum_{\mathbf{n}\in\mathbb{Z}^3\setminus 0} \frac{1}{\mathbf{n}^2} \simeq -8.9136\,,$$
$$J = \sum_{\mathbf{n}\in\mathbb{Z}^3\setminus 0} \frac{1}{\mathbf{n}^4} \simeq 16.5323\,. \tag{2.67}$$

Moreover, using the effective-range expansion to parametrize the phase-shift and the expansion in Eq. (2.66), Eq. (2.63) becomes

$$\eta^2 = \frac{a}{\pi L}\left(1 - \frac{a}{\pi L} I + \left(\frac{a}{\pi L}\right)^2 (I^2 - J) + O(L^{-3})\right). \tag{2.68}$$

With this one can write down the non-relativistic ground state energy shift as

$$\Delta E_0 = \frac{4\pi^2}{M_h L^2}\eta^2 = \frac{4\pi a}{M_h L^3}\left(1 - \frac{a}{\pi L} I + \left(\frac{a}{\pi L}\right)^2 (I^2 - J) + O(L^{-3})\right). \tag{2.69}$$

The expression above clearly shows that the leading order correction to the ground state energy level is of the order L^{-3}. Both the effective range r and relativistic correction enter at $O(L^{-6})$ [91, 92, 96]. Extension of this formalism, in the context of NREFT, to the three-particle sector will be discussed in Chap. 3

2.4.5 Two-Particle Decays

In Ref [43], Lellouch and Lüscher formulated a method for studying certain type of two-particle decay on the lattice that was based on the quantization condition approach. In general, QCD decays can be categorized into two groups. First group includes decays that are mediated via interactions other than the strong force[13], such as the electroweak decay of kaons $K \to \pi\pi$. The other group consists of decays which are mediated by the strong interactions, such as the QCD process $\rho \to \pi\pi$. The Lellouch-Lüscher formalism is apt for studying decays of the first kind and establishes the relation between infinite-volume decay matrix element and the finite-volume transition matrix element. Application of this method to the study of $K \to \pi\pi$ decay was carried out by the RBC and UKQCD collaborations [184–186].

In the case of kaon decay, $K \to \pi\pi$, perturbation theory can be employed as the Fermi constant is very small. In the following, $K^+ \to \pi^+\pi^0$ in the S-wave will be considered as this simplifies the discussion to a great extent[14]. Firstly, isospin $I = 1$ is not allowed for the two-pions states with $l = 0$ due to Bose symmetry. Secondly, $I = 0$ is also not allowed because of charge conservation symmetry. Hence, one only needs to consider the case of $I = 2$.

[13] Decays mediated via some type of symmetry violation also fall in this group. for example $\omega \to \pi\pi$, which occurs in the case of broken isospin symmetry.

[14] The discussion here closely follows Refs. [103, 183]

The infinite-volume amplitude in the above mentioned case is given by

$$\begin{aligned} T(K^+ \to \pi^+\pi^0) &= \langle \pi^+(\mathbf{p}_1)\pi^0(\mathbf{p}_2); \text{out}|\mathcal{H}_w(0)|K^+(\mathbf{P}); in\rangle \\ &= Ae^{i\,\delta_2(s)}\,. \end{aligned} \tag{2.70}$$

$\mathcal{H}_w$ here denotes the weak interaction Hamiltonian density and $\delta_2(s)$ corresponds to the isospin $I = 2$ S-wave phase shift. Note, the angular momentum index of the phase shift is dropped for notational convenience. In the finite volume, one-kaon state can be represented as $|K^+;\mathbf{P}\rangle$ having three-momenta $\mathbf{P}$. Moreover, states with quantum number of the $\pi^+\pi^0$ states can be represented by $|n;\mathbf{P}\rangle$. Hence, the finite volume equivalent of the decay amplitude can be defined with the help of the Euclidean correlator as follows:

$$\frac{\langle 0|\pi^+_{\mathbf{p}_1}(t_1)\pi^0_{\mathbf{p}_2}(t_1)H_w(K^+_{\mathbf{P}}(t_2))^\dagger|0\rangle}{\langle 0|\pi^+_{\mathbf{p}_1}(t_1)\pi^0_{\mathbf{p}_2}(t_1)(\pi^+_{\mathbf{p}_1}(t_2))^\dagger(\pi^0_{\mathbf{p}_2}(t_2))^\dagger|0\rangle\langle 0|K^+_{\mathbf{P}}(t_1)(K^+_{\mathbf{P}}(t_2))^\dagger|0\rangle} \xrightarrow[t_2\to-\infty]{t_1\to\infty} \langle n;\mathbf{P}|H_w|K^+;\mathbf{P}\rangle\,. \tag{2.71}$$

Here H_w is the Hamiltonian derived from the Hamiltonian density $\mathcal{H}_w$. Note that, the box size L is made implicitly large such that the energy of the states n is exactly equal to $E_K = M_K^2 + \mathbf{P}^2$ in the absence of weak interactions. Hence,

$$E_n^{(0)} = E_K\,. \tag{2.72}$$

When interactions are turned on, these energies will shift. These energy shifts can be calculated in the perturbation theory by expanding the weak Hamiltonian in orders of the weak coupling g_w. At the first order,

$$E_n = E_n^{(0)} \pm \langle n;\mathbf{P}|H_w|K^+;\mathbf{P}\rangle + O(g_w^2)\,. \tag{2.73}$$

Again, in infinite volume the process $\pi^+\pi^0 \to K^+ \to \pi^+\pi^0$ contributes to the amplitude $T(\pi^+\pi^0 \to \pi^+\pi^0)$ at $O(g_w)$. Writing the two-pion scattering amplitude as $T = T^{(0)} + \Delta T$, ΔT is given by

$$\Delta T = \frac{|A|^2 e^{2i\,\delta^2(s)}}{P^2 - M_K^2} = \pm\frac{|A|^2}{2E_n^{(0)}\langle n;\mathbf{P}|H_w|K^+;\mathbf{P}\rangle}e^{2i\,\delta^2(s)} + O(g_w^2)\,, \tag{2.74}$$

where P represents the four-momentum of the pion pair. With this the phase shift in the presence of the weak interaction can be defined up to first order in perturbation theory as

$$\bar{\delta}_2(s) = \delta_2(s) \pm \frac{q^*}{16\pi\sqrt{s}E_n^{(0)}}\frac{|A|^2}{\langle n;\mathbf{P}|H_w|K^+;\mathbf{P}\rangle} + O(g_w^2)\,. \tag{2.75}$$

Further, using the fact that E_n solves the Lüscher equation in the presence of weak interaction, the phase shift becomes,

$$\bar{\delta}_2(s_n) = k\pi - \phi^d(s_n)\,,\ \ \cot\phi^d(s) = -\frac{1}{\pi^{3/2}\gamma\eta}Z_{00}^d(1;s)\,, \tag{2.76}$$

where $k = 1, 2, \ldots$ and $s_n = E_n^2 - \mathbf{P}^2$. $\phi^{\mathbf{d}}(s_n)$ and $\delta_2(s_n)$ can be Taylor-expanded around $q_n^* = q_n^{*\,(0)}$

as follows:

$$\begin{aligned}\phi^{\mathbf{d}}(s_n) &= \phi^{\mathbf{d}}(s_n^{(0)}) + \phi^{\mathbf{d}'}(s_n^{(0)})\Delta q_n^* + O(g_w^2)\,,\\ \delta_2(s_n) &= \delta_2(s_n^{(0)}) + \delta_2'(s_n^{(0)})\Delta q_n^* + O(g_w^2)\,,\end{aligned} \tag{2.77}$$

with $s_n^{(0)} = (E_n^{(0)})^2 - \mathbf{P}^2 = M_K^2$. Δq_n^* can be defined as

$$\Delta q_n^* = q_n^* - q_n^{*(0)} = \pm\frac{E_n^{(0)}}{4q_n^{*(0)}}\langle n;\mathbf{P}|H_w|K^+;\mathbf{P}\rangle + O(g_w^2)\,. \tag{2.78}$$

The phase shift in the absence of weak interaction can again be replaced with $\delta_2(s_n^{(0)}) = k'\pi - \phi^d(s_n^{(0)})$ as $E_n^{(0)}$ solves the Lüscher equation in this case. Putting everything together, one ends up with the expression

$$\begin{aligned}|A|^2 &= \Phi_{LL}\left(\langle n;\mathbf{P}|H_w|K^+;\mathbf{P}\rangle\right)^2\,,\\ \Phi_{LL} &= 4\pi M_K\left(\frac{E_n^{(0)}}{q_n^{*(0)}}\right)^2\left(\delta_2'(M_K^2) + \phi^{\mathbf{d}'}(M_K^2)\right)\,.\end{aligned} \tag{2.79}$$

The expression above shows that the infinite-volume decay matrix element is proportional to the finite-volume matrix element. Here, Φ_{LL} denotes the proportionality constant and is called the Lellouch-Lüscher factor.

2.4.6 Three-particle Sector on Lattice

As stated above the Lüscher equation is not valid above the three-particle threshold, however, lattice simulation are already capable of probing this sector. Moreover, vast number of QCD resonances decay into three particles. Hence the necessity of an approach for extraction of physical observables from Lattice QCD even in the three-particle sector is apparent. The extension of Lüscher's approach to the three-particle is however not a trivial task.

Perturbation theory was employed to obtain the ground state energy shift [88, 90, 91, 94, 98, 99, 187] and excited state energy shift [97] by performing an expansion in $1/L$. This approach is however not applicable when resonances or shallow bound states are considered. Chap. 6 presents the result of such a perturbative calculation in the case of three-nucleon system. However, a quantization condition similar to the Lüscher equation, in the three-body sector which reproduces the perturbative results while also including resonances and shallow bound state is very attractive.

Currently, there exist three alternatives, although conceptually equivalent formalism for the three-particle quantization condition based on the fact that the three-particle S-matrix element uniquely determines the finite-volume energy spectra [65]. These are, the Relativistic Field Theory (RFT) [67, 68], Finite Volume Unitarity (FVU) [69] and Non-relativistic Field Theory (NREFT) [70, 71] approach.

All the three above-mentioned approaches involve the following steps. First, the integrals appearing in the infinite-volume three-particle scattering integral equations are replaced with finite-volume sums. The quantization condition is then written in terms of a vanishing determinant, similar to the Lüscher equation. Next, the parameters which parameterize the two- and three-body interactions are

determined by performing a fit to lattice energy levels via the quantization condition. Having obtained these parameters, the infinite-volume observables can be determined by solving the integral equations for the three-particle scattering amplitude. The quantization condition in the NREFT approach will be discussed in more details in the next chapter.

Moreover, the three-body equivalent to the two-body Lellouch-Lüscher (LL) formula was derived independently by two groups in Refs. [100–102]. In the two-body case, the LL-factor is a single function as shown in Eq. (2.79), whereas in the three-body case it is given by a matrix. This will also be discussed in some detail the next chapter and a numerical calculation for the LL-factor in the case of $K \to 3\pi$ will be detailed in Chap. 7.

2.4.7 Two-Particle Sector in the Presence of Long-Range Force

As stated above, Eq. (2.51) relates the two-body scattering amplitude to the phase shift below the inelastic threshold. Utilizing unitarity one can define the K-matrix as follows

$$\mathrm{Re}\, T_l^{-1}(s) = \frac{q^*}{16\pi\sqrt{s}} \cot\delta_l(s) \equiv K_l^{-1}(s)\,. \tag{2.80}$$

The advantage of defining the K-matrix is that it is a real-valued function both above and below threshold when short-range interactions are considered. However, when one has to include the effects of a lighter particle being exchanged (long-range force) in the scattering process of interest, this $K_l(s)$ becomes a complex-valued function due to the presence of the t-channel cut or the *left-hand cut*. A prominent example of such a situation is the one-pion exchange (OPE) in NN-scattering.

Consider the scattering of two particles with mass M and a lighter particle with mass m being exchanged in the t-channel. Given that $m \ll M$, the unprojected scattering amplitude $T(s)$ develops a pole at $t = m^2$, see Fig. 2.6, which translates to a pole in s at

$$s = 4M^2 - \frac{m^2}{\sin^2\left(\frac{\theta^*}{2}\right)}\,, \tag{2.81}$$

where θ^* represents a fixed choice of the CMS scattering angle.

When θ^* is varied from 0 to π the pole position in s changes from $s = 4M^2 - m^2$ to $s = -\infty$. Hence, the partial-wave projected scattering amplitude $T_l(s)$ develops a branch cut[15] between $s = 4M^2 - m^2$ and $s = -\infty$, as shown in Fig. 2.6. In such cases, the effective-range expansion is no more valid as the radius of convergence becomes very small. Hence, the ERE has to be modified in the case of presence of short- plus long-range interactions.

A modification to ERE was first suggested in the Refs. [188, 189], in the case of Coulomb plus nuclear potential. Following this study, many *two-range potentials* were investigated and modifications were suggested (see for e.g. [190–201]). A general modified effective range function for short- plus long-range potentials was developed by Haeringen and Kok in Ref. [64]. This MERF will be discussed briefly in the following paragraph.

Consider a two-range potential, of the form

$$V(r) = V_L(r) + V_S(r)\,, \tag{2.82}$$

[15] Note that n-light particle exchanges can lead to additional branch cuts that run for $s \leq 4M^2 - n^2m^2$.

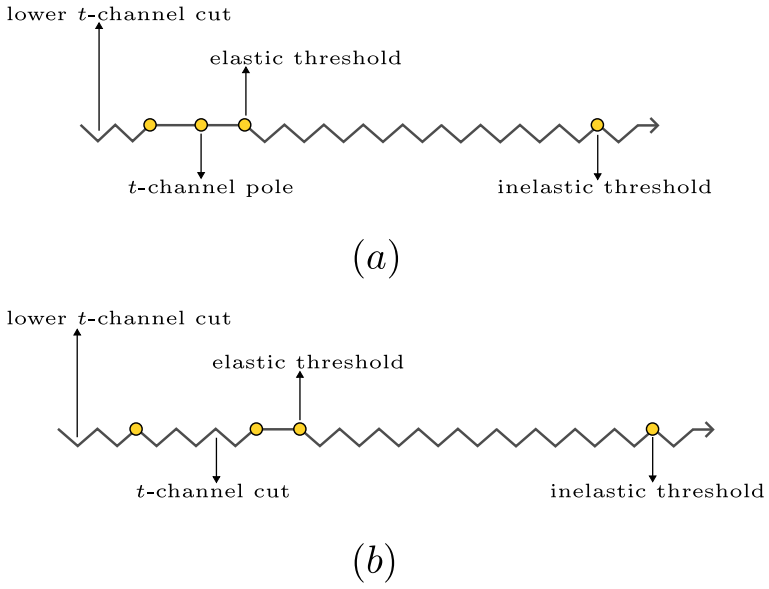

Figure 2.6: (a) The analytical structure of two-particle scattering amplitude $T(s)$ in the complex-s plane, for a fixed CM scattering angle. The wavy lines represents branch cuts. $T(s)$ develops a t-channel pole at $t = m^2$ below threshold in addition to the lower t-channel branch cuts coming from multi-meson exchanges. (b) The analytical structure of the partial-wave projected two-particle scattering amplitude $T_l(s)$, with the t-channel cut running from the t-channel pole to infinity.

where $V_L(r)$ is the long-range potential and $V_S(r)$ is the short-range potential. The potentials are assumed to be local and rotationally invariant. In this case, the MERF can be defined as follows:

$$K_l^M(s) = M_l(q^*) + \frac{(q^*)^{2l+1}}{|f_l(q^*)|^2}\big(\cot(\delta_l(s) - \sigma_l(s)) - i\big)\,, \tag{2.83}$$

where $\delta_l(s)$ represents the full phase shift and $\sigma_l(s)$ represents the phase shift in the presence of the long-range potential $V_L(r)$ only, i.e. $V_S(r) = 0$. $f_l(q^*)$ is the Jost function for the long-range potential which is defined in terms of the corresponding Jost solution $f_l(q^*, r)$ as follows,

$$f_l(q^*) = (q^*)^l e^{-il\pi/2}\frac{(2l+1)}{(2l+1)!!}\lim_{r\to 0} r^l f_l(q^*, r)\,. \tag{2.84}$$

The function $M_l(q^*)$ is given by,

$$M_l(q^*) = \frac{1}{l!}\Big(-\frac{iq^*}{2}\Big)^l \lim_{r\to 0}\frac{d^{2l+1}}{dr^{2l+1}} r^l \frac{f_l(q^*, r)}{f_l(q^*)}\,. \tag{2.85}$$

This approach uses the fact that typically the form of the long-range potential is known explicitly and the effects of $V_L(r)$ can be separated and included in the purely long-range functions $f_l(q^*)$ and $M_l(q^*)$. As a result of this separation the function $K_l^M(s)$ turns out to be a low-energy polynomial

and can be written in terms of the modified effective-range expansion as follows:

$$K_l^M(s) = -\frac{1}{\tilde{a}_S} + \frac{1}{2}(q^*)^2 \sum_{n=0}^{\infty} \tilde{r}_n \left(\frac{q^*}{\Lambda}\right)^{2n}, \tag{2.86}$$

where $(q^*)^2$ is of order of the light particle mass and Λ is of order of the heavy mass scale. Hence, the radius of convergence of the modified effective-range expansion is larger than that of the original effective-range expansion. Note that, in the limit $V_L \to 0$ the MREF reproduces the ERE.

A remark is in order, $M_l(q^*)$ is well defined if and only if $r^{-2l}V_L(r)$ is analytic at $r = 0$. This issue was discussed in detail in Ref. [202]. In case of a potential that does not obey this criteria, $M_l(q^*)$ can be defined by imposing a renormalization prescription.

In finite volume, the situation is even more non-trivial. The Lüscher equation is no more valid in the presence of short- plus long-range interaction. This is straightforward to see, if there is an energy level that lies on the t-channel cut region, the Lüscher equation will predict a real phase shift corresponding to a real K-matrix. However, as shown above the K-matrix in such a situation is clearly complex. The Lüscher equation is rooted in following fundamental assumptions. First, the relation $R/L \ll 1$ must be obeyed, where R is the range of the interaction, $R \sim 1/m$, where m is the mass of the lightest particle in the theory. Second, polarization corrections are exponentially suppressed ($\sim e^{-L/R}$) and can be dropped. Third, partial-wave mixing is small and hence a truncation can be made for $l = l_{\text{Max}}$. All three assumptions are violated in the presence of long-range forces [56].

Different approaches have been proposed in literature to extract physical observables from lattice in the presence of long-range forces. All of these approaches in general consider the long-range interactions explicitly. These approaches will be briefly discussed in the following.

In the Ref. [56], the authors have proposed to solve the quantization condition in the plane-wave basis instead of projecting on to the partial-waves. Then the plane wave basis is decomposed as a direct sum of irreps of the corresponding cubic or little group. The Lippmann–Schwinger equation (non-relativistic case) or Bethe–Salpeter equation (relativistic case) is solved to obtain the finite-volume spectrum. Moreover, an effective Hamiltonian is constructed using the long-range-interaction and a tower of operators involving contact terms and derivatives. The parameters of this Hamiltonian are extracted from the lattice energy levels, with which one can solve integral equations in the infinite volume to determine phase shift and other observables. The plane-wave basis was used in a study with the aim of extracting the pole of $T_{cc}(3875)^+$ from lattice data [57, 58].

Another approach, that modifies the two-body quantization condition was suggested by the authors of Refs. [59, 60]. In this approach, the short- and long-range part of the potential are split into different components. Then an auxiliary on-shell K-matrix denoted by $\overline{K}^{\text{os}}$ is defined which encodes all the short-range interactions. This $\overline{K}^{\text{os}}$ is then determined from a fit to the lattice energy levels, with which physical observables can be obtained by solving integral equations. This approach in essence is a two-step process.

Finally, in Ref. [61], the authors proposed to write down a three-body equation to deal with the problem of the t-channel cut. In this proposal DD^* scattering was considered and it was noted that the t-channel cut is absent in the three-body quantization condition for the $DD\pi$ system (D^* was assumed to be stable.). This was the case even when bound states in the $D\pi$ was below the elastic threshold. A comparative study of the three formalisms mentioned above was carried out in Ref. [63], which showed that any difference between the approaches could be removed by adjusting the short-range

couplings.

Developing an alternative approach to the above-mentioned problem was one of the primary goals of this research project. This *Modified Lüscher equation* approach will be detailed in Chap. 4. However, it may be pointed out that the result of this approach bears resemblances to the equations derived in Refs. [59, 60], in the sense that an alternative K-matrix is defined within the Modified Lüscher equation approach as well, although this K-matrix is directly related to the physical K-matrix via algebraic equations. Hence, the approach detailed in this thesis resembles the original Lüscher equation much closely and is a single-step formalism.

CHAPTER 3

Non-Relativistic Field Theory Approach in a Finite Volume

The aim of this chapter is to introduce the basic concepts of non-relativistic effective field theories, which are used throughout this thesis.

In the case, where the masses of particles are larger than the typical three-momenta, using a non-relativistic description proves to be advantageous. This is because the relativistic description contains a built-in hard scale which is equal to twice the particle mass (mass gap between particles and antiparticles). This hard scale leads to the violation of the power-counting rules in the small momenta. However, in the non-relativistic case, antiparticles are integrated out leaving behind only particles and conservation of particle number. This simplifies things drastically and revives the counting rules. Moreover, if one considers a process where it is reasonable to assume that particle-antiparticle creation and annihilation do not play a dominant role, then even if the three-momenta is of the order of the particle masses, the antiparticles can be integrated out. An example of such a situation is the kaon decay into three pions. It is reasonable to assume here that more than three pion intermediate states will not play a major part in the decay amplitude[1]. Hence, even though the final-state pion momenta are not very small compared to their masses, a non-relativistic description can be applied.

Using NREFTs in finite volume is beneficial as well. The two-body quantization condition can be derived with significant less effort in a NREFT framework. The reason for this is as follows, the irregular behavior in L, which is described by the Lüscher zeta-function, originates in s-channel bubble diagrams. In the NREFT framework the two-body scattering amplitude is given entirely by a tower of s-channel bubbles and hence in a finite volume reproduces the irregular L behavior correctly. Moreover, in the original Lüscher approach, the diagrams which involve creation and annihilation of particles and antiparticles lead to exponentially suppressed corrections whereas in the NREFT approach, these regular contributions are implicitly present in the LECs.

3.1 Non-Relativistic Effective Field Theories

In a NREFT the relevant degree of freedom are only the particle fields. One can start from a relativistic theory and use field transformation such as the Foldy-Wouthuysen transformation [203] to separate

[1] The kaon mass lies sufficiently below the five pion threshold.

the particle and antiparticle fields and then integrate out the antiparticle fields from the theory leaving behind the relevant particle fields. However, this process can be cumbersome and complicated. Rather, one can directly write down the most general non-relativistic Lagrangian involving all possible particle operators that obey the symmetries of the underlying theory. The fields showing up in this non-relativistic Lagrangian will contain either creation operators or annihilation operators. The couplings that show up in this Lagrangian, the so called LECs, can then be determined by *matching* to physical observables. The process of matching of a LEC involves calculation of an observable in the NREFT framework up to a relevant order in a given power counting scheme and then expressing the LEC in terms of the same observable calculated in the underlying theory. A suitable power counting scheme in a non-relativistic setup is provided by an expansion in powers of $|\mathbf{p}|/M = O(p)$, where M is the mass and $\mathbf{p}$ is the three-momenta of the particle. Moreover, regarding the time component, the quantity $p^0 - M$ is counted as $O(p^2)$.

The NREFT Lagrangian for a scalar particle of mass M which describes interaction between even number of particles in the final and initial state at the lowest order [103], is given by

$$\mathcal{L}_{\text{NREFT}} = \phi^\dagger \Big(i\partial_t - M + \frac{\nabla^2}{2M} + \dots \Big) \phi + \mathcal{L}_2 + \mathcal{L}_3 + \dots \,, \tag{3.1}$$

where $\mathcal{L}_2$ and $\mathcal{L}_3$ represent the Lagrangian in the two-body and three-body sector respectively, the ellipsis represents operators with higher number of fields and their derivatives and ϕ denotes a non-relativistic field that annihilates a particle given by

$$\phi(x) = \int \frac{d^3\mathbf{k}}{(2\pi)^3} a(\mathbf{k}) e^{-ikx} \,, \quad k^0 = M + \frac{k^2}{2M} \,. \tag{3.2}$$

Note that this Lagrangian is symmetric under the transformation $\phi \longrightarrow -\phi$. As stated above, the fields will either contain a creation operator or annihilation operator, hence the field ϕ is not hermitian. Moreover, since all operators contain equal number of ϕ and $\phi^\dagger$ fields, particle number is conserved.

Further, $\mathcal{L}_i$ with $i = 2, 3, \dots$ are defined as follows,

$$\mathcal{L}_i = \mathcal{L}_i^{(0)} + \mathcal{L}_i^{(2)} + \dots \,, \tag{3.3}$$

where the superscript represents the number of derivatives present in the operator (or the order of the operator in the power counting scheme). In the case of two-body and three-body sector,

$$\mathcal{L}_2^{(0)} = C_0 \phi^\dagger \phi^\dagger \phi \phi \,, \quad \mathcal{L}_3^{(0)} = D_0 \phi^\dagger \phi^\dagger \phi^\dagger \phi \phi \phi \,. \tag{3.4}$$

As mentioned above the LECs C_0 and D_0 are determined by matching to physical observables. However the coupling that comes with the term $\nabla^2/2M$ is fixed by *reparametrization invariance* [117, 204] and is equal to 1. This results from Lorentz-invariant nature of the underlying theory and leads to order by order recovery of relativistic dispersion law.

The non-relativistic propagator is given by

$$i\langle 0|T\phi(x)\phi^\dagger(y)|0\rangle = \int \frac{d^4k}{(2\pi)^4} \frac{e^{-ik(x-y)}}{M + \frac{\mathbf{k}^2}{2M} - k^0 - i\epsilon} \,. \tag{3.5}$$

This propagator has only one pole in the lower half of the complex k^0-plane. Hence, it vanishes for all $x^0 < y^0$, since there are no poles in the upper half of the complex k^0-plane. This results in vanishing contributions from all diagrams involving particles propagating backward in time. Furthermore, closed single-particle loops that arise when $x = y$ also vanishes. This can be seen by first performing the k^0 integral which results in a factor of $i\pi$, after which the remaining integral vanishes in dimensional regularization. These vanishing diagrams leads to a useful result in NREFT, which is, in the absence of relativistic corrections, the form of the propagator remains unchanged to all orders in perturbation theory. The form of the propagator will change only with the inclusion of relativistic corrections as the pole position will change, which is given by

$$k^0 = \sqrt{\mathbf{k}^2 + M^2} = M + \frac{\mathbf{k}^2}{2M} - \frac{\mathbf{k}^4}{8M^3} + \dots . \tag{3.6}$$

By the same arguments as above, diagrams with more loops vanish as well. An important consequence of this is that processes involving low number of particles are not contaminated by higher particle sectors. Hence, even though the ellipses in the Lagrangian in Eq. (3.1) denote an infinite tower of operators at leading order, only finite number of terms contribute explicitly to a particular process at a given order.

To construct the two-particle Lagrangian at $O(p^2)$, one can consider the momentum space scattering amplitude for the most general process $\phi(p_1) + \phi(p_2) \to \phi(q_1) + \phi(q_2)$ at the same order. This is justified as the scattering amplitude is the matrix element of the Lagrangian between free states at tree level. In the non-relativistic setup, in addition to conservation of total three-momenta $\mathbf{P} = \mathbf{p}_1 + \mathbf{p}_2 = \mathbf{q}_1 + \mathbf{q}_2$, Lorentz symmetry reduces to rotational symmetry which leads to six invariant quantities on which the two-particle scattering amplitude at $O(p^2)$ can depend on. These are given as follows:

$$\mathbf{p}^2\,,\ \mathbf{q}^2\,,\ \mathbf{P}^2\,,\ \mathbf{pP}\,,\ \mathbf{qP}\,,\ \mathbf{pq}\,, \tag{3.7}$$

with relative momentum of in-coming and out-going states defined as $\mathbf{p} = (\mathbf{p}_1 - \mathbf{p}_2)/2$ and $\mathbf{q} = (\mathbf{q}_1 - \mathbf{q}_2)/2$. The operators corresponding to $\mathbf{pP}$, $\mathbf{qP}$ and $\mathbf{pq}$ do not show up in the Lagrangian for identical particles due to Bose symmetry. This can be easily seen by considering the transformation $k_1 \leftrightarrow k_2$ for $k = p$ or q. The three independent three-momenta transform as $\mathbf{k} \to -\mathbf{k}$ and $\mathbf{P} \to \mathbf{P}$, which renders the last three combination in Eq. (3.7) odd under this transformation. Moreover, hermiticity requires the operators to be symmetric under the replacement $\mathbf{p} \leftrightarrow \mathbf{q}$. Hence the relevant Lagrangian at this order is given by

$$\mathcal{L}_2^{(2)} = C_1\Big((\phi^\dagger \overleftrightarrow{\nabla}^2 \phi^\dagger)(\phi\phi) + \text{h.c.}\Big) + C_2\Big((\phi^\dagger\phi^\dagger)\nabla^2(\phi\phi) + \text{h.c.}\Big)\,, \tag{3.8}$$

where the Galilean invariant derivative is given by $\overleftrightarrow{\nabla} = (\overrightarrow{\nabla} - \overleftarrow{\nabla})/2$. The arrows on top of ∇ indicates the direction in which the derivative acts. Higher order operators can be constructed in a similar manner.

An important remark is in order, the number of terms appearing in the Lagrangian can often be reduced by utilizing Equation of Motion (EOM). To see this one can consider the off-shell term that appears at $O(p^4)$ and is given by

$$O^{(4)}_{\text{off-shell}} = (\phi^\dagger \overleftrightarrow{\nabla}^4 \phi^\dagger)(\phi\phi) - (\phi^\dagger \overleftrightarrow{\nabla}^2 \phi^\dagger)(\phi \overleftrightarrow{\nabla}^2 \phi) + \text{h.c.} \tag{3.9}$$

This operator takes the following form in momentum space,

$$(\mathbf{p}^2 - \mathbf{q}^2)^2 \,, \tag{3.10}$$

which clearly vanishes when the momentum are taken on-shell, as $\mathbf{p}^2 = \mathbf{q}^2 = M\Big(P^0 - 2M - \mathbf{P}^2/(4M)\Big)$. Now, using EOM for the scalar fields,

$$\nabla^2\phi^\dagger = 2M(i\partial_t + M)\phi^\dagger \,, \quad \nabla^2\phi = -2M(i\partial_t - M)\phi \,, \tag{3.11}$$

the off-shell term in Eq. (3.9) can be reduced to a total derivative

$$O^{(4)}_{\text{off-shell}} = M^2(i\partial_t)^2(\phi^\dagger\phi^\dagger\phi\phi) \,, \tag{3.12}$$

and hence can be neglected.

3.2 Two-Body Sector

3.2.1 Matching in the Two-Body Sector

After writing down the Lagrangian, one has to determine the couplings that appear in different terms. As mentioned above this is done by matching physical observables in the NREFT and underlying theory. In the following section, matching is carried out in the two-particle sector. To this end the process $\phi(p_1) + \phi(p_2) \to \phi(q_1) + \phi(q_2)$ is considered.

In the two-body sector, the NREFT Lagrangian involves the following terms

$$\mathcal{L}_{\text{NREFT}} = \phi^\dagger\Big(i\partial_t - M + \frac{\nabla^2}{2M} + \frac{\nabla^4}{8M^3} + \dots\Big)\phi + \mathcal{L}_2 \,. \tag{3.13}$$

To determine the LECs, one can calculate the on-shell two-particle scattering amplitude in the NREFT and compare it to the same quantity calculated in the underlying relativistic theory (RT). This *matching condition* is given by

$$T_{\text{NREFT}}(\mathbf{p}_1, \mathbf{p}_2; \mathbf{q}_1, \mathbf{q}_2) = \prod_{i=1}^{2} \frac{T_{\text{RT}}(\mathbf{p}_1, \mathbf{p}_2; \mathbf{q}_1, \mathbf{q}_2)}{(2w(\mathbf{p}_i)2w(\mathbf{q}_i))^{\frac{1}{2}}} \,, \tag{3.14}$$

where T_{NREFT} and T_{RT} represent the NREFT and RT scattering amplitude respectively and $w(\mathbf{k}) = \sqrt{M^2 + \mathbf{k}^2}$. The different normalization of the one-particle states in relativistic and non-relativistic theory leads to the kinematic factors showing up in Eq. (3.14),

$$\begin{aligned} &\text{relativistic:} && \langle \mathbf{p}|\mathbf{q}\rangle = (2\pi)^3 2w(\mathbf{p})\delta^3(\mathbf{p} - \mathbf{q}) \,, \\ &\text{non-relativistic:} && \langle \mathbf{p}|\mathbf{q}\rangle = (2\pi)^3\delta^3(\mathbf{p} - \mathbf{q}) \,. \end{aligned} \tag{3.15}$$

After expanding both sides of Eq. (3.14) in series of three-momenta, the LECs appearing in T_{NREFT} are adjusted such that the matching condition is satisfied up to a given order[2]. This method allows

[2] Only the polynomial part has to be matched explicitly, the non-polynomial part turns out to be the same in both the

one to systematically include relativistic effects order by order. Although this inclusion is possible even at higher orders, the expressions become cumbersome and difficult to cast into an explicitly Lorentz-invariant form. To avoid such complications one can make slight modification to the NREFT framework to restore explicit Lorentz-covariance in the two-body sector [179, 205, 206].

To obtain an explicitly Lorentz-invariant form of the matching condition, following two steps are taken. First, the relativistic insertions in the internal lines are summed up to all orders. This leads to the hard scale M showing up in the propagator which leads to break down of the counting rules. Restoring the power counting rules boils down to adopting an additional renormalization prescription which will be discussed in a later paragraph. Second, the non-relativistic field ϕ is rescaled in order to deal away with difference of normalization of the one-particle states in the two theories[3]. The rescaling is defined as follows:

$$\phi(x) \to (2w)^{\frac{1}{2}}\phi(x)\,, \quad \text{with } w = \sqrt{M^2 - \nabla^2}\,, \tag{3.16}$$

with which the Lorentz-invariant matching condition can be written as

$$T_{\text{NREFT}}(\mathbf{p}_1, \mathbf{p}_2; \mathbf{q}_1, \mathbf{q}_2) = T_{\text{RT}}(\mathbf{p}_1, \mathbf{p}_2; \mathbf{q}_1, \mathbf{q}_2)\,. \tag{3.17}$$

Finally, summing up relativistic insertion to all orders leads to the following two-body Lagrangian

$$\mathcal{L}_{\text{NREFT}} = \phi^\dagger 2w(i\partial_t - w)\phi + \mathcal{L}_2^{(0)} + \mathcal{L}_2^{(2)} \ldots\,, \tag{3.18}$$

where

$$\mathcal{L}_2^{(0)} = C_0\phi^\dagger\phi^\dagger\phi\phi\,, \qquad \mathcal{L}_2^{(2)} = C_2\Big((w^\mu\phi)^\dagger(w_\mu\phi)^\dagger\phi\phi - M^2\phi^\dagger\phi^\dagger(\phi\phi) + \text{h.c.}\Big)\,, \tag{3.19}$$

with $w^\mu = (w, i\nabla)$ and the ellipses denote higher order terms.

As stated above, the explicit appearance of M in the propagator leads to breakdown of the power counting scheme. To restore the counting rules additional prescription has to be imposed. In the following, *threshold expansion* [211] is discussed with the example of the two-body loop integral in an arbitrary frame with CM four-momentum given by P^μ.

Consider the loop function

$$\begin{aligned} I(P) &= \int \frac{d^D k}{(2\pi)^D i} \frac{1}{4w(\mathbf{k})w(\mathbf{P}-\mathbf{k})(w(\mathbf{k}) - k^0 - i\epsilon)(w(\mathbf{P}-\mathbf{k}) - P^0 + k^0 - i\epsilon)} \\ &= \int \frac{d^d k}{(2\pi)^d} \frac{1}{4w(\mathbf{k})w(\mathbf{P}-\mathbf{k})(w(\mathbf{k}) + w(\mathbf{P}-\mathbf{k}) - P^0 - i\epsilon)}\,, \end{aligned} \tag{3.20}$$

where $d = D - 1$ and $P^0 = w(\mathbf{p}_1) + w(\mathbf{p}_2)$. The $i\epsilon$ prescription will be considered implicitly in the rest of the discussion to ease the notation. In threshold expansion, the integrand above is Taylor expanded in inverse powers of M and then the integral is performed in dimensional regularization after which the result is summed up to all orders. A useful identity needed to perform the above mentioned

theories in vicinity of the elastic threshold at a given order.

[3] the equivalence of S-matrix elements in the original theory and the rescaled field theory is ensured by the equivalence theorem [207–210].

procedure is

$$\frac{1}{2w^+2w^-}\left\{\frac{1}{w^+ + w^- - P^0} - \frac{1}{w^+ + w^- + P^0} + \frac{1}{w^+ - w^- + P^0} - \frac{1}{w^+ - w^- - P^0}\right\} = \frac{1}{2P^0\left(\mathbf{k}^2 - \left(\frac{\mathbf{kP}}{P^0}\right)^2 - (q^*)^2\right)}, \tag{3.21}$$

where $(q^*)^2 = s/4 - M^2$ with $s = (P^0)^2 - \mathbf{P}^2$ and $w^\pm = w(\mathbf{P}/2 \pm \mathbf{k})$. Only terms containing polynomial in momenta are left if the last three terms in the above identity are expanded in inverse powers of M. These terms can be added and subtracted in Eq. (3.20) after rescaling the integration momenta by $\mathbf{k} \to \mathbf{k} + \mathbf{P}/2$ to obtain the following form of the loop function:

$$I(P) = \int \frac{d^d k}{(2\pi)^d} \frac{1}{2P^0\left(\mathbf{k}^2 - \left(\frac{\mathbf{kP}}{P^0}\right)^2 - (q^*)^2\right)}, \tag{3.22}$$

which clearly does not have any explicit M dependence. The remaining integral can be evaluated by splitting the integration momentum $\mathbf{k}$ into perpendicular and parallel components with respect to $\mathbf{P}$ as follows:

$$\mathbf{k} = \frac{\mathbf{P}}{|\mathbf{P}|} k_\parallel + \mathbf{k}_\perp\,, \quad k_\parallel = \frac{\mathbf{kP}}{|\mathbf{P}|}\,, \tag{3.23}$$

with which one gets

$$I(p) = \frac{iq^*}{8\pi\sqrt{s}}\,. \tag{3.24}$$

The expression above is clearly Lorentz-invariant and is equal to the imaginary part of its counterpart in the relativistic theory. Further more, it is important to note that the replacement $(w^+ + w^- - P^0 - i\epsilon)^{-1} \to i\pi\delta(w^+ + w^- - P^0)$ is justified as only the absorptive part of the integral survives. Lastly, since the scattering amplitude in the two-body sector is entirely given by s-channel bubble diagrams described by $I(p)$, the calculation of T_{NREFT} in threshold expansion simplifies considerably.

The potential V in this case is defined through the interaction Hamiltonian H_I as follows:

$$\langle \mathbf{p}_1, \mathbf{p}_2 | H_I | \mathbf{q}_1, \mathbf{q}_2 \rangle = -(2\pi)^d \delta^d(\mathbf{p}_1 + \mathbf{p}_2 - \mathbf{q}_1 - \mathbf{q}_2) V(\mathbf{p}_1, \mathbf{p}_2; \mathbf{q}_1, \mathbf{q}_2)\,. \tag{3.25}$$

For example, the potential associated with the term $\mathcal{L}_2^{(0)} + \mathcal{L}_2^{(2)}$ is given by

$$V(\mathbf{p}_1, \mathbf{p}_2; \mathbf{q}_1, \mathbf{q}_2) = 4C_0 + 4C_2\Big((p_1.p_2) + (q_1.q_2) - 2M^2\Big)\,, \tag{3.26}$$

where p_i and q_j represent the on-shell four-momenta. An important point to note is that the potential is always given by a Lorentz-invariant polynomial as can be seen in the example above.

With the potential defined, the Lippmann-Schwinger equation for the T-matrix, depicted in Fig.

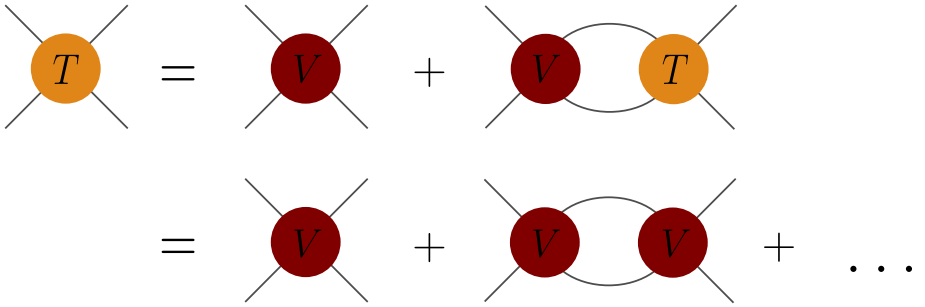

Figure 3.1: Schematic representation of the Lippmann-Schwinger equation in the NREFT with T representing the two-particle scattering amplitude and V denoting the potential corresponding to the interaction. The second line shows the Born series of the amplitude.

3.1, can be written as follows[4]:

$$T(\mathbf{p}_1,\mathbf{p}_2;\mathbf{q}_1,\mathbf{q}_2) = V(\mathbf{p}_1,\mathbf{p}_2;\mathbf{q}_1,\mathbf{q}_2) + \frac{1}{2}\int \frac{d^d k_1}{(2\pi)^d 2w(\mathbf{k}_1)}\frac{d^d k_2}{(2\pi)^d 2w(\mathbf{k}_2)} V(\mathbf{p}_1,\mathbf{p}_2;\mathbf{k}_1,\mathbf{k}_2) \times \frac{(2\pi)^d\delta^d(\mathbf{p}_1+\mathbf{p}_2-\mathbf{k}_1-\mathbf{k}_2)}{w(\mathbf{k}_1)+w(\mathbf{k}_2)-P^0} T(\mathbf{k}_1,\mathbf{k}_2;\mathbf{q}_1,\mathbf{q}_2)\,. \tag{3.27}$$

Moreover, the CM four-momentum is defined as $P = p_1 + p_2 = q_1 + q_2$ and relative four momenta are defined as $p = (p_1 - p_2)/2$ and $q = (q_1 - q_2)/2$ with which the potential can be expanded in partial-wave in the rest frame as follows:

$$V(\mathbf{p}_1,\mathbf{p}_2;\mathbf{q}_1,\mathbf{q}_2) = 4\pi \sum_{lm} \mathcal{Y}_{lm}(\mathbf{p}^*) V_l(|\mathbf{p}^*|,|\mathbf{q}^*|) \mathcal{Y}^*_{lm}(\mathbf{q}^*)\,, \tag{3.28}$$

where $\mathbf{p}^*$ and $\mathbf{q}^*$ are the relative three-momenta boosted to the rest frame which are defined as follows:

$$\begin{aligned}\mathbf{p}^* &= \mathbf{p} + \mathbf{P}\left((\gamma-1)\frac{\mathbf{pP}}{\mathbf{P}^2} - \gamma v \frac{p^0}{|\mathbf{P}|}\right),\\ \mathbf{q}^* &= \mathbf{q} + \mathbf{P}\left((\gamma-1)\frac{\mathbf{qP}}{\mathbf{P}^2} - \gamma v \frac{q^0}{|\mathbf{P}|}\right).\end{aligned} \tag{3.29}$$

Here, $\gamma = (1-v^2)^{-1/2}$ and $v = |\mathbf{P}|/P^0$. $\mathcal{Y}_{lm}(\mathbf{p}) = |\mathbf{p}|^l Y_{lm}(\hat{\mathbf{p}})$ denotes the solid harmonics with $Y_{lm}(\hat{\mathbf{p}})$ being the regular spherical harmonic function. Similarly the T-matrix can be expanded in partial-wave as

$$T(\mathbf{p}_1,\mathbf{p}_2;\mathbf{q}_1,\mathbf{q}_2) = 4\pi \sum_{lm} \mathcal{Y}_{lm}(\mathbf{p}^*) T_l(|\mathbf{p}^*|,|\mathbf{q}^*|) \mathcal{Y}^*_{lm}(\mathbf{q}^*)\,. \tag{3.30}$$

Defining the relative three-momentum $\mathbf{k} = (\mathbf{k}_1 - \mathbf{k}_2)/2$, the relative three-momentum boosted to the rest frame is defined as $\mathbf{k}^*$. With this the partial-wave projected Lippmann-Schwinger equation can be

[4] The NREFT label of the T-matrix is suppressed for notational convenience

written as

$$T_l(|\mathbf{p}^*|,|\mathbf{q}^*|) = V_l(|\mathbf{p}^*|,|\mathbf{q}^*|) + 2\pi \int \frac{d^d k_1}{(2\pi)^d 2w(\mathbf{k}_1)} \frac{d^d k_2}{(2\pi)^d 2w(\mathbf{k}_2)} \mathcal{Y}_{lm}(\mathbf{k}^*) V_l(|\mathbf{p}^*|,|\mathbf{k}^*|) \times \frac{(2\pi)^d \delta^d(\mathbf{p}_1+\mathbf{p}_2-\mathbf{k}_1-\mathbf{k}_2)}{w(\mathbf{k}_1)+w(\mathbf{k}_2)-P^0} \mathcal{Y}^*_{lm}(\mathbf{k}^*) T_l(|\mathbf{k}^*|,|\mathbf{q}^*|)\,. \tag{3.31}$$

Now, the replacement

$$\frac{\delta^d(\mathbf{p}_1+\mathbf{p}_2-\mathbf{k}_1-\mathbf{k}_2)}{w(\mathbf{k}_1)+w(\mathbf{k}_2)-P^0-i\epsilon} \to i\pi\delta^D(P-k_1-k_2) = i\pi\delta^D(P^*-k_1^*-k_2^*)\,, \tag{3.32}$$

can be made, as only the absorptive part contributes in dimensional regularization. Further simplification in the CM frame results in Eq. (3.31) being written as

$$T_l(|\mathbf{p}^*|,|\mathbf{q}^*|) = V_l(|\mathbf{p}^*|,|\mathbf{q}^*|) + \frac{i(q^*)^{2l+1}}{16\pi\sqrt{s}} V_l(|\mathbf{p}^*|,q^*) T_l(q^*,|\mathbf{q}^*|)\,. \tag{3.33}$$

Here, $s = (P^*)^2 = P^2$ and $(q^*)^2 = s/4 - M^2$. Therefore, the on-shell two-body T-matrix for a particular partial-wave l is given by

$$T_l(q^*,q^*) = T_l(s) = \frac{16\pi\sqrt{s}(q^*)^{-2l}}{16\pi\sqrt{s}(q^*)^{-2l} V_l^{-1}(s) - iq^*}\,, \tag{3.34}$$

where $V_l(s) = V_l(q^*,q^*)$. Note on the mass shell $q^* = |\mathbf{p}^*| = |\mathbf{q}^*|$. The LECs can then be fixed by matching this amplitude to its relativistic counterpart in the underlying theory. The relativistic K-matrix can be defined via the T-matrix and is related to the phase shift via unitarity,

$$K(\mathbf{p}_1,\mathbf{p}_2;\mathbf{q}_1,\mathbf{q}_2) = 4\pi \sum_{lm} \mathcal{Y}_{lm}(\mathbf{p}^*) K_l(|\mathbf{p}^*|,|\mathbf{q}^*|) \mathcal{Y}^*_{lm}(\mathbf{q}^*)\,,$$
$$K_l(q^*,q^*) = K_l(s) = \frac{16\pi\sqrt{s}}{(q^*)^{2l+1}\cot\delta_l(s)}\,. \tag{3.35}$$

The matching condition turns out to be

$$V_l(s) = K_l(s)\,. \tag{3.36}$$

The effective-range expansion can be used in the vicinity of the elastic threshold, i.e. $s = 4M^2$ where the NREFT is applicable, in order to match the LECs appearing in $V_l(s)$ to the scattering parameters of the underlying relativistic theory. This matching is straightforward to perform as both left-hand and right-hand side are polynomials in the variable $(q^*)^2$. In the case of s-wave,

$$V_l(s) = 4C_0 + 16C_2(q^*)^2 + \ldots\,,$$
$$K_l(s) = 32\pi a_0 M + 16\pi a_0^2 M\left(\frac{1}{a_0 M^2} + r_0\right)(q^*)^2 + \ldots\,, \tag{3.37}$$

the matching condition leads to

$$C_0 = 8\pi a_0 M\,,\quad C_2 = \pi a_0^2 M\left(\frac{1}{a_0 M^2} + r_0\right). \tag{3.38}$$

The advantage of the covariant NREFT formulation can be seen if one considers the matching condition in both covariant and original[5] formulations:

$$\begin{aligned} &\text{Covariant:} && K(\mathbf{p}_1,\mathbf{p}_2;\mathbf{q}_1,\mathbf{q}_2) = V(\mathbf{p}_1,\mathbf{p}_2;\mathbf{q}_1,\mathbf{q}_2)\,,\\ &\text{Original:} && K(\mathbf{p}_1,\mathbf{p}_2;\mathbf{q}_1,\mathbf{q}_2) = \prod_{i=1}^{2}(2w(\mathbf{p}_i)2w(\mathbf{q}_i))^{\frac{1}{2}} V_{\text{NREFT}}(\mathbf{p}_1,\mathbf{p}_2;\mathbf{q}_1,\mathbf{q}_2)\,. \end{aligned} \tag{3.39}$$

In the covariant formulation both K and V are polynomials in Lorentz-invariant quantities $(p.q)$ and s. Therefore, the LECs present in V and the scattering parameters appearing in K can be straightforwardly related to each other. However, in the original formulation things are a bit different. The kinematic factor, which appears due to a difference of normalization in relativistic and non-relativistic theory, results in the right hand side of the original formulation being a polynomial built from variables mentioned in Eq. (3.7) respecting the symmetries of the theory. This leads to superfluous couplings appearing in the theory which obey certain conditions. Hence, the covariant formulation automatically eliminates the redundant couplings due to explicit Lorentz invariance.

The covariant formulation also offers advantages in a finite volume. In addition to eliminating redundant couplings increasing the quality of the fit to the lattice energy spectrum, it also enables one to write down a quantization condition that is valid in an arbitrary moving frame. Moving frames, in general, cannot be treated in a non-covariant framework due to lack of explicit Lorentz invariance.

3.2.2 Lüscher Equation in the NREFT Formalism

As stated in the introduction, EFTs such as NREFT are an important tool for analysis of Lattice data. The LECs that appear in the Lagrangian of NREFT can be determined by performing a fit to the lattice energy spectra. With the LECs determined, infinite-volume observables can then be directly calculated using the NREFT Lagrangian. Hence, NREFT (and EFTs in general) bridge the gap between lattice data and physical observables. Moreover, NREFT offers a simplified approach for deriving the Lüscher equation as mentioned previously. Below the two-particle quantization condition is derived using the covariant formulation of NREFT and closely follows the derivation detailed in [48, 103].

Before proceeding to the derivation of the Lüscher equation, an important remark is in order. For EFTs to be applicable, the lattice needs to fulfill certain criteria. For an Euclidean lattice with lattice spacing a, spacial elongation L and temporal elongation L_T, obeying periodic boundary condition, the following should be satisfied

$$\frac{1}{L} \ll \Lambda \ll \frac{1}{a}\,, \tag{3.40}$$

where Λ represents the relevant hard scale. Since $1/L \ll \Lambda$, the same EFT is valid in both finite and infinite volume. This implies that the LECs which are determined by short-range physics, receive

[5] The matching condition in the original NREFT formulation can be derived following the same steps mentioned above.

exponentially suppressed contribution in $1/L$. Hence, finite-volume power-law suppressed effects can be studied without being contaminated by other lattice effects. With this condition being satisfied, EFTs can be effectively used to perform analyses on lattice data.

In a finite volume, rotational symmetry is broken which leads to different partial-waves mixing. Therefore, the partial-wave expansion of the finite-volume T-matrix[6], denoted by T^{fin}, is given by

$$T^{\text{fin}}(\mathbf{p}_1, \mathbf{p}_2; \mathbf{q}_1, \mathbf{q}_2) = 4\pi \sum_{lm,l'm'} \mathcal{Y}_{lm}(\mathbf{p}^*) T_{lm,l'm'}(|\mathbf{p}^*|, |\mathbf{q}^*|; \mathbf{P}) \mathcal{Y}^*_{l'm'}(\mathbf{q}^*) \,. \tag{3.41}$$

Here, the superscript is dropped on the projected T-matrix on the right-hand side for notational convenience. Moreover, definition of the potential V remains same in both the finite and infinite volume as it is purely determined by the EFT Lagrangian up to exponentially suppressed terms. Thus, Eq. (3.28) remains valid.

The on-shell Lippmann-Schwinger equation in finite volume[7], is then given by

$$T_{lm,l'm'}(s; \mathbf{P}) = \delta_{ll'}\delta_{mm'} V_l(s) + 4\pi \sum_{l''m''} V_l(s) H_{lm,l''m''}(s; \mathbf{P}) T_{lm,l'm'}(s; \mathbf{P}) \,, \tag{3.42}$$

where

$$H_{lm,l'm'}(s; \mathbf{P}) = \frac{1}{L^3} \sum_{\mathbf{k}_1 = 2\pi/L\mathbf{n}} \frac{\mathcal{Y}^*_{lm}(\mathbf{k}^*) \mathcal{Y}_{l'm'}(\mathbf{k}^*)}{2w(\mathbf{k}_1) 2w(\mathbf{P} - \mathbf{k}_1)(w(\mathbf{k}_1) + w(\mathbf{P} - \mathbf{k}_1) - P^0)} \,, \tag{3.43}$$

with $\mathbf{k}^*$ being the relative three-momentum boosted to the CM frame. Moreover, perpendicular and parallel components of $\mathbf{k}^*$ can be defined with respect to $\mathbf{P}$ as follows:

$$\mathbf{k}^* = (\gamma^{-1} k_{\parallel}, \mathbf{k}_{\perp}) \,, \quad \gamma = (1 - \nu^2)^{-\frac{1}{2}} \,. \tag{3.44}$$

Here, $\nu = |\mathbf{P}|/P^0$ on the mass shell and $k_{\parallel}$ and $\mathbf{k}_{\perp}$ are defined in Eq. (3.23). Using the identity,

$$\mathcal{Y}^*_{lm}(\mathbf{k}^*) \mathcal{Y}_{l'm'}(\mathbf{k}^*) = \frac{1}{\sqrt{4\pi}} \sum_{j=|l-l'|}^{l+l'} \sum_{s=-j}^{j} i^{j-l-l'} |\mathbf{k}^*|^{l+l'-j} C_{lm,js,l'm'} \mathcal{Y}^*_{js}(\mathbf{k}^*) \,, \tag{3.45}$$

the identity in Eq. (3.21) and the above mentioned definition of momentum with $\mathbf{k}^* \equiv \mathbf{r}$, $H_{lm,l'm'}(s; \mathbf{P})$ can be rewritten as

$$H_{lm,l'm'}(s; \mathbf{P}) = \frac{(q^*)^{l+l'+1} i^{l-l'}}{32\pi^2 \sqrt{s}} \mathcal{M}_{lm,l'm'}(s; \mathbf{P}) \,, \tag{3.46}$$

[6] Note that since asymptotic states are not defined in a finite volume, a formal definition of T-matrix does not exist in this case. However, an equivalent scattering amplitude T^{fin} which obeys the finite-volume version of the Lippmann-Schwinger equation can be defined by calculating the relevant LQCD correlation function in the EFT framework.

[7] In the finite-volume, integrals are replaced with pertinent summations.

with

$$\mathscr{M}_{lm,l'm'}(s,\mathbf{P}) = \frac{(-1)^l}{\pi^{3/2}\gamma}\sum_{j=|l-l'|}^{l+l'}\sum_{s=-j}^{j}\frac{i^j}{\eta^{j+1}}C_{lm,js,l'm'}\frac{i^j}{\eta^{j+1}}Z^{\mathbf{d}}_{js}(1;s)\,,$$
$$C_{lm,js,l'm'} = (-1)^{m'}i^{l-j+l'}\sqrt{(2l+1)(2j+1)(2l'+1)}\begin{pmatrix} l & j & l' \\ m & s & m' \end{pmatrix}\begin{pmatrix} l & j & l' \\ 0 & 0 & 0 \end{pmatrix}, \tag{3.47}$$

with $Z^{\mathbf{d}}_{js}(1;s)$ representing the Lüscher zeta-function defined as follows:

$$Z^{\mathbf{d}}_{lm}(1;s) = \sum_{\mathbf{r}\in P_{\mathbf{d}}}\frac{\mathcal{Y}_{lm}(\mathbf{r})}{r^2-\eta^2}\,,$$
$$P_{\mathbf{d}} = \left\{\mathbf{r}\in\mathbb{R}^3\middle| r_{\parallel} = \gamma^{-1}(n_{\parallel}-\frac{|\mathbf{d}|}{2})\,,\mathbf{r}_{\perp} = \mathbf{n}_{\perp}\,,\mathbf{n}\in\mathbb{Z}^3\right\}, \tag{3.48}$$

with $\mathbf{d} = \mathbf{P}L/(2\pi)$ and $\eta = q^*L/(2\pi)$. Using the fact that the potential can be expressed in terms of the infinite-volume phase shift and the poles of $T_{lm,l'm'}(s;\mathbf{P})$ corresponds to the finite-volume energy levels, the two-particle quantization condition can be written as

$$\det\mathscr{A} = 0\,,$$
$$\mathscr{A}_{lm,l'm'} = \delta_{ll'}\delta_{mm'}\cot\delta_l(s) - \mathscr{M}_{lm,l'm'}(s,\mathbf{P})\,. \tag{3.49}$$

Note that this expression is valid for arbitrary moving frame.

The above mentioned derivation clearly shows the convenience of using the covariant NREFT approach and its suitability for application to more complicated processes (see for e.g. [48]). In the next section, the three-body sector will be discussed within the NREFT framework.

3.3 Three-Body Sector

3.3.1 Matching in the Three-Body Sector

The matching condition in the case of the three-body sector can be written analogous to the two-body sector

$$T^{(3)}_{\text{NREFT}}(\mathbf{p}_1,\mathbf{p}_2,\mathbf{p}_3;\mathbf{q}_1,\mathbf{q}_2,\mathbf{q}_3) = \prod_{i=1}^{3}\frac{T^{(3)}_{\text{RT}}(\mathbf{p}_1,\mathbf{p}_2,\mathbf{p}_3;\mathbf{q}_1,\mathbf{q}_2,\mathbf{q}_3)}{(2w(\mathbf{p}_i)2w(\mathbf{q}_i))^{\frac{1}{2}}}\,. \tag{3.50}$$

Note that unlike the two-particle case, it is not straightforward to separate out the polynomial and non-polynomial contribution. Moreover, the three-body sector has more sources of non-polynomial contribution unlike the two-body sector where such terms only arise in bubble diagrams. In the following matching will be carried out in the original NREFT formulation, hence relativistic corrections need to be included at relevant order. Lastly, to make the notation less cumbersome and easily differentiate between the non-relativistic and relativistic amplitude, the definition $T^{(3)}_{\text{NREFT}} \equiv T_3$ and $T^{(3)}_{\text{RT}} \equiv \mathcal{M}_3$ will be used.

Since the definition of the regular part of the three-particle scattering amplitude at threshold is ambiguous, a consistent definition is needed. A simple and effective prescription in the three-body

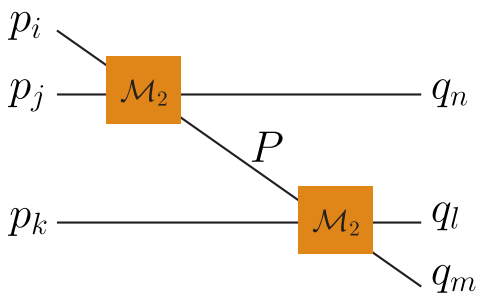

Figure 3.2: Most singular contribution to the three-particle revivalistic amplitude $\mathcal{M}_3^{\text{1PI}}$. The orange square represents the two-particle relativistic amplitude $\mathcal{M}_2$.

sector was laid out in Ref. [97] based on the on-shell amplitudes only. The rest of this section will follow this prescription closely.

One starts by considering the most singular piece of the scattering amplitude in the relativistic case, which is given by the sum of all one-particle reducible diagrams,

$$\mathcal{M}_3^{\text{1PI}}(\mathbf{p}_1,\mathbf{p}_2,\mathbf{p}_3;\mathbf{q}_1,\mathbf{q}_2,\mathbf{q}_3) = \sum_{\text{perm}(ijk)} \sum_{\text{perm}(lmn)} \frac{\mathcal{M}_2(\mathbf{p}_i,\mathbf{p}_j;\mathbf{q}_n,\mathbf{P})\mathcal{M}_2(\mathbf{p}_k,\mathbf{P};\mathbf{q}_l,\mathbf{q}_m)}{M^2 - P^2 - i\epsilon}\,, \tag{3.51}$$

where $\mathcal{M}_2$ represents the two-particle scattering amplitude, $\mathbf{p}_i, \mathbf{p}_j, \mathbf{p}_k$ and $\mathbf{q}_l, \mathbf{q}_m, \mathbf{q}_n$ denote the in-coming and out-going three-momenta and $P = p_i + p_j - q_n = q_l + q_m - p_k$. The Feynman diagram associated with this three-particle amplitude is depicted in Fig. 3.2. Note that the summation in the above expression account for the 9 possible permutations of the momenta.

Boosting the momenta to the CM frame, $\mathbf{k}^*$ representing the boosted momenta with $\mathbf{k} = \mathbf{p}, \mathbf{q}$ or $\mathbf{P}$, and using the identity

$$\frac{1}{M^2 - P^2} = \frac{1}{2w(\mathbf{P})}\left\{\frac{1}{w(\mathbf{P}) + w(\mathbf{p}_k) - w(\mathbf{q}_l) - w(\mathbf{q}_m)} + \frac{1}{w(\mathbf{P}) - w(\mathbf{p}_k) + w(\mathbf{q}_l) + w(\mathbf{q}_m)}\right\}, \tag{3.52}$$

the pole piece of the above mentioned amplitude can be defined as

$$\mathcal{M}_3^{\text{pole}}(\mathbf{p}_1,\mathbf{p}_2,\mathbf{p}_3;\mathbf{q}_1,\mathbf{q}_2,\mathbf{q}_3) = \sum_{\text{perm}(ijk)} \sum_{\text{perm}(lmn)} \frac{\overline{\mathcal{M}}_2(\mathbf{p}_i^*,\mathbf{p}_j^*;\mathbf{q}_n^*,\mathbf{P}^*)\overline{\mathcal{M}}_2(\mathbf{p}_k^*,\mathbf{P}^*;\mathbf{q}_l^*,\mathbf{q}_m^*)}{2w(\mathbf{P})(w(\mathbf{P}) + w(\mathbf{p}_k) - w(\mathbf{q}_l) - w(\mathbf{q}_m))}\,. \tag{3.53}$$

Here $\overline{\mathcal{M}}_2$ represents the on-shell two-body scattering amplitude.

The authors of Ref. [97] showed that for a particular choice of in-coming and out-going momenta, for example with unit vectors $\mathbf{e}_x, \mathbf{e}_y, \mathbf{e}_z$

$$\mathbf{p}_1 = \lambda\mathbf{e}_y\,, \qquad \mathbf{p}_2 = \lambda\left(\frac{\sqrt{3}}{2}\mathbf{e}_x - \frac{1}{2}\mathbf{e}_y\right), \qquad \mathbf{p}_3 = -\lambda\left(\frac{\sqrt{3}}{2}\mathbf{e}_x + \frac{1}{2}\mathbf{e}_y\right), \tag{3.54}$$

with $\mathbf{q}_i = -\mathbf{p}_i$, the difference between $\mathcal{M}_3$ and $\mathcal{M}_3^{\text{pole}}$ can be expanded in Laurent series near the

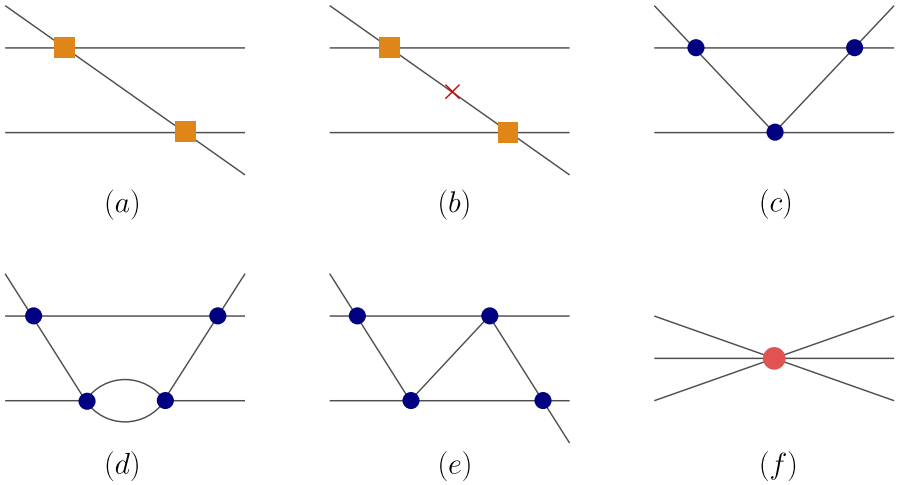

Figure 3.3: The six diagrams that contribute to the three-particle scattering amplitude in the NREFT. The orange squares here represents the two-particle scattering amplitude at $O(\mathbf{p}^2)$, The navy blue circles represents the vertices corresponding to the coupling C_0, the pink circle corresponds to the three-particle interactions associated with the coupling D_0. The red cross in diagram (b) corresponds to relativistic insertions $\mathbf{p}^4/(8M)$.

three-particle threshold as follows:

$$\mathrm{Re}\Big(\mathcal{M}_3(\lambda) - \mathcal{M}_3^{\mathrm{pole}}(\lambda)\Big) = \frac{1}{\lambda}\mathcal{M}_3^{(-1)} + \ln\frac{\lambda}{M}\mathcal{M}_3^{(l)} + \mathcal{M}_3^{(0)} + \dots\,. \tag{3.55}$$

Here, $\mathcal{M}_3^{(0)}$ denotes the threshold amplitude, the arbitrary scale appearing in the logarithm is chosen to be M and the ellipses represent terms that vanish in the limit $\lambda \to 0$. With the threshold amplitude defined in the relativistic case, a similar quantity needs to be defined in the non-relativistic case to carry out the matching of the three-body coupling.

In the NREFT, with the relevant Lagrangian given by

$$\begin{aligned}\mathcal{L}_{\mathrm{NREFT}} = {}& \phi^\dagger\Big(i\partial_t - M + \frac{\nabla^2}{2M} + \frac{\nabla^4}{8M^3}\Big)\phi + C_0\phi^\dagger\phi^\dagger\phi\phi \\ & + C_1\Big((\phi^\dagger \overleftrightarrow{\nabla}^2 \phi^\dagger)(\phi\phi) + \mathrm{h.c.}\Big) + C_2\Big((\phi^\dagger\phi^\dagger)\nabla^2(\phi\phi) + \mathrm{h.c.}\Big) + D_0\phi^\dagger\phi^\dagger\phi^\dagger\phi\phi\phi\,,\end{aligned} \tag{3.56}$$

there are six diagrams, shown in Fig. 3.3, that contribute to the regular part of the threshold amplitude when calculated in dimensional regularization.

The scattering amplitude from diagram (a) and (b) can be written down as,

$$T_3^{(a)} + T_3^{(b)} = \sum_{\mathrm{perm}(ijk)}\sum_{\mathrm{perm}(lmn)} \frac{T_2(\mathbf{p}_i,\mathbf{p}_j;\mathbf{q}_n,\mathbf{P})T_2(\mathbf{p}_k,\mathbf{P};\mathbf{q}_l,\mathbf{q}_m)}{w(\mathbf{P}) + w(\mathbf{p}_k) - w(\mathbf{q}_l) - w(\mathbf{q}_m) - i\epsilon}\,, \tag{3.57}$$

where T_2 represents the two-body scattering amplitude in the three-particle CM frame and $\mathbf{P} = \mathbf{p}_i + \mathbf{p}_j - \mathbf{q}_n = \mathbf{q}_l + \mathbf{q}_m - \mathbf{p}_k$. The two-body scattering amplitude can be determined using the

Lagrangian stated above, employing dimensional regularization in the loop integral and is given by

$$T_2(\mathbf{p}_i,\mathbf{p}_j;\mathbf{q}_n,\mathbf{P}) = 4C_0 - 16C_2\mathbf{Q}^2 - C_1((\mathbf{p}_i-\mathbf{p}_j)^2+(\mathbf{q}_n-\mathbf{P})^2) + i\frac{2MC_0^2}{\pi}P_{ij} - \frac{M^2C_0^3}{\pi^2}(P_{ij})^2 + O(\mathbf{p}^3)\,, \tag{3.58}$$

where $\mathbf{Q} = \mathbf{p}_1 + \mathbf{p}_2$ represents the two-body CM momentum, $P_{ij} = -M^2 + s_{ij}/4$ with $s_{ij} = (w(\mathbf{p}_i)+w(\mathbf{p}_j))^2 - (\mathbf{p}_i+\mathbf{p}_j)^2$. Now, since $w(\mathbf{p}_i)+w(\mathbf{p}_j) \neq w(\mathbf{q}_n)+w(\mathbf{P})$, this amplitude is not on-shell. However, the on-shell amplitude can be defined as follows

$$\begin{aligned}\overline{T}_2(\mathbf{p}_i,\mathbf{p}_j;\mathbf{q}_n,\mathbf{P}) &= T_2 + \delta T_2 \\ &= 4C_0 - 16C_2\mathbf{Q}^2 - 2C_1(\mathbf{p}_i-\mathbf{p}_j)^2 + i\frac{2MC_0^2}{\pi}P_{ij} - \frac{M^2C_0^3}{\pi^2}(P_{ij})^2 + O(\mathbf{p}^3)\,,\end{aligned} \tag{3.59}$$

with $\delta T_2 = -C_1((\mathbf{p}_i-\mathbf{p}_j)^2 - (\mathbf{q}_n-\mathbf{P})^2)$. Similar expressions can be written down for the other two-body scattering amplitude. With this, the finite part of the scattering amplitude of diagram (a) and (b) can be written as

$$T_3^{(a)} + T_3^{(b)} = \overline{T}_3^{(a+b)} - \sum_{\text{perm}(ijk)}\sum_{\text{perm}(lmn)} \frac{\overline{T}_2^{ij}\delta T_2^{lm} + \delta T_2^{ij}\overline{T}_2^{lm} + \overline{T}_2^{ij}\overline{T}_2^{lm}(\mathcal{F}-1)}{w(\mathbf{P})+w(\mathbf{p}_k)-w(\mathbf{q}_l)-w(\mathbf{q}_m)-i\epsilon}\,. \tag{3.60}$$

Here,

$$\begin{aligned}\overline{T}_3^{(a+b)} &= \prod_{i=1}^{3}\frac{1}{2w(\mathbf{p}_i)2w(\mathbf{q}_i))^{\frac{1}{2}}} \\ &\quad\times \sum_{\text{perm}(ijk)}\sum_{\text{perm}(lmn)} \frac{\mathcal{M}_2(s_{ij})\mathcal{M}_2(s_{lm})}{2w(\mathbf{P})(w(\mathbf{P})+w(\mathbf{p}_k)-w(\mathbf{q}_l)-w(\mathbf{q}_m)-i\epsilon)}\,, \\ \mathcal{F} &= \frac{(w(\mathbf{p}_i)w(\mathbf{p}_j)w(\mathbf{q}_l)w(\mathbf{q}_m))^{\frac{1}{2}}}{(w(\mathbf{p}_k)w(\mathbf{q}_n)w(\mathbf{P})w(\mathbf{P}))^{\frac{1}{2}}}\,.\end{aligned} \tag{3.61}$$

Moreover, $T_2^{\alpha\beta}$ represents the scattering amplitude involving particles with in-coming three-momenta $\mathbf{p}_\alpha$ and $\mathbf{p}_\beta$. The numerator and denominator of the second term in Eq. (3.60) can be expanded in momenta, resulting in the following expression

$$T_3^{(a)} + T_3^{(b)} - \overline{T}_3^{(a+b)} = -288MC_0C_1 + \frac{144C_0^2}{M} + \dots\,. \tag{3.62}$$

Next, the amplitude for diagram (c) is given by

$$\begin{aligned} T_3^{(c)} = 64C_0^3 \sum_{\mathrm{perm}(ijk)} \sum_{\mathrm{perm}(lmn)} \int \frac{d^D k}{(2\pi)^D i} \frac{1}{M - k^0 + \frac{\mathbf{k}^2}{2M} - i\epsilon} \\ \times \frac{1}{M - q_l^0 - q_m^0 + k^0 + \frac{(\mathbf{q}_l + \mathbf{q}_m - \mathbf{k})^2}{2M} - i\epsilon} \\ \times \frac{1}{M - p_i^0 - p_j^0 + k^0 + \frac{(\mathbf{p}_i + \mathbf{p}_j - \mathbf{k})^2}{2M} - i\epsilon} \,. \end{aligned} \tag{3.63}$$

This integral is ultraviolet finite and the explicit form is not necessary, rather for a given configuration of in-coming and out-going momenta one has

$$\mathrm{Re}\, T_3^{(c)} = \frac{C}{\lambda} \,, \tag{3.64}$$

where C is some constant.

Both diagram (d) and (e) are two-loop diagrams whose scattering amplitudes are given by

$$\begin{aligned} T_3^{(d)} = 128C_0^4 \sum_{\mathrm{perm}(ijk)} \sum_{\mathrm{perm}(lmn)} \int \frac{d^D k}{(2\pi)^D i} \int \frac{d^D l}{(2\pi)^D i} \frac{1}{M - k^0 + \frac{\mathbf{k}^2}{2M} - i\epsilon} \\ \times \frac{1}{M - q_l^0 - q_m^0 + k^0 + \frac{(\mathbf{q}_l + \mathbf{q}_m - \mathbf{k})^2}{2M} - i\epsilon} \\ \times \frac{1}{M - p_i^0 - p_j^0 + k^0 + \frac{(\mathbf{p}_i + \mathbf{p}_j - \mathbf{k})^2}{2M} - i\epsilon} \frac{1}{M - l^0 + \frac{\mathbf{l}^2}{2M} - i\epsilon} \\ \times \frac{1}{M - p_i^0 - p_j^0 + k^0 + l^0 + \frac{(\mathbf{p}_i + \mathbf{p}_j + \mathbf{p}_k - \mathbf{k} - \mathbf{l})^2}{2M} - i\epsilon} \,, \end{aligned} \tag{3.65}$$

$$\begin{aligned} T_3^{(e)} = 256C_0^4 \sum_{\mathrm{perm}(ijk)} \sum_{\mathrm{perm}(lmn)} \int \frac{d^D k}{(2\pi)^D i} \int \frac{d^D l}{(2\pi)^D i} \frac{1}{M - k^0 + \frac{\mathbf{k}^2}{2M} - i\epsilon} \\ \times \frac{1}{M - q_l^0 - q_m^0 + k^0 + \frac{(\mathbf{q}_l + \mathbf{q}_m - \mathbf{k})^2}{2M} - i\epsilon} \\ \times \frac{1}{M - p_i^0 - p_j^0 + l^0 + \frac{(\mathbf{p}_i + \mathbf{p}_j - \mathbf{l})^2}{2M} - i\epsilon} \frac{1}{M - l^0 + \frac{\mathbf{l}^2}{2M} - i\epsilon} \\ \times \frac{1}{M - p_i^0 - p_j^0 - p_k^0 + k^0 + l^0 + \frac{(\mathbf{p}_i + \mathbf{p}_j + \mathbf{p}_k - \mathbf{k} - \mathbf{l})^2}{2M} - i\epsilon} \,. \end{aligned} \tag{3.66}$$

These integrals are ultraviolet divergent and can be calculated in dimensional regularization. This

results in

$$\begin{aligned}
\mathrm{Re}\, T_3^{(d)} &= 2304\sqrt{3}C_0^4M^3\left(\mathscr{L}+\frac{1}{(4\pi)^3}\left(\ln\frac{\lambda^2}{M^2}+\delta^{(d)}\right)\right) = 2304\sqrt{3}C_0^4M^3\mathscr{L}+\mathrm{Re}\,\overline{T}_3^{(d)}\,,\\
\mathrm{Re}\, T_3^{(e)} &= -2304\frac{4\pi}{3}C_0^4M^3\left(\mathscr{L}+\frac{1}{(4\pi)^3}\left(\ln\frac{\lambda^2}{M^2}+\delta^{(e)}\right)\right) = -2304\frac{4\pi}{3}C_0^4M^3\mathscr{L}+\mathrm{Re}\,\overline{T}_3^{(e)}\,,
\end{aligned} \tag{3.67}$$

where

$$\mathscr{L} = \frac{(\mu^2)^{D-4}}{(4\pi)^3}\left(\frac{1}{D-4}-\Gamma'(1)-\ln 4\pi+\ln\frac{M^2}{\mu^2}\right). \tag{3.68}$$

Here, $\delta^{(d)}$ and $\delta^{(e)}$ are numbers given by Feynman parameter integrals (see Appendix A of Ref. [97]) and μ is the arbitrary scale of dimensional regularization.

Finally, diagram (f) is given by

$$T_3^{(f)} = 36D_0\,. \tag{3.69}$$

An important remark to make here is that the coupling D_0 has to be ultraviolet divergent to cancel out the divergences mentioned above. Hence, the renormalized coupling can be defined as follows:

$$D_0 = \frac{2C_0^4M^3}{\pi^3}(3\sqrt{3}-4\pi)(\mu^2)^{D-4}\left(\frac{1}{D-4}-\Gamma'(1)-\ln 4\pi\right)+D_0^r(\mu)\,. \tag{3.70}$$

Finally, with $\mu = M$ chosen for convenience, the matching condition for the three-body coupling is given by

$$36D_0^r(M) = 288MC_0C_1-\frac{144C_0^2}{M}+\overline{T}\,, \tag{3.71}$$

with $\overline{T}$ being the threshold amplitude defined by

$$\overline{T} = \lim_{\lambda\to 0}\mathrm{Re}\left(\prod_{i=1}^{3}\frac{\mathcal{M}_3}{(2w(\mathbf{p}_i)2w(\mathbf{q}_i))^{\frac{1}{2}}}-\overline{T}_3^{(a+b)}-T_3^{(c)}-\overline{T}_3^{(d)}-\overline{T}_3^{(e)}\right). \tag{3.72}$$

This expression can be simplified using Eq. (3.55) resulting in the following relation

$$\overline{T} = \frac{\mathcal{M}_3^{(0)}}{(2M)^3}-\frac{12M^3C_0^4}{\pi^3}(3\sqrt{3}\delta^{(d)}-4\pi\delta^{(e)})\,. \tag{3.73}$$

Using Eqs. (3.71) and (3.73), the three-body coupling in the NREFT can be matched to the relativistic three-particle threshold amplitude. Further the two-body coupling can be expressed in terms of the scattering parameters. The above procedure also highlights the fact that the two-body rescattering processes are responsible for producing the threshold singularities of the three-particle amplitude.

3.3.2 Perturbative Ground State Energy Shift in the NREFT Formulation

As mentioned previously, perturbation theory can be used to obtain the shift of the finite-volume energy levels by performing an expansion in $1/L$. This method provides an explicit formula which can be used to extract parameters of the theory from lattice calculation in the absence of resonances.

In the following Rayleigh-Schrödinger perturbation theory will be used along with the non-covariant NREFT formulation to re-derive Eq. (2.69) in a simpler and straightforward manner that allows for generalization to three- and more particle systems. This approach was first detailed in Ref. [91] with further modification carried out in Refs. [94, 97–99, 187]. Ref. [98] is followed closely below.

The relevant Lagrangian is given in Eq. (3.56). Note that the typical three-momenta on the lattice is of the order $2\pi/L$, hence each derivative suppresses the corresponding contribution to the energy by a factor of $1/L$. Therefore, the above mentioned Lagrangian is sufficient to calculate the energy shift up to $O(L^{-6})$. Further, as the non-covariant formulation is being used, relativistic corrections have to be included order by order.

The free energy of a state n in the finite volume is given by

$$E_n = \frac{1}{2M}(\mathbf{p}_1^2 + \mathbf{p}_2^2 + \cdots + \mathbf{p}_N^2)\,, \tag{3.74}$$

where the discretized momenta $\mathbf{p}_i = 2\pi\mathbf{n}_i/L$ and $n = \{\mathbf{n}_i\}$ with $i = 0, 1, \ldots, N$. Note that, in the following CM frame is considered, i.e. $\sum_{i=1}^{N}\mathbf{p}_i = 0$. Moreover, only the non-degenerate ground state is considered explicitly. The same treatment can be applied to the degenerate states with slight modifications and can be found, for example, in Refs. [97, 103].

The Hamiltonian of the system is give by

$$H = \int_{-L/2}^{L/2} d^3\mathbf{x}\,(\mathcal{H}_0 + \mathcal{H}_I) \tag{3.75}$$

with

$$\begin{aligned}
\mathcal{H}_0 &= -\phi^\dagger\Big(-M + \frac{\nabla^2}{2M}\Big)\phi\,,\\
\mathcal{H}_I &= -\phi^\dagger\Big(\frac{\nabla^4}{8M^3}\Big)\phi - C_0\phi^\dagger\phi^\dagger\phi\phi - C_1\Big((\phi^\dagger \overset{\leftrightarrow}{\nabla}^2 \phi^\dagger)(\phi\phi) + \text{h.c.}\Big)\\
&\quad - C_2\Big((\phi^\dagger\phi^\dagger)\nabla^2(\phi\phi) + \text{h.c.}\Big) - D_0\phi^\dagger\phi^\dagger\phi^\dagger\phi\phi\phi\,,
\end{aligned} \tag{3.76}$$

where ϕ and $\phi^\dagger$ represents the free fields which can be written in terms of a Fourier series in creation and annihilation operators as follows:

$$\begin{aligned}
\phi(\mathbf{x}, t) &= \frac{1}{L^3}\sum_{\mathbf{p}} \exp(-iE_\mathbf{p}t + i\mathbf{p}\mathbf{x})a_\mathbf{p}\,,\\
\phi^\dagger(\mathbf{x}, t) &= \frac{1}{L^3}\sum_{\mathbf{p}} \exp(iE_\mathbf{p}t - i\mathbf{p}\mathbf{x})a_\mathbf{p}^\dagger\,.
\end{aligned} \tag{3.77}$$

Here, $E_\mathbf{p} = M + \mathbf{p}^2/(2M)$ as the kinetic energy is completely given by the operator $\nabla^2/(2M)$ and the condition $[a_\mathbf{p}, a_\mathbf{p}^\dagger] = L^3\delta_{\mathbf{pq}}$ is obeyed. Further, the N-particle normalized state are represented by

$$|p\rangle = |\mathbf{p}_i, \ldots, \mathbf{p}_N\rangle = \frac{1}{L^{\frac{3N}{2}}\sqrt{N!}} a_{\mathbf{p}_1}^\dagger \ldots a_{\mathbf{p}_N}^\dagger |0\rangle\,, \tag{3.78}$$

where $p = (\mathbf{p}_1, \ldots, \mathbf{p}_N)$ and the closure relation is given by

$$\sum_{\mathbf{p}_1 \cdots \mathbf{p}_N} |\mathbf{p}_i, \ldots, \mathbf{p}_N\rangle\langle \mathbf{p}_i, \ldots, \mathbf{p}_N| = 1 \,. \tag{3.79}$$

Moreover, these states are eigenstates of H_0,

$$H_0|p\rangle = \sum_{i=1}^{N} E_{\mathbf{p}_i}|p\rangle \,. \tag{3.80}$$

Using the fact that the potential is determined by the interaction Hamiltonian, the Lippmann-Schwinger equation can be written in the operator form as follows:

$$\langle p|T|q\rangle = \langle p|H_I|q\rangle + \sum_k \frac{\langle p|H_I|k\rangle\langle k|T|q\rangle}{E - E_k} \,, \tag{3.81}$$

where T represents the T-matrix. Note that only the ground state is non-degenerate, all the other levels are degenerate. The contribution of the unperturbed ground state, $|0\rangle$, can be singled out and the above equation can be re-written as follows:

$$\begin{aligned} \langle p|T|q\rangle &= \langle p|\Omega|q\rangle + \frac{\langle p|\Omega|0\rangle\langle 0|T|q\rangle}{E - E_0} \,, \\ \langle p|\Omega|q\rangle &= \langle p|H_I|q\rangle + \sum_{k\neq 0} \frac{\langle p|H_I|k\rangle\langle k|\Omega|q\rangle}{E - E_k} \,. \end{aligned} \tag{3.82}$$

The pole position of the scattering matrix determines the energy shift of the level. If one sets the the external momenta to zero, i.e. $p = q = 0$, then the roots of the resulting equation given by

$$E - E_0 - \hat{\Omega}(E_0) = 0 \,, \tag{3.83}$$

correspond to the poles of the scattering T-matrix. Here, $\hat{\Omega}(E_0) = \langle 0|\Omega|0\rangle$. This equation is called the *secular equation* and has a form similar to a quantization condition. Since the energy shift $E - E_0$ is much smaller as compared to $|E_1 - E_0|$, the quantity $\hat{\Omega}(E_0)$ can be Taylor expanded such that one gets

$$E - E_0 = \hat{\Omega}(E_0) + \hat{\Omega}(E_0)\hat{\Omega}' + \frac{\hat{\Omega}^2(E_0)}{2}\hat{\Omega}'' + O((E - E_0)^3) \,, \tag{3.84}$$

where $E - E_0 = \hat{\Omega}(E_0)$ at leading order is used. Now, using Eq. (3.82), $\hat{\Omega}(E_0)$ can be written down in perturbation theory as

$$\hat{\Omega}(E_0) = \langle 0|\Omega|0\rangle = V_{00} + \sum_{p\neq 0} \frac{V_{0p}V_{p0}}{E_0 - E_p} + \sum_{p\neq 0}\sum_{q\neq 0} \frac{V_{0p}V_{pq}V_{q0}}{(E_0 - E_p)(E_0 - E_q)} + \ldots \,, \tag{3.85}$$

where $V_{pq} = \langle p|H_I|q\rangle$. Hence, using the above expression and Eq. (3.84), the perturbative energy

shift to the ground state energy can be written as

$$\begin{aligned}
\Delta E_1 &= V_{00}\,, \\
\Delta E_2 &= \sum_{p\neq 0} \frac{V_{0p}V_{p0}}{E_0 - E_p}\,, \\
\Delta E_2 &= \sum_{p\neq 0}\sum_{q\neq 0} \frac{V_{0p}V_{pq}V_{q0}}{(E_0 - E_p)(E_0 - E_q)} - V_{00}\sum_{p\neq 0}\frac{V_{0p}V_{p0}}{(E_0 - E_p)^2}\,.
\end{aligned} \tag{3.86}$$

The rather lengthy expression for ΔE_4 can be found in Ref. [103]. Using the explicit form of the potential these corrections can be easily calculated. For example, in the two-body case with the above mentioned Lagrangian,

$$\begin{aligned}
V_{pq} &= \langle \mathbf{p}_1\mathbf{p}_2|H_I|\mathbf{q}_1\mathbf{q}_2\rangle \\
&= \left\{ -\frac{2}{L^3}(C_0 - C_1(\mathbf{p}^2+\mathbf{q}^2)) - \frac{\mathbf{p}^4}{2M^3}\delta_{\mathbf{pq}}\right\}\delta_{\mathbf{p}_1+\mathbf{p}_2,\mathbf{q}_1+\mathbf{q}_2}\,,
\end{aligned} \tag{3.87}$$

with the relative momenta $\mathbf{k} = (\mathbf{k}_1 - \mathbf{k}_2)/2$. With this the corrections to the two-body ground state energy can be calculated up to $O(L^{-6})$ and is given by

$$\begin{aligned}
\Delta E^{(2)} = \frac{4\pi a_0}{ML^3}\Bigg\{ 1 - \frac{a_0}{\pi L}I + \left(\frac{a_0}{\pi L}\right)^2 (I^2 - J) - \left(\frac{a_0}{\pi L}\right)^3 (I^3 - 3IJ + K) \\
- \frac{\pi a_0}{M^2L^3} + \frac{2\pi a_0^2 r_0}{L^3}\Bigg\}\,,
\end{aligned} \tag{3.88}$$

where the couplings in the Lagrangian are matched to the two-body scattering parameters and the quantities I and J are defined in Eq. (2.67) and

$$K = \sum_{\mathbf{n}\in\mathbb{Z}^3\setminus 0} \frac{1}{\mathbf{n}^6} \simeq 8.40192\,. \tag{3.89}$$

An important remark needs to be made here. When calculating the higher order corrections, for example ΔE_2, divergent sums other than the ones represented by I can show up. These divergences need to be regularized and the same regularization scheme needs to be used in both the finite and infinite volume. In the case of ΔE_2 at $O(L^{-6})$, the formally divergent sum $\sum_{\mathbf{n}\in\mathbb{Z}^3\setminus 0} 1$ is present. This can be rewritten as

$$\sum_{\mathbf{n}\in\mathbb{Z}^3\setminus 0} 1 = -1 + \sum_{\mathbf{n}\in\mathbb{Z}^3} 1\,. \tag{3.90}$$

As no-scale integrals vanish in dimensional regularization, the above expression just becomes equal to -1. The expression in Eq. (3.88) agrees with Eq. (2.69) exactly up to $O(L^{-5})$.

Moreover, the above formula can be generalized to N-particle systems [103],

$$\begin{aligned}\Delta E^{(N)} = \frac{N!}{2!(N-2)!}\frac{4\pi a_0}{ML^3}\Bigg\{1 - \frac{a_0}{\pi L}I + \left(\frac{a_0}{\pi L}\right)^2 (I^2 + (2N-5)J) - \left(\frac{a_0}{\pi L}\right)^3 (I^3 + (2N-7)IJ \\ + (5N^2 - 41N + 63)K + 8(N-1)(2Q^r + R^r)) + (4N-9)\frac{\pi a_0}{M^2L^3} + (4N-6)\frac{2\pi a_0^2 r_0}{L^3}\Bigg\} \\ + \frac{N!}{3!(N-3)!}\left\{\frac{64\pi a_0^4}{ML^6}(3\sqrt{3} - 4\pi)\ln(\mu L) - \frac{6D_0^r(\mu)}{L^6}\right\}. \end{aligned} \tag{3.91}$$

For $N \geq 3$, two logarithmically divergent sums show up in the expression for ground state energy shift. These are given by

$$\begin{aligned} Q &= \frac{1}{L^{2d}(2\pi)^{2(d-3)}} \sum_{\mathbf{p},\mathbf{q}\neq 0} \frac{1}{\mathbf{p}^2\mathbf{q}^2(\mathbf{p}^2 + \mathbf{q}^2 + (\mathbf{p}+\mathbf{q})^2)}, \\ R &= \frac{1}{L^{2d}(2\pi)^{2(d-3)}} \sum_{\mathbf{p},\mathbf{q}\neq 0} \frac{1}{\mathbf{p}^4(\mathbf{p}^2 + \mathbf{q}^2 + (\mathbf{p}+\mathbf{q})^2)}. \end{aligned} \tag{3.92}$$

Now, dimensional regularization and Poisson's summation formula can be used to tame the divergences in these sums. This results in

$$\begin{aligned} Q &= \mu^{2(d-3)}\left\{\frac{1}{48\pi^2}\left(\ln(\mu L) - \frac{1}{2(d-3)}\right) + \frac{1}{(2\pi)^6}Q^r\right\}, \\ R &= \mu^{2(d-3)}\left\{-\frac{\sqrt{3}}{32\pi^3}\left(\ln(\mu L) - \frac{1}{2(d-3)}\right) + \frac{1}{(2\pi)^6}R^r\right\}, \end{aligned} \tag{3.93}$$

with the renormalized quantities given by

$$Q^r \simeq -102.1556\,, \quad R^r \simeq 19.1869\,. \tag{3.94}$$

The divergences that appear in the above equations are absorbed in the three-body coupling which leads to the definition of the renormalized three-body coupling given by

$$D_0 = \mu^{2(d-3)}\left\{-\frac{16\pi a_0^4}{3M(d-3)}(3\sqrt{3} - 4\pi) + D_0^r(\mu)\right\}. \tag{3.95}$$

Note, here μ is the arbitrary scale of dimensional regularization. Hence, if one carries out the renormalization of the three-body coupling in the infinite volume, the N-body ground state energy up to $O(L^{-6})$ does not contain any ultraviolet divergence. The expression in Eq. (3.91) offers a simple and efficient way to extract parameters of a theory from lattice measurements. The result of such a perturbative treatment of the three-nucleon system will be displayed in Chap. 6.

However, this method does have the drawback that it cannot be applied in the presence of resonances and shallow bound states. This can be easily seen from the fact that the expression for the ground state energy shift will converge slowly for large scattering length a_0 (given that L is of reasonable

size). Hence, a non-perturbative approach, a full fledged three-particle quantization condition, for a more general analysis of three-body lattice data is needed. The next section will introduce necessary framework required to achieve this.

3.3.3 Relativistic-Invariant Formulation of NREFT

A NREFT three-body quantization condition was derived in Refs. [70, 71] and it was cast into an explicitly relativistic-invariant form in Ref. [81]. This section aims to introduce the quantization condition in its manifestly invariant form following Ref. [81] closely.

The non-relativistic approach is very accurate when the typical momenta of particles are small compared to their masses. However, the momenta of light particles such as the pions may not be very small compared to their masses in typical processes of interest. In this case a relativistic-invariant treatment might result in sizable contribution from purely kinematic effects. Moreover, the quantization condition is a three-dimensional equation as the amplitudes entering it have to be on the mass shell to render it useful. Hence, the quantization condition contains sums (or integrals) over three-momenta and the fourth component is fixed on mass shell, and would benefit from being written in a relativistic-invariant form. Furthermore, the short-range three-body force which enters the infinite-volume Faddeev equation[8] can be parameterized such that the solutions of the Faddeev equation are invariant. However, in practice finding the explicit parametrization can be a very difficult task. In this case, casting the equations into a relativistically invariant form can be advantageous as the short-range three-body force term can be parameterized in terms of Lorentz-invariant quantities as shown in Ref. [212].

All expressions can be rewritten in a covariant manner by introducing an arbitrary timelike unit vector v^μ and considering the time evolution along the direction of this unit vector[9]. Lorentz-invariance guarantees that all choices of v^μ are physically equivalent. In addition to introduction of v^μ, one also needs to be express it in terms of the momenta which describes the process of interest. This ensures that the resulting amplitude is explicitly invariant as boosting the momenta will result in v^μ also being boosted.

The Lagrangian given in Eq. (3.18) can be reformulated in an arbitrary frame as follows:

$$\mathcal{L} = \phi^\dagger 2w_v(i(v\partial) - w_v)\phi + C_0\phi^\dagger\phi^\dagger\phi\phi + \dots\,, \tag{3.96}$$

where the arbitrary frame is defined by v_μ, $\phi(x)$ are the non-relativistic field as before, and ellipses denote higher order terms. The differential operator is given by

$$w_v = \sqrt{M^2 + \partial^2 - (v\partial)^2}\,. \tag{3.97}$$

The non-relativistic propagator for the free case is given by

$$i\langle 0|T(\phi(x)\phi^\dagger(y))|0\rangle = \int \frac{d^4k}{(2\pi)^4} e^{-ik(x-y)} D(k)\,, \tag{3.98}$$

[8] The finite-volume quantization condition also contains the three-body short-range term.

[9] By setting $v^\mu = v_0^\mu = (1, \mathbf{0})$, one can regain the original NREFT expressions.

with

$$D(k) = \frac{1}{2w_v(k)(w_v(k) - vk - i\epsilon)} \,. \tag{3.99}$$

Here, $w_v(k) = \sqrt{M^2 + k^2 + (vk)^2}$.

Similar to the original formulation of NREFT, to calculate the two-body scattering amplitude one has to evaluate bubble diagrams which come with the following loop integral:

$$I(P) = \int \frac{d^D k}{i(2\pi)^D} \frac{1}{2w_v(k)2w_v(P-k)(w_v(k) - vk - i\epsilon)(w_v(P-k) - v(P-k) - i\epsilon)} \,, \tag{3.100}$$

with the total CM momentum given by $P = p_1 + p_2 = q_1 + q_2$. Dimensional regularization can be used to make the above integral ultraviolet finite. However, threshold expansion has to be used in addition, to prevent the counting rules from breaking down (see Sec. 3.2.1). In this case ones uses the following identity

$$\frac{1}{2w_v(k)(w_v(k) - vk - i\epsilon)} = \frac{1}{M^2 - k^2 - i\epsilon} - \frac{1}{2w_v(k)(w_v(k) + vk - i\epsilon)} \,. \tag{3.101}$$

The other propagator obeys a similar expression. Next, the perpendicular component of the momenta can be defined with respect to the timelike unit vector v^μ as follows:

$$k_\perp^\mu = k^\mu - v^\mu vk \,, \quad (P-k)_\perp^\mu = (P-k)^\mu - v^\mu v(P-k) \,, \tag{3.102}$$

which are small compared to M. Moreover, threshold expansion can be used in the vicinity of the particle poles given by $vk = w_v(k)$ and $v(P-k) = w_v(P-k)$. The second term in the above identity can then be expanded and is given by

$$-\frac{1}{2w_v(k)(w_v(k) + vk - i\epsilon)} = -\frac{1}{4M^2} + \frac{k_\perp^2}{4M^4} + \cdots - \frac{M - vk}{8M^3} + \ldots \,. \tag{3.103}$$

Similar expression is obeyed by the other propagator. After threshold expanding, $I(P)$ is given by the single term

$$\begin{aligned} I(P) \equiv I(P^2) &= \int \frac{d^D k}{i(2\pi)^D} \frac{1}{(M^2 - k^2)(M^2 - (P-k)^2)} = \text{const} + \frac{\beta}{16\pi^2} \ln\left(\frac{\beta - 1}{\beta + 1}\right) \\ &= J(P^2) + \frac{i\beta}{16\pi} \,, \end{aligned} \tag{3.104}$$

with $s = P^2$, $\beta = (1 - 4M^2/(s + i\epsilon))^{1/2}$ and $J(P^2)$ representing a low-energy polynomial with real coefficients. The other terms that appear in the expression for $I(P)$ are of the form of low energy polynomials which vanish in dimensional regularization. Note that the loop function $I(P^2)$ vanishes at threshold, i.e. $s = 4M^2$ due to the renormalization prescription imposed.

The above mentioned expression is clearly Lorentz-invariant as it only depends on P^2. The difference between this expression and the expression for the loop function derived in the original NREFT, given by $J(P^2)$, boils down to a different choice of renormalization prescription used in the two cases.

Before moving to higher order terms, it is useful to look at the expression for the loop integral $I(P)$

in a finite volume.

In a finite volume one has to replace all the three-momenta integrals with finite-volume sums and hence the loop function is given by

$$I^{\text{fin}}(P) = \frac{1}{L^3}\sum_{\mathbf{k}}\int\frac{dk_0}{2\pi i}\frac{1}{2w_v(k)2w_v(P-k)} \times \frac{1}{(w_v(k)-vk-i\epsilon)(w_v(P-k)-v(P-k)-i\epsilon)}\,. \tag{3.105}$$

Using Eq. (3.101) and adding and subtracting the real part of the loop function in the infinite volume one gets the following expression:

$$I^{\text{fin}}(P) = \text{Re}\big(I(P^2)\big) + \Big(\frac{1}{L^3}\sum_{\mathbf{k}} - \mathcal{P}\int\frac{d^3\mathbf{k}}{(2\pi)^3}\Big) \times \int\frac{dk_0}{2\pi i}\Big[\frac{1}{(M^2-k^2-i\epsilon)(M^2-(P-k)^2-i\epsilon)} + \Gamma\Big]\,, \tag{3.106}$$

where the explicit expression for Γ is not needed as it only contributes to the exponentially suppressed term[10] and can be dropped. This results in any explicit v^μ dependence dropping out. The loop function can then be written as

$$I^{\text{fin}}(P) = J(s) + \Big(\frac{1}{L^3}\sum_{\mathbf{k}} - \mathcal{P}\int\frac{d^3\mathbf{k}}{(2\pi)^3}\Big)\int\frac{dk_0}{2\pi i}\frac{1}{(M^2-k^2-i\epsilon)(M^2-(P-k)^2-i\epsilon)}\,. \tag{3.107}$$

The k_0 integral can be evaluated, which results in the following expression:

$$\begin{aligned} I^{\text{fin}}(P) &= J(s) + \Big(\frac{1}{L^3}\sum_{\mathbf{k}} - \mathcal{P}\int\frac{d^3\mathbf{k}}{(2\pi)^3}\Big)\frac{w(\mathbf{k})+w(\mathbf{P}-\mathbf{k})}{2w(\mathbf{k})w(\mathbf{P}-\mathbf{k})\big((w(\mathbf{k})+w(\mathbf{P}-\mathbf{k}))^2-P_0^2\big)} \\ &= J(s) + \Big(\frac{1}{L^3}\sum_{\mathbf{k}} - \mathcal{P}\int\frac{d^3\mathbf{k}}{(2\pi)^3}\Big)\frac{w(\mathbf{k})+w(\mathbf{P}-\mathbf{k})}{4w(\mathbf{k})w(\mathbf{P}-\mathbf{k})(w(\mathbf{k})+w(\mathbf{P}-\mathbf{k})-P_0)}\,, \end{aligned} \tag{3.108}$$

where the above and bottom line differ by a low-energy polynomial in three-momentum given by $(4w(\mathbf{k})w(\mathbf{P}-\mathbf{k})(w(\mathbf{k})+w(\mathbf{P}-\mathbf{k})+P_0))^{-1}$, which leads to exponentially suppressed terms. The difference of the sum and integral can be related to the Lüscher-zeta function [213] and the loop function can be written down as:

$$I^{\text{fin}}(P) = J(s) + \frac{1}{4\pi^{3/2}\sqrt{s}L\gamma}Z_{00}^{\mathbf{d}}(1;s)\,. \tag{3.109}$$

[10] Γ contains the other three terms that come after using the identity given in Eq. (3.101) and depends on v^μ explicitly. After expanding the denominators in Γ using Eq. (3.103) and integrating over k_0, it leads to low-energy polynomials. These low-energy polynomials vanish in dimensional regularization in the infinite volume. In the finite volume, the difference of the sum and integral results in only exponentially suppressed terms that can be neglected [81].

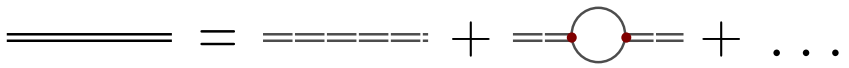

Figure 3.4: Diagrammatic representation of the Dyson equation obeyed by the full dimer propagator which is denoted by the double black lines. The free dimer propagator (σ) is represented by the double dashed gray lines while the particle propagator is represented by the single gray line. The dark red dots corresponds to vertex that converts particle pairs into dimer and vice versa.

At the next order the following term needs to be included in the two-particle Lagrangian,

$$\mathcal{L}_2^{(2)} = C_2\Big\{((w_\mu\phi)^\dagger(w^\mu\phi)^\dagger\phi\phi - M^2\phi^\dagger\phi^\dagger\phi\phi) + \text{h.c.}\Big\}\,, \tag{3.110}$$

where

$$w^\mu = v^\mu w_v + i\partial_\perp^\mu\,,\quad \partial_\perp^\mu = \partial^\mu - v^\mu v\partial\,. \tag{3.111}$$

Higher order terms can be written down in a similar manner starting from the original NREFT Lagrangian. The matching of the LECs appearing in the Lagrangian can be done following the steps[11] laid down in Sec. (3.2.1). At the end one gets the following expression for the on-shell two-body T-matrix

$$T_l(q^*,q^*) = T_l(s) = \frac{16\pi\sqrt{s}(q^*)^{-2l}}{16\pi\sqrt{s}(q^*)^{-2l}(V_l^{-1}(s) - \frac{(q^*)^{2l}}{2}J(s)) - iq^*}\,, \tag{3.112}$$

where $(q^*)^2 = (s/4 - M^2)$. One can write the amplitude T_l in terms of the phase shift using unitarity resulting in the following matching condition

$$16\pi\sqrt{s}(V_l^{-1}(s) - \frac{(q^*)^{2l}}{2}J(s)) = (q^*)^{2l+1}\cot\delta_l(s)\,. \tag{3.113}$$

Up to first order this expression reproduces the matching condition given in Eq. (3.38). Additional terms appear at second order onward.

Dimer Fields at the Lowest Order

To write down a three-body quantization condition, one needs to resum all the two-particle sub diagrams that are relevant for the three-body amplitude. To perform this, auxiliary fields can be introduced. These axillary fields are called *dimer fields* [134, 214]. In the following section these fields will be introduced at the lowest order, while the subsequent section will discuss the introduction of dimer fields at higher order.

The lowest order Lagrangian in the three-body sector can be written as

$$\mathcal{L}_{\text{NREFT}} = \phi^\dagger 2w_v(i(v\partial) - w_v)\phi + C_0\phi^\dagger\phi^\dagger\phi\phi + D_0\phi^\dagger\phi^\dagger\phi^\dagger\phi\phi\phi\,. \tag{3.114}$$

The introduction of the dimer fields in the above case leads to simplification in the three-body sector

[11] Note that on mass shell, for in-coming and out-going momenta $\tilde{p}_i^\mu = p_i^\mu$ and $\tilde{q}_i^\mu = q_i^\mu$ can be used, where the momenta are defined by $\tilde{p}_i^\mu = v^\mu w_v(p_i) + p_{i\perp}^\mu$. Moreover, the substitution $\tilde{k}_i^\mu \to k_i^\mu$ can be done in the loop integrals as the additional terms that arise from using the explicit expression of $\tilde{k}_i^\mu$ vanish in dimensional regularization [81].

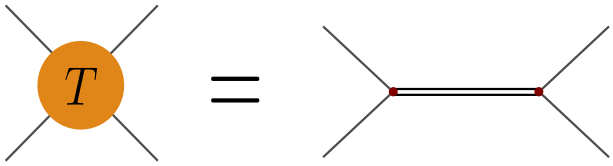

Figure 3.5: Relation between The two-particle scattering amplitude T and the full dimer propagator denoted by the double black lines. The particle propagator is represented by the single gray line and the dark red dots denote the vertices that convert between dimer and particle-pairs.

as the two-particle interactions are then given by an infinite sum of s-channel dimer exchanges and the particle-dimer interaction represent the three-particle interactions. The above Lagrangian can be rewritten in terms of particle field, $\phi(x)$, and dimer field, $\mathcal{T}(x)$ as follow:

$$\mathcal{L}_d = \phi^\dagger 2w_v(i(v\partial) - w_v)\phi + \sigma\mathcal{T}^\dagger\mathcal{T} + \frac{f_0}{2}(\mathcal{T}^\dagger\phi\phi + \text{h.c.}) + h_0\mathcal{T}^\dagger\mathcal{T}\phi^\dagger\phi\,, \tag{3.115}$$

where $\sigma = \pm 1$ for reasons which will become clear in the following. Next, the dimer fields can be integrated out and the generating functional can be written as

$$\begin{aligned} Z_d(j, j^\dagger) &= \int \mathcal{D}\phi\mathcal{D}\phi^\dagger \exp\left\{ i\int d^4x \left(\phi^\dagger 2w_v(i(v\partial) - w_v)\phi - \frac{f_0^2\phi^\dagger\phi^\dagger\phi\phi}{4(\sigma + h_0\phi^\dagger\phi)} + j^\dagger\phi + \phi^\dagger j\right)\right\} \\ &= \int \mathcal{D}\phi\mathcal{D}\phi^\dagger \exp\left\{ i\int d^4x \left(\phi^\dagger 2w_v(i(v\partial) - w_v)\phi - \sigma\frac{f_0^2}{4}\phi^\dagger\phi^\dagger\phi\phi \right.\right. \\ &\qquad \left.\left. + \frac{h_0 f_0^2}{4}\phi^\dagger\phi^\dagger\phi^\dagger\phi\phi\phi + \cdots + j^\dagger\phi + \phi^\dagger j\right)\right\}, \end{aligned} \tag{3.116}$$

where the integrand is expanded in powers of the field and the ellipses represent terms with more than six fields. Comparing Eq. (3.116) to the generating functional in the original theory given by

$$\begin{aligned} Z(j, j^\dagger) = \int \mathcal{D}\phi\mathcal{D}\phi^\dagger \exp\left\{ i\int d^4x \left(\phi^\dagger 2w_v(i(v\partial) - w_v)\phi + C_0\phi^\dagger\phi^\dagger\phi\phi \right.\right. \\ \left.\left. + D_0\phi^\dagger\phi^\dagger\phi^\dagger\phi\phi\phi + j^\dagger\phi + \phi^\dagger j\right)\right\}, \end{aligned} \tag{3.117}$$

one ends up with the following matching condition:

$$C_0 = -\sigma\frac{f_0^2}{4}\,, \quad D_0 = \frac{h_0 f_0^2}{4}\,. \tag{3.118}$$

This matching condition highlights the significance of σ. f_0^2 is always positive and hence $\sigma = \pm 1$ helps to account for the positive or negative sign of the S-wave scattering length. The dimer propagator

resummed to all orders is given by

$$i\langle 0|T(\mathcal{T}(x)\mathcal{T}^{\dagger}(y))|0\rangle = \int \frac{d^4P}{(2\pi)^4} e^{-iP(x-y)} D(P)\,. \tag{3.119}$$

The propagator $D(P)$ obeys the Dyson-Schwinger equation (depicted in Fig. 3.4):

$$D(P) = -\sigma - \frac{\sigma f_0^2}{2} I(P) D(P)\,, \tag{3.120}$$

with $I(P)$ defined in Eq. (3.104) representing the bubble integral. Using the result of this integral from the previous sections one gets

$$D(P) \equiv D(P^2) = \frac{16\pi\sqrt{s} f_0^{-2}}{16\pi\sqrt{s}(\sigma f_0^{-2} - \frac{1}{2}J(s)) - iq^*}\,. \tag{3.121}$$

Now, the two-particle T-matrix can be expressed in terms of the full dimer propagator by attaching dimer-particle vertices that convert the dimer into particle pairs, see Fig. 3.5. At leading order this results in the following expression:

$$T(\mathbf{p}_1, \mathbf{p}_2; \mathbf{q}_1, \mathbf{q}_2) = \tau_0(P^2) = f_0 D(P^2) f_0 = \frac{16\pi\sqrt{s}}{16\pi\sqrt{s}(\sigma f_0^{-2} - \frac{1}{2}J(s)) - iq^*}\,. \tag{3.122}$$

Dimer Fields at the Higher Order

Higher partial-waves are accounted in the NREFT framework via higher order operators involving derivatives acting on the fields. Hence, to include higher partial-waves in the present case, higher order operators in the original NREFT Lagrangian need to be rewritten in the particle-dimer picture. This can be done by including dimer fields with arbitrary spin [70, 71]. Below, the procedure for rewriting higher order operators in the particle-dimer picture will be discussed.

At $O(p^4)$ the following two-particle operators need to be included [81],

$$\begin{aligned}\mathcal{L}_2^{(4)} = {} & C_4^{\mathrm{S}}\Big((w_\mu\phi)^\dagger(w^\mu\phi)^\dagger - M^2\phi^\dagger\phi^\dagger\Big)\Big((w_\nu\phi)(w^\nu\phi) - M^2\phi\phi\Big) \\ & + \frac{5}{2}C_4^{\mathrm{D}}\Big(3(w_\mu\phi)^\dagger(w_\nu\phi)^\dagger(w^\mu\phi)(w^\nu\phi) - (w_\mu\phi)^\dagger(w^\mu\phi)^\dagger(w_\nu\phi)(w^\nu\phi) - M^4\phi^\dagger\phi^\dagger\phi\phi \\ & - \frac{M^2}{2}\big((w_\mu\phi)^\dagger(w^\mu\phi)^\dagger\phi\phi + \text{h.c.}\big)\Big)\,,\end{aligned} \tag{3.123}$$

where the operator associated with the coefficient C_4^{S} and C_4^{D} represent the S-wave and D-wave contributions respectively. The P-wave contribution is absent due to Bose symmetry in the identical particle case. With this operator the D-wave projected potential is given by

$$V_2(s) = 20C_4^{\mathrm{D}}(q^*)^4 P_2(\cos\theta)\,, \tag{3.124}$$

where $P_l(\cos\theta)$ represents the Legendre polynomials with $\cos\theta = (t-u)/(s-4M^2)$ and s, t, u being the Mandelstam variables.

As mentioned above, dimers with arbitrary spin can be included to account for interaction involving higher partial-waves [71]. Hence, tensor dimer fields $\mathcal{T}_{\mu_1,\ldots,\mu_l}$ are introduced corresponding to the angular momentum l. The dimer fields obey the following set of conditions[12]

$$v^{\mu_i}\mathcal{T}_{\mu_1,\ldots,\mu_l} = 0\,, \quad \text{for: } i = 1,\ldots,l\,. \tag{3.125}$$

Moreover, they are traceless in each pair of index and symmetric under the exchange of each pair of index. For notational convenience, $\mathcal{T}_{\mu_1,\ldots,\mu_l} \equiv \mathcal{T}_{n_l}$ will be used where $n_l = \mu_1,\ldots,\mu_l$.

$$\mathcal{L}_d = \phi^\dagger 2w_v(i(v\partial) - w_v)\phi + \sum_{l=0}^{\infty}\sigma_l\mathcal{T}_{n_l}^\dagger\mathcal{T}_{n_l} + \frac{1}{2}\sum_{l=0}^{\infty}(\mathcal{T}_{n_l}^\dagger O_{n_l} + \text{h.c.})\,, \tag{3.126}$$

where $O_{n_l} \equiv O_{\mu_1,\ldots,\mu_l}$ represents two-particle operators and $\sigma_l = \pm 1$. Integrating out the dimer fields, one ends up with the following Lagrangian describing the two-particle interactions:

$$\mathcal{L}_I = -\sum_l \frac{\sigma_l}{2}O_{n_l}^\dagger O_{n_l}\,. \tag{3.127}$$

The operators O_{n_l} can be constructed using the explicit form of the spherical functions and can be expressed in terms of a series given by the function $f_l(s) = f_l^{(0)} + \frac{1}{2}f_l^{(2)}(s-4M^2) + \ldots$, where $f_l^{(i)}$s are the coupling coefficient. In the D-wave, the lowest order two-particle operator is given by

$$\begin{aligned} O_2 \equiv O^{\mu\rho} = f_2^{(0)}\Big(&\frac{3}{2}(\phi(\overline{w}_\perp^\mu\overline{w}_\perp^\rho\phi) - (\overline{w}_\perp^\mu\phi)(\overline{w}_\perp^\rho\phi)) \\ &- \frac{1}{2}(g^{\mu\rho} - v^\mu v^\rho)(\phi(\overline{w}_\perp^\lambda\overline{w}_{\perp\lambda}\phi) - (\overline{w}_\perp^\lambda\phi)(\overline{w}_{\perp\lambda}\phi))\Big)\,, \end{aligned} \tag{3.128}$$

where $\overline{w}_\perp^\mu = \overline{w}^\mu - v^\mu(v\overline{w})$ with the operator $\overline{w}^\mu$ representing w^μ being boosted in the two-particle CMS with respect to the unit vector v^μ. This implies that the on-shell total momentum of the two particles is parallel to v^μ. Moreover, one has

$$\overline{w}^\mu = \Lambda_\rho^\mu w^\rho\,, \tag{3.129}$$

where Λ_ρ^μ represents the Lorentz transformation.

Rewriting the two-particle operators in momentum space leads to simpler and compact expressions. The total on-shell momentum of two particle can be defined as $P = \widetilde{p}_1 + \widetilde{p}_2$, with $\widetilde{p}_i$ being the on-shell momenta of the particles with $i = 1, 2$. P^μ can be made parallel to v^μ by considering the following boost:

$$\overline{P}^\mu = \Lambda_\rho^\mu P^\rho = \sqrt{P^2}v^\mu\,, \quad \Lambda_\rho^{-1\,\mu}v^\rho = \frac{P^\mu}{\sqrt{P^2}}\,. \tag{3.130}$$

With this one can write down,

$$\boldsymbol{v}^2\overline{\mathbf{P}} = \boldsymbol{v}(\boldsymbol{v}\overline{\mathbf{P}})\,, \quad |\boldsymbol{v}|\overline{P}^0 = v^0|\overline{\mathbf{P}}|\,. \tag{3.131}$$

The above identities can be used to rewrite operators appearing in the Lagrangian in momentum space.

[12] These conditions ensure that independent degree of freedom is equal to $2l + 1$.

The lowest-order two-particle D-wave term in $\mathcal{L}_I$ is then given by

$$\widetilde{O}^{\mu\rho}(p)\widetilde{O}_{\mu\rho}(q) = 16(f_2^{(0)})^2\Big(\frac{9}{4}(\bar{p}_\perp\bar{q}_\perp)^2 - \frac{3}{4}(\bar{p}_\perp)^2(\bar{q}_\perp)^2\Big)\,, \tag{3.132}$$

where $\widetilde{O}^{\mu\rho}$ is the momentum space equivalent of $O^{\mu\rho}$, $\bar{p}_\perp^\mu = \bar{p}^\mu - v^\mu(v\bar{p})$ with $\bar{p}^\mu = (\bar{p}_1^\mu - \bar{p}_2^\mu)/2$. Using the identities defined above and Lorentz-invariance, the above expression can be simplified in the laboratory frame as follows:

$$\widetilde{O}^{\mu\rho}(p)\widetilde{O}_{\mu\rho}(q) = 24(f_2^{(0)})^2(q^*)^4 P_2(\cos\theta)\,. \tag{3.133}$$

Using Eq. (3.124) one gets the matching condition

$$(f_2^{(0)})^2 = \frac{5}{6}C_4^{\mathrm{D}}\,. \tag{3.134}$$

Higher partial-waves and terms with more derivative can be included in the particle-dimer picture in a similar manner.

Next, consider the full dimer propagator,

$$i\langle 0|T(\mathcal{T}_{n_l}(x)\mathcal{T}^\dagger_{n_{l'}}(y))|0\rangle = \int \frac{d^4P}{(2\pi)^4}e^{-iP(x-y)}D_{n_l n_{l'}}(P)\,, \tag{3.135}$$

with $D_{n_l n_{l'}}(P)$[13] being a matrix with Lorentz indices that obeys the following equation

$$D_{n_l n_{l'}}(P) = -\delta_{n_l n_{l'}}\sigma_l - \frac{\sigma_l}{2}(q^*)^{2l}f_l(s)I(P^2)f_{l'}(s)D_{n_l n_{l'}}(P)\,, \tag{3.136}$$

where the function $f_l(s)$ enters via the particle-dimer vertex in the loop, see Fig. 3.5. The loop function $I(P^2)$ is defined in Eq. (3.104). Now, the two-particle scattering amplitude can be related to $D_{n_l n_{l'}}(P)$ by,

$$T(s) = \sum_{n_l n_{l'}} Y_{n_l}(\bar{p})\tau_{n_l n_{l'}}(s)Y_{n_{l'}}(\bar{q}) = \sum_{n_l n_{l'}} Y_{n_l}(\bar{p})f_l(s)D_{n_l n_{l'}}(P)f_{l'}(s)Y_{n_{l'}}(\bar{q})\,, \tag{3.137}$$

where $\bar{p}$ and $\bar{q}$ are defined via Lorentz transformation given in Eq. (3.130) and

$$\sum_{n_l} \equiv \sum_{l=0}^{\infty}\sum_{\mu_1,\ldots,\mu_l}\,. \tag{3.138}$$

Moreover the function $Y_{n_l}(\bar{p})$ is defined as follows:

$$Y_{n_l}(\bar{p}) = Y_{\mu_1,\ldots,\mu_l}(\bar{p}) = (\frac{s}{4} - M^2)^{-l/2}\mathcal{Y}_{\mu_1,\ldots,\mu_l}(\bar{p})\,, \tag{3.139}$$

with a particle of spin l being described by the tensor $\mathcal{Y}_{\mu_1,\ldots,\mu_l}$. For example, for $l = 2$ one has

[13] Note that $D_{n_l n_{l'}}$ is diagonal in l, l' space in the infinite volume but not in the finite volume.

$\mathcal{Y}_{\mu\nu} = (3p_\mu p_\nu - (g_{\mu\nu} - v_\mu v_\nu)p^2)/2$.

After projecting the T-matrix on the left side onto partial-waves and using unitarity to relate it to the phase shift, one can write down the following matching condition

$$\sigma_l f_l^{-2}(s) - \frac{(q^*)^{2l}}{2} J(s) = \frac{(q^*)^{2l+1}}{16\pi\sqrt{s}} \cot\delta_l(s) \,. \tag{3.140}$$

The left-hand side of the above equation is a polynomial in the Lorentz-invariant quantity s with coefficient $f_l^{(i)}$ and the right-hand side can be expressed in terms of the scattering parameters via the effective-range expansion. Since both the sides can be expressed in terms of a polynomial series in the variable $(q^*)^2$, a one-to-one correspondence between number of couplings $f_l^{(i)}$s and scattering parameters exists.

The Three-Body Force

After having constructed the particle-dimer Lagrangian in the two-body sector, one has to also include a short-range three-body interaction term. One starts by first considering the process involving three identical scalar particle, $\phi(p_1) + \phi(p_2) + \phi(p_3) \to \phi(q_1) + \phi(q_2) + \phi(q_3)$. In this case, the set of Lorentz-invariant quantities are given by [212]

$$\begin{aligned} &s = (p_1 + p_2 + p_3)^2 = (q_1 + q_2 + q_3)^2 \,, \\ &s_{ij} = (p_i + p_j)^2 \,, \;\; s'_{ij} = (q_i + q_j)^2 \;\; i, j = 1, 2, 3, \; i \neq j \,, \\ &t^{ij} = (p_i - q_j)^2 \,, \;\; i, j = 1, 2, 3 \,. \end{aligned} \tag{3.141}$$

One can impose consistent power counting rules by defining the following quantities:

$$\Delta = s - 9M^2 \,, \;\; \Delta_p^i = s_{jk} - 4M^2 \,, \;\; \Delta_q^i = s'_{jk} - 4M^2 \,. \tag{3.142}$$

Here, the label $i, j, k = 1, 2, 3$ with $i \neq j \neq k$. The magnitude of the generic momentum $\mathbf{p}$ counts as $O(\epsilon)$ where ϵ is a small generic parameter. Hence, the above mentioned quantities count as $O(\epsilon^2)$.

On the mass shell, these quantities obey the following identities[14] [212]:

$$\begin{aligned} &\sum_{i=1}^{3} \Delta_p^i = \sum_{i=1}^{3} \Delta_q^i = \Delta \,, \\ &\sum_{j=1}^{3} t^{ij} = \Delta_p^i - \Delta \,, \\ &\sum_{i=1}^{3} t^{ij} = \Delta_q^j - \Delta \,, \end{aligned} \tag{3.143}$$

where $i = 1, 2, 3$. Since identical particles are considered here, further constraints can be imposed on the three-body force term by utilizing Bose symmetry and time-reversal symmetry. By Bose symmetry,

[14] For a general $n \to m$ process, the independent degree of freedom N, is given by $N = 3(n + m) - 10$ due to Poincaré invariance.

the three-body interaction should be invariant under the exchange of any pair of in-coming and out-going particles, and by time-reversal symmetry, in-coming and out-going states can be exchanged. This leads to

$$\begin{aligned} p_i \leftrightarrow p_j \;&:\; \Delta_p^i \leftrightarrow \Delta_p^j \;\; t^{ik} \leftrightarrow t^{jk}\,, \\ q_i \leftrightarrow q_j \;&:\; \Delta_q^i \leftrightarrow \Delta_q^j \;\; t^{ki} \leftrightarrow t^{kj}\,, \\ p_i \leftrightarrow q_i \;&:\; \Delta_p^i \leftrightarrow \Delta_q^i \;\; t^{ij} \leftrightarrow t^{ji}\,, \end{aligned} \tag{3.144}$$

where $i, j, k = 1, 2, 3$ and in the last line $i, j = 1, 2, 3$ has to be taken simultaneously. Using the fact that the three-body force $\mathcal{F}_3$ at tree level is short ranged in nature and can be expanded in the quantities $\Delta, \Delta_p^i, \Delta_q^i$ and t^{ij} while also imposing the constraints discussed above, $\mathcal{F}_3$ can be written down as

$$\mathcal{F}_3 = \alpha_0 + \alpha_2 \Delta + O(\epsilon^4)\,, \tag{3.145}$$

where α_0 and α_2 are real coefficients due to unitarity.

The particle-dimer picture differs from the three-particle picture in the following important ways. Since dimer and ϕ particles are not identical all partial-waves have to be considered. Moreover, dimer fields posses spin while ϕ particles are spinless scalars. Lastly, equation of motion cannot be used to constraint the number of independent terms appearing in the Lagrangian. Below scalar dimers will be considered and Ref [81] will be followed closely.

The tree level particle-dimer scattering amplitude in the case of scalar dimer, assuming here dimer fields represent unphysical auxiliary fields, depend on the following quantities:

$$s = (p+P)^2 = (q+Q)^2\,,\;\; t = (p-q)^2 = (P-Q)^2\,,\;\; \sigma_p^2 = P^2\,,\;\; \sigma_q^2 = Q^2\,, \tag{3.146}$$

where P and Q represents the momenta of the in-coming and out-going dimer fields respectively and p and q represents the momenta of the in-coming and out-going particle fields respectively. Analogous to the explicit three-particle case, the following quantities can be defined to impose consistent power counting rules:

$$\Delta = s - 9M^2 = O(\epsilon^2)\,,\;\; \Delta_{p/q} = \sigma_{p/q}^2 - 4M^2 = O(\epsilon^2)\,,\;\; t = O(\epsilon^2)\,, \tag{3.147}$$

where all transverse momenta $p_\perp$ count as $O(\epsilon)$. The potential in this case, can be expanded in Taylor series and is given by

$$V_d(s, t, \sigma_p^2, \sigma_q^2) = h_0 + h_1(s - 9M^2) + h_2 t + h_3(\sigma_p^2 + \sigma_q^2 - 8M^2) + O(\epsilon^4)\,, \tag{3.148}$$

where time-reversal symmetry was used. Moreover, the coefficients h_i are real due to unitarity.

All the coupling mentioned above are not independent and only couplings that contribute to the on-shell three-particle amplitude should be considered. These couplings can then be matched to the three-body force term given above. To obtain the three-particle on-shell amplitude from the potential, one has to attach particle-dimer vertices and sum over all possible permutations of in-coming and out-going state. The vertex is defined by the function $f_0(\sigma^2) = f_0^{(0)} + f_0^{(2)}(\sigma^2 - 4M^2)$ with $\sigma^2 = \sigma_p^2, \sigma_p^2$ at $O(\epsilon^2)$. Moreover, as any of the three-particle in the initial or final state can be the spectator particle, the kinematic quantities have to be labeled with the spectator particle index

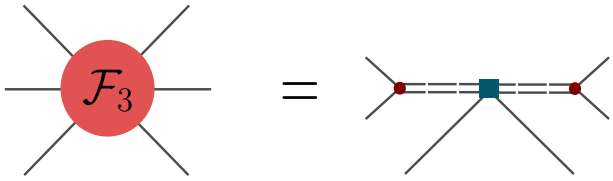

Figure 3.6: The three-particle force term expressed in terms of the short-range particle-dimer interaction. The double dashed gray lines denote the free dimer propagator, the particle propagator is represented by the single gray line, the dark red dots represent particle-dimer conversion vertices and the dark cyan rectangle corresponds to the particle-dimer interaction vertex.

$i, j = 1, 2, 3$ which have to be summed over at the end. The quantities $\Delta_{p/q}$ and t are then defined as

$$\Delta_p^i = P_i^2 - 4M^2\,, \quad \Delta_q^i = Q_i^2 - 4M^2\,, \quad t^{ij} = (p_i - q_j)^2\,. \tag{3.149}$$

These quantities obey the identities given in Eq. (3.143).

With this the three-particle amplitude is given by

$$T_3^{\text{tree}} = \sum_{i,j=1}^{3} f_0(\sigma_q^{i\,2}) V_d(s, t^{ij}, \sigma_q^{i\,2}, \sigma_p^{j\,2}) f_0(\sigma_p^{j\,2}) + O(\epsilon^4)\,. \tag{3.150}$$

Using Eq. (3.145) the matching condition can be written down as

$$\mathcal{F}_3 = \alpha_0 + \alpha_2 \Delta = \sum_{i,j=1}^{3} f_0(\sigma_p^{i\,2}) V_d(s, t^{ij}, \sigma_p^{i\,2}, \sigma_q^{j\,2}) f_0(\sigma_q^{j\,2})\,. \tag{3.151}$$

This expression clearly shows that only one of the coupling h_1, h_2, h_3 is independent and any two of these coupling can be set to zero with any loss of generality. The diagrammatic representation of this matching condition is shown in Fig. 3.6.

An important remark is in order here. The above discussion is relevant only in the absence of physical dimer (two-particle shallow bound state). In the presence of physical dimers, both σ_p^2 and σ_q^2 will be determined by the dimer mass squared. Thus, particle-dimer scattering amplitude can be directly matched to effective-range parameters.

At the order considered above only S-wave contributes. At higher order in ϵ, the scattering angle θ can be defined as follows:

$$t - 2M^2 = \frac{(s + M^2 - \sigma_q^2)(s + M^2 - \sigma_p^2) - (\lambda(M^2, s, \sigma_p^2)\lambda(M^2, s, \sigma_q^2))^{\frac{1}{2}} \cos\theta}{4s}\,, \tag{3.152}$$

where $\lambda(\alpha, \beta, \gamma) = \alpha^2 + \beta^2 + \gamma^2 - 2(\alpha\beta + \beta\gamma + \gamma\alpha)$ represents the Källén-function. Hence, the particle-dimer amplitude at tree level can be expanded in a series of finite number of Legendre polynomial at any given order in ϵ.

Now to include higher partial-wave, dimer fields with arbitrary spin needs to be included. To proceed, Lorentz transformations can be used to remove redundant coupling and write down an

appropriate basis for the field $\mathcal{T}_{\mu_1,\ldots,\mu_l}$. This Lorentz transformation is given by

$$\underline{\Lambda}^{\mu}_{\rho} v^{\rho} = v^{\mu}_{0}\,, \quad \underline{\mathcal{T}}_{\mu_1,\ldots,\mu_l} = \underline{\Lambda}^{\mu_1}_{\rho_1} \ldots \underline{\Lambda}^{\mu_l}_{\rho_l} \mathcal{T}_{\rho_1,\ldots,\rho_l}\,. \tag{3.153}$$

Note that, if one of the indices of $\mathcal{T}$ is zero then the transformed field $\underline{\mathcal{T}}$ becomes zero due to the constraint given in Eq. (3.125). Moreover, the transformed field can be expanded in terms of the dimer field components $\mathcal{T}_{lm}$, given by

$$\underline{\mathcal{T}}_{\mu_1,\ldots,\mu_l} = \sum_{m=-l}^{l} C^{lm}_{\mu_1,\ldots,\mu_l} \mathcal{T}_{lm}\,, \tag{3.154}$$

where $C^{lm}_{\mu_1,\ldots,\mu_l}$ are purely numerical coefficients that can be determined from the spherical functions.

With this, the potential is given by the matrix element of the interaction Hamiltonian and can be boosted to the rest frame as follows:

$$\begin{aligned}\langle p, P; \mu_1', \ldots \mu_{l'}' | H_I | q, Q; \mu_1 \ldots \mu_l \rangle = (\underline{\Lambda}^{-1})^{\rho_1'}_{\mu_1'} \ldots (\underline{\Lambda}^{-1})^{\rho_{l'}'}_{\mu_{l'}'} (\underline{\Lambda}^{-1})^{\rho_1}_{\mu_1} \ldots (\underline{\Lambda}^{-1})^{\rho_l}_{\mu_l} \\ \times \sum_{m'=-l'}^{l'} \sum_{m=-l}^{l} C^{l'm'}_{\rho_1',\ldots,\rho_{l'}'} C^{lm}_{\rho_1,\ldots,\rho_l} \langle \underline{p}; l'm' | H_I | \underline{q}; lm \rangle\,.\end{aligned} \tag{3.155}$$

Here, (lm) and $(l'm')$ represents the dimer field's angular momentum and $\underline{k}^{\mu}$ for $k = p, q$ is defined as follows:

$$\underline{k}^{\mu} = \underline{\Lambda}^{\mu}_{\rho} k^{\rho}\,. \tag{3.156}$$

Note that, the same Lorentz transformation can be used to transform the above matrix element to the CM frame. The partial-wave projection of $\langle \underline{p}; l'm' | H_I | \underline{q}; lm \rangle$ is then given by

$$\begin{aligned}\langle \underline{p}; l'm' | H_I | \underline{q}; lm \rangle &= V_d^{lm,l'm'}(s, t, \sigma_p^2, \sigma_q^2) \\ &= 4\pi \sum_{JM} \sum_{L'L} \mathcal{Y}^{L'l'}_{JM}(\underline{\mathbf{p}}, m') \mathcal{H}_{JL'L}(\Delta, \Delta_p, \Delta_q) (\mathcal{Y}^{Ll}_{JM}(\underline{\mathbf{q}}, m))^*\,,\end{aligned} \tag{3.157}$$

with the function $\mathcal{Y}^{Ll}_{JM}(\underline{\mathbf{p}}, m)$ is given by

$$\mathcal{Y}^{Ll}_{JM}(\underline{\mathbf{p}}, m) = \langle L(M-m), lm | JM \rangle \mathcal{Y}_{L(M-m)}(\underline{\mathbf{p}})\,. \tag{3.158}$$

Here, J, M represents the total angular momentum, whereas L and L' are the orbital angular momentum between the out-going and in-coming particle-dimer pairs respectively. Lastly, its should be noted that the quantity $\mathcal{H}^{ll'}_{JLL'}(\Delta, \Delta_p, \Delta_q)$ expanded in powers of ϵ, is a polynomial in its arguments.

Now, the interaction Lagrangian corresponding to this matrix element can be written down as follows:

$$\mathcal{L}_I = 4\pi \sum_{lm} \sum_{l'm'} \sum_{JM} \sum_{LL'} \mathcal{T}^{\dagger}_{lm} \Big(\mathcal{Y}^{Ll}_{JM}(i\nabla, m) \phi^{\dagger} \Big) \mathcal{H}^{ll'}_{JLL'}(\Delta, \overleftarrow{\Delta}_d, \overrightarrow{\Delta}_d) \Big((\mathcal{Y}^{L'l'}_{JM}(i\nabla, m'))^* \phi \Big) \mathcal{T}_{l'm'}\,, \tag{3.159}$$

where the operator Δ_d acts on the dimer fields in the direction given by the arrow above the operator

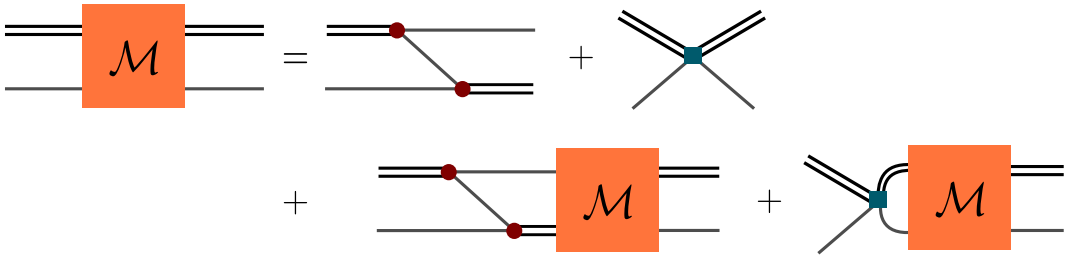

Figure 3.7: Diagrammatic representation of the Faddeev equation for the particle-dimer scattering amplitude $\mathcal{M}$. The full dimer propagator is denoted by the double black lines while the particle propagator is represented by the single gray line. The dark red dots denote particle-dimer conversion vertices whereas the dark cyan rectangle corresponds to the particle-dimer interaction vertex.

and Δ acts on the particle-dimer pairs.

A few important remarks are in order. First, a more generic form of Eq. (3.157) can be written down involving v^μ explicitly using an additional Lorentz transformation to the CM frame, but this expression is cumbersome and complicated. Second, invariant quantities involving the unit vector v^μ need to be included in the list of Lorentz-invariant quantities on which the tree-level amplitude can depend on. However, since the external momentum is expressed in terms of v^μ, these structures explicitly involving v^μ can be neglected. Finally, in the present context the dimer fields were introduced with the aim of simplifying the bookkeeping in order to write down the three-particle quantitation condition, in general matching of the three-body coupling to the underlying theory is not needed. Rather, the LECs appearing in the three-particle sector is fixed by fitting to the LQCD energy spectrum. Then these fitted parameters are used to calculated infinite-volume physical observables. With particle-dimer Lagrangian ready, the next section will introduce the *Faddeev equations* in the infinite volume.

3.3.4 Faddeev Equation in the Particle-Dimer Picture

The three-body amplitude is defined via the well-known Faddeev equations [215]. The Faddeev equations for the particle-dimer amplitude is diagrammatically shown in Fig. 3.7. Note that, here off-shell dimer fields need to be considered as at the end external vertices will be attached in order to obtain the three-particle amplitude. Moreover, the case of scalar dimers will be considered first and then the result will be generalized to dimer with spin following the steps laid down in Ref [81].

The Faddeev equation in the case of particle-dimer scattering is given by

$$\mathcal{M}(p,q) = \mathrm{Z}(p,q) + \int^{\Lambda_v} \frac{d^3k_\perp}{(2\pi)^3 2w_v(k)} \mathrm{Z}(p,k) D((K-k)^2) \mathcal{M}(k,q)\,, \tag{3.160}$$

where

$$\int^{\Lambda_v} \frac{d^3k_\perp}{(2\pi)^3 2w_v(k)} G(k) = \int \frac{d^4k}{(2\pi)^3} \delta(k^2 - M^2)\theta(\Lambda^2 + k^2 - (vk)^2) G(k)\,. \tag{3.161}$$

Here, the four-momenta of the external particles are denoted by p, q and the four-momenta of the dimers are given by $P = \sigma_p = K - p$ and $Q = \sigma_q = K - q$ with K being the total momentum of the

particle-dimer pair. Moreover, $x_\perp^\mu = x^\mu - v^\mu(vx)$ with x^μ representing an arbitrary vector.

An important point to note here is that while dimensional regularization was used in the two-body sector, in the particle-dimer picture one has to use the cutoff regularization scheme to account for non-perturbative treatment of the complex diagrams involved. Here, Λ represents this momentum cutoff.

The Kernel $\mathrm{Z}(p,q)$ is defined by the tree-level particle-dimer amplitude, corresponding to the first two diagrams in Fig. 3.7, and is given by

$$\mathrm{Z}(p,q) = \frac{f_0(s_p) f_0(s_q)}{2w_\nu(K-p-q)(w_\nu(p)+w_\nu(q)+w_\nu(K-p-q)-\nu K - i\epsilon)} + V_d(s,t,\sigma_p^2,\sigma_q^2)\,, \quad (3.162)$$

where

$$\begin{aligned} s_p &= (w_\nu(p)+w_\nu(K-p-q))^2 + (K-q)_\perp^2\,, \\ s_q &= (w_\nu(q)+w_\nu(K-p-q))^2 + (K-p)_\perp^2\,. \end{aligned} \quad (3.163)$$

Now, the variables s_p and s_q can be traded off for the off-shell dimer momentum by using the relation

$$\begin{aligned} s_q - \sigma_p^2 &= s_q - (K-q)^2 \\ &= (w_\nu(q)+w_\nu(K-p-q)+w_\nu(p)-\nu K)(w_\nu(q)+w_\nu(K-p-q)-w_\nu(p)+\nu K)\,, \end{aligned} \quad (3.164)$$

with a similar expression holding for $s_p - \sigma_q^2$. The term in the left bracket above cancels with the denominator. Now using the fact that the function $f_0(s)$ is a polynomial in the variable $s - 4M^2$ one can replace $f_0(s_{p/q})$ with $f_0(\sigma_{p/q}^2)$ absorbing the difference in the regular part of the second term in the kernel. With this the kernel becomes

$$\mathrm{Z}(p,q) = \frac{f_0(\sigma_p^2) f_0(\sigma_q^2)}{2w_\nu(K-p-q)(w_\nu(p)+w_\nu(q)+w_\nu(K-p-q)-\nu K - i\epsilon)} + \widetilde{V}_d(s,t,\sigma_p^2,\sigma_q^2)\,, \quad (3.165)$$

where $\widetilde{V}_d(s,t,\sigma_p^2,\sigma_q^2)$ is the modified short-range part. Note that the appearance of v^μ in the three-body short-range part is not problematic as at the end one always relates v^μ to K^μ.

Next, the three-particle on-shell amplitude can be calculated from the particle-dimer amplitude by attaching external vertices and summing over all possible combinations of spectator particles, see Fig. 3.8. Moreover, diagrams where only subsystems of two particles interact need to be included, these diagrams are referred to as disconnected diagrams. Hence, the on-shell three-particle scattering

amplitude is given by:

$$\begin{aligned}
T_3(p_1,p_2,p_3;q_1,q_2,q_3) &= T_3^{\text{dis}} + T_3^{\text{con}}\,,\\
T_3^{\text{dis}} &= \sum_{i,j=1}^{3}(2\pi)^3\delta^3(p_{i\perp}-q_{j\perp})2w_v(p_i)\tau((K-p_i)^2)\,,\\
T_3^{\text{con}} &= \sum_{i,j=1}^{3}\tau((K-p_i)^2)\mathcal{M}(p_i,q_j)\tau((K-q_j)^2)\,,
\end{aligned} \tag{3.166}$$

where $\tau((K-k)^2) = f_0(\sigma_k^2)D((K-k)^2)f_0(\sigma_k^2)$ with $\sigma_k^2 = (K-k)^2 - 4M^2$ was used.

An important remark needs to be made here. All expression above are manifestly Lorentz-invariant as the vector v^μ also transforms under Lorentz transformation along with the other vectors. Hence, by expressing v^μ in terms of the external momenta all amplitudes are rendered manifestly Lorentz-invariant.

The above expressions can be straightforwardly generalized to dimers with spin by replacing each quantity with corresponding matrix in Lorentz space:

$$\begin{aligned}
\mathcal{M} &\to \mathcal{M}_{n_l n_{l'}}\,,\\
\mathrm{Z} &\to \mathrm{Z}_{n_l n_{l'}}\,,\\
D &\to D_{n_l n_{l'}}\,.
\end{aligned} \tag{3.167}$$

With these replacements, the Faddeev equation becomes

$$\begin{aligned}
\mathcal{M}_{n_l n_{l'}}(p,q) &= \mathrm{Z}_{n_l n_{l'}}(p,q)\\
&\quad + \sum_{n_{l''}n_{l'''}}\int^{\Lambda_v}\frac{d^3k_\perp}{(2\pi)^3 2w_v(k)}\mathrm{Z}_{n_l n_{l''}}(p,k)D_{n_{l''}n_{l'''}}((K-k)^2)\mathcal{M}_{n_{l'''}n_{l'}}(k,q)\,.
\end{aligned} \tag{3.168}$$

The three-particle on-shell amplitude can then be defined as

$$\begin{aligned}
T_3(p_1,p_2,p_3;q_1,q_2,q_3) &= T_3^{\text{dis}} + T_3^{\text{con}}\,,\\
T_3^{\text{dis}} &= \sum_{i,j=1}^{3}(2\pi)^3\delta^3(p_{i\perp}-q_{j\perp})2w_v(p_i)\sum_{n_l n_{l'}}Y_{n_l}(\bar{p}^{(i)})\tau_{n_l n_{l'}}((K-p_i)^2)Y_{n_{l'}}(\bar{q}^{(j)})\,,\\
T_3^{\text{con}} &= \sum_{i,j=1}^{3}\sum_{n_l n_{l'} n_{l''} n_{l'''}}Y_{n_l}(\bar{p}^{(i)})\tau_{n_l n_{l'}}((K-p_i)^2)\\
&\quad\times\mathcal{M}_{n_{l'}n_{l''}}(p_i,q_j)\tau_{n_{l''}n_{l'''}}((K-q_j)^2)Y_{n_{l'''}}(\bar{q}^{(j)})\,,
\end{aligned} \tag{3.169}$$

where the function $Y_{n_l}(\bar{p})$ are defined in Eq. (3.139). Moreover, $\bar{p}^{(i)}$ is defined via the Lorentz transformation in Eq. (3.130) and the i in the superscript labels the spectator particle.

As mentioned earlier, cutoff regularization has to be used to render the particle-dimer amplitude UV finite. This leads to the coupling appearing in the particle-dimer interaction term becoming cutoff-dependent to counter the explicit Λ dependence. Moreover, the momentum in the dimer

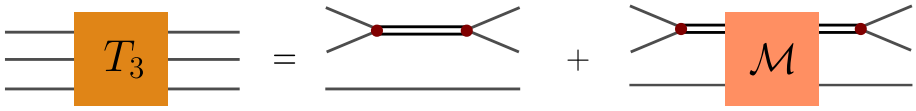

Figure 3.8: The three-particle scattering amplitude T_3 expressed in terms of the particle-dimer scattering amplitude $\mathcal{M}$. The full dimer propagator is denoted by the double black lines while the particle propagator is represented by the single gray line. The dark red dots denote particle-dimer conversion vertices.

propagator entering the Faddeev equation runs up to the hard scale given by Λ. The effective-range expansion is not a good approximation of the two-particle scattering amplitude at such high energies. This leads to the dimer propagator developing subthreshold poles called *spurious poles*. For the S-wave two-particle scattering amplitude in NREFT with $q^* = i\kappa$, the poles are at

$$\kappa_{1,2} = \frac{1 \mp \sqrt{1 - 2r_0/a_0}}{r_0} \,. \tag{3.170}$$

Note that the effective-range expansion is used up to $O((q^*)^2)$. The case where $a_0, r_0 > 0$ and $a_0 \gg r_0 \simeq \Lambda^{-1}$ constitutes an interesting situation. Here, the pole at κ_1 represents a shallow bound state (such as the deutron) and hence a stable dimer whereas the second pole at κ_2 represents a unphysical spurious pole. Even though the spurious pole lies far below threshold and outside the region of applicability of the theory, these poles still need to be integrated over in the particle-dimer integral equation. This can lead to unphysical behavior. Fortunately, these poles can be canceled out by adjusting the renormalization prescription of the short-range three-body interactions as shown in Refs. [216], in the infinite volume, and [217], in the finite volume.

3.3.5 Quantization Condition in the Three-Particle Sector

Similar to the infinite volume, the Faddeev equation can be written down for the particle-dimer amplitude in the finite volume by replacing all the integrals with the pertinent sums. In the following only the S-wave case is considered for simplicity, however for higher partial-waves one can again use the replacement given in Eq. (7.17) and the expressions can be straightforwardly modified.

In a finite volume, the Faddeev equation is given by

$$\mathcal{M}^{\text{fin}}(p,q) = \mathrm{Z}(p,q) + \frac{1}{L^3} \sum_{\mathbf{k}=\frac{2\pi\mathbf{n}}{L}} \frac{\theta(\Lambda^2 + M^2 - (vk)^2)}{2w(\mathbf{k})} \mathrm{Z}(p,k) D^{\text{fin}}(K-k) \mathcal{M}^{\text{fin}}(k,q) \,, \tag{3.171}$$

where L is the length of the finite-volume cubic box, assuming periodic boundary condition, $k^\mu = (w(\mathbf{k}), \mathbf{k})$ with $w(\mathbf{k}) = \sqrt{M^2 + \mathbf{k}^2}$ and $\mathbf{n} \in \mathbb{Z}^3$. Note that the definition of the kernel $\mathrm{Z}(p,q)$ remains the same as in infinite volume. The quantity $\mathcal{M}^{\text{fin}}$ represents the finite-volume particle-dimer amplitude and $D^{\text{fin}}(K)$ is defined as follows:

$$D^{\text{fin}}(K) = \frac{16\pi\sqrt{s}(f_0(s))^{-2}}{q^* \cot\delta_0(s) - \frac{2}{\sqrt{\pi}L\gamma} Z_{00}^{\mathbf{d}}(1;s)} \,, \tag{3.172}$$

where $Z_{00}^{\mathbf{d}}(1;s)$ is the Lüscher-zeta function defined in Eq. (3.48), $s = K^2$, $\gamma = \left(1 - \mathbf{K}^2/K_0^2\right)^{-1/2}$, $(q^*)^2 = (s/4 - M^2)$ and $\mathbf{d} = \mathbf{K}L/(2\pi)$.

While writing down the above expression one assumes that $s > 0$, for $s < 0$ one simply has to carry out the following replacement $D^{\text{fin}}(K) \to D(K^2)$ as below the two-particle threshold these two quantities only differ by exponentially suppressed corrections which can be neglected.

Similar to the case in the two-particle sector, the poles of the three-particle scattering amplitude corresponds to the finite-volume energy levels. The three-particle scattering amplitude is determined by the particle-dimer scattering amplitude and hence the poles of $\mathcal{M}^{\text{fin}}$ determine the finite-volume energy spectrum. Therefore the quantization condition takes the form of a determinant equation given by [81]:

$$\begin{aligned} &\det \mathscr{A}^{(3)} = 0\,, \\ &\mathscr{A}^{(3)}(p,q) = L^3 2w(\mathbf{p})\delta_{\mathbf{pq}}(D^{\text{fin}}(K-p))^{-1} - \mathrm{Z}(p,q)\,, \end{aligned} \tag{3.173}$$

where p, q are momenta that obey the condition $\Lambda^2 + M^2 - (vp)^2 \geq 0$, $\Lambda^2 + M^2 - (vq)^2 \geq 0$. Note that, unlike the two-particle case, here the determinant is also taken over the space of on-shell spectator momentum (in addition to angular momentum). The quantization condition can be partially diagonalized by projecting on the irreps of the octahedral group as shown in Ref. [177].

The three-body quantization condition given in Eq. (3.173) relates the finite-volume energy spectrum to the infinite-volume physical observables. Considering the rest frame for simplicity, i.e. $v^\mu = v_0^\mu = (1, \mathbf{0})$, the extraction process proceeds as follows: first, the relevant terms in the NREFT Lagrangian are identified based on the process considered and truncation is made based on power counting arguments. This leads to the relevant Lagrangian containing only a finite number of terms. After this step, the two-particle couplings are fixed by fitting to the finite-volume energy spectrum obtained from LQCD calculation using the Lüscher equation. These two-particle couplings can be directly related to scattering parameters via the ERE which corresponds to physical observables. Next, a cutoff Λ needs to be chosen, with which the three-body quantization condition can be used to fix the remaining LECs to the three-particle energy spectrum obtained from LQCD. With all the parameters successfully fitted[15] in the NREFT Lagrangian, the Faddeev equation can be solved in the infinite volume using the same cutoff[16] Λ to calculate infinite-volume physical observables in the three-particle sector.

3.3.6 Three-Particle Decay in Relativistic-Invariant Formulation of NREFT

After writing the Quantization condition in the three-particle sector, it is possible to move on to studying three-particle decay on the lattice. In order to do this, an analogue of the LL-factor needs to be derived in the three-particle sector as well. This three-body analogue of the LL-factor was derived in the NREFT setting in Ref. [100] and in the RFT setting in Ref. [102]. The LL-factor in moving frames was derived in the relativistic-invariant NREFT framework in Ref. [101]. The LL-factor for

[15] The LECs in the infinite volume and finite volume only differ by exponentially suppressed corrections and hence can be neglected.

[16] As stated earlier, the three-particle LECs are cutoff dependent and hence the same cutoff needs to be used in both finite and infinite volume.

three-particle decay will be derived in the relativistic-invariant NREFT setup in this section following Ref. [101] closely.

Before starting the derivation of the LL-factor in the three-particle case, an important issue needs to be addressed. Typically, NREFT is applied to systems where the typical momenta of particles denoted by p is very small compared to the mass of the lightest particle in the theory denoted by M, i.e. $p/M \ll 1$. This is in general not true in the case of three-particle decay such as the kaon-decay. However, if the decay amplitude can be approximated by a low-energy polynomial, the NREFT treatment can still be applied accurately. In the case kaon decay to three pions, the real part of the decay amplitude is measured very accurately and can be fit to a polynomial of low order in the Mandelstam variable s_i in whole region of the Dalitz plot as shown in Ref. [218]. Hence, the NREFT approach is applicable in this case. However, it should be noted that this may not be true for every three-particle decay and each case has to be dealt with accordingly. More generally, the NREFT approach can be used when it is known already that the inelastic channels do not play an important role in the process under consideration.

One starts with the particle-dimer Lagrangian derived in the previous sections and applies the Lorentz transformation of the type given in Eq. (3.153) to write down the Lagrangian in the following form:

$$\begin{aligned}\mathcal{L}_d &= \phi^\dagger 2w_v(i(v\partial) - w_v)\phi + \sum_{lm}\sigma_l\mathcal{T}^\dagger_{lm}\mathcal{T}_{lm} + \sum_{lm}(\mathcal{T}^\dagger_{lm}O_{lm} + \text{h.c.}) \\ &+ 4\pi\sum_{lm}\sum_{l'm'}\sum_{JM}\sum_{LL'}\mathcal{T}^\dagger_{lm}\Big(\mathcal{Y}^{Ll}_{JM}(\underline{\mathbf{w}},m)\phi^\dagger\Big)\mathcal{H}^{ll'}_{JL'L}(\Delta,\overleftarrow{\Delta}_d,\overrightarrow{\Delta}_d)\Big((\mathcal{Y}^{L'l'}_{JM}(\underline{\mathbf{w}},m'))^*\phi\Big)\mathcal{T}_{l'm'}\,, \qquad (3.174)\end{aligned}$$

where

$$\begin{aligned}\mathcal{T}_{lm} &= \sum_{\mu_1\ldots\mu_l}(C^{-1})^{lm}_{\mu_1\ldots\mu_l}\underline{\Lambda}^{\mu_1}_{\rho_1}\ldots\underline{\Lambda}^{\mu_l}_{\rho_l}\mathcal{T}^{\rho_1\ldots\rho_l}\,, \\ O_{lm} &= \sum_{\mu_1\ldots\mu_l}(C^{-1})^{lm}_{\mu_1\ldots\mu_l}\underline{\Lambda}^{\mu_1}_{\rho_1}\ldots\underline{\Lambda}^{\mu_l}_{\rho_l}O^{\rho_1\ldots\rho_l}\,. \qquad (3.175)\end{aligned}$$

As stated before $C^{lm}_{\mu_1\ldots\mu_l}$ are pure numerical coefficients that can be determined from the spherical functions. Here, l denotes the spin of the dimer and $m = -l,\ldots l$.

The Lorentz transformation matrix associated with the transformation above can be defined as follows:

$$\underline{\Lambda}^{\mu\rho}(v) = g^{\mu\rho} - \frac{v^\mu v^\rho}{1+(vv_0)} - \frac{v_0^\mu v_0^\rho}{1+(vv_0)} + \frac{v^\mu v_0^\rho + v_0^\mu v^\rho}{1+(vv_0)}(vv_0) - (v^\mu v_0^\rho - v_0^\mu v^\rho)\,. \qquad (3.176)$$

The Faddeev equation for particle-dimer amplitude in this case can then be written down as follows:

$$\begin{aligned}\mathcal{M}_{l'm',lm}(p,q) &= \mathrm{Z}_{l'm',lm}(p,q) \\ &+ \sum_{l''m''}\int^{\Lambda_v}\frac{d^3k_\perp}{(2\pi)^3 2w_v(k)}\mathrm{Z}_{l'm',l''m''}(p,k)D_{l''}((K-k)^2)\mathcal{M}_{l''m'',lm}(k,q)\,, \qquad (3.177)\end{aligned}$$

where $\mathcal{M}_{l'm',lm}(p,q)$ is the particle-dimer scattering amplitude with (lm) and $(l'm')$ denoting the

spin and magnetic quantum number of the dimer in the initial and final state respectively and the dimer propagator is denoted by $D_l((K-k)^2)$. The kernel takes the following form

$$\begin{aligned}\mathrm{Z}_{l'm',lm}(p,q) = &\frac{4\pi(\mathcal{Y}_{l'm'}(\tilde{\mathbf{p}}))^* f_{l'}(s_p) f_l(s_q)\mathcal{Y}_{lm}(\tilde{\mathbf{q}})}{2w_v(K-p-q)(w_v(p)+w_v(q)+w_v(K-p-q)-vK-i\epsilon)} \\ &+ 4\pi \sum_{JM}\sum_{LL'} \mathcal{Y}^{L'l'}_{JM}(\underline{\mathbf{p}},m')\mathcal{H}^{l'l}_{JL'L}(\Delta,\Delta_p,\Delta_q)\big((\mathcal{Y}^{Ll}_{JM}(\underline{\mathbf{q}},m)\big)^*\,, \end{aligned} \tag{3.178}$$

where

$$\begin{aligned}&\tilde{p}^\mu = \frac{1}{2}\underline{\Lambda}^{\mu\rho}(v)\Lambda_{\rho\alpha}(v,v_p)(\hat{q}-\hat{k})_\alpha\,, \quad \tilde{q}^\mu = \frac{1}{2}\underline{\Lambda}^{\mu\rho}(v)\Lambda_{\rho\alpha}(v,v_q)(\hat{p}-\hat{k})_\alpha\,,\\ &k^\mu = K^\mu - p^\mu - q^\mu\,, \quad v_p^\mu = \frac{(\hat{q}+\hat{k})^\mu}{\sqrt{s_p}}\,, \quad v_q^\mu = \frac{(\hat{p}+\hat{k})^\mu}{\sqrt{s_q}}\,,\\ &s_p = (\hat{q}+\hat{k})^2\,, \quad s_q = (\hat{p}+\hat{k})^2\,,\\ &\Delta = (K^2-9M^2)\,, \quad \Delta_p = (K-\hat{p})^2-4M^2\,, \quad \Delta_q = (K-\hat{q})^2-4M^2\,, \end{aligned} \tag{3.179}$$

with $\hat{x}^\mu = x^\mu - v^\mu(av) + v^\mu w_v(x)$ for a general vector x^μ and

$$\Lambda^{\mu\rho}(v,u) = g^{\mu\rho} - \frac{u^\mu u^\rho}{1+(vu)} - \frac{v^\mu v^\rho}{1+(vu)} + \frac{u^\mu v^\rho + v^\mu u^\rho}{1+(vu)}(vu) - (u^\mu v^\rho - v^\mu u^\rho)\,. \tag{3.180}$$

With this the three-particle quantization condition can be written down following the steps laid in the previous section as follows:

$$\begin{aligned}&\det \mathcal{A}^{(3)} = 0\,,\\ &\mathcal{A}^{(3)}_{l'm',lm}(p,q) = L^3 2w(\mathbf{p})\delta_{\mathbf{pq}}\Big(D^{\mathrm{fin}}_{l'm',lm}(K-p)\Big)^{-1} - \mathrm{Z}_{l'm',lm}(p,q)\,. \end{aligned} \tag{3.181}$$

Now, in addition to the terms mentioned in $\mathcal{L}_d$ one also has to include the kinetic term of the heavy particle which is given by

$$\mathcal{L}_h = h^\dagger 2w_v^h(i(v\partial) - w_v^h)h\,, \tag{3.182}$$

where h represents the heavy particle field and $w_v^h = \sqrt{M_h^2 + \partial^2 - (v\partial)^2}$ with M_h denoting the mass of the heavy particle.

Moreover, one has to also consider the term describing the decay of the heavy particle into the light particle-dimer pair. This is represented by the following term:

$$\mathcal{L}_G = \sqrt{4\pi}\sum_{lm}\frac{(-1)^l}{\sqrt{2l+1}}\Big(h^\dagger G_l(\Delta_d)\big((\mathcal{Y}_{l,-m}(\underline{\mathbf{w}})\big)^*\phi\big)\mathcal{T}_{lm} + \mathrm{h.c.}\Big)\,, \tag{3.183}$$

where $G_l(\Delta_d) = G_l^{(0)} + G_l^{(1)}\Delta_d + \ldots$ is a low-energy polynomial with $G_l^{(i)}$s representing the effective coupling in the theory[17]. The operator Δ_d acts on the dimer field with its action defined

[17] These couplings are assumed to be proportional to some small parameters in the underlying theory, for example the Fermi coupling in the case of weak decays.

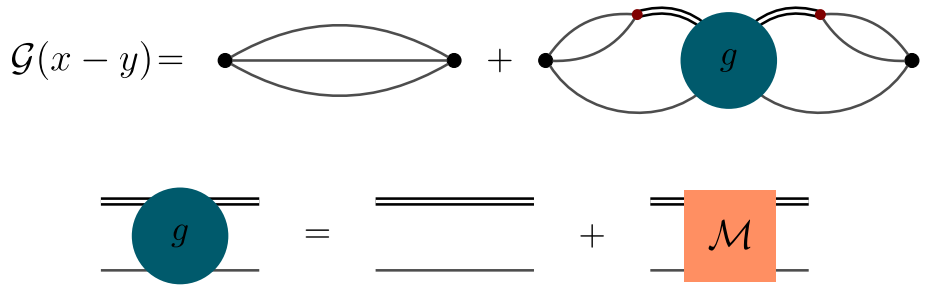

Figure 3.9: The Two-point function $\mathcal{G}(x-y)$ calculated in NREFT. The particle-dimer scattering amplitude is defined by $\mathcal{M}$. The double black line represents the full dimer propagator while the single gray line represents the particle propagator. The dark red dots correspond to the particle-dimer conversion vertices. The quantity g is given in Eq. (3.191).

by $\Delta_d T_{lm}(P) = (P^2 - 4M^2)T_{lm}(P)$. The tree level Lagrangian given in Refs. [205, 206] can be reproduced by integrating out the dimer fields. Finally, the full Lagrangian is given by

$$\mathcal{L} = \mathcal{L}_d + \mathcal{L}_h + \mathcal{L}_G \,. \tag{3.184}$$

Two-Point Function and Matrix Element

To derive the LL-factor in the three-particle case, one starts with the two-point function

$$\mathcal{G}(x-y) = \langle 0|T(O(x)O(y))|0\rangle \,, \tag{3.185}$$

where $O(x) = \phi^3(x)$ is a simple choice for source and sink operator. Inserting a complete set of eigenstates of the finite-volume Hamiltonian represented by $|n\rangle$ leads to

$$\mathcal{G}(x-y) = \sum_n e^{iP_n(x-y)} |\langle 0|O(0)|n\rangle|^2 \,, \tag{3.186}$$

where $\mathbf{P}_n = 2\pi\mathbf{n}/L$, $\mathbf{n} \in \mathbb{Z}^3$ represents the three-momentum of the intermediate states and it is assumed that $P_n^0 > |\mathbf{P}|$ with P_n^0 being the time component. Note that translational invariance was used in the expression above. Performing Wick rotation[18] to the Euclidean space one gets [101]

$$\mathcal{G}(x-y) = \sum_n e^{-P_{n,\parallel}(x-y)_\parallel} e^{-iP_{n,\perp}(x-y)_\perp} |\langle 0|O(0)|n\rangle|^2 \,, \tag{3.187}$$

where for an arbitrary vector a^μ the parallel and perpendicular components are defined as follows:

$$a_\parallel = va \,, \qquad a_\perp^\mu = a^\mu - v^\mu a_\parallel \,. \tag{3.188}$$

[18] Defining Wick rotation in the case of a quantization axis chosen parallel to the vector v^μ is a subtle issue and can be done by defining parallel and perpendicular components of the vectors involved and then analytically continuing to the Euclidean space.

Moreover, this quantity $\mathcal{G}(x-y)$ can also be calculated in the NREFT framework. One starts with the expression of $\mathcal{G}(x-y)$ in the infinite volume in the Minkowski space, which is given by

$$\mathcal{G}(x-y) = 3^2 \int \frac{dK_\parallel}{2\pi i} \frac{dK_\perp}{(2\pi)^3} e^{-iK_\perp (x-y)_\perp} e^{-iK_\parallel (x-y)_\parallel} \mathcal{G}(K)\,, \tag{3.189}$$

with $\mathcal{G}(K) = \mathcal{G}_0(K) + \mathcal{G}_1(K)$ and

$$\begin{aligned}
\mathcal{G}_0(K) &= \frac{2}{3} \int \frac{d^3k_{1,\perp}}{(2\pi)^3 2w_v(k_1)} \frac{d^3k_{2,\perp}}{(2\pi)^3 2w_v(k_2)} \\
&\quad \times \frac{1}{2w_v(K-k_1-k_2)\big(w_v(k_1)+w_v(k_2)+w_v(K-k_1-k_2)-K_\parallel - i\epsilon\big)}\,, \\
\mathcal{G}_1(K) &= 4\pi \sum_{lm,l'm'} \int \frac{d^3k_{1,\perp}}{(2\pi)^3 2w_v(k_1)} \frac{d^3k_{2,\perp}}{(2\pi)^3 2w_v(k_2)} \frac{d^3k_{3,\perp}}{(2\pi)^3 2w_v(k_3)} \frac{d^3k_{4,\perp}}{(2\pi)^3 2w_v(k_4)} \\
&\quad \times \frac{\mathcal{Y}_{l'm'}(\tilde{\mathbf{k}}_1) f_{l'}((K-k_3)^2)}{2w_v(K-k_1-k_3)\big(w_v(k_1)+w_v(k_3)+w_v(K-k_1-k_3)-K_\parallel - i\epsilon\big)} \\
&\quad \times g_{l'm',lm}(k_3,k_4;K) \\
&\quad \times \frac{f_l((K-k_4)^2)(\mathcal{Y}_{lm}(\tilde{\mathbf{k}}_2))^*}{2w_v(K-k_2-k_4)\big(w_v(k_2)+w_v(k_4)+w_v(K-k_2-k_4)-K_\parallel - i\epsilon\big)}\,.
\end{aligned} \tag{3.190}$$

Here, $\tilde{\mathbf{k}}_1, \tilde{\mathbf{k}}_2$ denote the relative momenta of the particle pairs which is boosted to the CM frame of the relevant dimers and the quantity $g_{l'm',lm}(k_3,k_4;K)$ is defined as follows:

$$\begin{aligned}
g_{l'm',lm}(k_3,k_4;K) &= \delta_{ll'}\delta_{mm'} 2w_v(k_3)\delta^3(k_{3,\perp}-k_{4,\perp}) D_l(K-k_3) \\
&\quad + D_{l'}(K-k_3)\mathcal{M}_{l'm',lm}(k_3,k_4) D_l(K-k_4)\,.
\end{aligned} \tag{3.191}$$

The Fig. 3.9 shows the graphical representation of $\mathcal{G}(x-y)$. The spectral representation can be used to write the particle-dimer scattering amplitude in terms of the wave function $\varphi_n^{l'm'}(k_3)$ and its conjugate $\bar{\varphi}_n^{lm}(k_4)$, with the label n representing the eigenvalues of the Hamiltonian, as follows:

$$\mathcal{M}_{l'm',lm}(k_3,k_4) = \sum_n \frac{\varphi_n^{l'm'}(k_3)\bar{\varphi}_n^{lm}(k_4)}{P_{n,\parallel} - K_\parallel - i\epsilon}\,. \tag{3.192}$$

The wave function introduced above obeys the homogeneous Faddeev equation which can be obtained by substituting the above expression in the Faddeev equation and identifying the pole contributions on both the sides. This equation is given by

$$\varphi_n^{lm}(k) = \sum_{l'm'} \int^{\Lambda_v} \frac{d^3q_\perp}{(2\pi)^3 2w_v(q)} \mathcal{Z}_{lm,l'm'}(k,q) D_l(K-q) \varphi_n^{l'm'}(q)\,. \tag{3.193}$$

Moreover, the normalization of the wave function can be fixed by using well-known techniques, c.f. Refs. [219, 220], and is given by

$$\begin{aligned}1 = &\sum_{lm}\int^{\Lambda_v}\frac{d^3q_\perp}{(2\pi)^3 2w_v(q)}\bar{\varphi}_n^{lm}(q)\left(\frac{d}{dK_\parallel}D_l(K-q)\right)\varphi_n^{lm}(q)\Big|_{K_\parallel=P_{n,\parallel}}\\ &+\sum_{l'm',lm}\int^{\Lambda_v}\frac{d^3q_\perp}{(2\pi)^3 2w_v(q)}\frac{d^3k_\perp}{(2\pi)^3 2w_v(k)}\\ &\times\bar{\varphi}_n^{l'm'}(q)D_{l'}(K-q)\left(\frac{d}{dK_\parallel}Z_{l'm',lm}(q,k)\right)D_l(K-k)\varphi_n^{lm}(k)\Big|_{K_\parallel=P_{n,\parallel}}.\end{aligned}\tag{3.194}$$

Now, one also needs the analogue of the two-point function in a finite volume. Since discretization is done in the rest frame, the integration momenta have to be boosted to the rest frame. This is done by using

$$\frac{d^3k_{i,\perp}}{(2\pi)^3 2w_v(k_i)}\to\frac{d^3\mathbf{k}_i}{(2\pi)^3 2w(\mathbf{k}_i)}\,,\qquad\frac{d^3K_\perp}{(2\pi)^3 2\sqrt{P_n^2-K_\perp^2}}\to\frac{d^3\mathbf{K}}{(2\pi)^3 2\sqrt{P_n^2+\mathbf{K}^2}}\,.\tag{3.195}$$

Note that the volume of the box needs to be adjusted such that $P_n^0=\sqrt{M_h^2+\mathbf{P}_n^2}$.

The two-point function in the finite volume can then be written down using Eqs. (3.191) and (3.192) in Eq. (3.190) and integrating over $K_\parallel$ as follows:

$$\begin{aligned}\mathcal{G}(x-y) = 3^2\frac{4\pi}{L^{15}}&\sum_{lm,l'm',l''m'',l'''m'''}\sum_{\mathbf{k}_1\mathbf{k}_2\mathbf{k}_3\mathbf{k}_4}e^{-iK_\perp(x-y)_\perp}e^{-iP_{n,\parallel}(x-y)_\parallel}\\ &\times\frac{\sqrt{M_h^2-K_\perp^2}}{2w(\mathbf{k}_1)2w(\mathbf{k}_2)2w(\mathbf{k}_3)2w(\mathbf{k}_4)\sqrt{M_h^2+\mathbf{K}^2}}\\ &\times\frac{\mathcal{Y}_{l'm'}(\tilde{\mathbf{k}}_1)f_{l'}((K-k_3)^2)D^{\text{fin}}_{l'm',l'''m'''}(K-k_3)\varphi_n^{l'''m'''}(k_3)}{2w_v(K-k_1-k_3)\big(w_v(k_1)+w_v(k_3)+w_v(K-k_1-k_3)-P_{n,\parallel}\big)}\\ &\times\frac{\bar{\varphi}_n^{l'''m'''}(k_4)D^{\text{fin}}_{l''m'',lm}(K-k_4)f_l((K-k_4)^2)(\mathcal{Y}_{lm}(\tilde{\mathbf{k}}_2))^*}{2w_v(K-k_2-k_4)\big(w_v(k_2)+w_v(k_4)+w_v(K-k_2-k_4)-P_{n,\parallel}\big)}+\ldots\,,\end{aligned}\tag{3.196}$$

where the pole contribution at $K_\parallel=P_{n,\parallel}$ with $P_n^2=M_h^2$ and given $\mathbf{K}$ is singled out. Moreover,

$$K_\perp^0=-\frac{\mathbf{v}^2}{v_0}P_{n,\parallel}+\frac{\mathbf{vK}}{v_0}\,,\quad\mathbf{K}_\perp=\mathbf{K}-\mathbf{v}P_{n,\parallel}\,.\tag{3.197}$$

The ellipses in the above expression denote the other single-pole contributions that appear in the spectral decomposition of the scattering amplitude which cancel out in the rest frame. Since the framework considered here is explicitly Lorentz-invariant this property should also be inherited to the moving frames.

The expression above can be analytically continued to the Euclidean space and compared to Eq. (3.187) to extract the matrix element $|\langle 0|O(0)|n\rangle|$ as follows:

$$|\langle 0|O(0)|n\rangle| = \frac{3\sqrt{4\pi}}{L^{\frac{3}{2}}}\left(\frac{M_h}{\sqrt{M_h^2+\mathbf{K}^2}}\right)^{\frac{1}{2}}\Bigg|\sum_{lm,l'm'}\frac{1}{L^6}\sum_{\mathbf{k}_1\mathbf{k}_3}^{\Lambda_v} \times \frac{\mathcal{Y}_{l'm'}(\tilde{\mathbf{k}}_1)f_{l'}((K-k_3)^2)D^{\text{fin}}_{l'm',lm}(K-k_3)\varphi_n^{lm}(k_3)}{2w(\mathbf{k}_1)2w(\mathbf{k}_3)2w_v(K-k_1-k_3)\big(w_v(k_1)+w_v(k_3)+w_v(K-k_1-k_3)-P_{n,\|}\big)}\Bigg|, \tag{3.198}$$

where $K^\mu = \big((P_{n,\|}+\mathbf{vK})/v_0, \mathbf{K}\big)$ and the cutoff Λ_v is explicitly mentioned. Now, the vector v^μ can be fixed along the vector K^μ as there is no summation in the variable $\mathbf{K}$. This leads to $K^\mu_\perp = 0$.

The finite-volume analogue of the wave function also obeys the homogeneous Faddeev equation given by

$$\varphi_n^{lm}(k) = \sum_{l'm',l''m''}\sum_{\mathbf{q}}^{\Lambda_v}\frac{1}{L^3 2w(\mathbf{q})}\mathcal{Z}_{lm,l''m''}(k,q)D^{\text{fin}}_{l''m'',l'm'}(K-q)\varphi_n^{l'm'}(q) \tag{3.199}$$

and the normalization can be fixed via the following expression:

$$\begin{aligned}1 = &\sum_{lm,l'm'}\sum_{\mathbf{q}}^{\Lambda_v}\frac{1}{L^3 2w(\mathbf{q})}\bar{\varphi}_n^{lm}(q)\left(\frac{d}{dK_\|}D^{\text{fin}}_{lm,l'm'}(K-q)\right)\varphi_n^{lm}(q)\Big|_{K_\|=P_{n,\|}}\\ &+\sum_{lm,l'm',l''m'',l'''m'''}\sum_{\mathbf{qk}}^{\Lambda_v}\frac{1}{L^6 2w(\mathbf{q})2w(\mathbf{k})}\bar{\varphi}_n^{l'm'}(q)D^{\text{fin}}_{l'm',l''m''}(K-q)\\ &\times\left(\frac{d}{dK_\|}\mathcal{Z}_{l''m'',l'''m'''}(q,k)\right)D^{\text{fin}}_{l'''m''',lm}(K-k)\varphi_n^{lm}(k)\Big|_{K_\|=P_{n,\|}}.\end{aligned} \tag{3.200}$$

Decay Matrix Element

Next, Consider the following two-point function

$$\mathcal{G}_h(x) = \langle 0|T(O(x)\mathcal{J}_h^\dagger(0))|0\rangle\,, \tag{3.201}$$

where the current $\mathcal{J}_h^\dagger(z) = \frac{\delta\mathcal{L}_G}{\delta h(z)}$ acts as the source operator for the field $h(z)$. Inserting a complete set of states in the above expression and using translational invariance one gets,

$$\mathcal{G}_h(x) = \sum_n e^{-iP_{n,\|}x_\|}e^{-iP_{n,\perp}x_\perp}\langle 0|O(0)|n\rangle\langle n|\mathcal{J}_h^\dagger(0)|0\rangle\,. \tag{3.202}$$

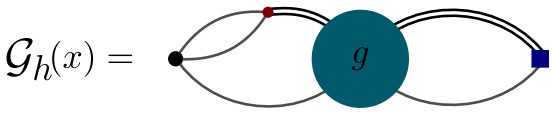

Figure 3.10: The two-point function $\mathcal{G}_h(x)$ calculated in the NREFT. The full dimer propagator is represented by the double black lines whereas the single gray line represents the particle propagator. The dark red dot corresponds to the particle-dimer conversion vertex and the dark blue square corresponds the sink operator $\mathcal{J}_h^\dagger(0)$.

Again this quantity can be calculated in the NREFT in the infinite volume and is given by

$$\begin{aligned}\mathcal{G}_h(x) = 3 \int \frac{K_\parallel}{2\pi i} \frac{d^3K_\perp}{(2\pi)^3} e^{-iK_\parallel x_\parallel} e^{-iK_\perp x_\perp} \\ \times 4\pi \sum_{lm,l'm'} \frac{(-1)^{l'}}{\sqrt{2l'+1}} \int \frac{d^3k_{1,\perp}}{(2\pi)^3 2w_v(k_1)} \frac{d^3k_{2,\perp}}{(2\pi)^3 2w_v(k_2)} \frac{d^3k_{3,\perp}}{(2\pi)^3 2w_v(k_3)} \\ \times \frac{f_l((K-k_2)^2)\mathcal{Y}_{lm}(\tilde{\mathbf{k}}_2) g_{lm,l'm'}(k_2,k_3;K)\mathcal{Y}_{l',-m'}(\underline{\mathbf{k}}_3) G_l((K-k_3)^2)}{2w_v(K-k_1-k_2)\big(w_v(k_1)+w_v(k_2)+w_v(K-k_1-k_2)-K_\parallel-i\epsilon\big)},\end{aligned} \tag{3.203}$$

where G_l is defined below Eq. (3.183). This two-point function is shown graphically in Fig. 3.10.

The finite-volume counterpart of the above mentioned two-point function can be written down by following the steps given in the previous section and is given by

$$\begin{aligned}\mathcal{G}_h(x) = 3 \sum_{lm,l'm',l''m'',l'''m'''} \frac{4\pi}{L^{12}} \frac{(-1)^{l'}}{\sqrt{2l'+1}} \sum_{\mathbf{k}_1\mathbf{k}_2\mathbf{k}_3} \frac{e^{-iP_{n,\parallel}x_\parallel} M_h}{2w(\mathbf{k}_1)2w(\mathbf{k}_2)2w(\mathbf{k}_3)\sqrt{M_h^2+\mathbf{K}^2}} \\ \times f_l((K-k_2)^2)\mathcal{Y}_{lm}(\tilde{\mathbf{k}}_2) D^{\text{fin}}_{lm,l''m''}(K-k_2)\varphi_n^{l''m''}(k_2) \\ \times \frac{\bar{\varphi}_n^{l'''m'''}(k_3) D^{\text{fin}}_{l'''m''',l'm'}(K-k_3)\mathcal{Y}_{l',-m'}(\underline{\mathbf{k}}_3) G_l((K-k_3)^2)}{2w_v(K-k_1-k_2)\big(w_v(k_1)+w_v(k_2)+w_v(K-k_1-k_2)-P_{n,\parallel}\big)} + \dots,\end{aligned} \tag{3.204}$$

where the pole contribution at $K_\parallel = P_{n,\parallel}$ with $P_n^2 = M_h^2$ for a given $\mathbf{K}$ is displayed explicitly. Comparing this expression to the one in Eq. (3.202) and using Eq. (3.198), one gets

$$\begin{aligned}L^{\frac{3}{2}}\langle n|\mathcal{J}_h^\dagger(0)|0\rangle = \pm\sqrt{4\pi}\left(\frac{M_h}{\sqrt{M_h^2+\mathbf{K}^2}}\right)^{\frac{1}{2}} \sum_{lm,l'm'} \frac{(-1)^{l'}}{\sqrt{2l'+1}} \sum_{\mathbf{k}}^{\Lambda_v} \frac{1}{L^3 2w(\mathbf{k})} \\ \times \bar{\varphi}_n^{lm}(k) D^{\text{fin}}_{lm,l'm'}(K-k)\mathcal{Y}_{l',-m'}(\underline{\mathbf{k}}) G_l((K-k)^2)\,.\end{aligned} \tag{3.205}$$

The finite-volume decay matrix element is real-valued and hence the ± sign gives the phase of this quantity. Although, the choice of sign is a subtle issue and is detailed in Ref. [102], similar to Ref. [101], in rest of this section the above mentioned matrix element will be defined with the positive sign.

$$\langle\phi(\mathbf{k}_1)\phi(\mathbf{k}_2)\phi(\mathbf{k}_3);\text{out}|\,\mathcal{J}_h^\dagger(0)|0\rangle =$$

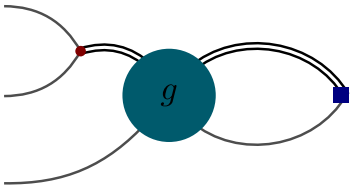

Figure 3.11: Graphical representation of the infinite-volume decay matrix element. The full dimer propagator is represented by the double black lines whereas the single gray line represents the particle propagator. The dark red dot corresponds to the particle-dimer conversion vertex.

Moreover, in the infinite volume the decay matrix element is given by

$$\begin{aligned}\langle\phi(\mathbf{k}_1)\phi(\mathbf{k}_2)\phi(\mathbf{k}_3);\text{out}|\mathcal{J}_h^\dagger(0)|0\rangle = 4\pi \sum_{lm,l'm'} \frac{(-1)^{l'}}{\sqrt{2l'+1}} \sum_{j=1}^{3} \int \frac{d^3k_\perp}{(2\pi)^3 2w_\nu(k)} f_l((K-k_j)^2)\mathcal{Y}_{lm}(\tilde{\mathbf{k}}_j) \\ \times g_{lm,l'm'}(k_j,k;K)\mathcal{Y}_{l',-m'}(\underline{\mathbf{k}})G_l((K-k)^2)\,. \end{aligned} \tag{3.206}$$

This decay matrix element is explicitly Lorentz-invariant and is shown in Fig. 3.11.

LL Formula in the Three-particle Sector

As stated before the quantity $G_l(\Delta_d)$ is a low-energy polynomial and can be expanded as follows:

$$G_l(\Delta_d) = G_l^{(0)} + G_l^{(1)}\Delta_d + \dots\,, \tag{3.207}$$

implying that at any given order in the NREFT power counting, only a finite number of couplings $G_l^{(i)}$ need to be considered. For a generic small parameter ϵ with $p_\perp = O(\epsilon)$, at $O(\epsilon^{2n})$, $N = (n+1)(n+2)/2$ couplings $G_l^{(i)}$ need to be taken into account with $i = 0,\dots,n-l/2$. Note that, the operator Δ_d counts as $O(\epsilon^2)$ and the function $\mathcal{Y}_{l,-m}(\underline{\mathbf{k}})$ counts as $O(\epsilon^l)$ where l represents a given even angular momentum quantum number. This number N can be further reduced based on symmetry arguments.

Consider a lattice setup ζ with the total momentum represented by $\mathbf{K}_\zeta$ and box length represented by L_ζ. One can then write down the finite-volume decay matrix element in this lattice setup after expanding $G_l((K-k)^2)$ as follows:

$$L_\zeta^{\frac{3}{2}}\langle n|\mathcal{J}_h^\dagger(0)|0\rangle_\zeta = \sum_{l=0}^{2n}\sum_{i=0}^{n-l/2} a_l^{(i)}(K_\zeta,L_\zeta)G_l^{(i)} \equiv \sum_{\alpha=1}^{N} a_{\zeta\alpha}G_\alpha\,, \tag{3.208}$$

where the expression for $a_l^{(i)}(K_\zeta,L_\zeta)$ can be obtained by comparing the above expression to Eq. (3.205).

The infinite-volume decay matrix element can also be written down in a similar form and is given by

$$\langle\phi(\mathbf{k}_1)\phi(\mathbf{k}_2)\phi(\mathbf{k}_3);\text{out}|\mathcal{J}_h^\dagger(0)|0\rangle = \sum_{l=0}^{2n}\sum_{i=0}^{n-l/2} A_l^{(i)}(K)G_l^{(i)} \equiv \sum_{\alpha=1}^{N} A_\alpha(K)G_\alpha\,, \tag{3.209}$$

where K represents the total momentum of the three-particle system and the expression for $A_l^{(i)}(K)$ can be obtained by comparing the above expression to Eq. (3.206).

The dependence of the infinite-volume matrix element on the couplings $G_l^{(i)}$ can be removed by making N measurements of the finite-volume decay matrix element in different lattice setups and using Eq. (3.208), resulting in the following expression

$$\langle \phi(\mathbf{k}_1)\phi(\mathbf{k}_2)\phi(\mathbf{k}_3); \text{out}|\mathcal{J}_h^\dagger(0)|0\rangle = \sum_{\zeta=1}^{N} (\Phi_3)_\zeta L_\zeta^{\frac{3}{2}} |\langle n|\mathcal{J}_h^\dagger(0)|0\rangle|_\zeta \,. \tag{3.210}$$

Here $(\Phi_3)_\zeta$ represents the LL-factor in the three-particle case and is given by

$$(\Phi_3)_\zeta = \sum_{\alpha=1}^{N} A_\alpha(K)(a^{-1})_{\alpha\zeta} \,, \tag{3.211}$$

with

$$\begin{aligned} A_\alpha(K) &= \left(A_0^{(0)}(K)\, A_0^{(1)}(K)\, \ldots\, A_0^{(N)}(K)\, \ldots\, A_{2n}^{(0)}(K)\right), \\ a &= \begin{pmatrix} a_0^{(0)}(K_1,L_1) & a_0^{(1)}(K_1,L_1) & \ldots & a_0^{(N)}(K_1,L_1) & \ldots & a_{2n}^{(0)}(K_1,L_1) \\ \vdots & & \ddots & & & \vdots \\ a_0^{(0)}(K_N,L_N) & a_0^{(1)}(K_N,L_N) & \ldots & a_0^{(N)}(K_N,L_N) & \ldots & a_{2n}^{(0)}(K_N,L_N) \end{pmatrix} \end{aligned} \tag{3.212}$$

and a^{-1} being the inverse of the matrix a. Note that the lattice size L_ζ has to be fixed such that $K^0 = \sqrt{M_h^2 + \mathbf{K}_\zeta^2}$ for every ζ.

Similar to the two-particle case, the LL-factor in the three-particle case only depends on the short-range interaction of the light particle. However, unlike the two-particle case, the LL-factor here is a matrix. The process of extracting the infinite-volume decay amplitude proceeds as follows: first, the LECs in the two-body and three-body sector are fixed by fitting to the finite-volume energy spectra using the respective quantization conditions. With this, the amplitudes $A_l^{(i)}(K)$ and $a_l^{(i)}(K,L)$ can be determined. Next, the finite-volume decay matrix element is extracted in different moving frames, ensuring the energy level of the moving heavy particle coincides with the energy of the three-particle eigenstate by fixing the box size as needed. Finally, the infinite-volume decay amplitude can be calculated using the LL-factor as derived above. One of the aims of this research project was to apply this compact formalism to the weak decay of kaon into three pions and determine the LL-factor. This will be detailed in Chap. 7.

CHAPTER 4

Lüscher Equation with Long-Range Forces

The content of the following chapter is based on the publication

- R. Bubna, H.-W. Hammer, F. Müller, J.-Y. Pang, A. Rusetsky and J.-J. Wu, *Lüscher equation with long-range forces*, JHEP **05** (2024) 168, arXiv: 2402.12985 [hep-lat]

A modified version of the Lüscher equation is derived in the presence of the long-range force caused by the exchange of a light particle. This long-range force leads to strong partial-wave mixing and the t-channel sub-threshold singularities. The modified Lüscher equation enables one to circumvent these problems effectively. The approach detailed in the following is intrinsically linked to the so-called modified effective-range expansion (MERE) in the infinite volume. Moreover, a detailed comparison with the two recently proposed alternative approaches was also discussed.

In systems such as the NN system, exchange of light particles lead to the partial-wave projected amplitude developing a t-channel cut which lies relatively close to the threshold. The original Lüscher's method is no more applicable, as it would predict a real K-matrix in this region, where the K-matrix is complex. Moreover, above threshold the presence of long-range interactions result in the partial-wave expansion converging very slowly. The aim of this project was to address these issue and provide a modified Lüscher equation for extracting physical observables from lattice data in the presence of long-range interactions. Technical considerations such as spin, relativistic kinematics or moving frames are relegated to future publications.

To achieve the goal of modifying the Lüscher equation, the long-range and short-range part of the potential were split and then the modified effective-range expansion introduced in Ref. [64] was used. The MERE utilizes the fact that the long-range potential is explicitly known. Furthermore, the MERE helps to define a modified effective-range function which is a low-energy polynomial with a larger radius of convergence than the original ERE. The project started with recasting the MERE in the language of NREFT, following Ref. [222] closely. An important point to note here is that the functions, corresponding to the long-range part, entering the MERE are only defined for "superregular" potentials [202]. Potentials such as the Yukawa potential, considered here, which do not fall in the category of superregular potential have to be modified. This modification boils down to imposing a renormalization prescription. The choice of this renormalization prescription does not affect the result, albeit some regularization schemes would be more numerically stable than others. Moreover, the long-range potential is assumed to be local and spherically symmetric. These constraints on the long-range part play an important role in the derivation of MERE. It was explicitly shown that the

modified effective-range function is indeed a low-energy polynomial and all the effects related to the long-range part were included in functions that do not depend on the short-range part.

At the next step, the MERE was then reformulated in a finite volume using the eigenvectors of the long-range part of the Hamiltonian and replacing integrals with finite-volume sums. After that, a modified quantization condition with the long-range part split off was derived. This modified equation requires the definition of the modified Lüscher function. Even though this modified function is free of UV divergence, due to the renormalization prescription imposed on the potential, it still requires a matching to ensure consistency with its infinite-volume counterpart. This issue was discussed in detail both above and below threshold. The author independently checked all the formula given in the text. Moreover, numerical tests with the long- plus short-range potential were carried out by the author, which verified the analytical results. However, these tests were not included in the final text.

The modified Lüscher function can be calculated explicitly as the long-range potential is a well-known function whereas the parameters of short-range interaction which is encoded in the modified effective-range function can be fit from lattice data. At the end, this approach with the modified Lüscher equation was qualitatively compared to existing approaches proposed in Refs. [56, 57, 60–62]. A complete numerical implementation of the modified Lüscher equation is considered in the next chapter.

4.1 Introduction

In recent decades, the Lüscher method [33] has become a standard tool for the extraction of the scattering phase shifts from the finite-volume energy levels, measured in lattice QCD. The method has been generalized to the case of moving frames, particles with spin and coupled two-body channels (see here [34–36, 39, 41, 42, 223–228] for a representative list of references). In all cases, the formalism is based on the fundamental assumptions, namely:

- The interactions between particles are short-range. The relation $R/L \ll 1$ holds, where R is the characteristic range of interaction and L denotes the size of the cubic box (the spatial extension of the lattice) in which the system is placed. The quantity R is typically given by the inverse of the lightest mass in the theory, $R \sim M^{-1}$.

- Owing to the condition $R/L \ll 1$, the polarization corrections, proportional to $\exp(-L/R)$, are strongly suppressed and can be neglected. This allows one to write down an equation (referred to as the Lüscher equation or the two-body quantization condition), which determines the finite-volume spectrum in terms of the observables (S-matrix elements) only. The details of the short-range interactions do not matter.

- Again, owing to the condition $R/L \ll 1$, the partial-wave mixing is small, and it is possible to truncate higher partial-waves in the Lüscher equation.

Obviously, the condition $R/L \ll 1$ is violated, when the scattering in the presence of the electromagnetic interactions is considered (QCD+photons on the lattice). Moreover, at physical quark masses the pions are rather light, which leads to problems in the study of nucleon-nucleon interactions on the lattice. Namely, as explicitly demonstrated in the recent paper [56], the partial-wave mixing at the physical point in the Lüscher equation for the NN scattering is indeed substantial. A closely related problem is the appearance of the so-called t-channel (left-hand) cut in the NN partial-wave scattering

amplitudes, running from negative infinity till $s = (2m_N)^2 - M_\pi^2$ along the real axis in the complex s-plane, see, e.g., [59, 60] (Here, m_N and M_π denote the nucleon and the pion masses, respectively.). Since $M_\pi \ll m_N$ in nature, the gap between the t-channel cut and the right-hand unitarity cut is very small. On the other hand, as seen in the latest studies of the NN scattering on the lattice, many energy levels are located on the t-channel cut (see, e.g., Fig. 3 in Ref. [55]). The standard Lüscher approach is obviously not applicable in this case. Note also that NN scattering is not only the physically interesting process where these problems emerge. For example, in the description of the $T_{cc}(3875)^+$ state the same problem shows up in full glory. Moreover, it can be seen that the structure of the singularities is completely different in the two cases $M_\pi < M_{D^*} - M_D$ and $M_\pi > M_{D^*} - M_D$, and hence reveals a critical dependence on the values of quark masses used in the lattice calculations [58].

As a remedy to the above problems, the authors of Ref. [56] have advocated solving the quantization condition in the three-dimensional plane-wave basis, in order to determine the parameters of the effective chiral Lagrangian directly from the fit to the lattice energy levels.[1] A similar method has recently been applied to the analysis of lattice data aimed at the extraction of the $T_{cc}(3875)^+$ pole [57, 58].[2] This proposal solves the problem in principle and translates the output of lattice calculations into the parameters of the effective Hamiltonian. The phase shifts and other infinite-volume observables are then obtained by solving integral equations in the infinite volume. As a side remark, note that a (conceptually) similar solution is adopted in all formulations of the three-body quantization condition [67–71, 231], where no other approach to the problem has been found so far. However, in the much simpler two-body case, one is tempted to look further for the alternatives (similar to the Lüscher formula) which directly express the finite-volume two-body spectrum in terms of the physical observables.

An alternative solution, which has been suggested recently [59, 60], is based on splitting the hadron interactions into the long-range and short-range components that are then treated separately. In this respect, the approach described in these papers is conceptually close to the one pursued in the present work. While a detailed comparison of all existing approaches will be given at the end of this work, we still mention here the most important difference between Refs. [59, 60] and our approach. Namely, in Refs. [59, 60] an auxiliary on-shell K-matrix $\bar{K}^{\text{os}}$ has been introduced, which has to be determined from the fit to the lattice data. Once this is done, one should solve the integral equations, in order to arrive at the physical amplitudes. So, it is essentially a two-step process. In our approach an analog of this auxiliary K-matrix is introduced as well. However, its relation to the physical amplitude has an algebraic form and there is no need to solve integral equations. From this point of view, our approach is closer to the original Lüscher single-step formalism than the approach described in Refs. [59, 60].

Note also that in Ref. [61], in the context of the study of the $T_{cc}(3875)^+$ meson, it was proposed to solve the problem of the t-channel cut by writing down three-body equations, even in case of a stable D^* meson. Below, we shall consider this proposal in more detail. Here we only note that, in latter case, it is very close to the solution proposed in Refs. [56–58].

For completeness, we also note that, the two-body quantization condition (as well as the two-body Lellouch-Lüscher formula) in the presence of the Coulomb force was considered in Refs. [232–234]. In the final expressions, the Coulomb potential has been treated perturbatively in the fine structure

[1] Albeit all calculations in Ref. [56] have been carried out in the framework of the chiral EFT, one could choose here any EFT that allows a *controllable* expansion of the scattering amplitude in some small parameter(s) in the energy region of interest.

[2] Note also that earlier the same method has been used in the continuum, namely, for the study of the energy dependence of the NN scattering amplitude at non-physical quark masses as well [229, 230].

constant. Such a treatment can be justified for sufficiently small values of the box size L.

The aim of the present chapter is to address the problem of the long-range force in the Lüscher equation in a general fashion and to derive a modified Lüscher equation, which has a much larger domain of applicability than the original one. To simplify life as much as possible, in the present situation we do not consider the theories with massless particles – the inclusion of QED is relegated to future publications. Furthermore, we ignore purely technical issues like the inclusion of spin, relativistic kinematics or moving frames. The key observation that allows one to achieve the stated objective is that the long-range part of the potential, which gives rise to all above problems, is usually well known and can be expressed in terms of few parameters that can be accurately measured on the lattice. The short-range part of potential is unknown and should be fitted to the lattice data on the two-body energy levels by using the modified Lüscher equation.

We shall see below that the method to achieve the above goal is to reformulate the so-called modified effective-range expansion (MERE) [64] in a finite volume. To this end, in Sect. 4.2 we invest a certain effort to relate MERE to the non-relativistic effective theory (NREFT) framework along the lines described in Ref. [222] and discuss, in particular, the inclusion of the non-derivative couplings which were omitted in Ref. [222]. The latter framework can be directly recast in a finite volume, as done in Sect. 4.3, and leads to a modified quantization condition with the long-range part split off. Section 4.4 is dedicated to the comparison of our approach to alternative ones known in the literature. The numerical implementation of the proposed framework constitutes a separate piece of work and will not be considered here.

4.2 Modified Effective-Range Expansion in the Effective Field Theory Framework

4.2.1 Modified Effective-Range Expansion

In Ref. [64], van Haeringen and Kok consider a non-relativistic scattering problem for a sum of two local, rotationally invariant potentials:

$$V(r) = V_L(r) + V_S(r)\,. \tag{4.1}$$

Here, $V_L(r)$ and $V_S(r)$ denote the long-range and short-range parts of the potential, respectively. Due to the long-range nature of the full potential, the effective-range expansion in the partial-wave with the angular momentum ℓ,

$$q^{2\ell+1}\cot\delta_\ell(q) = -\frac{1}{a_\ell} + \frac{1}{2}\,r_\ell q^2 + \cdots\,, \tag{4.2}$$

has a very small radius of convergence. This happens, e.g., if the effective range r_ℓ and the subsequent coefficients (shape parameters) are unnaturally large. However, for a general long-range potential it is also possible that the radius of convergence is zero, as in the case of a Coulomb potential.

Further, the authors define the function

$$K_\ell^M(q^2) = M_\ell(q) + \frac{q^{2\ell+1}}{|f_\ell(q)|^2}\,\left(\cot(\delta_\ell(q) - \sigma_\ell(q)) - i\right)\,. \tag{4.3}$$

Here, $\delta_\ell(q), \sigma_\ell(q)$ denote, respectively, the full phase shift and the phase shift in the problem with the long-range potential $V_L(r)$ only (i.e., setting $V_S(r) = 0$). Furthermore,

$$M_\ell(q) = \frac{1}{\ell!}\left(-\frac{iq}{2}\right)^\ell \lim_{r\to 0} \frac{d^{2\ell+1}}{dr^{2\ell+1}}\, r^\ell \frac{f_\ell(q,r)}{f_\ell(q)}\,, \tag{4.4}$$

where $f_\ell(q,r)$ is the Jost solution in the case $V_S(r) = 0$, and

$$f_\ell(q) = \frac{q^\ell e^{-i\ell\pi/2}(2\ell+1)}{(2\ell+1)!!} \lim_{r\to 0} r^\ell f_\ell(q,r)\,. \tag{4.5}$$

The main result of Ref. [64] consists in demonstrating the fact that the quantity $K_\ell^M(q^2)$, defined by Eq. (4.3), is a polynomial in the variable q^2, with a radius of convergence much larger than the original version of the effective-range expansion, displayed in Eq. (4.2).

The derivation given in Ref. [64], however, has a caveat that has been briefly mentioned already in the same paper and was discussed in more detail in Ref. [202]. Namely, the quantity $M_\ell(q)$ is well-defined, if and only if the potential $V_L(r)$ is regular enough at the origin, so that $r^{-2\ell}V_L(r)$ stays analytic at $r = 0$. The class of such potentials is termed "superregular" in Ref. [202]. The usual Coulomb or Yukawa potentials do not belong to this class, even for S-wave scattering.

If one is dealing with potentials which are not superregular, one has to use certain convention on top of Eq. (4.4) in order to define the quantity $M_\ell(q)$. This is nothing but a renormalization prescription that has to be imposed on the ultraviolet-divergent loop containing an arbitrary number of instantaneous "exchanges" corresponding to the potential $V_L(r)$. A non-trivial problem consists in a mathematically consistent formulation of the renormalization prescription, using the same language as used in the derivation of Eqs. (4.3) and (4.4). There exists a well-known exact solution of the problem for any ℓ in case of the Coulomb interaction that is given in the textbooks, see, e.g., [235]. The solution for a general potential which is less singular than $r^{-3/2}$ is discussed in Ref. [202] albeit only in the case $\ell = 0$ and, roughly speaking, boils down to a subtraction of the q-independent (divergent) constant from $M_\ell(q)$. We are not, however, aware of the discussion of the case $\ell \neq 0$ in the literature. The term that is divergent at $r \to 0$ can be identified in this case as well. However, its coefficient is q-dependent, in general, and the challenge consists in showing that this coefficient is a low-energy polynomial in q^2 in the wide region determined by the heavy scale. For this reason, here we adopt a different strategy. Namely, we truncate the partial-wave expansion $\ell \le \ell_{\rm max}$ from the beginning and regularize the potential $V_L(r)$ in order to render it superregular. For example, a kind of the Pauli-Villars regularization will perfectly do the job in case of the Yukawa potential we shall be primarily dealing with:

$$V_L(r) = \frac{g e^{-M_\pi r}}{r} \to \frac{g e^{-M_\pi r}}{r} - \sum_{i=1}^{2\ell_{\rm max}+1} c_i \frac{g e^{-M_i r}}{r}\,. \tag{4.6}$$

Here, $M_i = n_i M$, where M denotes a typical heavy scale of the theory (determined, for instance, by the inverse range in $V_S(r)$), whereas n_i are numbers of order unity. The requirement that the first

$2\ell_{\text{max}} + 1$ terms in the Laurent expansion vanish leads to the following linear system of equations:

$$\begin{aligned} 1 &= \sum_{i=1}^{2\ell_{\text{max}}+1} c_i \,, \\ \frac{M_\pi}{M} &= \sum_{i=1}^{2\ell_{\text{max}}+1} c_i n_i \,, \\ &\cdots \,, \\ \left(\frac{M_\pi}{M}\right)^{2\ell_{\text{max}}} &= \sum_{i=1}^{2\ell_{\text{max}}+1} c_i n_i^{2\ell_{\text{max}}} \,. \end{aligned} \tag{4.7}$$

It is straightforwardly seen that the regularized potential is indeed superregular for all $\ell \leq \ell_{\text{max}}$. Note, however, that the $2\ell_{\text{max}} + 1$ equations in Eq. (4.7) do not determine the n_i and c_i uniquely. The constants n_i have to be picked such that the masses $M_i = n_i M$ are of order M and different from each other. This ensures that Eq. (4.7) has a solution and no unnaturally large coefficients c_i emerge.

Finally, in the splitting $V(r) = V_L(r) + V_S(r)$, one could modify both $V_L(r)$ and $V_S(r)$, adding and subtracting the same string of the short-range Yukawa terms. This will render $V_L(r)$ superregular and will not change the interpretation of $V_S(r)$ as a short-range potential. Hence, the above regularization serves solely the purpose of recasting the potential into the form that obeys the requirements of Ref. [64].

4.2.2 NREFT Framework

In the literature, there have been several attempts to reformulate the modified effective-range expansion in the effective field theory language [222, 232, 236, 237]. We shall mainly follow the path outlined in these papers and derive an analog of Eq. (4.3) in the effective field theory setting. In order to do this, we recall that, in the non-relativistic effective field theory, the scattering amplitude is merely a solution of the Lippmann-Schwinger (LS) equation with the potential determined by a matrix element of the interaction Lagrangian between the free two-particle states. We still assume that the potential is a sum of long-range and short-range parts, but do not assume anymore that the potential is local. The short-range potential in momentum space is a familiar low-energy polynomial. Its partial-wave expansion can be written in the following form

$$\langle \mathbf{p}|V_S|\mathbf{q}\rangle = 4\pi \sum_{\ell m} Y_{\ell m}(\hat{p}) V_S^\ell(p,q) Y_{\ell m}^*(\hat{q}) \,. \tag{4.8}$$

Here,

$$V_S^\ell = (pq)^\ell \sum_{a=0}^{\infty} \sum_{b=0}^{a} C_\ell^{ab} (p^2)^b (q^2)^{a-b} \,, \qquad C_\ell^{ab} = C_\ell^{ba} \,. \tag{4.9}$$

Furthermore, $p = |\mathbf{p}|$, $\hat{p}$ denotes a unit vector in direction of $\mathbf{p}$, and $Y_{\ell m}(\hat{p})$ are the spherical harmonics. Writing down explicitly the first few terms in the potential, one gets

$$\langle \mathbf{p}|V_S|\mathbf{q}\rangle = C_0^{00} + 3C_1^{00}\mathbf{pq} + C_0^{10}(\mathbf{p}^2 + \mathbf{q}^2) + \cdots \,, \tag{4.10}$$

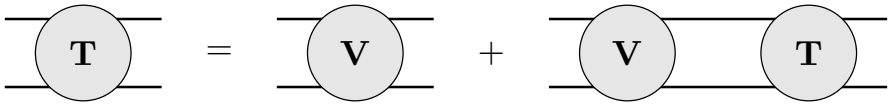

Figure 4.1: Lippmann-Schwinger equation for the full T matrix (circle marked T) in momentum space. The circle marked V indicates the full potential while the pair of internal solid lines represent the free two-particle Green function G_0. Closed loops imply a momentum integration.

which in the position space corresponds to a sum of a δ-like potential and the derivatives thereof. The long-range potential might be taken to be the regularized Yukawa potential, corresponding to an exchange of a light particle, see above. In any case, it is assumed to be local. Furthermore, ultraviolet divergences will be present in the LS equation, in general. We assume that these divergences are regularized and renormalized in a standard fashion (say, the power-divergence subtraction (PDS) scheme, bearing the case of NN scattering in mind). Since the presence of a long-range force non-trivially affects only the infrared behavior of the theory, it is expected that the issue of renormalization is inessential in the present context. To simplify things, one could also merely assume that the momentum cutoff is performed at a very large value Λ, and the Λ-dependent effective couplings are adjusted order by order to reproduce the behavior of the S-matrix elements at low momenta.

The fully off-shell LS equation for the T matrix is illustrated in Fig. 4.1. The corresponding integral equation in momentum space is given by

$$T(\mathbf{p},\mathbf{q};q_0^2+i\varepsilon) = V(\mathbf{p},\mathbf{q}) + \int \frac{d^3\mathbf{k}}{(2\pi)^3}\,\frac{V(\mathbf{p},\mathbf{k})T(\mathbf{k},\mathbf{q};q_0^2+i\varepsilon)}{\mathbf{k}^2-q_0^2-i\varepsilon}\,, \tag{4.11}$$

where the explicit expression for the two-particle Green function

$$\langle\mathbf{p}|G_0(q_0^2+i\varepsilon)|\mathbf{q}\rangle = \frac{(2\pi)^3\delta^3(\mathbf{p}-\mathbf{q})}{\mathbf{p}^2-q_0^2-i\varepsilon}\,. \tag{4.12}$$

was used and the regularization of the momentum integration with the cutoff Λ is left implicit. The partial-wave amplitudes are defined as follows:

$$T(\mathbf{p},\mathbf{q};q_0^2+i\varepsilon) = 4\pi\sum_{\ell m} Y_{\ell m}(\hat{p})T_\ell(p,q;q_0^2+i\varepsilon)Y^*_{\ell m}(\hat{q})\,. \tag{4.13}$$

The phase shift is related to the on-shell partial-wave amplitudes via:

$$T_\ell(q_0,q_0;q_0^2+i\varepsilon) \doteq T_\ell(q_0) = \frac{4\pi}{q_0\cot\delta_\ell(q_0)-iq_0}\,. \tag{4.14}$$

Next, we split the full potential into the long- and short-range parts, $V = V_L + V_S$, and define the scattering amplitude T_L and the Green function G_L for the long-range potential only. This construction is shown diagrammatically in Fig. 4.2. The first line gives the LS equation for T_L, while the second line gives the expression for G_L in terms of G_0 and T_L. Both quantities are needed for the NREFT

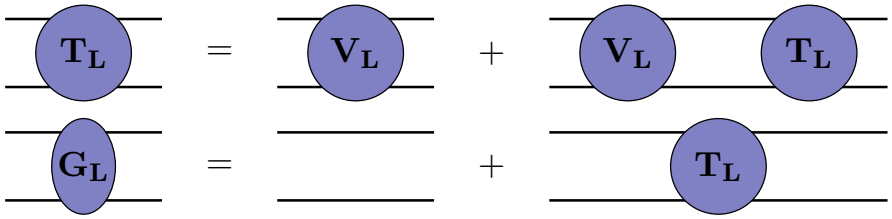

Figure 4.2: Definition of the scattering amplitude T_L (first line) and Green function G_L (second line) for the long-range interaction only. Further notation as in Fig. 4.1

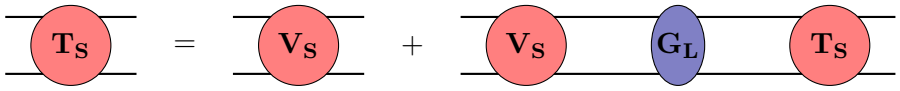

Figure 4.3: Diagrams for the short-range T matrix T_L. Note that the loop integration now involves G_L instead of G_0. Further notation as in Fig. 4.1

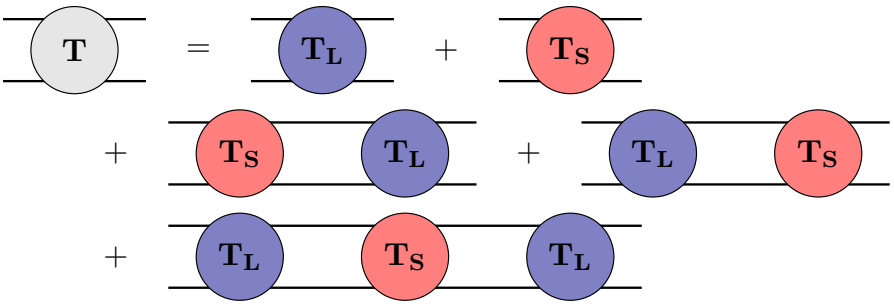

Figure 4.4: Diagrams for the full T matrix expressed through T_L and T_S. Further notation as in Fig. 4.1

formulation of the modified effective-range expansion. The explicit expressions read

$$\begin{aligned} T_L(q_0^2+i\varepsilon) &= V_L + V_L G_0(q_0^2+i\varepsilon) T_L(q_0^2+i\varepsilon)\,, \\ G_L(q_0^2+i\varepsilon) &= G_0(q_0^2+i\varepsilon) + G_0(q_0^2+i\varepsilon) T_L(q_0^2+i\varepsilon) G_0(q_0^2+i\varepsilon)\,. \end{aligned} \tag{4.15}$$

Moreover, we define the short-range T matrix T_S,

$$T_S(q_0^2+i\varepsilon) = V_S + V_S G_L(q_0^2+i\varepsilon) T_S(q_0^2+i\varepsilon)\,. \tag{4.16}$$

which is shown diagrammatically in Fig. 4.3. Note that the loop integration now involves G_L instead of G_0. Using these definitions, the full T matrix can be expressed as

$$\begin{aligned} T(q_0^2+i\varepsilon) &= T_L(q_0^2+i\varepsilon) \\ &+ (1 + T_L(q_0^2+i\varepsilon) G_0(q_0^2+i\varepsilon)) T_S(q_0^2+i\varepsilon) (G_0(q_0^2+i\varepsilon) T_L(q_0^2+i\varepsilon) + 1)\,, \end{aligned} \tag{4.17}$$

which is illustrated in Fig. 4.4. This amounts to adding T_L and T_S dressed by T_L in all possible ways.

The above expressions are of course familiar from the theory of scattering on two potentials. Note that we have used operator notation in Eqs. (4.15, 4.16, 4.17) to keep the notation clear. The integrations over intermediate states will only be shown explicitly in the following when required for

clarity.

In order to simplify life further, we assume that the long-range potential is repulsive and does not create bound states. Then, the spectral representation of the long-range Green function takes the form:

$$\langle \mathbf{p}|G_L(q_0^2+i\varepsilon)|\mathbf{q}\rangle = \int \frac{d^3\mathbf{k}}{(2\pi)^3}\,\frac{\langle \mathbf{p}|\psi_{\mathbf{k}}^{(\pm)}\rangle\langle\psi_{\mathbf{k}}^{(\pm)}|\mathbf{q}\rangle}{\mathbf{k}^2-q_0^2-i\varepsilon}\,, \tag{4.18}$$

where $\psi_{\mathbf{k}}^{(\pm)}$ denote the eigenfunctions of the Hamiltonian $H_L = H_0 + V_L$, corresponding to the eigenvalue $\mathbf{k}^2$, and $(\pm)$ specifies outgoing/ingoing boundary conditions on the wave function. These wave functions can be constructed with the use of the Møller operators:

$$\begin{aligned} |\psi_{\mathbf{k}}^{(\pm)}\rangle &= (1+G_0(k^2\pm i\varepsilon)T_L(k^2\pm i\varepsilon))|\mathbf{k}\rangle \doteq \Omega(k^2\pm i\varepsilon)|\mathbf{k}\rangle\,,\\ \langle\psi_{\mathbf{k}}^{(\pm)}| &= \langle\mathbf{k}|(1+T_L(k^2\mp i\varepsilon)G_0(k^2\mp i\varepsilon)) \doteq \langle\mathbf{k}|\Omega^\dagger(k^2\pm i\varepsilon)\,. \end{aligned} \tag{4.19}$$

Now, let us consider the Born series for the quantity

$$\begin{aligned} &\langle \mathbf{p}|\Omega^\dagger(q_0^2-i\varepsilon)T_S(q_0^2+i\varepsilon)\Omega(q_0^2+i\varepsilon)|\mathbf{q}\rangle\\ =\;& \int_{\mathbf{k}_1,\mathbf{k}_2}\langle \mathbf{p}|\Omega^\dagger(q_0^2-i\varepsilon)|\mathbf{k}_1\rangle\langle\mathbf{k}_1|V_S|\mathbf{k}_2\rangle\langle\mathbf{k}_2|\Omega(q_0^2+i\varepsilon)|\mathbf{q}\rangle\\ +\;& \int_{\mathbf{k}_1,\mathbf{k}_2,\mathbf{k}_3,\mathbf{k}_4,\mathbf{l}}\langle \mathbf{p}|\Omega^\dagger(q_0^2-i\varepsilon)|\mathbf{k}_1\rangle\langle\mathbf{k}_1|V_S|\mathbf{k}_2\rangle\langle\mathbf{k}_2|\psi_{\mathbf{l}}^{(+)}\rangle\frac{1}{\mathbf{l}^2-q_0^2-i\varepsilon}\,\langle\psi_{\mathbf{l}}^{(+)}|\mathbf{k}_3\rangle\\ &\quad\times\langle\mathbf{k}_3|V_S|\mathbf{k}_4\rangle\langle\mathbf{k}_4|\Omega(q_0^2+i\varepsilon)|\mathbf{q}\rangle+\cdots\,, \end{aligned} \tag{4.20}$$

where we have used the abbreviation

$$\int_{\mathbf{k}_1} \equiv \frac{d^3\mathbf{k}_1}{(2\pi)^3}\,. \tag{4.21}$$

On the energy shell $p^2 = q^2 = q_0^2$, the above expression simplifies to

$$\begin{aligned} &\langle \mathbf{p}|\Omega^\dagger(q_0^2-i\varepsilon)T_S(q_0^2+i\varepsilon)\Omega(q_0^2+i\varepsilon)|\mathbf{q}\rangle\\ =\;& \int_{\mathbf{k}_1,\mathbf{k}_2}\langle\psi_{\mathbf{p}}^{(-)}|\mathbf{k}_1\rangle\langle\mathbf{k}_1|V_S|\mathbf{k}_2\rangle\langle\mathbf{k}_2|\psi_{\mathbf{q}}^{(+)}\rangle\\ +\;& \int_{\mathbf{k}_1,\mathbf{k}_2,\mathbf{k}_3,\mathbf{k}_4,\mathbf{l}}\langle\psi_{\mathbf{p}}^{(-)}|\mathbf{k}_1\rangle\langle\mathbf{k}_1|V_S|\mathbf{k}_2\rangle\langle\mathbf{k}_2|\psi_{\mathbf{l}}^{(+)}\rangle\frac{1}{\mathbf{l}^2-q_0^2-i\varepsilon}\,\langle\psi_{\mathbf{l}}^{(+)}|\mathbf{k}_3\rangle\\ &\quad\times\langle\mathbf{k}_3|V_S|\mathbf{k}_4\rangle\langle\mathbf{k}_4|\psi_{\mathbf{q}}^{(+)}\rangle+\cdots\,. \end{aligned} \tag{4.22}$$

The partial-wave expansion of the asymptotic wave functions is defined as follows:

$$\langle \mathbf{p}|\psi_{\mathbf{k}}^{(\pm)}\rangle = \sum_{\ell m} Y_{\ell m}(\hat{p})\psi_\ell^{(\pm)}(k,p)Y_{\ell m}^*(\hat{k})\,. \tag{4.23}$$

Furthermore,

$$\left(\psi_\ell^{(-)}(k,p)\right)^* = e^{2i\sigma_\ell(k)}\left(\psi_\ell^{(+)}(k,p)\right)^* , \tag{4.24}$$

where $\sigma_\ell(k)$ denotes the scattering phase shift in case of the long-range potential only. Now, the partial-wave expansion of the quantity defined in Eq. (4.22) is given by

$$\langle \mathbf{p}|\Omega^\dagger(q_0^2 - i\varepsilon)T_S(q_0^2 + i\varepsilon)\Omega(q_0^2 + i\varepsilon)|\mathbf{q}\rangle = 4\pi \sum_{\ell m} Y_{\ell m}(\hat{p})e^{2i\sigma_\ell(q_0)}B_\ell(q_0)Y_{\ell m}^*(\hat{q}) , \tag{4.25}$$

where

$$B(\mathbf{p},\mathbf{q};q_0^2 + i\varepsilon) = \tilde{V}_S(\mathbf{p},\mathbf{q}) + \int \frac{d^3\mathbf{k}}{(2\pi)^3}\,\frac{\tilde{V}_S(\mathbf{p},\mathbf{k})B(\mathbf{k},\mathbf{q};q_0^2 + i\varepsilon)}{\mathbf{k}^2 - q_0^2 - i\varepsilon} , \tag{4.26}$$

$$\tilde{V}_S(\mathbf{p},\mathbf{q}) = \langle \psi_\mathbf{p}^{(+)}|V_S|\psi_\mathbf{q}^{(+)}\rangle , \tag{4.27}$$

and $B_\ell(q_0)$ is equal to the partial-wave amplitude $B_\ell(p,q;q_0^2)$ on the energy shell $p^2 = q^2 = q_0^2$. In analogy to Eq. (4.14), one may write

$$B_\ell(q_0) = \frac{4\pi}{q_0\cot\tilde{\delta}_\ell(q_0) - iq_0} . \tag{4.28}$$

Using Eqs. (4.17) and (4.25), one finally gets:

$$\tilde{\delta}_\ell(q_0) = \delta_\ell(q_0) - \sigma_\ell(q_0) . \tag{4.29}$$

4.2.3 Non-Derivative Interactions

Let us first restrict ourselves to $\ell = 0$ and assume that only the coupling C_0^{00} is different from zero. Then, the potential $\tilde{V}_S$ is separable:

$$\tilde{V}_S(\mathbf{p},\mathbf{q}) = \left(\tilde{\psi}_\mathbf{p}^{(+)}(0)\right)^* C_0^{00}\tilde{\psi}_\mathbf{q}^{(+)}(0) . \tag{4.30}$$

Here, $\tilde{\psi}_\mathbf{q}^{(+)}(\mathbf{r})$ stands for the wave function in the coordinate space. Then, on the energy shell $|\mathbf{q}| = q_0$, the S-wave amplitude takes the form

$$B_0(q_0) = \frac{|\tilde{\psi}_\mathbf{q}^{(+)}(0)|^2}{(C_0^{00})^{-1} - \langle G_L^0(q_0)\rangle} , \tag{4.31}$$

where

$$\langle G_L^0(q_0)\rangle = \int \frac{d^3\mathbf{k}}{(2\pi)^3}\,\frac{|\tilde{\psi}_\mathbf{k}^{(+)}(0)|^2}{\mathbf{k}^2 - q_0^2 - i\varepsilon} . \tag{4.32}$$

Let us now assume that the conditions of Ref. [64] are fulfilled and, namely, the long-range potential V_L is local. It is convenient to define the partial-wave expansion of the Green function in the momentum/coordinate spaces as follows:

$$\begin{aligned}\langle \mathbf{p}|G_L(q_0^2+i\varepsilon)|\mathbf{q}\rangle &= 4\pi\sum_{\ell m}\mathcal{Y}_{\ell m}(\mathbf{p})G_L^\ell(p,q;q_0^2+i\varepsilon)\mathcal{Y}^*_{\ell m}(\mathbf{q})\,,\\ \langle \mathbf{r}|G_L(q_0^2+i\varepsilon)|\mathbf{w}\rangle &= 4\pi\sum_{\ell m}\mathcal{Y}_{\ell m}(\mathbf{r})\tilde{G}_L^\ell(r,w;q_0^2+i\varepsilon)\mathcal{Y}^*_{\ell m}(\mathbf{w})\,,\end{aligned} \tag{4.33}$$

with $\mathcal{Y}_{\ell m}(\mathbf{z}) = z^\ell Y_{\ell m}(\hat{z})$. Then,

$$\langle G_L^\ell(q_0)\rangle = \lim_{r,w\to 0}\tilde{G}_L^\ell(r,w;q_0^2+i\varepsilon)\,. \tag{4.34}$$

Using the result of Appendix A.1, we can write

$$\langle G_L^\ell(q_0)\rangle = \frac{1}{4\pi\left((2\ell+1)!!\right)^2}M_\ell(q_0) + \text{real polynomial in } q_0^2\,, \tag{4.35}$$

where $M_\ell(q_0)$ is given by Eq. (4.4). The real polynomial can be safely dropped as it corresponds to the choice of the renormalization prescription.

Next, we express the wave function at the origin, which appears in Eq. (4.31), through the scattering wave function $\phi_0(k,r) \doteq \phi_0(k,k,r)$ defined in Eq. (A.3). Using

$$|\tilde{\psi}_{\mathbf{k}}(0)| = \lim_{r\to 0}\left|\frac{\phi_0(k,r)}{kr}\right| = \frac{1}{|f_0(k)|} \tag{4.36}$$

along with Eqs. (4.28) and (4.31), we obtain

$$\frac{4\pi}{C_0^{00}} = M_0 + \frac{q_0}{|f_0(q_0)|^2}\left(\cot\tilde{\delta}_0(q_0) - i\right) \tag{4.37}$$

for the S-wave phase shift. The essence of the modified effective-range expansion is now crystal clear: it has a larger radius of convergence which is governed by the short-range potential only.

4.2.4 Derivative Interactions

Consider now the situation when the matrix element of the potential V_S is a generic low-energy polynomial defined in Eq. (4.10). This is no more true for the potential $\tilde{V}_S(\mathbf{p},\mathbf{q})$, defined in Eq. (4.27). Here, we wish to address the structure of the latter in more detail. The partial-wave expansion of the V_S is given in Eq. (4.8). Convoluting this equation with the wave functions, integrals of the following type emerge

$$A_\ell^a = \int\frac{d^3\mathbf{p}}{(2\pi)^3}\,\mathcal{Y}^*_{\ell m}(\mathbf{p})(\mathbf{p}^2)^a\langle \mathbf{p}|\psi_{\mathbf{k}}^{(+)}\rangle\,. \tag{4.38}$$

One can now use the identity

$$(\mathbf{p}^2)^a = (\mathbf{p}^2 - \mathbf{k}^2 + \mathbf{k}^2)^a = (\mathbf{p}^2 - \mathbf{k}^2)^a + a(\mathbf{p}^2 - \mathbf{k}^2)^{a-1}\mathbf{k}^2 + \cdots , \tag{4.39}$$

and rewrite Eq. (4.38) as

$$A_\ell^a = \lim_{\mathbf{r}\to 0} \mathscr{Y}^*_{\ell m}(i\nabla) \sum_{b=0}^{a} \frac{(-1)^{a-b} a!}{b!(a-b)!} (\mathbf{k}^2)^b (\mathbf{k}^2 + \triangle)^{a-b} \tilde{\psi}^{(+)}_{\mathbf{k}}(\mathbf{r}) . \tag{4.40}$$

Here, as in Ref. [64], it is assumed that the long-range potential $V_L(r)$ is local and spherically symmetric. Furthermore, consider the case $\ell = 0$ first. Using the Schrödinger equation, one then gets

$$(\mathbf{k}^2 + \triangle)\psi^{(+)}_{\mathbf{k}}(\mathbf{r}) = \text{const} \cdot V_L(r)\psi^{(+)}_{\mathbf{k}}(\mathbf{r}) \to \text{const} \cdot V_L(0)\psi^{(+)}_{\mathbf{k}}(0) , \quad \text{as } \mathbf{r} \to 0 . \tag{4.41}$$

In the case of a regularized Yukawa coupling, the quantity $V_L(0)$ is finite.

Acting now with the operator $(\mathbf{k}^2 + \triangle)$ on both sides of this equation once more, one gets a term, containing V_L^2, as well as terms with the space derivatives acting on $V_L(r)$. Continuing this operation, we get a string of terms, containing $\nabla_{i_1} \ldots \nabla_{i_k} V_L(r)$. Furthermore, owing to the rotational symmetry,

$$\lim_{r\to 0} \nabla_{i_1} \ldots \nabla_{i_k} V_L(r) = \begin{cases} (\delta_{i_1 i_2} \cdots \delta_{i_{k-1} i_k} + \text{perm}) V_k , & \text{even } k , \\ 0 & \text{odd } k . \end{cases} \tag{4.42}$$

One could stick to the dimensional regularization here, in which all V_k are finite. Furthermore, in the dimensional regularization, $V_k \sim \mu^k$, where μ denotes the small mass scale of the long-distance potential (the pion mass M_π, in case of Yukawa interactions). We remind the reader that we are dealing here with the long-distance (infrared) problems, for which the details of the ultraviolet renormalization should not matter.

The Kronecker δ-symbols, which are present in Eq. (4.42), can be further contracted with $\nabla_{i_1} \cdots$ acting on the wave function, turning them into the Laplacians $\triangle$ that can be again eliminated with the use of the Schrödinger equation. At the end of the day, for $\ell = 0$,

$$A_0^a = \sum_{b=0}^{a} (\mathbf{k}^2)^b h_0^{a-b} \tilde{\psi}^{(+)}_{\mathbf{k}}(\mathbf{0}) , \tag{4.43}$$

where the coefficients h_0^{a-b} are expressed through $V_L(0)$ and the derivatives of the potential at the origin. It is important to mention that the mass scale in the derivatives is set by the long-range potential and, therefore, the expansion in the derivatives is converging fast.

Next, consider the case $\ell \neq 0$ and restore the factor $\mathscr{Y}^*_{\ell m}(i\nabla)$ in the expression for A_ℓ^a. This factor contains exactly ℓ derivatives which should be commuted through all potentials to the right. Performing the limit $\mathbf{r} \to 0$, it is straightforward to ensure that

$$\begin{aligned} A_\ell^a &= \sum_{b=0}^{a} (\mathbf{k}^2)^b h_\ell^{a-b} \lim_{\mathbf{r}\to 0} \mathscr{Y}^*_{\ell m}(i\nabla) \tilde{\psi}^{(+)}_{\mathbf{k}}(\mathbf{r}) \\ &\doteq 4\pi \sum_{b=0}^{a} c_\ell (\mathbf{k}^2)^{a-b} h_\ell^b \lim_{r\to 0} i^\ell \frac{\phi_\ell(k,r)}{k r^{\ell+1}} Y^*_{\ell m}(\hat{k}) , \end{aligned} \tag{4.44}$$

where

$$c_\ell \delta_{mm'} = \lim_{\mathbf{r}\to 0} \mathcal{Y}^*_{\ell m}(i\nabla)\mathcal{Y}_{\ell m'}(\mathbf{r}) = \frac{i^\ell \ell!(2\ell+1)}{4\pi}\delta_{mm'}\,. \tag{4.45}$$

Furthermore, using

$$\lim_{r\to 0}\frac{\phi_\ell(k,r)}{kr^{\ell+1}} = \frac{k^\ell}{f_\ell(k)(2\ell+1)!!}\,, \tag{4.46}$$

one obtains

$$\begin{aligned}\tilde{V}^\ell_S(p,q) &= \frac{1}{[(2\ell+1)!!]^2 f^*_\ell(p) f_\ell(q)}\,(pq)^\ell \bar{V}^\ell_S(p,q)\,,\\ \bar{V}^\ell_S(p,q) &= \sum_{a=0}^{\infty}\sum_{b=0}^{a}\tilde{C}^{ab}_\ell (p^2)^b (q^2)^{a-b}\,.\end{aligned} \tag{4.47}$$

In the above expression, the couplings $\tilde{C}^{ab}_\ell$ are expressed through C^{ab}_ℓ in form of the series in the small scale μ. In other words, no unnaturally large couplings emerge. This property is crucial for arguing that the sum, given in the above equation, still represents a low-energy polynomial. To summarize, $\tilde{V}^\ell_S(p,q)$ unlike $V^\ell_S(p,q)$, is *not* a low-energy polynomial. The difference is however minimal and boils down to the Jost functions that enter the expression as a multiplicative factor.

At the next step, we carry out the partial-wave expansion in Eq. (4.26) and use the following ansatz for the partial-wave amplitude:

$$B_\ell(p,q;q_0^2+i\varepsilon) = \frac{1}{[(2\ell+1)!!]^2 f^*_\ell(p) f_\ell(q)}\,(pq)^\ell \bar{B}_\ell(p,q;q_0^2+i\varepsilon)\,. \tag{4.48}$$

This gives

$$\bar{B}_\ell(p,q;q_0^2+i\varepsilon) = \bar{V}^\ell_S(p,q) + \int \frac{k^2 dk}{2\pi^2}\,\frac{k^{2\ell}}{[(2\ell+1)!!]^2|f_\ell(k)|^2}\,\frac{\bar{V}^\ell_S(p,k)\bar{B}_\ell(k,q;q_0^2+i\varepsilon)}{k^2-q_0^2-i\varepsilon}\,. \tag{4.49}$$

Let us now define a new amplitude that obeys an integral equation with a regular kernel:

$$\begin{aligned}R_\ell(p,q;q_0^2) &= \bar{V}^\ell_S(p,q)\\ &+ \int \frac{k^2 dk}{2\pi^2}\,\frac{k^{2\ell}}{[(2\ell+1)!!]^2|f_\ell(k)|^2}\,\frac{\bar{V}^\ell_S(p,k)R_\ell(k,q;q_0^2)-\bar{V}^\ell_S(p,q_0)R_\ell(q_0,q;q_0^2)}{k^2-q_0^2}\,.\end{aligned} \tag{4.50}$$

These two amplitudes on the energy shell are related by

$$\begin{aligned}\bar{B}_\ell(q_0,q_0;q_0^2+i\varepsilon) &= R_\ell(q_0,q_0;q_0^2) + \bar{B}_\ell(q_0,q_0;q_0^2+i\varepsilon)R_\ell(q_0,q_0;q_0^2)\\ &\times \int \frac{k^2 dk}{2\pi^2}\,\frac{k^{2\ell}}{[(2\ell+1)!!]^2|f_\ell(k)|^2}\,\frac{1}{k^2-q_0^2-i\varepsilon}\,.\end{aligned} \tag{4.51}$$

Note that $R_\ell(p,q;q_0^2)$, like $\bar{V}_S^\ell(p,q)$, is a low-energy polynomial. Identifying $K_\ell^M(q_0^2) = \Big[R_\ell(q_0,q_0;q_0^2)\Big]^{-1}$, we obtain:

$$B_\ell(q_0) = \frac{q_0^{2\ell}}{|f_\ell(q_0)|^2[(2\ell+1)!!]^2}\left\{K_\ell^M(q_0,q_0) - \langle G_L^\ell(q_0)\rangle\right\}^{-1} . \tag{4.52}$$

Finally, using Eqs. (4.28) and (4.35), one arrives at the modified effective-range expansion as given in Eq. (4.3), with $K_\ell^M(q_0^2)$ being a low-energy polynomial.

To summarize, using effective field theory methods, we have rederived the modified effective-range expansion formula of Ref. [64], where the effects of the long-range interactions are separated and included in the functions $f_\ell(q)$ and $M_\ell(q)$ that do not depend on the short-range potential V_S. This neat separation is, however, based on the assumption that the long-range potential $V_L(r)$ is local. The most important cases of the long-range force: the one-pion exchange as well as Coulomb interactions are exactly of this type. It can be further expected that, with some effort, the method could be generalized to the case of a finite sum $V_1(r) + (\triangle V_2(r) + V_2(r)\triangle) + \nabla V_3(r)\nabla + \ldots$, albeit the final formula probably takes a more complicated form (Here, the couplings in front of $V_1(r), V_2(r), V_3(r), \ldots$ are assumed to be of natural size.). Here, we are not pursuing this idea further. On the other hand, a generic non-local long-range potential (say, a separable potential with a very smooth cutoff) is most likely not amenable to this kind of treatment at all. In other words, in general, there are two mass scales present in the potential V_L – the one associated with the momentum transfer and the one associated with the relative momentum in the CM frame, respectively. A long-range potential, in which the former scale is small whereas the latter scale is of a natural size, can be treated with the method in a similar way as described above.

4.3 Modified Lüscher Equation

4.3.1 Derivation of the Quantization Condition

In a finite box, the Green function $G_L(q_0^2)$, which enters in the equation for $T_S(q_0^2)$, can be expanded in a sum over all eigenvectors of the Hamiltonian H_L in a finite volume:

$$\langle \mathbf{p}|G_L(q_0^2)|\mathbf{q}\rangle = \sum_n \frac{\langle \mathbf{p}|\psi_n\rangle\langle\psi_n|\mathbf{q}\rangle}{q_n^2 - q_0^2} . \tag{4.53}$$

Furthermore, the finite-volume spectrum of the system is determined by the pole positions of the full T-matrix that can be written down in a form of a finite-volume analog of Eq. (4.17). Using the fact that the poles of T_L will eventually cancel [238] (see also Appendix A.2), it is straightforward to conclude that the spectrum will be determined by the poles of T_S. Moreover, it is easily seen that no spurious poles emerge, since the poles that emerge in G_L are shifted by the short-range interaction. Using now the basis of eigenfunctions of the Hamiltonian H_L and defining the quantity

$$B^{nm}(q_0^2) = \langle\psi_n|T_S(q_0^2)|\psi_m\rangle , \tag{4.54}$$

we get

$$B^{nm} = \tilde{V}_S^{nm} + \sum_k \tilde{V}_S^{nk} \frac{1}{q_k^2 - q_0^2} B^{km} , \qquad \tilde{V}_S^{nm} = \langle \psi_n | V_S | \psi_m \rangle . \tag{4.55}$$

(The dependence of B^{nm} on q_0^2 is suppressed hereafter). Furthermore, using the partial-wave expansion

$$v_{\ell m}^n = \frac{1}{L^3} \sum_{\mathbf{p}} \mathcal{Y}_{\ell m}^*(\mathbf{p}) \langle \mathbf{p} | \psi_n \rangle , \tag{4.56}$$

we get

$$\langle \psi_n | V_S | \psi_m \rangle = 4\pi \sum_{\ell m, \ell' m'} \left(v_{\ell m}^n \right)^* \bar{V}_S^\ell(q_n, q_m) \delta_{\ell\ell'} \delta_{mm'} v_{\ell' m'}^m . \tag{4.57}$$

The next steps in the derivation repeat those in the infinite volume. We use the following ansatz for the matrix B

$$B^{nm} = 4\pi \sum_{\ell m} \left(v_{\ell m}^n \right)^* \bar{B}_{\ell m, \ell' m'}(q_n, q_m; q_0^2) v_{\ell' m'}^m , \tag{4.58}$$

and get

$$\begin{aligned} \bar{B}_{\ell m, \ell' m'}(q_n, q_m; q_0^2) &= \bar{V}_S^\ell(q_n, q_m) \delta_{\ell\ell'} \delta_{mm'} \\ + \sum_k \sum_{\ell'' m''} \bar{V}_S^\ell(q_n, q_k) & \frac{4\pi v_{\ell m}^k \left(v_{\ell'' m''}^k \right)^*}{q_k^2 - q_0^2} \bar{B}_{\ell'' m'', \ell' m'}(q_k, q_m; q_0^2) . \end{aligned} \tag{4.59}$$

Define again

$$\begin{aligned} R_{\ell m, \ell' m'}(q_n, q_m; q_0^2) &= \bar{V}_S^\ell(q_n, q_m) \delta_{\ell\ell'} \delta_{mm'} + \sum_k \sum_{\ell'' m''} \frac{4\pi v_{\ell m}^k \left(v_{\ell'' m''}^k \right)^*}{q_k^2 - q_0^2} \\ \times \left(\bar{V}_S^\ell(q_n, q_k) R_{\ell'' m'', \ell' m'}(q_k, q_m; q_0^2) \right. & \left. - \bar{V}_S^\ell(q_n, q_0) R_{\ell'' m'', \ell' m'}(q_0, q_m; q_0^2) \right) . \end{aligned} \tag{4.60}$$

The infinite-volume limit in this (subtracted) equation can be performed, and the quantity $R_{\ell m, \ell' m'}(p, q; q_0^2)$ tends to $\delta_{\ell\ell'} \delta_{mm'} R_\ell(p, q; q_0^2)$ in this limit. On the mass shell, with $q_n^2 = q_m^2 = q_0^2$ we, therefore, obtain

$$\begin{aligned} \bar{B}_{\ell m, \ell' m'}(q_0, q_0; q_0^2) &= \delta_{\ell\ell'} \delta_{mm'} R_\ell(q_0, q_0; q_0^2) \\ + \sum_{\ell'' m''} & R_\ell(q_0, q_0; q_0^2) H_{\ell m, \ell'' m''}(q_0) \bar{B}_{\ell'' m'', \ell' m'}(q_0, q_0; q_0^2) , \end{aligned} \tag{4.61}$$

where

$$H_{\ell m,\ell' m'}(q_0) = 4\pi \sum_k \frac{v^k_{\ell m}\left(v^k_{\ell' m'}\right)^*}{q_k^2 - q_0^2} = \frac{4\pi}{L^6} \sum_{\mathbf{p},\mathbf{q}} \mathcal{Y}^*_{\ell m}(\mathbf{p}) \langle \mathbf{p}|G_L(q_0^2)|\mathbf{q}\rangle \mathcal{Y}_{\ell' m'}(\mathbf{q})\,. \tag{4.62}$$

The modified quantization condition, derived from Eq. (4.61) takes the form $\det \mathscr{A} = 0$. Using again, as in Eq. (4.52), the definition $K^M_\ell(q_0^2) = \left[R_\ell(q_0, q_0; q_0^2)\right]^{-1}$, we arrive at the following expression for the matrix $\mathscr{A}_{\ell m,\ell' m'}$:

$$\mathscr{A}_{\ell m,\ell' m'}(q_0) = \delta_{\ell\ell'}\delta_{mm'} K^M_\ell(q_0^2) - H_{\ell m,\ell' m'}(q_0)\,. \tag{4.63}$$

4.3.2 Calculation of the Function $H_{\ell m,\ell' m'}(q_0)$

Owing to our choice of the superregular long-range potential, the quantity $H_{\ell m,\ell' m'}(q_0)$ is free of the ultraviolet divergences for $\ell, \ell' \leq \ell_{\text{max}}$. However, one still needs a finite renormalization, in order to ensure that the definition of the function $H_{\ell m,\ell' m'}(q_0)$ in a finite volume is consistent with its infinite-volume counterpart. Below, we shall consider the cases $q_0^2 < 0$ and $q_0^2 > 0$ separately.

Negative Energies, $q_0^2 < 0$

In the case $q_0^2 < 0$, a consistent definition of the loop function is given by

$$H_{\ell m,\ell' m'}(q_0) = (H_{\ell m,\ell' m'}(q_0) - H^\infty_{\ell m,\ell' m'}(q_0)) + \frac{1}{4\pi}\,\delta_{\ell\ell'}\delta_{mm'} M_\ell(q_0)\,. \tag{4.64}$$

It should be mentioned here that the functions $f_\ell(p, r)$ and hence $M_\ell(p)$ are analytic in the upper half of the complex p-plane.[3] Consequently, $M_\ell(q_0)$ is well-defined for negative values of q_0^2, taking into account the presence of the infinitesimal positive imaginary part in q_0^2. Furthermore, using Eqs. (4.15), (4.62) and applying the Poisson formula, one gets:

$$H_{\ell m,\ell' m'}(q_0) - H^\infty_{\ell m,\ell' m'}(q_0) = H^{(1)}_{\ell m,\ell' m'}(q_0) + H^{(2)}_{\ell m,\ell' m'}(q_0) + H^{(3)}_{\ell m,\ell' m'}(q_0)\,, \tag{4.65}$$

where

$$\begin{aligned}
H^{(1)}_{\ell m,\ell' m'}(q_0) &= 4\pi \sum_{\mathbf{n}} \int \frac{d^3\mathbf{p}}{(2\pi)^3} \frac{\mathcal{Y}^*_{\ell m}(\mathbf{p})\left(e^{i\mathbf{p}\mathbf{n}L} - 1\right)\mathcal{Y}_{\ell' m'}(\mathbf{p})}{\mathbf{p}^2 - q_0^2}\,,\\
H^{(2)}_{\ell m,\ell' m'}(q_0) &= 4\pi \sum_{\mathbf{n},\mathbf{s}} \int \frac{d^3\mathbf{p}}{(2\pi)^3} \frac{d^3\mathbf{q}}{(2\pi)^3} \left(e^{i\mathbf{p}\mathbf{n}L - i\mathbf{s}\mathbf{q}L} - 1\right) \frac{\mathcal{Y}^*_{\ell m}(\mathbf{p})}{\mathbf{p}^2 - q_0^2} \langle \mathbf{p}|T_L(q_0^2)|\mathbf{q}\rangle \frac{\mathcal{Y}_{\ell' m'}(\mathbf{q})}{\mathbf{q}^2 - q_0^2}\,,\\
H^{(3)}_{\ell m,\ell' m'}(q_0) &= 4\pi \int \frac{d^3\mathbf{p}}{(2\pi)^3} \frac{d^3\mathbf{q}}{(2\pi)^3} \frac{\mathcal{Y}^*_{\ell m}(\mathbf{p})}{\mathbf{p}^2 - q_0^2} \left(\langle \mathbf{p}|T_L(q_0^2)|\mathbf{q}\rangle - \langle \mathbf{p}|T^\infty_L(q_0^2)|\mathbf{q}\rangle\right) \frac{\mathcal{Y}_{\ell' m'}(\mathbf{q})}{\mathbf{q}^2 - q_0^2}\,.
\end{aligned} \tag{4.66}$$

[3] Considering the Born series of the Green function $G_L(q_0^2)$, it is easy to get convinced that $M_\ell(q_0)$ is real everywhere below threshold.

The first term here is the standard Lüscher zeta-function. In order to calculate the remaining two terms, let us consider the LS equation for $T_L(q_0^2)$ (a finite-volume counterpart of Eq. (4.15)). Carrying out the partial-wave expansion

$$\begin{aligned}\langle \mathbf{p}|V_L|\mathbf{q}\rangle &= 4\pi \sum_{\ell m} Y_{\ell m}(\hat{p}) V_L^\ell(p,q) Y^*_{\ell m}(\hat{q})\,,\\ \langle \mathbf{p}|T_L(q_0^2)|\mathbf{q}\rangle &= 4\pi \sum_{\ell m,\ell' m'} Y_{\ell m}(\hat{p}) T_L^{\ell m,\ell' m'}(p,q;q_0^2) Y^*_{\ell' m'}(\hat{q})\,,\end{aligned} \tag{4.67}$$

one gets

$$\begin{aligned}&T_L^{\ell m,\ell' m'}(p,q;q_0^2) = \delta^{\ell\ell'}\delta^{mm'} V_L^\ell(p,q)\\ &+\ 4\pi \sum_{\ell'' m'} \int_0^\infty \frac{k^2 dk}{(2\pi)^3} V_L^\ell(p,k) \frac{f_{\ell m,\ell'' m''}(k) + f_{\ell m,\ell'' m''}(-k)}{k^2 - q_0^2} T_L^{\ell'' m'',\ell' m'}(p,q;q_0^2)\,,\end{aligned} \tag{4.68}$$

where

$$f_{\ell m,\ell'' m''}(k) + f_{\ell m,\ell'' m''}(-k) = \int d\Omega\, Y^*_{\ell m}(\hat{k}) \sum_{\mathbf{n}} e^{-i\mathbf{k}\mathbf{n}L} Y_{\ell'' m''}(\hat{k})\,. \tag{4.69}$$

The quantity $f_{\ell m,\ell'' m''}(k)$ is analytic in the upper half-plane of the variable k and vanishes exponentially, when $\mathrm{Im}\, k \to +\infty$. Note that $\ell + \ell'$ is always even for identical particles.

For the following discussion, it is convenient to define $V_L^\ell(p,q)$ for negative arguments,

$$V_L^\ell(p,q) = (-1)^\ell V_L^\ell(-p,q) = (-1)^\ell V_L^\ell(p,-q) = V_L^\ell(-p,-q)\,, \tag{4.70}$$

and, hence, from Eq. (4.68) one concludes that

$$\begin{aligned}T_L^{\ell m,\ell' m'}(p,q;q_0^2) &= (-1)^\ell T_L^{\ell m,\ell' m'}(-p,q;q_0^2) = (-1)^{\ell'} T_L^{\ell m,\ell' m'}(p,-q;q_0^2)\\ &= T_L^{\ell m,\ell' m'}(-p,-q;q_0^2)\,.\end{aligned} \tag{4.71}$$

This means that the integration over the variable k can be extended over the whole real axis, from $-\infty$ to $+\infty$:

$$\begin{aligned}&T_L^{\ell m,\ell' m'}(p,q;q_0^2) = \delta^{\ell\ell'}\delta^{mm'} V_L^\ell(p,q)\\ &+\ 4\pi \sum_{\ell'' m'} \int_{-\infty}^\infty \frac{k^2 dk}{(2\pi)^3} V_L^\ell(p,k) \frac{f_{\ell m,\ell'' m''}(k)}{k^2 - q_0^2} T_L^{\ell'' m'',\ell' m'}(p,q;q_0^2)\,,\end{aligned} \tag{4.72}$$

Using now the fact that $f_{\ell m,\ell'' m''}(k)$ is analytic in the upper half-plane, one may shift the variables $p,q,k \to p,q,k+i\sigma$. The value of σ is restricted by the singularities appearing in the free Green function as well as in the potential $V_L^\ell(p,q)$. Namely, σ must fulfill the condition $\sigma < |q_0|$, for the free Green function to stay regular. The restriction coming from the potential does not depend on q_0. For instance, in case of Yukawa interaction, we have $\sigma < M_\pi/2$. The quantity σ should obey both conditions. Performing the contour shift in the second and third lines of Eq. (4.66) as well, one sees that the finite-volume corrections to $H_{\ell m,\ell' m'}(q_0)$ are suppressed by the factor $e^{-\sigma L}$.

Positive Energies, $q_0^2 > 0$

For $q_0^2 > 0$, the Poisson formula can not be used. The infinite-volume limit of the quantity $H_{\ell m,\ell m}(q_0)$ in this case implies using the principal value prescription. Furthermore, from unitarity one can straightforwardly conclude that

$$\begin{aligned}((2\ell+1)!!)^2\langle G_L^\ell(q_0)\rangle &= ((2\ell+1)!!)^2\langle G_L^\ell(q_0)\rangle_{\text{p.v.}} \\ &+ i\frac{q_0^{2\ell+1}}{4\pi}\,\frac{(1+F^\ell(q_0))^2}{1-iq_0R_L^\ell(q_0,q_0;q_0^2)/(4\pi)}\,,\end{aligned} \tag{4.73}$$

where

$$F_\ell(q_0) = \frac{1}{q_0^\ell}\ \text{p.v.}\int_0^\infty \frac{p^2dp}{2\pi^2}\,\frac{p^\ell R_L^\ell(p,q_0;q_0^2)}{p^2-q_0^2}\,. \tag{4.74}$$

Here, R_L^ℓ denotes the K-matrix for the scattering on the long-range potential. Furthermore, since, by definition, $\text{Im}\,\langle G_L^\ell(q_0)\rangle_{\text{p.v.}} = 0$, with the use of Eqs. (4.3) and (4.35) one obtains, on the one hand,

$$\text{Im}\,\langle G_L^\ell(q_0)\rangle = \frac{q_0^{2\ell+1}}{4\pi((2\ell+1)!!)^2}\,\frac{1}{|f_\ell(q_0)|^2}\,, \tag{4.75}$$

and, on the other hand,

$$\begin{aligned}\text{Im}\,\langle G_L^\ell(q_0)\rangle &= \frac{q_0^{2\ell+1}}{4\pi((2\ell+1)!!)^2}\,\frac{(1+F^\ell(q_0))^2}{1+q_0^2R_L^\ell(q_0,q_0;q_0^2)/(4\pi)^2} \\ &= \frac{q_0^{2\ell+1}}{4\pi((2\ell+1)!!)^2}\left|1+\frac{1}{q_0^\ell}\int_0^\infty\frac{p^2dp}{2\pi^2}\,\frac{p^\ell T_L^\ell(p,q_0;q_0^2)}{p^2-q_0^2-i\varepsilon}\right|^2\,.\end{aligned} \tag{4.76}$$

Using now Eq. (4.19) and performing the partial-wave expansion of the on-shell function in analogy with Eq. (A.2), we obtain:

$$\frac{\phi_\ell(q_0,r)}{q_0r} = j_\ell(q_0r) + \int_0^\infty\frac{p^2dp}{2\pi^2}\,\frac{j_\ell(pr)T_L^\ell(p,q_0;q_0^2)}{p^2-q_0^2-i\varepsilon}\,, \tag{4.77}$$

where $\phi_\ell(q_0,r)$ is the on-shell wave function. Performing the limit $r\to 0$ in this equation, we get:

$$\lim_{r\to0}(2\ell+1)!!\frac{\phi_\ell(q_0r)}{(q_0r)^{\ell+1}} = 1+\frac{1}{q_0^\ell}\int_0^\infty\frac{p^2dp}{2\pi^2}\,\frac{p^\ell T_L^\ell(p,q_0;q_0^2)}{p^2-q_0^2-i\varepsilon}\,. \tag{4.78}$$

Finally, from Eq. (4.46), one concludes that Eqs. (4.75) and (4.76) are consistent. This represents a nice check of our approach.

A consistent definition of the quantity $H_{\ell m,\ell' m'}(q_0)$ is given by

$$H_{\ell m,\ell' m'}(q_0) = (H_{\ell m,\ell' m'}(q_0) - H^\infty_{\ell m,\ell' m'}(q_0)) + \delta_{\ell\ell'}\delta_{mm'}((2\ell+1)!!)^2\langle G_L^\ell(q_0)\rangle_{\text{p.v.}}\,, \tag{4.79}$$

where $H^{\infty}_{\ell m,\ell' m'}(q_0)$ is defined by a counterpart of Eq. (4.62), with sums replaced by integrals with the principal-value prescription everywhere. Note also that, since the potential is superregular, no ultraviolet divergences arise except in the free loop containing no potential exchange. There, it can be handled, as usual, by using dimensional regularization and cancels anyway in the difference of the finite-volume and the infinite-volume contributions.

Neglecting exponentially suppressed contributions from the long-range interactions, one could reduce the calculation of the function $H_{\ell m,\ell' m'}(q_0)$ to the solution of the system of linear equations in the angular-momentum basis. This equation has the following form:

$$H_{\ell m,\ell' m'}(q_0) = H^{0}_{\ell m,\ell' m'}(q_0) + \sum_{\ell m,\ell'' m''} H^{0}_{\ell m,\ell'' m''}(q_0) q_0^{2\ell} R_L^{\ell''}(q_0) H_{\ell'' m'',\ell' m'}(q_0)\,. \tag{4.80}$$

Here, $R_L^{\ell}(q_0) = 4\pi \tan\sigma_\ell(q_0)/q_0$ are the partial-wave on-shell K-matrices, corresponding to the long-range potential, and

$$H^{0}_{\ell m,\ell' m'}(q_0) = \frac{4\pi}{L^3} \sum_{\mathbf{k}} \frac{\mathcal{Y}^*_{\ell m}(\mathbf{k}) \mathcal{Y}_{\ell' m'}(\mathbf{k})}{\mathbf{k}^2 - q_0^2}\,. \tag{4.81}$$

This quantity can be expressed through a linear combination of the Lüscher zeta-functions. The quantity $H^{\infty}_{\ell m,\ell' m'}(q_0)$ should be taken equal to zero in this case.

Note however that neglecting exponential corrections coming from the long-range potential might be dangerous. This is seen, for example, from the fact that, below threshold, $q_0^2 < 0$, the quantity $R_L^{\ell}(q_0)$ develops the t-channel singularity that was mentioned earlier, whereas the exact function $H_{\ell m,\ell' m'}(q_0)$ is of course regular there. The derivation of the modified quantization condition, which was presented above, nicely demonstrates the origin of the problem and a way to circumvent it. In fact, the problem is handmade and is not present in Eq. (4.63). It emerges first, when one tries to evaluate $H_{\ell m,\ell' m'}(q_0)$ from Eq. (4.80) and continue analytically below threshold. All this is perfectly consistent with the discussion in the recent paper [60].

4.3.3 Partial-Wave Mixing

Above threshold, the modified zeta-function is determined from Eq. (4.80) or from the pertinent equation in the plane-wave basis. Since V_L is a long-range potential, it is expected that many partial-waves will contribute to this expression. However, this is not a problem, since V_L is a well-known function, with parameters that are determined very precisely elsewhere (e.g., the pion mass and the pion axial-vector coupling, in case of the one-pion exchange potential). Hence, the solution of Eq. (4.80) does not require a fit to lattice data. On the other hand, the short-range interaction, encoded in the function $K_\ell^M(q_0^2)$, is determined from the fit. One expects that the partial-wave mixing effect in the modified Lüscher equation is small, exactly because of the short-range nature of these interactions.

4.3.4 Exponentially Suppressed Effects

Up to now, we have consistently dropped the exponentially suppressed effects. However, as mentioned already in the introduction, these effects can turn relatively large, owing to the small mass scale. In the case of, say, NN scattering, one may indirectly estimate the size of the exponential effects, comparing the finite-volume spectra obtained in the plane-wave basis with the solutions of the modified Lüscher

equation with the same input. A simpler method to estimate the size of the exponential effects is the comparison of the modified Lüscher functions $H_{\ell m,\ell' m'}(q_0)$, calculated in the plane-wave basis and in the angular-momentum basis. This comparison does not involve any parameters that characterize the short-range interactions.

There is one place, however, where one already knows that the exponential effects are important. We remind the reader that the energy levels, which lie on the t-channel cut, are indeed observed in the NN system on the lattice [55]. Physical bound states cannot be present there and, hence, the infinite-volume limit of the Lüscher equation does not predict a pole in this region. The observed poles can only emerge because of the exponential contributions.

4.3.5 The Case with the Short-Range Potential Only

The limit $V_L(r) \to 0$ is trivial. In this limit, the Jost function $f_L(q) = 1$, $\sigma_\ell(q) = 0$, and Eq. (4.3) reduces to the familiar expression

$$K_\ell^M(q^2) = q^{2\ell+1} \cot \delta_\ell(q) \,. \tag{4.82}$$

Furthermore, the modified Lüscher zeta-function $H_{\ell m,\ell' m'}$ reduces to the conventional one, $Z_{\ell m,\ell' m'}$, and Eq. (4.63) turns into the original Lüscher equation.

4.4 Comparison with the Existing Approaches

So far, several different frameworks (including the present one) have been proposed to treat the finite-volume scattering in the presence of the long-range forces. All three approaches have one thing in common – namely, they all treat the long-range part of the potential explicitly, without trying to approximate it by a string of contact interactions (like in the derivation of the ordinary Lüscher equation). After that point, the paths start to diverge.

In the recent paper [60] a modified two-body quantization condition has been derived in the presence of both the long- and short-range forces. The authors present their central result in two different forms. Namely, Eq. (3.63) of that paper is written down in a plane wave *and* angular-momentum basis. From this point of view, it bears strong resemblance with the approach of Ref. [56], however, with a conceptual difference. Namely, all short-range interactions in Ref. [60] are summed up and enter the quantization condition through an auxiliary *on-shell* K-matrix $\bar{K}^{\text{os}}$. No particular parameterization of the *on-shell* K-matrix $\bar{K}^{\text{os}}$ is specified. We note, however, that for any realistic application to lattice data involving partial-wave mixing such a parameterization would be required. In contrast, the long- and short-range interactions are treated on equal footing in Ref. [56], and the short-range K-matrix is implicitly parameterized in terms of the effective couplings appearing in the Hamiltonian.

Furthermore, in Eqs. (5.3) and (5.4) of Ref. [60] the authors recast their central result in the angular-momentum basis. This result bears close analogy to our modified quantization condition. For example, the quantity F^T from their Eq. (5.4) is similar to our modified Lüscher function $H_{\ell m,\ell' m'}(q_0)$. The main difference, as already noted in the introduction, is that the authors of Ref. [60] propose a two-step procedure for the analysis of lattice data. Namely, at the first step, an auxiliary matrix $\bar{K}^{\text{os}}$ is determined from data. At the next step, $\bar{K}^{\text{os}}$ is substituted into the integral equation which is solved to obtain the physical K-matrix. We propose to unite these two steps in one – in our approach, the

auxiliary K-matrix is related to the physical one at the same CM energy through a simple algebraic expression.

Last but not least, it has been recently proposed to solve the t-channel problem in the two-body scattering by writing down three-body scattering equations [61]. In particular, the t-channel cut that emerges close to threshold in DD^* scattering (assuming a stable D^*) does not show up in the three-body quantization condition for the $DD\pi$ system, even if the bound state in the $D\pi$ subsystem lies below the elastic threshold. The results seems surprising at a first glance. Let us recall however that the three-body quantization condition is written down in the space of spectator momenta. Hence, in case of the stable D^* meson, this approach, up to the exponentially suppressed contributions should be algebraically equivalent to the plane-wave solution proposed in Refs. [56–58]. Note however that, in difference to the latter, the approach of Ref. [61] allows for a smooth transition to the case of an unstable D^* meson.[4]

To summarize, the difference between the existing approaches mainly boils down to the following two points:

1. *Technical convenience.* The quantization condition can be written down in the plane-wave basis as well as in the angular-momentum basis. Given modern computing capacities, the difference between these two representations is not a decisive factor anymore. Despite this, we still prefer a more compact representation in the angular-momentum basis, which reduces to a single algebraic equation if the partial-wave mixing for the short-range interactions can be neglected. The same statement applies to relating physical observables to quantities extracted from the fit to lattice data. For example, in order to relate $\bar{K}^{\text{os}}$ to the physical K-matrix, integral equations need to be solved [60], whereas the corresponding link in our approach is given by a simple algebraic relation.

2. *The choice of quantities extracted from lattice data.* This is a more subtle issue. In an idealized world with single-channel scattering and no partial-wave mixing, the Lüscher equation just gives the scattering phase in terms of the level energy. In realistic situations, however, one often needs a parameterization of the K-matrix in order to solve the quantization condition. Without any doubt, the use of an effective Hamiltonian provides such a parameterization within the range of applicability of this particular EFT. In this case, the quantities that are extracted from data at first hand are the couplings of the effective Hamiltonian. However, expressing the lattice energy levels directly in terms of the physical K-matrix, in our opinion, renders the approach more flexible: for example, one might use different EFTs (or expansions) in different energy regions to cover a larger energy range.

4.5 Conclusions

i) In this chapter, we have derived a modified Lüscher equation in the presence of both the long-range and short-range interactions. The presence of the former leads to several (interrelated) conceptual difficulties in the standard Lüscher equation. Namely,

[4] Note also that the calculation of the infinite-volume scattering amplitude in the region of the t-channel cut has been carried out earlier in Ref. [239]. In these calculations it was explicitly shown that the particle-dimer amplitude develops the left-hand singularity. The method of Ref. [61] essentially stems from this observation.

- The partial-wave expansion may converge slowly, and hence there could be a significant admixture of the higher partial waves in the Lüscher equation that complicates the analysis of data.
- The long-range interactions lead to a t-channel cut in the scattering amplitude that moves very close to the threshold, if the range of the interactions increases. Using lattice energy levels that lie below the t-channel threshold in the Lüscher equation is inconsistent.
- The exponentially suppressed contributions could be still significant for not so large values of L.

Our approach which, loosely speaking, represents a re-formulation of the modified effective-range expansion of Ref. [64] in a finite volume, is capable to address all above challenges.

ii) Several alternative approaches have appeared recently in the literature [56, 60, 61]. Here, a detailed comparison to these approaches is given. We argue that our method is conceptually closest to the original Lüscher framework. It allows to directly extract the scattering phase shift from the measured energy spectrum, if the partial-wave mixing for the short-range interactions is negligible and if the parameters of the long-range potential (i.e., the mass and the coupling of the pion) are known accurately for a given lattice ensemble. Hence, it should be possible to analyze lattice data analog to the original Lüscher approach once the modified Lüscher function is available.

iii) The modified Lüscher function, which incorporates the long-range interaction, is a central ingredient of our approach. In the present chapter we consider the evaluation of this function in great detail, paying particular attention to the issues of the ultraviolet divergences and renormalization. Once this function, which does not depend on the unknown parameters of the short-range force, is calculated and tabulated, the analysis of data exactly follows the standard pattern. An explicit calculation of this function is however a rather challenging enterprise and will be discussed in a separate publication.

iv) Note that here we deliberately ignored all issues related with the spin of particles, moving frames, relativistic effects, etc. All this is inessential in the context of the problems considered here and would only blur the discussion.

v) It remains to be seen, whether the Coulomb interaction can be treated consistently in the same manner, and whether the results would add something substantial to the findings of Refs. [232–234]. Here, it should be also mentioned that, due to the removal of the zero mode of the Coulomb field in case of periodic boundary conditions, the resulting Lagrangian is not local anymore. This, in its turn, might cause problems in the matching of the non-relativistic effective field theory, which is used for the derivation of the Lüscher equation, to its relativistic counterpart (see, e.g., Ref. [240]). In this context, it would be interesting to explore the possibility of using different boundary conditions. An alternative to this would be to use the formulation with massive protons, see, e.g. [241].

vi) The major challenge consists in using the same method in the three-particle problem. For instance, it remains to be seen, whether the long-range one-pion exchange force in the three-nucleon system can be separated as neatly from the short-range interactions as done in case of the nucleon-nucleon scattering.

CHAPTER 5

Modified Lüscher Zeta-Function and the Modified Effective Range Expansion in the Presence of a Long-Range Force

The content of the following chapter is based on the publication

- R. Bubna, H.-W. Hammer, B.-L. Hoid, J.-Y. Pang, A. Rusetsky and J.-J. Wu, *Modified Lüscher zeta-function and the modified effective range expansion in the presence of a long-range force*, JHEP **10** (2025) 197, arXiv: 2507.18399 [hep-lat]

In the following chapter an efficient numerical algorithm was proposed for the calculation of the modified Lüscher zeta-function, derived in the Chap. 4, in the presence of a long-range force. Further, using the formalism developed in the previous chapter, synthetic data on the finite-volume energy levels, generated in a toy model, were analyzed. It was explicitly shown that in contrast to the standard Lüscher approach, the truncation of higher partial-waves has very little effect on the final result. Furthermore, the regularization and renormalization of the modified Lüscher zeta-function was described and discussed in detail, as well as the problems arising within the cutoff regularization were detailed. Finally, it was also shown that one obtains modified effective-range expansion parameters of natural size in all partial-waves while using the renormalization scheme proposed in the following chapter.

In recent times, there has been great amount of interest in systems on lattice where long-range force plays an important role. Two such ongoing studies are the calculation of DD^* spectrum and $T_{cc}^+(3875)$ state properties. As discussed in the previous chapter, analysis of lattice data in case of any system where long-range force plays an important role, Lüscher equation is no more applicable. One has to employ a different approach. One such approach was detailed and derived in Chap. 4. In this project this approach, the Modified Lüscher Equation, was implemented numerically while carrying out analysis of mock data generated in a toy model. Several technical issues such as, partial-wave mixing, renormalization of the Lüscher zeta-function and exponentially suppressed corrections are discussed in detail. For this numerical implementation only the center-of-mass frame and the A_1^+ representation of the octahedral group were considered. Anything beyond these considerations is relegated to further studies.

The project started with a brief overview of the formalism derived in Chap. 4. Further, the quantization condition derived previously is rewritten in a form that makes it suitable for numerical

calculation. This rewriting leads to only the regular part of the modified Lüscher zeta-function entering the quantization condition. Moreover, no partial-wave expansion of the long-range potential is needed and the Lippmann-Schwinger equation is solved in the plane-wave basis in the finite volume. Jin-Yi Pang along with the author developed a numerical routine to evaluate this regular part of the modified Lüscher function efficiently up to G-wave. The modified Lüscher function was then compared to the original Lüscher function and key differences were discussed.

The toy model, considered in the project, involved a long-range Yukawa potential and a short-range Yukawa potential. The synthetic spectrum was generated by solving the finite-volume quantization condition for this model in the plane-wave basis and identifying the eigenvalues of the Hamiltonian (Hamiltonian approach). The proposed approach should give a result for the energy levels which differ from the Hamiltonian approach energy levels only by exponentially small corrections. Hence, these energy levels were used to test the validity of the proposed approach. The modified Lüscher equation was then solved for this model, considering only S- and G-wave, and the results were compared to the synthetic data generated. It was shown that energy levels predicted by the present approach were much more accurate than the original Lüscher's method. Furthermore, it was shown that the partial-wave expansion converges very fast in the case of modified Lüscher equation as in some cases retaining only the S-wave contribution was enough to reproduce the exact answer. Lastly, since the modified Lüscher equation accurately reproduced the same energy levels as in the Hamiltonian approach, it was concluded that the exponentially suppressed corrections are indeed very small.

For fitting of parameters using the modified effective range function one also needs to calculate the divergent loop function in the infinite volume. This loop function corresponds to a series of bubble diagrams with increasing number of long-range interaction insertions. For a given l, there are $2l + 1$ divergent loops. As discussed in the previous chapter this UV divergence can be dealt with by imposing a renormalization prescription such as the Pauli-Villars or cut-off regularization. However, these regularization schemes become numerically inconvenient at higher l. In the following project, dimensional regularization was used to render these loops finite. An efficient method for the calculation of the loop function in S- and G-wave were developed and discussed in detail. The author contributed to this derivation and employed the VEGAS routine to evaluate the real and imaginary part of the loop function in the S- and G-wave. Moreover, the limit $M \to 0$ was considered, in which the long-range potential considered here reduces to the Coulomb potential. The author verified that the result for the loop function in the present approach matches to the result in literature for the Coulomb potential up to the choice of renormalization prescription. Finally, the modified effective range function was compared to the standard effective range function and it was shown explicitly that the region of applicability of the modified function is greater than the standard one.

5.1 Introduction

The recent surge of interest to the two-body finite-volume quantization condition in the presence of a long-range force [56, 57, 60–63, 221, 243–247] can be attributed, first and foremost, to the ongoing studies of two specific problems in lattice QCD. These are the calculation of the D^*D spectrum and the properties of the $T_{cc}^+(3875)$ state [248–251], as well as to the extraction of the baryon-baryon scattering phase shifts from the two-baryon spectrum [55, 252, 253].[1] At physical quark masses, both these systems feature a long-range force that emerges from the one-pion exchange. This leads to

[1] For an alternative approach to the study of these systems by using HAL QCD method, see, e.g., [254–256].

several interrelated problems in the analysis of lattice data, all stemming from the fact that the scale that defines the effective range of interactions could become sizable as compared to the inverse of the box size L. (For the systems in question, this scale is of order of the pion mass or even less.) Namely, the exponentially suppressed corrections, which are usually neglected in the derivation of the Lüscher equation [33], may become relevant. Furthermore, the standard Lüscher approach relies on the truncation of higher partial-waves. However, as one knows, the convergence of the partial-wave expansion in the presence of a long-range force is poor, and many terms have to be kept in this expansion in order to achieve a reasonable accuracy. Last but not least, it is well known that the partial-wave scattering amplitudes in quantum field theory develop the so-called left-hand cut in the complex s-plane. In case of NN scattering, the beginning of this cut lies just 5 MeV below the elastic NN threshold. In general, the width of the gap between left- and right-hand cuts is related to the effective range of the interactions and is very small for the systems considered here. It is also clear that, for the analysis of the energy levels which lie on or in the vicinity of the left-hand cut, the standard Lüscher method is not applicable.

In recent years, several approaches have been proposed to address the problems mentioned above. The work done within the HAL QCD approach [254–256] is conceptually very different from the rest and will not be considered here. Furthermore, a very straightforward approach, uses an effective field theory based Hamiltonian and treats long- and short-range interactions on equal footing [56]. This approach parameterizes the interactions in terms of effective couplings which are, by definition, devoid of any singularities, in contrast to the S-matrix elements. The scattering equations are then solved directly in a finite volume, producing the finite-volume spectrum that is fitted to the data. In order to avoid large partial-wave mixing effects and the emergence of the left-hand cut, the equations are solved in the plane-wave basis, without resorting to the partial-wave expansion. In this way, one also takes into account exponentially suppressed corrections, apart from those that are implicitly included in the effective couplings and are determined by a heavy scale. At the final stage, one solves the same equation in the infinite volume in order to determine S-matrix elements, using the values of the couplings extracted from the fit to the lattice spectrum. We further note that the approach, where the two-body scattering is "embedded" into the three-body problem (see, e.g., [61, 62]), is based on similar premises. Namely, below the breakup threshold, it is equivalent to the two-body equation written down in the plane-wave basis, where the sum is performed over the spectator three-momentum, while, of course, these two approaches differ above the breakup threshold. An alternative approach, using the finite-volume version of the N/D method, has also been proposed recently [244].

Another group of approaches is based on the explicit splitting of the interaction into the known long-range and the unknown short-range parts [60, 221, 243]. In particular, here we shall concentrate on the approach developed in Ref. [221], which uses the finite-volume generalization of the so-called modified effective range expansion by van Haeringen and Kok [64]. Here, the long-range interaction is treated in the plane-wave basis, whereas the partial-wave expansion for the short-range part is still performed. This expansion is assumed to be converging well, which will be explicitly verified below. As a result, one obtains a modified Lüscher equation with a little partial-wave mixing, which allows one to extract the scattering phase pretty much in the same way as in the standard Lüscher approach. We would like to stress that we do not plan a comparison of different approaches with the aim of determining the best one. As far as we can see, all of them are conceptually equivalent and the decision of which one to use should be based on mere convenience, see Ref. [63] for more discussion on this issue.

The aim of the present chapter is to demonstrate the numerical implementation of the formalism

developed in Ref. [221], carrying out the analysis of synthetic data generated in a toy model. In the course of this, we shall address all issues mentioned in the beginning, namely, the size of the exponentially suppressed corrections, partial-wave mixing, and the analysis of the data in the region of the left-hand cut. Another important issue that we consider in the present article is the renormalization. In particular, the modified Lüscher zeta-function, which enters the modified Lüscher equation, is given by an infinite sum of diagrams corresponding to the multiple insertions of the long-range potential into a two-particle loop. These diagrams are ultraviolet-divergent, with the degree of divergence growing with the angular momentum of a given partial-wave. It can be seen that the cutoff regularization becomes inconvenient in higher partial-waves, since power-law divergences force the parameters of the effective-range expansion to be of an unnatural size. We therefore opt for the dimensional regularization and provide an efficient numerical algorithm for the calculation of the above-mentioned multi-loop integral in this regularization. It should be stressed that the results of these studies are relevant beyond the applications in the analysis of the finite-volume lattice data and can be used for the study of the few-body systems in the presence of several interactions with very different scales.

The layout of the chapter is as follows. In order to render the chapter self-contained, we review the key formulae from Ref. [221] in Sect. 5.2. This material is essential for the understanding of the rest of the chapter. In Sect. 5.3, we consider the calculation of the modified Lüscher zeta-function and the analysis of the (synthetic) data. Finally, in Sect. 5.4, we consider the renormalization of the modified Lüscher zeta-function in dimensional regularization and the modified effective-range expansion. To separate the conceptual issues from unnecessary technical details, we work exclusively in the center-of-mass frame and concentrate on the A_1^+ representation of the octahedral group. Furthermore, we assume that the long-range part of the potential is given by a simple Yukawa interaction corresponding to the exchange of a light particle with a mass M. Going beyond these assumptions forms the subject of a separate investigation.

5.2 Modified Effective-Range Expansion and Modified Lüscher Equation

In the infinite volume, the two-body scattering amplitude T obeys the Lippmann-Schwinger equation

$$T(\boldsymbol{p},\boldsymbol{q};q_0^2) = V(\boldsymbol{p},\boldsymbol{q}) + \int \frac{d^3\boldsymbol{k}}{(2\pi)^3}\,\frac{V(\boldsymbol{p},\boldsymbol{k})T(\boldsymbol{k},\boldsymbol{q};q_0^2)}{\boldsymbol{k}^2 - q_0^2}\,, \tag{5.1}$$

where the variable q_0^2 is understood to have a small positive imaginary part, $q_0^2 + i\epsilon$, above threshold as usual (q_0 denotes the magnitude of the relative three-momenta on shell). The potential $V = V_L + V_S$ is given by a sum of a long- and short-range parts. The long-range part is known and local. In the following, we assume that it is given by the Yukawa potential corresponding to the exchange of a particle with the mass M (the pion)

$$V_L(\boldsymbol{p},\boldsymbol{q}) = \frac{4\pi g}{M^2 + (\boldsymbol{p}-\boldsymbol{q})^2}\,. \tag{5.2}$$

In case of the NN scattering within the chiral effective theory, for example, in the ${}^3P_0$ partial-wave, $g = mM^2 g_A^2/(16\pi F_\pi^2) \simeq 0.073\,m$, where m, $g_A \simeq 1.27$ and $F_\pi \simeq 92.3\,\text{MeV}$ denote the nucleon mass,

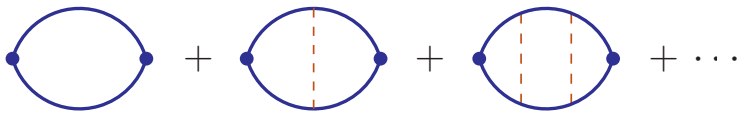

Figure 5.1: Perturbative expansion of the function $M_\ell(q_0)$ defined in Eq. (5.5) in the coupling constant g. One-pion-exchange ladders to all orders contribute to this expansion. The filled dots correspond to the insertion of $\mathcal{Y}^*_{\ell m}(\boldsymbol{p})$ and $\mathcal{Y}_{\ell' m'}(\boldsymbol{q})$.

axial-vector coupling constant and the pion decay constant, respectively. We shall use this value of g in the toy model considered below.

The short-range part is generally unknown and non-local. Its expansion in momenta takes the form

$$V_S(\boldsymbol{p},\boldsymbol{q}) = C_0^{00} + 3C_1^{00}\boldsymbol{p}\boldsymbol{q} + C_0^{10}(\boldsymbol{p}^2+\boldsymbol{q}^2) + \cdots . \tag{5.3}$$

Note that in the derivation of the modified effective-range expansion, it is usually assumed that the long-range potential is superregular. In the partial-wave with angular momentum ℓ this means that $r^{-2\ell}V_L(r)$ stays analytic at $r \to 0$. The potential in Eq. (5.2) does not fulfill this condition, even for $\ell = 0$. One could use different types of regularizations here, e.g., Pauli-Villars regularization as in Ref.[221], or merely a sharp cutoff. As we shall see, however, this method is numerically inconvenient, when higher partial-waves are included. The loops with one-pion exchanges are divergent and produce high powers of the cutoff mass. Renormalization implies that these large polynomial contributions are included in the short-range couplings $C_0^{00}, C_1^{00}, C_0^{10}\ldots$, rendering them to be unnaturally large. We shall therefore argue in favor of the dimensional regularization and introduce a renormalization scheme where such large contributions are absent from the beginning.

The modified effective-range expansion for the scattering phase shift on the full potential V can be written in the following form

$$K_\ell^M(q_0^2) = M_\ell(q_0) + \frac{q_0^{2\ell+1}}{|f_\ell(q_0)|^2}\left(\cot(\delta_\ell(q_0)-\sigma_\ell(q_0)) - i\right). \tag{5.4}$$

Here, $K_\ell^M(q_0^2)$ denotes the so-called modified effective range function, whereas $M_\ell(q_0)$ is given by

$$\delta_{\ell\ell'}\delta_{mm'}M_\ell(q_0) = (4\pi)^2\int\frac{d^3\boldsymbol{p}}{(2\pi)^3}\frac{d^3\boldsymbol{q}}{(2\pi)^3}\,\mathcal{Y}^*_{\ell m}(\boldsymbol{p})\langle\boldsymbol{p}|G_L(q_0)|\boldsymbol{q}\rangle\mathcal{Y}_{\ell' m'}(\boldsymbol{q}), \tag{5.5}$$

where $\mathcal{Y}_{\ell m}(\boldsymbol{p}) = p^\ell Y_{\ell m}(\hat{p})$ and $Y_{\ell m}(\hat{p})$ denotes the conventional spherical function. Furthermore, $G_L(q_0)$ is the Green function for the scattering on the long-range potential only, which obeys the following equation

$$\langle\boldsymbol{p}|G_L(q_0)|\boldsymbol{q}\rangle = \frac{(2\pi)^3\delta^3(\boldsymbol{p}-\boldsymbol{q})}{\boldsymbol{p}^2-q_0^2} + \frac{1}{\boldsymbol{p}^2-q_0^2}\int\frac{d^3\boldsymbol{k}}{(2\pi)^3}V_L(\boldsymbol{p},\boldsymbol{k})\langle\boldsymbol{k}|G_L(q_0)|\boldsymbol{q}\rangle. \tag{5.6}$$

Expanding the quantity $G_L(q_0)$ in perturbative series, it is seen that $M_\ell(q_0)$ is given by the sum of loops with zero, one, two,... insertions of the one-pion exchange, see Fig. 5.1. Of course, the above

expressions do not make sense as they stand, since the integrals entering some of the expressions diverge in the ultraviolet. Some regularization/renormalization is implicit in these expressions. Other quantities that enter into Eq. (5.4), are the phase shift on the full potential $\delta_\ell(q_0)$, the phase shift on the long-range potential $\sigma_\ell(q_0)$, and the Jost function for the long-range potential $f_\ell(q_0)$. Thus, all quantities on the right-hand side of this equation, except $\delta_\ell(q_0)$, can be evaluated from the known potential V_L prior to performing any lattice calculations. The rationale for splitting the potential into the long- and short-range parts is manifested in the properties of $K_\ell^M(q_0^2)$. Namely, while the effective range expansion of the conventional K-matrix, obtained without such a splitting, has a very small radius of convergence due to the proximity of the left-hand cut, $K_\ell^M(q_0^2)$ stays regular in the left-hand region.

The modified Lüscher equation, which is based on the same splitting, performed in a finite volume, is given by $\det\left[\mathscr{A}(q_0)\right] = 0$, where

$$\mathscr{A}_{\ell m,\ell' m'}(q_0) = \frac{1}{4\pi}\,\delta_{ll'}\delta_{mm'}K_\ell^M(q_0^2) - H_{\ell m,\ell' m'}(q_0)\,. \tag{5.7}$$

In Eq. (5.7), the quantity $H_{\ell m,\ell' m'}(q_0)$ is defined as (cf. with Eq. (5.5))

$$H_{\ell m,\ell' m'}(q_0) = \frac{4\pi}{L^6}\sum_{\boldsymbol{p},\boldsymbol{q}} \mathscr{Y}^*_{\ell m}(\boldsymbol{p})\langle \boldsymbol{p}|G_L(q_0)|\boldsymbol{q}\rangle \mathscr{Y}_{\ell' m'}(\boldsymbol{q})\,, \tag{5.8}$$

where $G_L(q_0)$ is given by Eq. (5.6), with the integration replaced by summation over the discrete momenta $\boldsymbol{p} = 2\pi\boldsymbol{n}/L\,,\ \boldsymbol{q} = 2\pi\boldsymbol{n}'/L$, with $\boldsymbol{n}\,,\boldsymbol{n}' \in \mathbb{Z}^3$.

Owing to the lack of the rotational invariance, the finite-volume quantization condition is not diagonal in angular momentum. Partial diagonalization is achieved using the octahedral symmetry of the cubic lattice. To this end, one defines (see, e.g., [33, 36, 179])

$$\delta_{\sigma\rho}\mathscr{A}^\Gamma_{t\ell,t'\ell'}(q_0) = \sum_{mm'}\left(c^{\Gamma\sigma t}_{\ell m}\right)^*\mathscr{A}_{\ell m,\ell' m'}(q_0)c^{\Gamma\rho t'}_{\ell' m'}\,. \tag{5.9}$$

Here, Γ denotes a particular irreducible representation (irrep) of the octahedral group, and t, t' are indices that label different copies of the same irrep Γ contained in the irreps of the rotation group characterized by angular momenta ℓ, ℓ' respectively. Furthermore, σ, ρ label basis vectors in the irrep Γ, and $c^{\Gamma\sigma t}_{\ell m}$, $c^{\Gamma\rho t'}_{\ell' m'}$ denote the pertinent Clebsh-Gordan coefficients. The quantization condition in a given irrep is now given by $\det\left[\mathscr{A}^\Gamma(q_0)\right] = 0$. Finally, the spherical harmonics after the projection onto the irrep Γ are defined as

$$\mathscr{Y}^{\Gamma\sigma t}_\ell(\boldsymbol{p}) = \sum_m c^{\Gamma\sigma t}_{\ell m}\mathscr{Y}_{\ell m}(\boldsymbol{p})\,. \tag{5.10}$$

Owing to the Wigner-Eckart theorem, the sum in the r.h.s. of Eq. (5.9) yields the factor $\delta_{\sigma\rho}$ with the coefficient that does not depend on σ and ρ. For this reason, one may fix $\sigma = \rho$ to any value in the calculations. For this reason, and in order to avoid clutter of indices, in the following we suppress σ, ρ in all expressions.

5.3 Modified Lüscher Zeta-Function and the Analysis of Data

5.3.1 Calculation of the Zeta-Function

In this section we shall concentrate on the calculation of the quantity that enters the matrix $\mathscr{A}^{\Gamma}_{t\ell,t'\ell'}(q_0)$ from Eq. (5.9):

$$H^{\Gamma}_{t\ell,t'\ell'}(q_0) = \frac{4\pi}{L^6}\sum_{\boldsymbol{p},\boldsymbol{q}}\left(\mathscr{Y}^{\Gamma t}_{\ell}(\boldsymbol{p})\right)^{*}\langle \boldsymbol{p}|G_L(q_0)|\boldsymbol{q}\rangle \mathscr{Y}^{\Gamma t'}_{\ell'}(\boldsymbol{q})\,. \tag{5.11}$$

In the infinite volume, the summation is replaced by integration, and we have

$$\begin{aligned} H^{\Gamma,\infty}_{t\ell,t'\ell'}(q_0) &= \sum_{mm'}\left(c^{\Gamma t}_{\ell m}\right)^{*} H^{\infty}_{\ell m,\ell' m'}(q_0) c^{\Gamma t'}_{\ell' m'} \\ &= \frac{1}{4\pi}\sum_{mm'}\left(c^{\Gamma t}_{\ell m}\right)^{*}\delta_{\ell\ell'}\delta_{mm'}\mathrm{Re}\left[M_\ell(q_0)\right] c^{\Gamma t'}_{\ell' m'} \\ &= \frac{1}{4\pi}\delta_{\ell\ell'}\delta_{mm'}\delta_{tt'}\mathrm{Re}\left[M_\ell(q_0)\right]\,. \end{aligned} \tag{5.12}$$

One further defines

$$\begin{aligned} \Delta H^{\Gamma}_{t\ell,t'\ell'}(q_0) &= H^{\Gamma}_{t\ell,t'\ell'}(q_0) - H^{\Gamma,\infty}_{t\ell,t'\ell'}(q_0) \\ &= H^{\Gamma}_{t\ell,t'\ell'}(q_0) - \frac{1}{4\pi}\delta_{\ell\ell'}\delta_{tt'}\mathrm{Re}\left[M_\ell(q_0)\right]\,. \end{aligned} \tag{5.13}$$

The matrix that enters in the quantization condition, takes the form

$$\mathscr{A}^{\Gamma}_{t\ell,t'\ell'}(q_0) = \frac{1}{4\pi}\delta_{\ell\ell'}\delta_{tt'}K^{M}_{\ell}(q_0^2) - H^{\Gamma}_{t\ell,t'\ell'}(q_0)\,. \tag{5.14}$$

Using Eq. (5.4) and the unitarity relation, which relates the imaginary part of $M_\ell(q_0)$ with the Jost function $f_\ell(q_0)$, the matrix $\mathscr{A}$ can be finally rewritten in the following form

$$\mathscr{A}^{\Gamma}_{t\ell,t'\ell'}(q_0) = \frac{q_0^{2\ell+1}}{4\pi|f_\ell(q_0)|^2}\delta_{\ell\ell'}\delta_{tt'}\cot(\delta_\ell(q_0)-\sigma_\ell(q_0)) - \Delta H^{\Gamma}_{t\ell,t'\ell'}(q_0)\,. \tag{5.15}$$

The advantage of this transformation consists in the fact that the quantity ΔH does not contain ultraviolet divergences. Indeed, let us consider the quantity $G_L(q_0)$, which enters the expression of the matrix H. The free Green function in the finite-volume version of the Lippmann-Schwinger equation (5.6) can be split into two parts, according to

$$\frac{1}{\boldsymbol{p}^2-q_0^2} = \underbrace{\left(\frac{1}{\boldsymbol{p}^2+\mu^2}+\frac{\mu^2+q_0^2}{(\boldsymbol{p}^2+\mu^2)^2}+\cdots+\frac{(\mu^2+q_0^2)^n}{(\boldsymbol{p}^2+\mu^2)^{n+1}}\right)}_{=G_1} + \underbrace{\frac{(\mu^2+q_0^2)^{n+1}}{(\boldsymbol{p}^2+\mu^2)^{n+1}(\boldsymbol{p}^2-q_0^2)}}_{=G_2}\,. \tag{5.16}$$

Here, μ is an arbitrary scale, and the number of the subthreshold subtractions n is taken large enough to ensure the ultraviolet convergence of all sums after the angular-momentum truncation, when G_L is replaced by G_2. Furthermore, defining the scattering amplitude T_1 through the Lippmann-Schwinger equation $T_1 = V_L + V_L G_1 T_1$, we get

$$G_L = \underbrace{G_1 + G_1 T_1 G_1}_{=G_\mu} + \underbrace{(1 + G_1 T_1)\tilde{G}(T_1 G_1 + 1)}_{=G_f}\,, \tag{5.17}$$

where

$$\tilde{G} = G_2 + G_2 T_1 \tilde{G}\,. \tag{5.18}$$

The infinite-volume limit in the above equations are easily performed by replacing sums by integrals. Then, we have

$$\begin{aligned}\Delta H^{\Gamma}_{t\ell,t'\ell'}(q_0) &= \frac{4\pi}{L^6}\sum_{\boldsymbol{p},\boldsymbol{q}}\left(\mathcal{Y}^{\Gamma t}_{\ell}(\boldsymbol{p})\right)^*\langle \boldsymbol{p}|G_\mu(q_0)+G_f(q_0)|\boldsymbol{q}\rangle\mathcal{Y}^{\Gamma t'}_{\ell'}(\boldsymbol{q}) \\ &- 4\pi\int\frac{d^3\boldsymbol{p}}{(2\pi)^3}\frac{d^3\boldsymbol{q}}{(2\pi)^3}\left(\mathcal{Y}^{\Gamma t}_{\ell}(\boldsymbol{p})\right)^*\langle \boldsymbol{p}|G^\infty_\mu(q_0)+G^\infty_f(q_0)|\boldsymbol{q}\rangle\mathcal{Y}^{\Gamma t'}_{\ell'}(\boldsymbol{q})\,. \end{aligned}\tag{5.19}$$

The key property of this expression is that the quantity G_μ does not have a singular denominator in the physical region. Consequently, $G_\mu - G^\infty_\mu$ is suppressed by factors of $\exp(-\mu L)$ and can be safely neglected.[2] After dropping $G_\mu - G^\infty_\mu$, the remainder contains the subtracted propagator G_f only and is ultraviolet-finite both in a finite and in the infinite volume separately. In this manner, the quantity ΔH can be straightforwardly evaluated using numerical methods. Ultraviolet divergences are absent. No partial-wave expansion is involved for the long-range potential, and the Lippmann-Schwinger equation in a finite volume is solved in a plane-wave basis.

In Fig. 5.2 we plot the modified Lüscher zeta-function[3] $H^{\Gamma}_{t\ell,t'\ell'}(q_0)$ (see Eq. (5.11)) vs. the standard Lüscher zeta-function obtained from $H^{\Gamma}_{t\ell,t'\ell'}(q_0)$ at $g = 0$. The angular momenta take the values $\ell, \ell' = 0, 4$, and $q_0^2 = E/M$. The labels t, t' are neglected, because multiple representations are not present. The calculations of the modified Lüscher zeta-function are done for two different values of the parameter μ. As seen from Fig. 5.2, the results are practically independent of μ, which serves as a very good check on the calculations.

The calculated modified and standard functions are very similar to each other, except for a small horizontal shift. A difference, however, emerges in the vicinity of the lowest energy level corresponding to the relative momentum $\boldsymbol{p} = (0, 0, 0)$: except in the case $\ell = \ell' = 0$, the standard Lüscher zeta-function does not have a pole here. However, the modified function is a solution of the Lippmann-Schwinger type equation, where all momenta are present in the intermediate state, and therefore it develops a pole at the energy corresponding to the lowest level. For a better visibility, the

[2] A warning is in order: for certain values of the parameters, the quantities G_μ and G_f can develop subthreshold poles that cancel in the sum. However, one can always adjust the free parameter μ, so that these poles lie far outside the region of interest.

[3] Strictly speaking, $H^{\Gamma}_{t\ell,t'\ell'}(q_0)$ in the free case is given by a linear combination of the zeta-functions with known group-theoretical coefficients. For brevity, we shall refer to $H^{\Gamma}_{t\ell,t'\ell'}(q_0)$ as to the zeta-function as well.

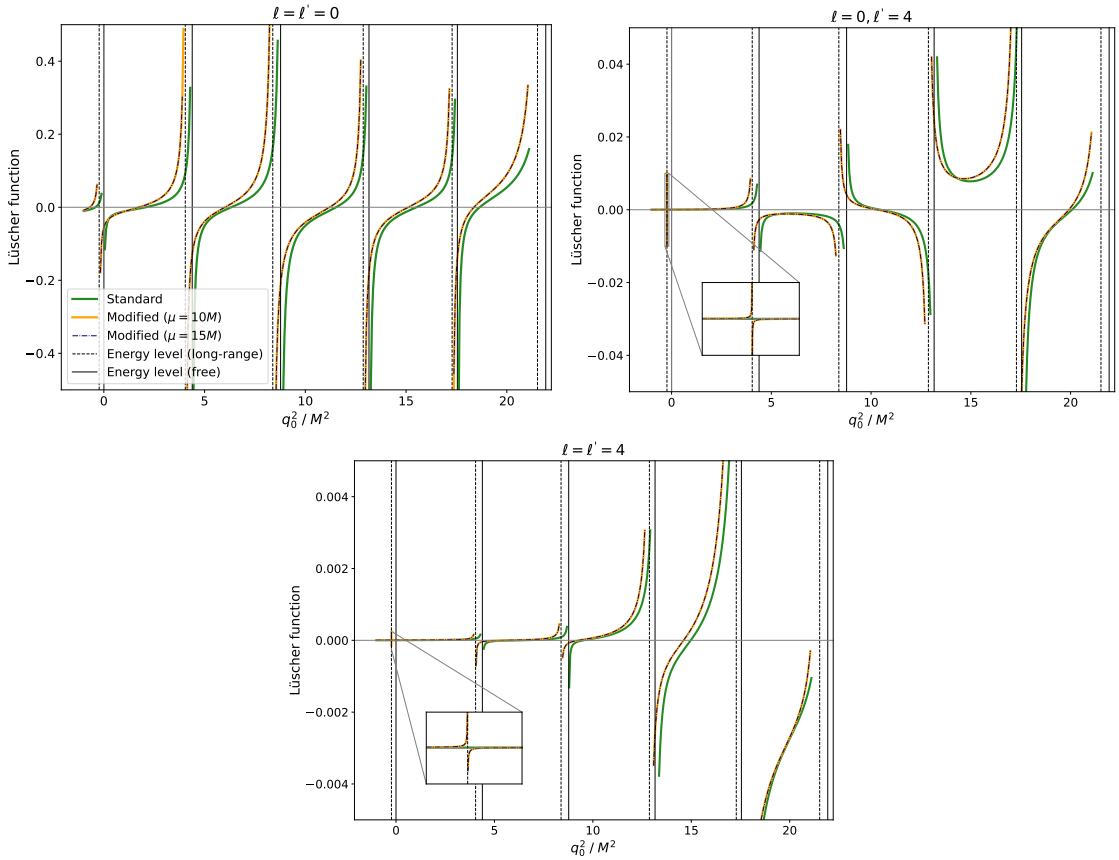

Figure 5.2: Modified Lüscher zeta-function vs. standard Lüscher zeta-function for two different values of parameter μ: $\mu = 10M$ and $\mu = 15M$. The size of the box is fixed by $ML = 3$. As seen, the difference between these two values of μ is not seen by a bare eye. Furthermore, the vicinity of the lowest energy level is zoomed in the last two plots, where the modified function, unlike the standard one, has a pole.

singular behavior of the modified Lüscher zeta-function in this energy region is zoomed in for the cases $\ell = 0, \ell' = 4$ and $\ell = \ell' = 4$.

5.3.2 Analysis of the Synthetic Data

The potential of the toy model, which are used to produce the synthetic lattice data, is given by a sum of the long- and short-range parts:

$$V(\boldsymbol{p}, \boldsymbol{q}) = \frac{4\pi g}{M^2 + (\boldsymbol{p} - \boldsymbol{q})^2} + \frac{4\pi g_S}{M_S^2 + (\boldsymbol{p} - \boldsymbol{q})^2}\,, \tag{5.20}$$

with $g_S/g = -2.74$. In addition, we set the ratio $m/M = 6.7$. Moreover, we treat M_S/M as a free parameter, in order to observe a smooth transition from the short-range to the long-range interaction.

First of all, note that one can easily solve the finite-volume quantization condition with the above potential, finding the eigenvalues of the Hamiltonian in the plane-wave basis. These solutions will be

used to test the validity of our method, since both approaches coincide up to the exponentially small corrections. Note also that, in the Hamiltonian approach, one can mimic the truncation of higher partial-waves in the Lüscher equation. To this end, one has merely to project the input potential onto the partial-waves and drop higher partial-waves in this projection.

As we know, one of the fundamental problems in using Lüscher equation in the presence of a long-range force consists in a slow convergence of the partial-wave expansion. In order to compare the convergence speed in case of the standard/modified Lüscher approach, we retain only S- and G-waves in the quantization condition. The equation (5.14) then yields

$$D(E) = \left(\frac{1}{4\pi}\, K_0^M(q_0) - H_{00}(q_0)\right) - \frac{\left(H_{04}(q_0)\right)^2}{\left(\frac{1}{4\pi}\, K_4^M(q_0) - H_{44}(q_0)\right)} = 0\,. \tag{5.21}$$

Here the labels t, t' are omitted for brevity. In case of the standard Lüscher equation, $K_\ell^M(q_0)$ is replaced by $K_\ell(q_0)$, and $H_{\ell\ell'}(q_0)$ by the expression evaluated at $g = 0$. If only the S-wave is taken into account, the second term in the expression (5.21) is dropped. Calculations are done for two values $M_S/M = 10$ and $M_S/M = 2$, corresponding to the two extreme cases.

Let us start with the excited states. The solutions of the quantization condition for the first few excited levels and for $M_S/M = 10$ are seen in Fig. 5.3. This plot beautifully demonstrates the advantage of the modified quantization condition with respect to the standard one. Namely, while taking into account the partial-waves with $\ell = 0, 4, \ldots$, the solution of the standard Lüscher equation slowly converges to the exact solution. In contrast, the solution of the modified quantization condition with the S-wave only already reproduces the exact energy level, and adding the G-wave does not change anything – the two curves cannot be distinguished from each other.

The pattern, described above, remains practically unchanged in case of $M_S/M = 2$, shown in Fig. 5.4, which describes a borderline situation with V_S almost long-range. Now, adding the G-wave leads to a visible effect, but still the convergence of the modified quantization condition is much better as compared to the standard one.

Few comments are in order. First, as seen, the exponentially suppressed effects are very small, because the solutions of the quantization condition reproduce very well the finite-volume spectrum of the Hamiltonian in the plane-wave basis. Second, the convergence of the partial-wave expansion is rather uneven. This can be seen better from Fig. 5.5, which shows the finite-volume spectrum of the Hamiltonian with the full potential projected onto different partial-waves. As seen, for example, the contribution of the G-wave to the 2nd excited state is rather small, and the higher partial-waves contribute significantly. A qualitative discussion of this phenomenon is given in appendix A.3. In general, as expected, the convergence becomes slower for higher partial-waves, with relative momentum increased.

Last but not least, we would like to note that in the situation when the short-range is completely absent (i.e., when $V_S = 0$), the energy levels are given by the poles of the modified Lüscher zeta-function $H_{\ell\ell'}(q_0)$. In Figs. 5.3 and 5.4, these poles are indicated by empty circles. It is seen that, even for $M_S = 10M$, the effect of setting $V_S = 0$ is sizable. However,the S-wave contribution alone suffices to reproduce the exact answer. This means that the partial-wave expansion in the modified Lüscher equation converges very fast indeed, and the truncation to the S-wave yields a very good approximation, in difference to the standard approach.

The ground state is considered separately. First, note that the convergence of the partial-wave

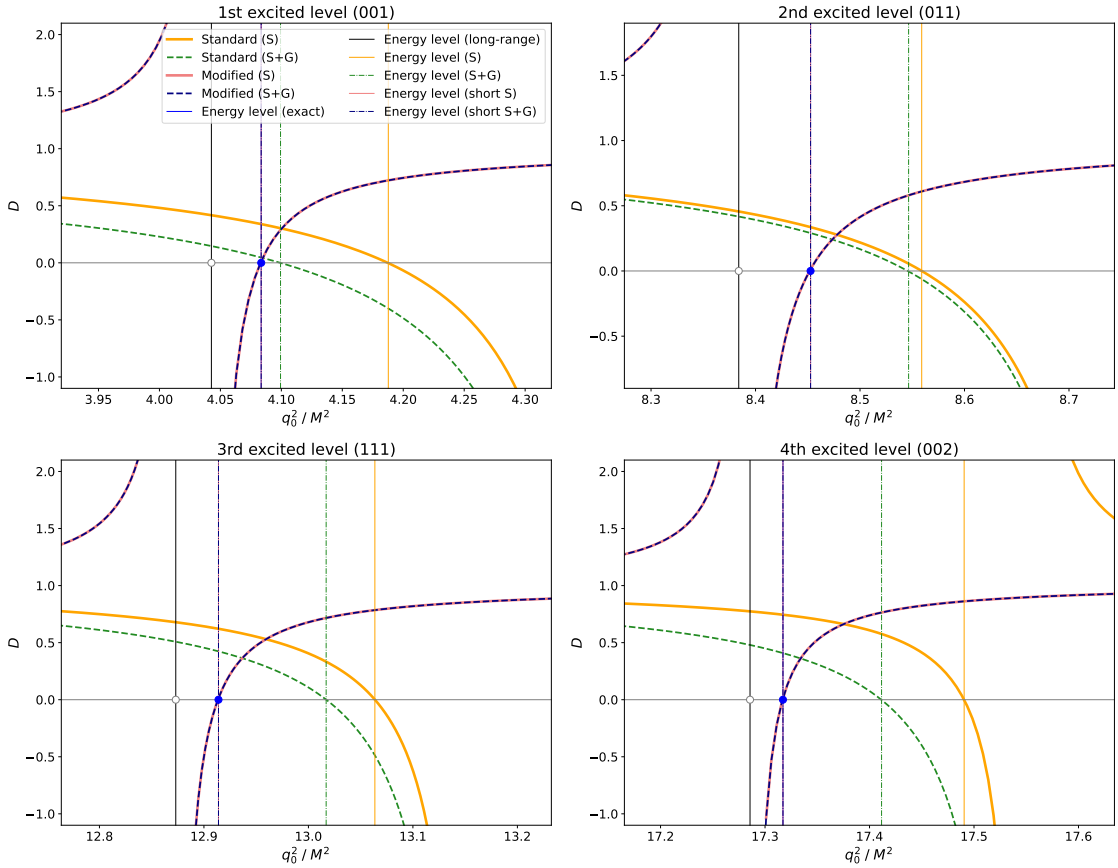

Figure 5.3: The solution of the quantization condition for the first few excited levels (both the standard and modified Lüscher equation). The partial-wave expansion is truncated, retaining only S-wave, or S- and G-waves. For comparison, the eigenvalues of the Hamiltonian are shown by vertical lines: exact, projected on S, S+G waves, only the short-range part projected on S, S+G waves. In addition, we show a solution with the long-range potential only, i.e., $V_S = 0$. The values of the parameters used are $M_S = 10M$, $ML = 3$. In the title of each plot, we indicate an unperturbed plane-wave state momentum, to which this state reduces in the absence of the interaction.

expansion in the Hamiltonian approach is very good[4], see Fig. 5.5, even for the standard case. The solution of the quantization condition, however, shown in Fig. 5.6 presents different picture. The modified quantization condition still provides a very accurate solution at $M_S/M = 10$ and a quite accurate solution at $M_S/M = 2$. The standard Lüscher equation, however, is completely off. The reason for this is the proximity of the left-hand cut which leads to large exponential corrections. As expected, these corrections are strongly suppressed in the modified quantization condition as compared to the standard one.

In order to understand this result qualitatively, let us introduce a characteristic parameter that determines, how far the left-hand cut is located from a given energy level. In the case of standard

[4] It is worth to mention that for some particular excited state, the G-wave contribution is obvious suppressed, for example, the 2nd excited level which is around the momentum of $(0, 1, 1)$. A detailed discussion is presented in App. A.3.

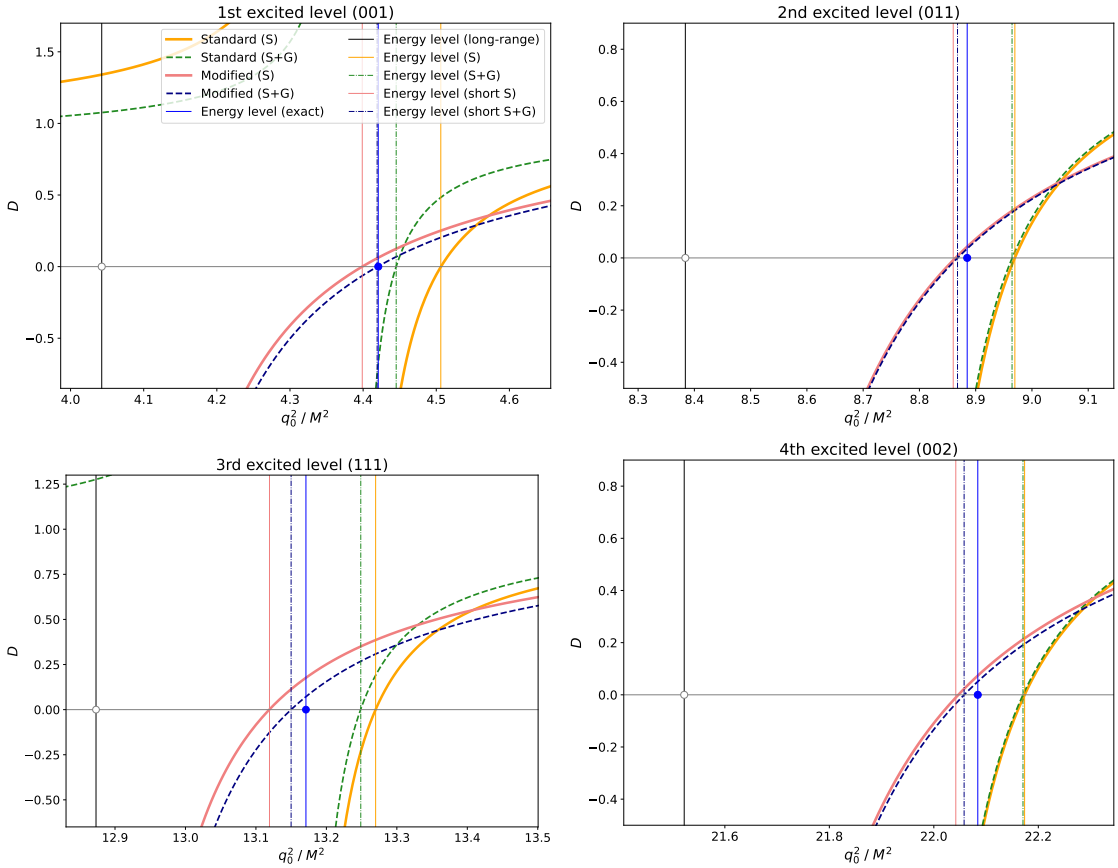

Figure 5.4: The same as in Fig. 5.3, but for $M_S = 2M$.

and modified Lüscher equations, the left hand starts at $q_0^2/M^2 = -1/4$ and $q_0^2/M^2 = -M_S^2/4M^2$, respectively. If one divides this quantity by the value of q_0^2/M^2 corresponding to the ground state (taken from the figure) and extracts the square root, one ends up with a ratio of momentum scales. In the case of the standard Lüscher equation, this ratio is equal to 1.1 and 1.9 for $M_S = 10M$ and $M_S = 2M$, respectively. In the modified case, this ratio becomes 11 and 3.8, respectively. This, in our opinion, explains why the exponential corrections in the modified case are much smaller than in the standard setting. It would be interesting to see, which value a similar parameter takes in the analysis of data carried out in Ref. [249], since this might provide a rough estimate of the exponential corrections which are neglected in this analysis.

5.4 Modified Effective-Range Expansion in the Left-Hand Cut Region

5.4.1 Calculation of the Loop Function $M_\ell(q_0)$

The function $M_\ell(q_0)$ is given by Eq. (5.5). As already mentioned, this quantity is ultraviolet-divergent. One way to regularize this divergence is to render the long-range potential superregular, e.g., by using

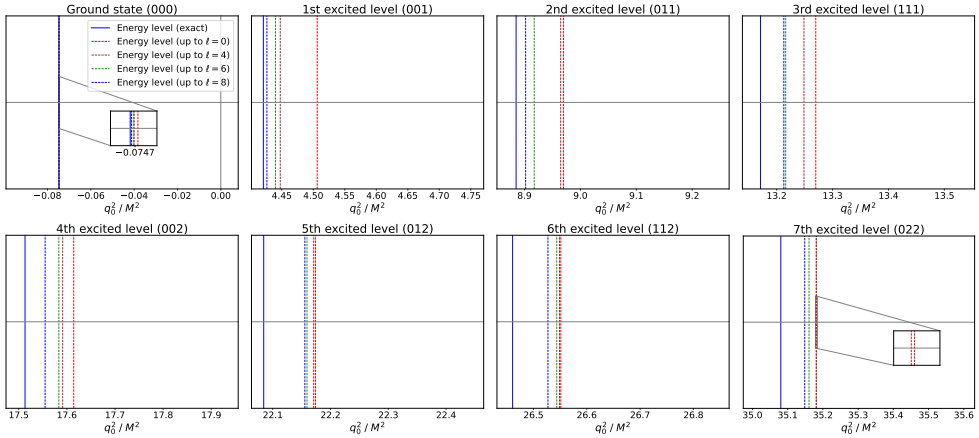

Figure 5.5: Checking the convergence of the partial-wave expansion in the energy spectrum of the Hamiltonian. The values of the parameters used are $M_S = 10M$ and $ML = 3$.

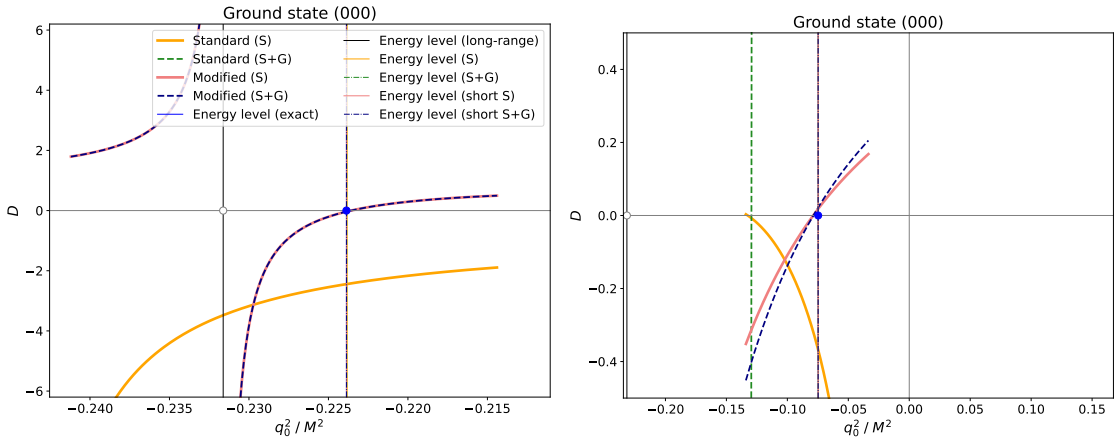

Figure 5.6: The solution of the quantization condition (both standard and modified) for the ground state. The values of the parameters are $ML = 3$ and $M_S = 10M$ (left panel), $M_S = 2M$ (right panel). There is no solution of the standard quantization condition in case $M_S = 10M$.

the Pauli-Villars regularization or a sharp cutoff. The price to pay for using this straightforward procedure is that the coefficients of the modified effective-range expansion if the function $K_\ell^M(q_0^2)$ are not of natural size anymore. Indeed, let Λ denote the (large) cutoff mass used in the regularization. For a given ℓ, the loop diverges as $\Lambda^{2\ell+1}$. Since in the modified effective-range expansion this loop enters in a combination $K_\ell^M(q_0^2) - M_\ell(q_0)$, it is clear that this polynomial with large coefficients has to be absorbed into $K_\ell^M(q_0^2)$. At the practical level, the cutoff regularization becomes numerically inconvenient for even not so large values of ℓ.[5] For this reason, we propose to use dimensional regularization instead, where the power divergences are absent. However, in this case, we encounter

[5] It should be mentioned that the problem of the ultraviolet divergences in the modified effective-range expansion has been observed in the literature before, see, e.g., Ref. [257].

another problem. Namely, the quantity $G_L(q_0)$, which enters the expression for $M_\ell(q_0)$, contains an infinite sum of one-pion exchange ladder diagrams (see Fig. 5.1) and is determined through the solution of an integral equation. It is not obvious how one can use dimensional regularization to tame divergences in the integral equation.

The key observation that allows one to solve the problem is that each consequent term in the Born series of $G_L(q_0)$ has a lower index of divergence than the previous one. Therefore, only a finite number of terms in the expansion diverge. One can use this property and split $G_L(q_0)$ into two parts: $G_L(q_0) = G_L^{\text{div}}(q_0) + G_0(q_0) T_L^{\text{fin}} G_0(q_0)$, and, correspondingly, $M_\ell(q_0) = M_\ell^{\text{div}}(q_0) + M_\ell^{\text{fin}}(q_0)$, where

$$\begin{aligned} G_L^{\text{div}}(q_0) &= \underbrace{\left(G_0(q_0) + G_0(q_0) V_L G_0(q_0) + \cdots\right)}_{2\ell+2 \text{ terms}}, \\ T_L^{\text{fin}} &= \underbrace{\left(V_L + V_L G_0(q_0) V_L + \cdots\right)}_{2\ell+2 \text{ terms}} + V_L G_0(q_0) T_L^{\text{fin}}. \end{aligned} \tag{5.22}$$

The integral equation that determines T_L^{fin} is of a Lippmann-Schwinger type and can be numerically solved by using standard techniques. The loop integral, containing T_L^{fin}, is free of ultraviolet divergences. Hence all calculations can be carried out in $d = 3$ dimensions.

The remainder is given by the following expression:

$$M_\ell^{\text{div}}(q_0) = 4\pi \int \frac{d^3\boldsymbol{p}}{(2\pi)^3} \frac{d^3\boldsymbol{q}}{(2\pi)^3} (pq)^\ell P_\ell(\hat{p}\cdot\hat{q}) \langle \boldsymbol{p} | G_L^{\text{div}}(q_0) | \boldsymbol{q} \rangle . \tag{5.23}$$

In order to carry out dimensional regularization in the above expression, one should first define Legendre polynomials $P_\ell(x)$ in d dimensions. This definition is not unique. However, using different definitions reduces to adding a finite polynomial in q_0^2 to $M_\ell^{\text{div}}(q_0)$ and hence can be accounted for by adjusting the renormalization prescription. Our definition is based on the use of the d-dimensional harmonic polynomials $\mathcal{Y}^{(\ell)}_{i_1\cdots i_\ell}(\boldsymbol{p}) = y_{i_1\cdots i_\ell, j_1\cdots j_\ell} p_{j_1}\cdots p_{j_\ell}$, which have the following properties:

- $\mathcal{Y}^{(\ell)}_{i_1\cdots i_\ell}(\boldsymbol{p})$ is a polynomial in the components of the vector $\boldsymbol{p}$;
- $\mathcal{Y}^{(\ell)}_{i_1\cdots i_\ell}(\boldsymbol{p})$ is symmetric and traceless in any pair of indices.

The examples of harmonic polynomials for $\ell = 0, 1, 2, 3, 4$ are given below:

$$\begin{aligned} \mathcal{Y}^{(0)}(\boldsymbol{p}) &= 1, \\ \mathcal{Y}^{(1)}_i(\boldsymbol{p}) &= p_i, \\ \mathcal{Y}^{(2)}_{ij}(\boldsymbol{p}) &= p_i p_j - \frac{1}{d}\boldsymbol{p}^2, \\ \mathcal{Y}^{(3)}_{ijk}(\boldsymbol{p}) &= p_i p_j p_k - \frac{1}{d+2}\boldsymbol{p}^2(\delta_{ij}p_k + \delta_{ik}p_j + \delta_{jk}p_i), \\ \mathcal{Y}^{(4)}_{ijkl}(\boldsymbol{p}) &= p_i p_j p_k p_l - \frac{1}{d+4}\boldsymbol{p}^2(\delta_{ij}p_k p_l + \delta_{ik}p_j p_l + \delta_{il}p_j p_k + \delta_{jk}p_i p_l + \delta_{jl}p_i p_k + \delta_{kl}p_i p_j) \\ &\quad + \frac{1}{(d+2)(d+4)}\boldsymbol{p}^4(\delta_{ij}\delta_{kl} + \delta_{ik}\delta_{jl} + \delta_{il}\delta_{jk}), \end{aligned} \tag{5.24}$$

and so on. The coefficients $y_{i_1\cdots i_\ell, j_1\cdots j_\ell}$ can be easily read off from these expressions. Furthermore,

$$(pq)^\ell P_\ell(\hat{p}\cdot\hat{q}) = c_d^{(\ell)} \sum_{i_i,\cdots,i_\ell} \mathscr{Y}^{(\ell)}_{i_1\cdots i_\ell}(\boldsymbol{p})\mathscr{Y}^{(\ell)}_{i_1\cdots i_\ell}(\boldsymbol{q})\,. \tag{5.25}$$

This gives

$$\begin{aligned}
P_0(\hat{p}\cdot\hat{q}) &= 1\,,\\
(pq)P_1(\hat{p}\cdot\hat{q}) &= (\boldsymbol{pq})\,,\\
(pq)^2P_2(\hat{p}\cdot\hat{q}) &= \frac{d}{d-1}\left((\boldsymbol{pq})^2 - \frac{1}{d}\,\boldsymbol{p}^2\boldsymbol{q}^2\right),\\
(pq)^3P_3(\hat{p}\cdot\hat{q}) &= \frac{d+2}{d-1}\left((\boldsymbol{pq})^3 - \frac{3}{d+2}\,(\boldsymbol{pq})\boldsymbol{p}^2\boldsymbol{q}^2\right),\\
(pq)^4P_4(\hat{p}\cdot\hat{q}) &= \frac{(d+2)(d+4)}{d^2-1}\left((\boldsymbol{pq})^4 - \frac{6}{d+4}\,(\boldsymbol{pq})^2\boldsymbol{p}^2\boldsymbol{q}^2 + \frac{3}{(d+2)(d+4)}\,\boldsymbol{p}^4\boldsymbol{q}^4\right),
\end{aligned} \tag{5.26}$$

and so on. The normalization constant $c_d^{(\ell)}$ is chosen so that $P_\ell(1) = 1$ for all d.

Since our calculations are restricted to the A_1^+ irrep of the octahedral group for demonstration purposes, it suffices to consider the angular momenta $\ell = 0, 4$.

The Case $\ell = 0$

In this case, only the two-loop diagram $M^{\mathsf{div}}_{0,2}(q_0)$ (the second diagram in Fig. 5.1) should be considered. The one-loop diagram with no pion exchange can be easily evaluated in dimensional regularization and the rest is ultraviolet-finite. The two-loop diagram in dimensional regularization is given by

$$\begin{aligned}
M^{\mathsf{div}}_{0,2}(q_0) &= 4\pi\int\frac{d^d\boldsymbol{p}}{(2\pi)^d}\,\frac{d^d\boldsymbol{q}}{(2\pi)^d}\,\frac{1}{\boldsymbol{p}^2-q_0^2}\,\frac{4\pi g}{M^2+(\boldsymbol{p}-\boldsymbol{q})^2}\,\frac{1}{\boldsymbol{q}^2-q_0^2}\\
&= \int_0^1 \mathscr{D}_{xy}\int\frac{d^d\boldsymbol{p}}{(2\pi)^d}\,\frac{d^d\boldsymbol{q}}{(2\pi)^d}\,\frac{\Gamma(3)\,(4\pi)^2 g}{\Big(x_1(\boldsymbol{p}^2-q_0^2)+y(M^2+(\boldsymbol{p}-\boldsymbol{q})^2)+x_2(\boldsymbol{q}^2-q_0^2)\Big)^3}\,,
\end{aligned} \tag{5.27}$$

where

$$\mathscr{D}_{xy} = dx_1dx_2dy\,\delta(1-x_1-x_2-y)\,. \tag{5.28}$$

One can rewrite the above expression in a compact form, introducing a 2-dimensional column $\boldsymbol{Q}_\alpha$, $\alpha = 1, 2$, where $\boldsymbol{Q}_1 = \boldsymbol{p}$ and $\boldsymbol{Q}_2 = \boldsymbol{q}$. Then,

$$M^{\mathsf{div}}_{0,2}(q_0) = \int_0^1 \mathscr{D}_{xy}\int\frac{d^{2d}\boldsymbol{Q}}{(2\pi)^{2d}}\,\frac{\Gamma(3)\,(4\pi)^2 g}{\left(\sum\limits_{\alpha,\beta}\boldsymbol{Q}_\alpha C_{\alpha\beta}\boldsymbol{Q}_\beta + \Delta\right)^3}\,, \tag{5.29}$$

where

$$C = \begin{pmatrix} x_1 + y & -y \\ -y & y + x_2 \end{pmatrix}, \qquad \Delta = yM^2 - (x_1 + x_2)q_0^2 \,. \tag{5.30}$$

One can now perform orthogonal transformations in order to diagonalize the matrix C. The result looks as

$$M_{0,2}^{\mathsf{div}}(q_0) = \int_0^1 \mathscr{D}_{xy} \int \frac{d^{2d}\boldsymbol{Q}}{(2\pi)^{2d}} \frac{\Gamma(3)\,(4\pi)^2 g}{\left(\sum\limits_\alpha \boldsymbol{Q}_\alpha \lambda_\alpha \boldsymbol{Q}_\alpha + \Delta\right)^3}, \tag{5.31}$$

where λ_α denote the eigenvalues of the matrix C. Rescaling further the momenta $\boldsymbol{Q}_\alpha \to \lambda_\alpha^{-1/2}\boldsymbol{Q}_\alpha$, we get:

$$\begin{aligned} M_{0,2}^{\mathsf{div}}(q_0) &= \int_0^1 \mathscr{D}_{xy} \int \frac{d^{2d}\boldsymbol{Q}}{(2\pi)^{2d}} \frac{\Gamma(3)\,(4\pi)^2 g \det(C)^{-d/2}}{\left(\sum\limits_\alpha \boldsymbol{Q}_\alpha \boldsymbol{Q}_\alpha + \Delta\right)^3} \\ &= \frac{\Gamma(3-d)g}{(4\pi)^{d-2}} \int_0^1 \mathscr{D}_{xy} \det(C)^{-d/2} \Delta^{d-3} \,. \end{aligned} \tag{5.32}$$

We further introduce the new variables $x_1 = \rho\tau$ and $x_2 = \rho(1-\tau)$, with $0 \le \rho, \tau \le 1$. Defining the dimensionless quantity $z = q_0^2/M^2$ and carrying out the integration in y, we get

$$\begin{aligned} M_{0,2}^{\mathsf{div}}(q_0) &= \frac{\Gamma(3-d)g(M^2)^{d-3}}{(4\pi)^{d-2}} \int_0^1 \rho d\rho d\tau ((1-\rho) - \rho z)^{d-3} (\rho(1-\rho) + \rho^2\tau(1-\tau))^{-d/2} \\ &= \frac{\Gamma(3-d)g(M^2)^{d-3}}{(4\pi)^{d-2}} \int_0^\infty ds \int_0^1 d\tau (s-z)^{d-3} (s + \tau(1-\tau))^{-d/2} \\ &= -\frac{g}{2(d-3)} + \text{UV finite}, \end{aligned} \tag{5.33}$$

where a new integration variable $s = (1-\rho)/\rho$ was introduced.

As anticipated, the two-loop diagram is ultraviolet divergent. One could use, for example, MS or $\overline{\text{MS}}$ renormalization scheme, using M (as the only available mass) as a renormalization scale. The advantage of such a procedure consists in the fact that no large polynomials should be absorbed in $K_\ell^M(q_0^2)$ anymore. It should be pointed, however, that using this scheme becomes more complicated for higher values of ℓ, even if the above statement still applies. Namely, there are more divergent diagrams for higher ℓ, and the factors $(d-3)^{-1}$ may arise either from the prefactor containing the Γ-function, or the integral over the variable s, and the separation of the all ultraviolet-divergent terms becomes involved. We find that a simple solution to the problem is to impose a different renormalization prescription, namely, to subtract first few terms in the Taylor expansion at threshold $z = 0$. In the case we are considering, a single subtraction suffices, since the divergent term is a constant:

$$\hat{M}_{0,2}^{\mathsf{div}}(q_0) = M_{0,2}^{\mathsf{div}}(q_0) - M_{0,2}^{\mathsf{div}}(0) \,. \tag{5.34}$$

For higher ℓ, more subtractions are necessary.

The Case $\ell = 4$

In the section above we have considered the case $\ell = 0$ in great detail, including the discussion of the ultraviolet regularization and the choice of the renormalization prescription. Most of the techniques, used here, can be applied for higher values of ℓ without change. In this case, however, there are more divergent diagrams. The N-loop diagram can be written as follows:

$$\begin{aligned} M_{4,N}^{\text{div}}(q_0) &= 4\pi \int \frac{d^d\boldsymbol{Q}_1}{(2\pi)^d} \cdots \frac{d^d\boldsymbol{Q}_N}{(2\pi)^d} \frac{1}{\boldsymbol{Q}_1^2 - q_0^2} \frac{4\pi g}{M^2 + (\boldsymbol{Q}_1 - \boldsymbol{Q}_2)^2} \cdots \frac{(Q_1 Q_N)^4 P_4(\hat{Q}_1 \cdot \hat{Q}_N)}{\boldsymbol{Q}_N^2 - q_0^2} \\ &= \int_0^1 \mathscr{D}_{xy} \int \frac{d^d\boldsymbol{Q}_1}{(2\pi)^d} \cdots \frac{d^d\boldsymbol{Q}_N}{(2\pi)^d} \frac{h_N (Q_1 Q_N)^4 P_4(\hat{Q}_1 \cdot \hat{Q}_N)}{D^{2N-1}}, \end{aligned} \tag{5.35}$$

where $h_N = \Gamma(2N-1)\,(4\pi)^N g^{N-1}$ and

$$D = x_1(\boldsymbol{Q}_1^2 - q_0^2) + y_1(M^2 + (\boldsymbol{Q}_1 - \boldsymbol{Q}_2)^2) + \cdots + x_N(\boldsymbol{Q}_N^2 - q_0^2)\,. \tag{5.36}$$

Here, the Feynman parameters x_i, $i = 1, \ldots, N$ and $y_i, i = 1, \ldots, N-1$ are associated with the Green function $(\boldsymbol{Q}_i^2 - q_0^2)^{-1}$ and the pion propagator $(M^2 + (\boldsymbol{Q}_i - \boldsymbol{Q}_{i+1})^2)^{-1}$, respectively, and $\mathscr{D}_{xy} = dx_1 \cdots dx_N dy_1 \cdots dy_{N-1} \delta(1 - x_1 - \cdots - x_N - y_1 - \cdots - y_{N-1})$. The tridiagonal matrix C takes the following form

$$C = \begin{pmatrix} x_1 + y_1 & -y_1 & 0 & 0 & 0 & \cdots & 0 \\ -y_1 & x_2 + y_1 + y_2 & -y_2 & 0 & 0 & \cdots & 0 \\ 0 & -y_2 & x_3 + y_2 + y_3 & -y_3 & 0 & \cdots & 0 \\ & & \cdots & & & & -y_{N-1} \\ 0 & \cdots & 0 & 0 & 0 & -y_{N-1} & x_N + y_{N-1} \end{pmatrix} \tag{5.37}$$

Let the matrix O be an orthogonal matrix that diagonalizes C: $(OCO^T)_{\alpha\beta} = \lambda_\alpha \delta_{\alpha\beta}$. The variable transformation $\boldsymbol{Q}_\alpha \to O_{\alpha\beta}\lambda_\beta^{-1/2}\boldsymbol{Q}_\beta$ transforms the denominator into

$$D \to \sum_\alpha \boldsymbol{Q}_\alpha \boldsymbol{Q}_\alpha + \Delta, \qquad \Delta = (y_1 + \cdots + y_{N-1})M^2 - (x_1 + \cdots + x_N)q_0^2\,. \tag{5.38}$$

The multi-loop integral is then rewritten in the following form:

$$M_{4,N}^{\text{div}}(q_0) = \int_0^1 \mathscr{D}_{xy} \int \frac{d^{Nd}\boldsymbol{Q}}{(2\pi)^{Nd}} \frac{\det(C)^{-d/2} h_N c_d^{(4)}}{D^{2N-1}} \left(N_4 - \frac{6}{d+4} N_2 + \frac{3}{(d+2)(d+4)} N_0 \right). \tag{5.39}$$

In order to simplify notations, we further introduce the multiindex $A = (\alpha, i)$ and $B = (\beta, j)$. Here $\alpha, \beta = 1, \ldots N$ and $i, j = 1, 2, 3$ label the loop momentum and the space index of the Nd-dimensional vector $\boldsymbol{Q} = (\boldsymbol{Q}_1, \cdots, \boldsymbol{Q}_N)$. We further define $v_\alpha^{(1)} = O_{1\alpha}\lambda_\alpha^{-1/2}$ and $v_\beta^{(N)} = O_{1\beta}\lambda_\beta^{-1/2}$. The terms in

the numerator of the Feynman integral can be written in the following compact notation ($K = 0, 2, 4$)

$$N_K = v^{(1)}_{\alpha_1} \cdots v^{(1)}_{\alpha_4} \, v^{(N)}_{\beta_1} \cdots v^{(N)}_{\beta_4} \, \Phi^{(K)}_{i_1 \cdots i_4, j_1 \cdots j_4} \, Q_{A_1} \cdots Q_{A_4} Q_{B_1} \cdots Q_{B_4} \,, \tag{5.40}$$

where

$$\begin{aligned} \Phi^{(0)}_{i_1 \cdots i_4, j_1 \cdots j_4} &= \delta_{i_1 i_2} \delta_{i_3 i_4} \delta_{j_1 j_2} \delta_{j_3 j_4} \,, \\ \Phi^{(2)}_{i_1 \cdots i_4, j_1 \cdots j_4} &= \delta_{i_1 i_2} \delta_{j_1 j_2} \delta_{i_3 j_3} \delta_{i_4 j_4} \,, \\ \Phi^{(4)}_{i_1 \cdots i_4, j_1 \cdots j_4} &= \delta_{i_1 j_1} \delta_{i_2 j_2} \delta_{i_3 j_3} \delta_{i_4 j_4} \,. \end{aligned} \tag{5.41}$$

Since the denominator of the Feynman integral depends only on the Nd-dimensional vector squared, it is possible to average over the directions. We define

$$\begin{aligned} \langle Q_A Q_B \rangle &= a_1 \, Q^2 \, \Pi^{(1)}_{AB} \,, \\ \langle Q_{A_1} Q_{A_2} Q_{B_1} Q_{B_2} \rangle &= a_2 \, Q^4 \, \Pi^{(2)}_{A_1 A_2 B_1 B_2} \,, \\ \langle Q_{A_1} Q_{A_2} Q_{A_3} Q_{B_1} Q_{B_2} Q_{B_3} \rangle &= a_3 \, Q^6 \, \Pi^{(3)}_{A_1 A_2 A_3 B_1 B_2 B_3} \,, \\ \langle Q_{A_1} Q_{A_2} Q_{A_3} Q_{A_4} Q_{B_1} Q_{B_2} Q_{B_3} Q_{B_4} \rangle &= a_4 \, Q^8 \, \Pi^{(4)}_{A_1 A_2 A_3 A_4 B_1 B_2 B_3 B_4} \,. \end{aligned} \tag{5.42}$$

It is clear that the quantities Π are symmetric with respect to the permutations of any of two indices. Furthermore,

$$\begin{aligned} \Pi^{(1)}_{AB} &= \delta_{AB} \,, \\ \Pi^{(2)}_{A_1 A_2 B_1 B_2} &= \delta_{A_1 A_2} \Pi^{(1)}_{B_1 B_2} + \delta_{A_1 B_1} \Pi^{(1)}_{A_2 B_2} + \delta_{A_1 B_2} \Pi^{(1)}_{A_2 B_1} \,, \\ \Pi^{(3)}_{A_1 A_2 A_3 B_1 B_2 B_3} &= \delta_{A_1 A_2} \Pi^{(2)}_{A_3 B_1 B_2 B_3} + \delta_{A_1 A_3} \Pi^{(2)}_{A_2 B_1 B_2 B_3} + \delta_{A_1 B_1} \Pi^{(2)}_{A_2 A_3 B_2 B_3} \\ &+ \delta_{A_1 B_2} \Pi^{(2)}_{A_2 A_3 B_1 B_3} + \delta_{A_1 B_3} \Pi^{(2)}_{A_2 A_3 B_1 B_2} \,, \\ \Pi^{(4)}_{A_1 A_2 A_3 A_4 B_1 B_2 B_3 B_4} &= \delta_{A_1 A_2} \Pi^{(3)}_{A_3 A_4 B_1 B_2 B_3 B_4} + \delta_{A_1 A_3} \Pi^{(3)}_{A_2 A_4 B_1 B_2 B_3 B_4} \\ &+ \delta_{A_1 A_4} \Pi^{(3)}_{A_2 A_3 B_1 B_2 B_3 B_4} + \delta_{A_1 B_1} \Pi^{(3)}_{A_2 A_3 A_4 B_2 B_3 B_4} \\ &+ \delta_{A_1 B_2} \Pi^{(3)}_{A_2 A_3 A_4 B_1 B_3 B_4} + \delta_{A_1 B_3} \Pi^{(3)}_{A_2 A_3 A_4 B_1 B_2 B_4} \\ &+ \delta_{A_1 B_4} \Pi^{(3)}_{A_2 A_3 A_4 B_1 B_2 B_3} \,, \end{aligned} \tag{5.43}$$

and so on. The normalization constants $a_1, \ldots, a_4$ can be easily determined, taking the trace on both sides of Eq. (5.42)

$$\begin{aligned} a_1 &= \frac{1}{dN} \,, \qquad a_2 = \frac{1}{dN(dN+2)} \,, \qquad a_3 = \frac{1}{dN(dN+2)(dN+4)} \,, \\ a_4 &= \frac{1}{dN(dN+2)(dN+4)(dN+6)} \,. \end{aligned} \tag{5.44}$$

It remains to substitute the above formulae into Eq. (5.40) and evaluate the numerator after averaging over the directions. After the lengthy but straightforward calculations we arrive at a compact expression

$$M_{4,N}^{\mathrm{div}}(q_0) = \int_0^1 \mathscr{D}_{xy} \int \frac{d^{Nd}\boldsymbol{Q}}{(2\pi)^{Nd}} \frac{\det(C)^{-d/2} h_N c_d^{(4)} a_4 \, (d-1)d(d+1)(d+6)\, f_{1N}^4 \, Q^8}{(Q^2+\Delta)^{2N-1}}\,, \tag{5.45}$$

where $f_{\alpha\beta}$ denotes the matrix element of C^{-1}:

$$f_{\alpha\beta} = \sum_\gamma O_{\alpha\gamma} \lambda_\gamma^{-1} O_{\beta\gamma} = \det(C)^{-1} \mathrm{Adj}(C)_{\alpha\beta}\,, \tag{5.46}$$

where $\mathrm{Adj}(C)$ is the adjugate of the matrix C. Carrying out the integration over $\boldsymbol{Q}$, we finally get

$$\begin{aligned} M_{4,N}^{\mathrm{div}}(q_0) &= \frac{g^{N-1} c_d^{(4)} a_4}{(4\pi)^{N(d/2-1)}} \frac{\Gamma(Nd/2+4)\Gamma(N(2-d/2)-5)}{\Gamma(Nd/2)} \\ &\times \int_0^1 \mathscr{D}_{xy}\, \det(C)^{-d/2-4} \left(\mathrm{Adj}(C)_{1N}\right)^4 \Delta^{N(d/2-2)+5}\,. \end{aligned} \tag{5.47}$$

In order to carry out integrations, it is convenient to group the variables x_i and y_i separately:

$$\begin{aligned} x_1 &= \rho\tau_1, \qquad x_2 = \rho(1-\tau_1)\tau_2, \quad \cdots \quad x_N = \rho(1-\tau_1)\cdots(1-\tau_{N-1})\,, \\ y_1 &= (1-\rho)t_1, \qquad y_2 = (1-\rho)(1-t_1)t_2, \quad \cdots \quad y_{N-1} = (1-\rho)(1-t_1)\cdots(1-t_{N-2})\,, \\ s &= (1-\rho)/\rho\,. \end{aligned} \tag{5.48}$$

As already mentioned, the quantity $M_{4,N}^{\mathrm{div}}(q_0)$ is ultraviolet divergent. It contains a simple pole in $(d-3)$ to all orders that can emerge in different places. For *even* values of N, the pole emerges in $\Gamma(N(2-d/2)-5)$, whereas the integration over the variable s yields a finite result in dimensional regularization, because the index of divergence is half-integer in $d=3$ dimensions. For *odd* values of N, the prefactor is finite, and the pole emerges from the integration over s. Integrating over the variables τ_i and t_i does not produce any divergences. All diagrams with $N>10$ are ultraviolet-finite.

Separating the poles in multi-loop diagrams is a rather involved enterprise. On the other hand, applying the subtraction at threshold (or any other point below threshold, with a subtraction scale of order of M) can be done straightforwardly. We shall fix our renormalization prescription by subtracting from the multi-loop diagram the first few terms of the Taylor expansion in the variable $z = q_0^2/M^2$. The polynomial of the fourth order in z should be subtracted for $N=2$, the polynomial of the third order for $N=3,4$, the polynomial of the second order for $N=5,6$, and so on. It is clear that this procedure does not introduce large mass scale and, hence, the coefficients of the modified effective-range expansion in $K_\ell^M(q_0^2)$ will be of natural size.

5.4.2 Results of Numerical Calculations for $M_\ell(q_0)$

In this section we shall present the results of numerical calculations for $\ell = 0, 4$. After subtracting the ultraviolet divergences, the calculation over Feynman parameters in $d=3$ dimensions were carried by using the VEGAS routine [258, 259]. The Lippmann-Schwinger equation (5.22) that determines T_L^{fin} is discretized on Gaussian mesh points and solved by using matrix inversion.

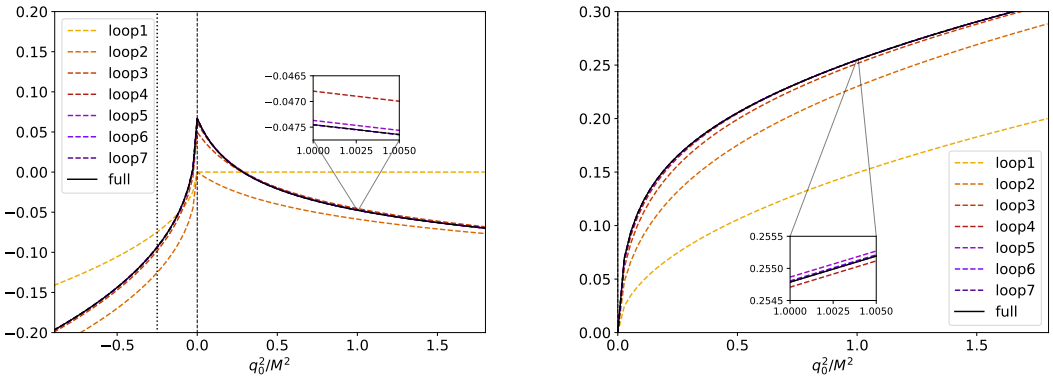

Figure 5.7: The real and imaginary parts of the function $M_\ell(q_0)$ for $\ell = 0$. The imaginary part is zero below threshold. The full solution corresponds to the sum of the $M_\ell^{\text{div}}(q_0)$ (up to two loops) and $M_\ell^{\text{fin}}(q_0)$, see Eq. (5.22). For comparison, the perturbative result up to 7 loops is shown. The vertical lines in the left panel correspond to the elastic threshold and the beginning of the left-hand cut.

In Fig. 5.7 the real and imaginary parts of the function $M_\ell(q_0)$ for $\ell = 0$ are plotted. The full solution $M_\ell(q_0) = M_\ell^{\text{div}}(q_0) + M_\ell^{\text{fin}}(q_0)$ is given by a sum of two terms, where the former contains perturbative contributions up to two loops. For comparison, we also plot the result of perturbative calculations up to and including 7 loops. It is seen that, for a given value of the coupling g, the perturbative series converges rapidly, so the result in 4 loops and higher becomes visually indistinguishable from the full solution.

In Fig. 5.8 the result of the calculation in case $\ell = 4$ is shown. Now, $M_\ell^{\text{div}}(q_0)$ contains 10 terms, and $M_\ell^{\text{fin}}(q_0)$ is so small that it cannot be distinguished with a bare eye. As one sees from the figure, the convergence is again very good and, after calculating a few loops, the full solution does not change anymore. Note that oscillations in the real part are an artifact of the subtraction and do not have an effect on the convergence.

Last but not least, note that only repulsive interactions are considered at present. In case of attractive interactions, bound states can emerge in the spectrum and the Born series is no longer convergent. In our approach, these bound state poles show up in $M_\ell^{\text{fin}}(q_0)$.

5.4.3 Coulomb Interactions

In the limit $M \to 0$, our long-range force reduces to the Coulomb force, for which the analytic solution is known [176, 191]. In this case, we have to identify the dimensionful constant g with $g = 2\mu_r\alpha$, where μ_r is the reduced mass and α denotes the fine structure constant. The quantity $M_\ell(q_0)$ becomes the function of the dimensionless variable $\eta = \alpha\mu_r/q_0$. Restricting ourselves, for simplicity, to the case $\ell = 0$, we get

$$M_0(q_0) = 2\alpha\mu_r\left\{\eta^2\sum_{n=1}^{\infty}\frac{1}{n(n^2+\eta^2)} - \log\eta + \Gamma'(1)\right\}. \tag{5.49}$$

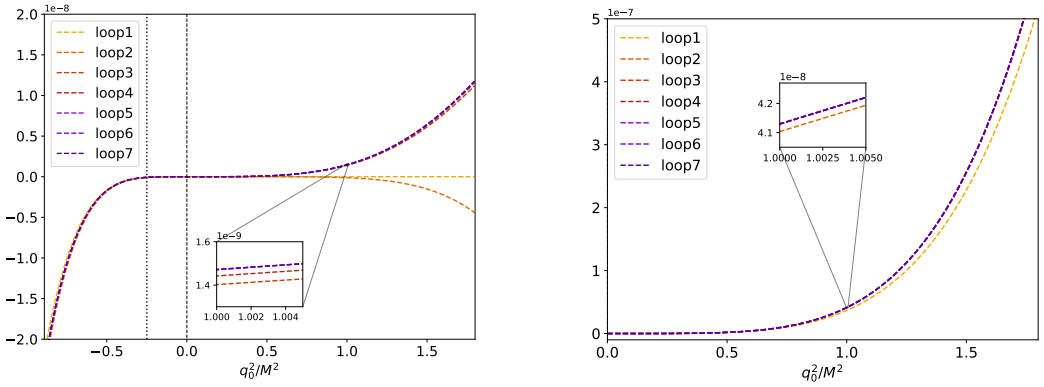

Figure 5.8: The real and imaginary parts of the function $M_\ell(q_0)$ for $\ell = 4$. The imaginary part is zero below threshold. The perturbative expansion converges very rapidly, so that the contribution of $M_\ell^{\text{fin}}(q_0)$ is invisible by the bare eye and is not shown (see also the zoomed-in windows). The vertical lines in the left panel correspond to the elastic threshold and the beginning of the left-hand cut.

We have checked that, in the limit $M \to 0$, the expression in the curly brackets in Eq. (5.32) indeed yields the term $-\log \eta$ up to an inessential constant contribution. Fixing of this contribution amounts to setting the renormalization prescription. Higher order terms in the expansion in η are obtained from the multi-loop integrals. The loops with odd N are purely imaginary and do not contribute. We have (numerically) checked that the first few coefficients of the expansion of $M_\ell(q_0)$ indeed reproduce those obtained from Eq. (5.49) with a very good precision. Thus, our expression for $M_\ell(q_0)$ indeed reduces to the known one from Refs. [176, 191] in the massless limit.

5.4.4 Modified Effective-Range Expansion Function

As mentioned above, the modified quantization condition allows one to extract the modified effective range function $K_\ell^M(q_0^2)$ both above and below threshold and, in particular, in the left-land cut region where the standard Lüscher approach fails. Here we wish to construct $K_\ell^M(q_0^2)$ in the whole energy range and ensure that it is smooth and real everywhere, in contrast to the standard K-matrix. We carry out calculations in the model described by the potential (5.20) and restrict ourselves, for simplicity, to the case $\ell = 0$.

It should be pointed out that the analytic continuation of the solution of the Lippmann-Schwinger equation below threshold is by no means a trivial affair. As discussed, e.g., in Ref. [260], when $q_0^2 < -M^2$, the path of momentum integration in the Lippmann-Schwinger integration, which originally runs from 0 to infinity, should be deformed in order to avoid the singularities of the potential. The left-hand cut starts higher, at $q_0^2 = -M^2/4$. Since the analysis in the left-hand cut region is our primary interest, we restrict the energy interval by $q_0^2 > -M^2$. Albeit, with some additional effort, the analysis can be extended to the larger region $q_0^2 > -M_S^2/4$.

Another subtle issue is the definition of the effective-range expansion below threshold. The

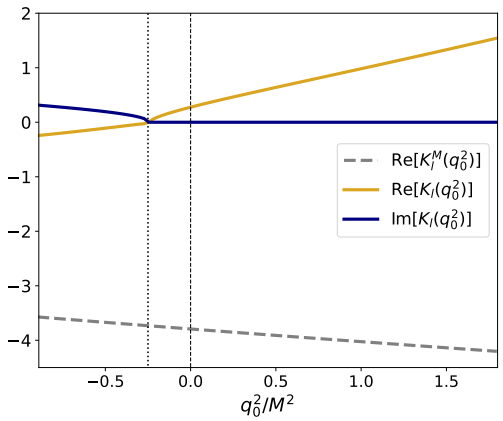

Figure 5.9: Real and imaginary parts (in arbitrary units) of the standard effective range function $K_\ell(q_0^2)$ (solid lines) vs. the real part of the modified effective range function $K_\ell^M(q_0^2)$ (dashed line) in the S-wave ($\ell = 0$). The imaginary part of $K_\ell^M(q_0^2)$ is zero everywhere in the interval considered. The position of the left-hand threshold is shown by a vertical dotted line.

definition (5.4) applies above threshold. In the interval $-M^2 < q_0^2 < 0$ we use the following definition:

$$K_\ell^M(q_0^2) = M_\ell(q_0) + \frac{4\pi q_0^{2\ell}}{|f_\ell(q_0)|^2} \frac{1}{T_\ell(q_0) - T_\ell^L(q_0)}, \tag{5.50}$$

where $T_\ell(q_0), T_\ell^L(q_0)$ denote the full and the long-range fully on-shell scattering amplitudes (these amplitudes become complex in the left-hand cut region, however the difference $T_\ell(q_0) - T_\ell^L(q_0)$ stays real). The Jost function is also real in the considered subthreshold interval and is given by

$$f_\ell(q_0)^{-1} = 1 + \frac{1}{q_0^\ell} \int_0^\infty \frac{p^2 dp}{2\pi^2} \frac{p^\ell}{p^2 - q_0^2} T_\ell^L(p, q_0; q_0^2), \qquad T_\ell^L(q_0) = T_\ell^L(p, q_0; q_0^2). \tag{5.51}$$

In Fig. 5.9 we show the modified effective range function $K_\ell^M(q_0^2)$ vs. the standard one $K_\ell(q_0^2)$. The difference is clearly visible. While the standard function displays a singular structure at the left-land threshold and becomes complex below it, the modified effective range function is almost linear in the whole interval considered. Moreover, it does not demonstrate any sign of a singular behavior even very close to $q_0^2 = -M^2$, in agreement with the claim that the convergence radius of the modified effective-range expansion is set by the short-range scale M_S.

5.5 Conclusions

i) In the present chapter we discussed the numerical implementation of the modified Lüscher equation, proposed in Ref. [221]. We chose to demonstrate the essential features of the implementation, using a simple toy model: two spinless non-relativistic particles interacting through a sum of two Yukawa potentials, having different ranges. Furthermore, the center-of-

mass frame was chosen from the beginning, and we restricted ourselves to the case of the A_1^+ irrep of the octahedral group only. All these are purely technical restrictions and can be easily removed in the analysis of real lattice data.

ii) In addition to the above, we assumed that the long-range force is perturbative and does not create bound states/low-lying resonances alone. In contrast to the other assumptions, this one is more restrictive and might require additional scrutiny. For the time being, we however stick to this assumption, because it is justified for the real physical systems which are studied on the lattice at present.

iii) We went step by step and presented a simple but rather accurate and fast algorithm for the calculation of the modified Lüscher zeta-function shown in Fig. 5.1. This quantity is ultraviolet-divergent as its renormalization is a non-trivial issue, especially in higher partial-waves. From the point of numerical algorithms, a cutoff is a preferred choice. However, cutoff regularization leads to the very large subtraction terms in higher partial-waves that affects the accuracy of calculations. From this point of view, dimensional regularization is preferred because in this case the subtraction terms are of natural size in all partial-waves. We derive explicit expressions for the renormalized n-loop exchange diagrams in dimensional regularization, using a subtraction scheme that does not produce unnaturally large polynomial contributions.

iv) The solutions of the quantization condition (both modified and standard ones) are compared with the exact finite-volume spectrum of the Hamiltonian, calculated in the plane-wave basis. The results confirm all our expectations. First of all, exponential corrections are very small for all levels except the ground state, where they are increased owing to the proximity of the left-hand cut. Furthermore, the convergence of the partial-wave expansion is very good in the modified case and poor in the standard case. Indeed, the standard case implies the partial-wave expansion of the whole potential, whereas in the modified case only the short-range potential is expanded in partial-waves, the long-range part is treated in the plane-wave basis as a whole.

v) If the modified Lüscher zeta-function for a known long-range potential is calculated and tabulated in advance, the analysis of lattice data proceeds exactly in the same manner as in the case of the standard Lüscher equation. The truncation in partial-waves, which involves short-range potential only, is justified. This potentially renders the proposed approach very convenient for the analysis of lattice data.

CHAPTER 6

Finite-Volume Energy Shift of the Three-Nucleon Ground State

The content of the following chapter is based on the publication

- R. Bubna, F. Müller and A. Rusetsky, *Finite-volume energy shift of the three-nucleon ground state*, Phys. Rev. D **108**.1 (2023) 014518, arXiv: 2304.13635 [hep-lat]

It should be noted that this project was a part of the Master's thesis of the author and hence only results from the project are displayed in the following chapter.

In this project non-relativistic effective field theory is used to carry out a perturbative calculation of the three-nucleon ground state energy shift in a finite-volume cubic box of size L. The energy shift is evaluated up to and including $O(L^{-6})$. Convergence of the resulting perturbative series is studied numerically for the physical values of the scattering lengths.

The perturbative calculation of finite-volume energy shifts offers an simple and straightforward method to fit lattice data. Even though it cannot be used in the presence of bound states or resonances, it can be still applied to situations where using the full three-body quantization condition would be an overkill. The perturbative framework was not applied to a system of three-fermions like the three-nucleon system before. This project aimed to derive the energy shift to the ground state in the case of three-fermions, with focus on the three-nucleon system. An important point to note here is that, due to the large scattering length in the case of nucleons, the box size required for a convergent series is very large and probably out of reach for the time being. However, the perturbative formula derived within this project can be still applied to other three-fermion systems.

The project started with writing down the relevant non-relativistic Lagrangian given in Refs. [136, 261] and identifying the terms which would contribute up to and including $O(L^{-6})$. Matching of the two-body LECs appearing in the Lagrangian was carried out using the methods detailed in the previous chapters.

For deriving the ground state energy shift it was assumed that the scattering length is of natural size and its ratio with the box size L was very small compared to 1. With this assumption, dimensional regularization was used to tame the UV divergence arising from divergent diagrams. Following Ref. [97], the three-particle relativistic on-shell amplitude can be parametrized in terms of a single variable λ by making a choice of the incoming and outgoing three-momenta. Taking the limit $\lambda \to 0$ results in the amplitude becoming singular, however the regular part of the threshold amplitude can still be

obtained by subtracting singular terms in a systematic manner. With the relativistic amplitude defined, the author evaluated the relevant six diagrams that contribute three-particle threshold amplitude in the NREFT and hence derived the matching condition for the three-body coupling. The procedure laid out in Refs. [91, 97, 98] were closely followed to derive the three-nucleon ground state energy shift.

With the Lagrangian set-up the interaction Hamiltonian was identified. The author along with Fabian Müller derived the states that are allowed in the finite volume. Symmetries of the system and Pauli's exclusion principle were utilized to write down all relevant states, including intermediate ones. These states were then used to calculate the matrix element of each term appearing in the interaction Hamiltonian. The author plugged in the matrix elements in the formula for Rayleigh-Schrödinger perturbation theory and carried out the summation over the intermediate states to derive the three-nucleon ground state energy shift up to and including $O(L^{-6})$. The result was independently checked by Fabian Müller. As discussed in the previous chapter, it was shown that the divergent term of the three-body coupling exactly cancel out the divergence arising from the finite-volume sums. Further, one can trade the three-body coupling for the three-particle relativistic threshold amplitude to write down the ground state energy shift of the three-nucleon system in terms of S-matrix elements.

The physical nucleon scattering lengths were then substituted in the derived formula up to $O(L^{-5})$, as the three-particle threshold amplitude is required at the next order, to provide an estimate of L required for the perturbative series to converge reliably. It was noted that the perturbative series converges for very large and impractical L.

6.1 Perturbative Shift to the Ground State Energy

Using the Lagrangian given in Refs. [136, 261] and following the steps described in Secs. 3.3.1 and 3.3.2, the following energy shift to the ground state of the three-nucleon system is obtained:

$$
\begin{aligned}
E_3 &= \frac{6\pi}{M}(a_s + a_t)\,, \\
E_4 &= -\frac{6}{M}(a_s^2 + a_t^2)I\,, \\
E_5 &= \frac{3}{2M\pi}\Big[4(a_s^3 + a_t^3)I^2 - (a_s + a_t)(5a_s^2 - 14a_s a_t + 5a_t^2)J\Big]\,, \\
E_6 &= \frac{6}{M\pi^2}\Big[-(a_s^4 + a_t^4)I^3 + (4a_s^4 - 3a_s^3 a_t - 3a_s a_t^3 + 4a_t^4)IJ \\
&\quad - \frac{3}{2}(a_s + a_t)^2(a_s^2 - 7a_s a_t + a_t^2)K - \frac{1}{4}(a_s^4 + 24a_s^3 a_t + 78a_s^2 a_t^2 + 24a_s a_t^3 + a_t^4)Q^r \\
&\quad - \frac{1}{2}(a_s^4 + 6a_s^3 a_t + 18a_s^2 a_t^2 + 6a_s a_t^3 + a_t^4)R^r\Big] \\
&\quad + \frac{6\pi^2}{M^3}(a_s^2 + a_t^2) + \frac{12\pi^2}{M}(a_s^3 \hat{r}_s + a_t^3 \hat{r}_t) \\
&\quad + \frac{2\pi}{M}\Big[3\sqrt{3}\{a_s^4 + 6a_s^3 a_t + 18a_s^2 a_t^2 + 6a_s a_t^3 + a_t^4\} \\
&\quad - \pi\{a_s^4 + 24a_s^3 a_t + 78a_s^2 a_t^2 + 24a_s a_t^3 + a_t^4\}\Big] \ln(\mu L) + 4\eta_3^r(\mu)\,.
\end{aligned}
\tag{6.1}
$$

Here, $a_{s,t}$ represents the NN scattering length, $\hat{r}_{s,t} = r_{s,t} - 1/(a_{s,t}M^2)$ with $r_{s,t}$ representing the effective range in the pertinent channel, M denotes the nucleon mass and $\eta_3^r(\mu)$ is the renormalized three-nucleon coupling.

In the final result, the quantity $\eta_3^r(\mu)$ in E_6 should be replaced by $\mathscr{M}_3^{(0)}$ through the matching condition. The dependence on μ disappears, as it should. In the above expressions, I, J, K are the finite quantities that arise from regularizing the above mentioned momentum sums. These are given by

$$\begin{aligned} I &= \sum_{\mathbf{n}\neq 0} \frac{1}{\mathbf{n}^2} = -8.91363291781\ldots, \\ J &= \sum_{\mathbf{n}\neq 0} \frac{1}{\mathbf{n}^4} = 16.532315959\ldots, \\ K &= \sum_{\mathbf{n}\neq 0} \frac{1}{\mathbf{n}^6} = 8.401923974433\ldots. \end{aligned} \tag{6.2}$$

Q^r and R^r are the finite parts obtained after renormalizing the double sums over momenta using the $\overline{\text{MS}}$ scheme. These are given by

$$\begin{aligned} &\frac{1}{L^{2d}} \sum_{\mathbf{p},\mathbf{q}\neq 0} \frac{1}{\mathbf{p}^2\mathbf{q}^2(\mathbf{p}^2+\mathbf{q}^2+(\mathbf{p}+\mathbf{q})^2)} \\ &= \mu^{2(d-3)} \left\{ \frac{1}{48\pi^2} \left(\ln(\mu L) - \frac{1}{2(d-3)} \right) + \frac{1}{(2\pi)^6} Q^r \right\}, \end{aligned} \tag{6.3}$$

$$\begin{aligned} &\frac{1}{L^{2d}} \sum_{\mathbf{p}\neq 0} \frac{1}{\mathbf{p}^4} \sum_{\mathbf{q}} \frac{1}{(\mathbf{p}^2+\mathbf{q}^2+(\mathbf{p}+\mathbf{q})^2)} \\ &= \mu^{2(d-3)} \left\{ -\frac{\sqrt{3}}{32\pi^3} \left(\ln(\mu L) - \frac{1}{2(d-3)} \right) + \frac{1}{(2\pi)^6} R^r \right\}. \end{aligned} \tag{6.4}$$

Numerical values of the finite quantities are given by

$$\begin{aligned} Q^r &= -102.1556055\ldots, \\ R^r &= 19.186903\ldots. \end{aligned} \tag{6.5}$$

The calculation of these quantities is described in Refs. [91, 97, 98], where these values are taken from. Note that the divergent term of the three-body coupling η_3 is exactly the one that is needed to cancel the divergence in the finite-volume sums. This serves as a nice check of the calculations. At the end, one may replace $\eta_3^r(\mu)$ by the threshold amplitude $\mathscr{M}_3^{(0)}$, expressing the energy shift solely in terms of the observable S-matrix elements. In this form, the final perturbative formula is valid in case of unnaturally large scattering lengths and very large values of L.

We find it very instructive to study the convergence of the obtained perturbative formula for different values of L. As an input, we use the following values of the two-body scattering lengths [262]:

$$a_s = -23.7148(43)\text{fm}, \qquad a_t = 5.4112(15)\text{fm}, \tag{6.6}$$

In Fig. 6.1 we plot $E_3/L^3, E_4/L^4$ and E_5/L^5 as functions of L. We do not consider E_6 in order to

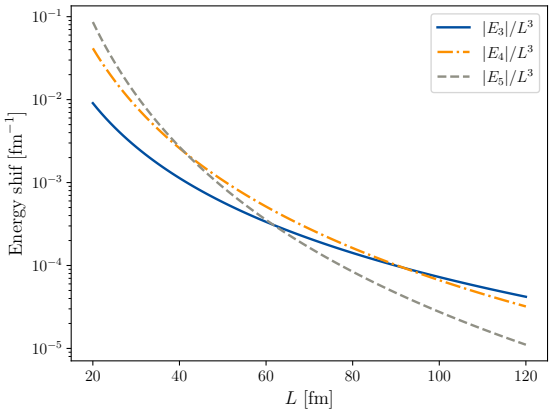

Figure 6.1: The three-particle energy shift at different orders plotted against the box size L.

avoid blurring the discussion due to the inclusion of the three-body coupling. For comparison, in Fig. 6.2 we plot the two-particle energy shift in the triplet and singlet channels, using formulae from, e.g., Ref. [91][1].

From the plots in Fig. 6.1 it is seen that, for $L \lesssim 45\,\text{fm}$, $E_5/L^5 > E_4/L^4 > E_3/L^3$. This clearly indicates that, in this case, perturbation theory is not applicable for small L. For L above 90 fm the ordering of the corrections to the ground state energy seems to be correct and, naively, one would assume that perturbation theory is applicable above this value. However, the convergence is expected to be very slow and hence, in order to achieve a decent convergence rate, one would need to go to the very high values of L. Furthermore, comparison to Fig. 6.2 shows that the convergence in the two-particle sector is much faster, albeit still beyond reach for the present-day lattice QCD calculations.

6.2 Conclusions and Outlook

i) Using the non-relativistic effective theory, we have derived a perturbative expansion of the finite-volume shift of the three-nucleon ground state energy up to and including order L^{-6}. The matching to the threshold three-nucleon amplitude has also been carried out in perturbation theory.

ii) It is known that S-wave nucleon-nucleon scattering lengths have unnaturally large values that affects the convergence of the standard perturbative series. As a result, the lowest-order term to the two-body amplitude should be resummed to all orders. Despite this fact, a strict perturbative derivation of the finite-volume shift is still valid. The difference is hidden in expressing of the two and three-body observables through the effective couplings and does not affect the final formula of the energy shift in terms of the observables.

[1] In that paper, the expressions for two identical scalars are given. However, to the order we are working, the nucleon-nucleon Lippmann-Schwinger equation in the singlet/triplet channels looks identical to its scalar counterpart. Consequently, one can use the formulae from Ref. [91] also here.

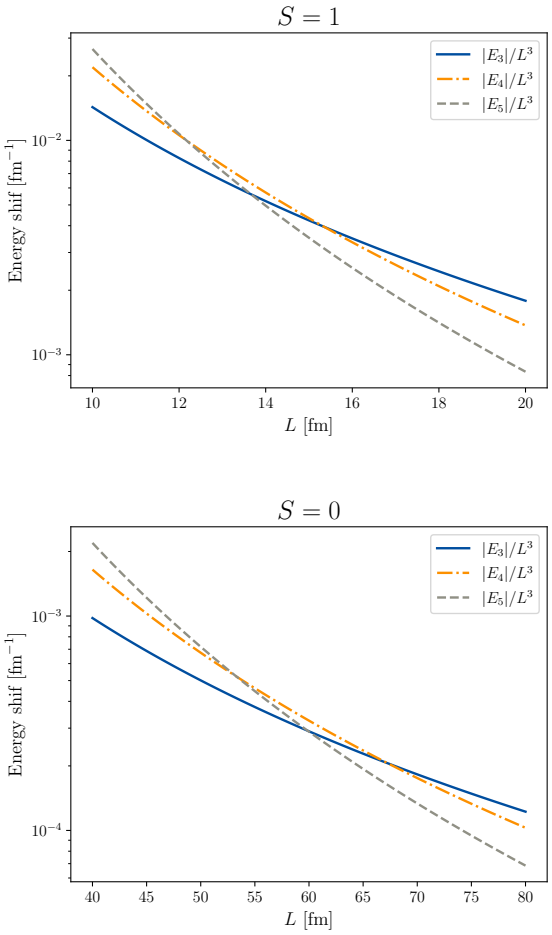

Figure 6.2: The two-particle energy shift in the spin triplet and singlet channels, at different orders, against the box size L.

iii) Numerically, at physical values of the scattering lengths, the perturbative series converges only at unrealistically high values of L. Furthermore, the convergence in the three-particle sector is substantially slower than in case of two nucleons.

iv) A full-fledged three-fermion quantization condition has become available recently [87]. In our opinion, in the future, the derived perturbative expression may provide a useful testing ground for the general framework, controlling, in particular, a consistent inclusion of the relativistic effects for particles with spin. These effects are technically challenging in the explicitly relativistic-invariant framework and are almost trivial in the non-relativistic setting used here.

CHAPTER 7

Lellouch-Lüscher Factor for the $K \to 3\pi$ Decays

The content of the following chapter is based on the publication

- J.-Y. Pang, R. Bubna, F. Müller, A. Rusetsky and J.-J. Wu, *Lellouch-Lüscher factor for the $K \to 3\pi$ decays*, JHEP **05** (2024) 269, arXiv: 2312.04391 [hep-lat]

The explicit expression for the Lellouch-Lüscher (LL) factor in the case of $K \to 3\pi$ decays was derived at leading order, without derivative couplings. Several important technical aspects are addressed in details in this project, such as the proper decomposition into the isospin amplitudes, the choice of a minimal set of effective couplings and the renormalization, as well as the algorithm for the solution of the pertinent Faddeev equations in the infinite volume which is based on the contour deformation method. Most importantly, the numerical results obtained in this project demonstrates that the three-body force contributes very little to the LL factor, paving the way for the study of $K \to 3\pi$ decays on the lattice.

In this project the relativistic-invariant formulation of NREFT was used to numerically evaluate the LL factor in the case of kaon decay into three pions in different isospin channels. In the context of NREFT and moving frames, the three-body LL factor was derived in Ref. [101]. Even though several technical aspects are detailed in the following chapter, the main goal of this project was to numerically evaluate the LL factor in the case of kaon decay and to identify whether the three-pion couplings need to be known explicitly or a rough approximation of the three-pion amplitude based on ChPT is enough for the determination of the LL factor. If the LL factor is relatively insensitive to the three-body force, the determination of three-pion couplings from the lattice spectrum can be skipped completely, simplifying the calculation greatly.

The most general NREFT Lagrangian for the present case was written down in both the three-particle and particle-dimer picture. The author along with Fabian Müller and Jin-Yi Pang carried out the matching in both the two-body and three-body sector as well as the matching of the decay Lagrangian. Techniques laid out in Chap. 3 was used for carrying out the matching. At this point, it is important to ask whether irrelevant operators, that do not contribute at tree-level, contribute at higher orders. Considering the structure of the vertex function for kaon decay and three-pion amplitude, it was shown that these operators remain irrelevant even at higher orders.

The author derived the Faddeev equation for the particle-dimer amplitude for different isospin channels under consideration. The amplitude in the isospin $J = 2$ channel turns out to be cut-off independent without the need of a three-body force term due to negative sign of the Clebsh-Gordan

coefficient. Moreover, due to the absence of physical dimers there exists only one three-pion amplitude in the isospin $J = 1$ channel. Hence, only two independent cut-off dependent couplings need to be matched in the three-body sector (one for $J = 1$ and one for $J = 3$). The particle-dimer amplitude at threshold is singular at $E = 3M_\pi$. The regular part of the amplitude was read off from the result given in Ref. [95]. With this, the expression for three-particle amplitude and corresponding wave-functions were derived by the author.

The particle-dimer couplings were then matched to the three-pion threshold amplitude. The author along with Jin-Yi Pang derived the three-pion threshold amplitude at tree-level in ChPT and carried out the matching. A tree-level calculation was sufficient as the LL factor evaluated numerically shows high insensitivity to the three-body amplitude. With all the necessary set-up completed, the LL factor for kaon decay was derived.

The kernel of the Faddeev equation in the infinite volume contains logarithmic singularities, hence the integration contour needs to be deformed to solve this equation. The author, Fabian Müller and Jin-Yi Pang independently implemented contour deformation routines for solving the Faddeev equation in the infinite volume. Further, the finite-volume energy spectrum in rest frame and moving frames were obtained by solving the three-body quantization condition and hence the finite-volume wave functions were evaluated. With all the necessary pieces, the LL factor was numerically evaluated for $K \to 3\pi$ decays. The value of three-body threshold amplitude, obtained from ChPT, was varied in a wide interval to test the sensitivity of the LL factor. It was determined that the LL factor exhibited negligible dependence on the three-particle amplitude.

7.1 Introduction

In the recent years, first results of the lattice studies of the spectrum in the three-particle systems have started to appear. These results have been analyzed by using three different but conceptually equivalent formalisms known as Relativistic Field Theory (RFT) [67, 68], Non-Relativistic Effective Field Theory (NREFT) [70, 71] and Finite-Volume Unitarity (FVU) [69, 231] approaches. The references to the activities in the field that include both formal developments as well as actual simulations on the lattice are collected here [29, 30, 65–71, 73–75, 77, 78, 81–87, 92, 95–102, 137–140, 212, 231, 264–292]. For more information on the subject, we refer the reader to the two recent reviews on the subject [72, 293].

One of the most intriguing and challenging tasks in the three-particle sector is the study of the three-particle decays. Here, we exclusively focus on the decays which proceed via the weak or electromagnetic forces – in other words, these particles would be absolutely stable in pure QCD. A classic example for this kind of decays is given by $K \to 3\pi$. Here, one could also count the decays that proceed via the isospin breaking (the most prominent example of this sort is given by the $\eta \to 3\pi$). Putting differently, the η is stable in pure *isospin-symmetric* QCD, with $m_u = m_d$, and the decay amplitude is proportional to the quark mass difference $(m_d - m_u)$ (the higher-order terms in this small parameter will be neglected). A completely different picture emerges where both the formation and the decay of a particle (resonance) is caused by strong interactions which are described by the QCD Lagrangian alone. In this case, analytic continuation into the complex plane becomes inevitable. We shall not consider such processes in the present chapter.

The main conceptual problem in the determination of the decay amplitudes on the lattice are caused by the presence of the final-state interactions. Since the mass of the decaying particle lies above the

sum of the masses of the decay products, the propagators in the Feynman diagrams that describe final-state interaction may become singular in the integration region. This, at a fixed energy, leads to an irregular dependence of the measured matrix element on the lattice volume, rather than to the exponentially suppressed finite-volume corrections which emerge in the observables of stable particles. Lellouch and Lüscher [43] have shown that, in case of two-particle decays, this singular behavior is contained in a single function (the so-called LL factor), which relates the decay amplitudes in the infinite and in a finite volume. A crucial property of this function is that it depends on the dynamics in the final state (the two-body phase shifts, in this case[1]), but not on the interactions that lead to the decay. Further development of these ideas can be found in Refs. [41, 48, 295] which include, in particular, the generalization to the moving frames and the multi-channel decays.

An analog of the LL formula for the three-particle decays has been derived only very recently, independently by two groups [100–102]. Albeit there is no substantial conceptual difference between the two- and three-particle cases (for example, the functions that describe an irregular volume-dependence also in the three-particle case depend solely on the parameters of the final-state interactions), an algebraic structure of the final expressions is much more cumbersome and obscure. In particular, there exists only one LL factor in the two-body decays, owing to the kinematic constraints (the magnitude of the relative momentum in the two-body decays is fixed by energy-momentum conservation). On the contrary, the three-body decays are characterized by an (infinite) tower of effective couplings that describe the dependence of the decay amplitudes on different kinematical invariants. Consequently, the LL factor is not a single function but a matrix, which should be truncated in actual calculations.

The aim of the present chapter is to consider a single physical process, the kaon decay into three pions, and to work out the LL factor explicitly for this process in different isospin channels. In order to achieve this goal, the NREFT approach will be used. The choice of the process was not completely arbitrary – we believe that the three-pion decay of the kaon will likely be one of the first three-particle decays studied using lattice QCD, not least since it is considered as one of the sources of information about CP violation in the light quark sector (see, e.g., [296]). Moreover, we believe that, taking into account the expected accuracy of lattice calculations at the present stage, in the beginning it will be reasonable to truncate all interactions in the two- and three-pion sectors at the lowest order, i.e., to consider only non-derivative couplings in the S-wave. These approximations will allow us to put the final result in a much more compact and transparent form, suitable for a direct use by lattice practitioners, even if the calculation of the most interesting CP-odd observables (for instance, the asymmetry of slopes in the decays of K^+ and K^- [297]) will, at the end, require the inclusion of the higher-order derivative couplings at next-to-leading order.[2] Such a generalization can be however performed in a straightforward manner, using the methods described in the present chapter.[3] In order not to overload the presentation with the technical details, we omit these higher-order terms in the following.

Furthermore, there are several technical issues that were addressed only very briefly, or not addressed at all in the previous work on the problem that was carried out within the NREFT framework. Since the kaons can decay into different isospin channels, one has to explicitly write down the Faddeev

[1] In general, the LL factor receives contributions from an infinite tower of the partial-waves, see, e.g., [294].

[2] For more details on the counting scheme in the effective theory, we refer to [205, 206].

[3] The only (small) complication that may arise here is related to the emergent spurious poles in the two-body pion-pion scattering amplitude that could be however removed, using the method described in Refs. [216, 217, 298].

equations in these channels.[4] Moreover, as it is well known [134, 214], these Faddeev equations need to be renormalized. A choice of a minimal set of three-body couplings that suffices to render amplitudes cutoff-independent is rather non-trivial and will be discussed below. Moreover, we discuss an algorithm which will be used for a numerical solution of these Faddeev equations in the infinite volume. This algorithm is based on the deformation of the integration contour into the complex plane and has been known for a long time in the non-relativistic scattering theory. The discussion in case of relativistic kinematics in the literature is much more fragmented, and we shall attempt to fill this gap in the present chapter.

The main objective here is however not of a technical nature. Namely, we shall try to find an answer to the question, whether a prior knowledge of the exact values of the three-body couplings, which describe short-range three-body interactions, is essential for the determination of the LL factor. If the answer to this question were positive, it would substantially complicate the extraction of the decay amplitudes on the lattice. Indeed, for this, one would have to first accurately extract the three-pion couplings from the measured spectrum of three pions, which is quite a challenging task. Fortunately, it turns out that the LL factor shows very little dependence on the three-body force. For this reason, even a rough estimate of the three-body amplitude, based on Chiral Perturbation Theory (ChPT), will be sufficient for an accurate calculation of the LL factor which is essentially determined through the S-wave $\pi\pi$ scattering lengths alone. This, in turn, paves the way for a direct extraction of the $K \to 3\pi$ amplitudes in lattice QCD, circumventing, at the initial stage, the determination of the three-pion couplings from the measured lattice spectrum.

The layout of the chapter is the following. In Sect. 7.2 we write down the most general effective Lagrangian for the problem at hand (both in three-particle and particle-dimer picture). The matching between these alternative descriptions has been carried out, and an explicit expression for the LL factor in $K \to 3\pi$ decays is derived. In Sect. 7.3, the Faddeev equations in different isospin channels are explicitly written down and the renormalization issues are addressed. The matching to the relativistic amplitudes that will ultimately enable one to express the three-body couplings in the Lagrangian through the three-body amplitudes calculated in ChPT, is discussed. In Sect. 7.4, these Faddeev equations in the infinite volume are solved by using the contour rotation technique. Furthermore, the finite-volume energy spectrum of the three-pion system is obtained by solving the quantization condition and the finite-volume wave function are determined. All these are necessary ingredients for the calculation of the LL factor. We finally check the sensitivity of the calculated LL factor to the input values of the short-range part of the three-body threshold amplitude and find that in a wide interval, the LL factor practically does not depend on this input. Sect. 7.5 contains our conclusions.

7.2 Derivation of the $K \to 3\pi$ LL Formula

7.2.1 The Lagrangian in the Three-Particle Picture

In the following, we will consider the decay of a positively charged kaon K^+ into three pions, which is induced via weak interactions. There are two decay channels: $K^+ \to \pi^0\pi^0\pi^+$ and $K^+ \to \pi^+\pi^+\pi^-$. In order to describe the decay $K \to 3\pi$ within the NREFT approach, we adapt the Lagrangian given in

[4] Note that, in the RFT framework, the inclusion of the different isospin channels has been considered in Ref. [102].

[206], rewriting it in an arbitrary frame defined by the four-velocity v^μ:

$$\begin{aligned}\mathcal{L} = &\sum_{i_3} \pi^\dagger_{i_3}\, 2w_v \left(i(v\partial) - w_v\right) \pi_{i_3} + \mathcal{L}_2 + \mathcal{L}_3 \\ &+ K^\dagger_+\, 2W_v \left(i(v\partial) - W_v\right) K_+ + \mathcal{L}_K\,,\end{aligned} \tag{7.1}$$

where $w_v = \sqrt{M_\pi^2 + \partial^2 - (v\partial)^2}$ and $W_v = \sqrt{M_K^2 + \partial^2 - (v\partial)^2}$ and M_π and M_K denote the masses of pions and kaons respectively. Note that we work in the basis with physical particles, so that the triplet of pion fields is given by $\pi_{i_3} = (\pi_+, \pi_0, \pi_-)$. At the leading order in the power counting the two-body Lagrangian reads as

$$\begin{aligned}\mathcal{L}_2 = &\frac{1}{2} C_1\, \pi_0^\dagger \pi_0^\dagger \pi_0 \pi_0 + 2\, C_2 \left(\pi_+^\dagger \pi_0^\dagger \pi_+ \pi_0 + \pi_-^\dagger \pi_0^\dagger \pi_- \pi_0\right) + C_3 \left(\pi_+^\dagger \pi_-^\dagger \pi_0 \pi_0 + \text{h.c.}\right) \\ &+ 2\, C_4\, \pi_+^\dagger \pi_-^\dagger \pi_+ \pi_- + \frac{1}{2} C_5 \left(\pi_+^\dagger \pi_+^\dagger \pi_+ \pi_+ + \pi_-^\dagger \pi_-^\dagger \pi_- \pi_-\right)\,,\end{aligned} \tag{7.2}$$

while the three-body Lagrangian is given by

$$\begin{aligned}\mathcal{L}_3 = &D_1 \left(\pi_+^\dagger \pi_+ + \pi_0^\dagger \pi_0 + \pi_-^\dagger \pi_-\right)^3 \\ &+ D_2 \left(2\pi_+^\dagger \pi_-^\dagger - \pi_0^\dagger \pi_0^\dagger\right) \left(\pi_+^\dagger \pi_+ + \pi_0^\dagger \pi_0 + \pi_-^\dagger \pi_-\right) \left(2\pi_+ \pi_- - \pi_0 \pi_0\right).\end{aligned} \tag{7.3}$$

The weak kaon decays are described by the Lagrangian

$$\mathcal{L}_K = G_1 \left(K_+^\dagger \pi_0 \pi_0 \pi_+ + \text{h.c.}\right) + G_2 \left(K_+^\dagger \pi_+ \pi_+ \pi_- + \text{h.c.}\right)\,. \tag{7.4}$$

At higher orders, all Lagrangians are amended by the terms that contain space derivatives of all fields. A consistent power counting emerges, if one counts three-momenta as $\mathbf{p} = O(\delta)$, where δ stands for a generic small parameter.[5] Again, for consistency, one should count the difference $M_K - 3M_\pi$ as a quantity of order δ^2 [206]. As mentioned above, here the higher-order terms in δ, corresponding to the derivative couplings, are not considered.

To summarize, the following couplings emerge at leading order in the three-particle picture:

- The couplings $C_i\,,\ i = 1, \ldots, 5$, describing non-derivative pion-pion interactions in different isospin channels. These can be expressed through the S-wave $\pi\pi$ scattering lengths a_0, a_2 in a standard manner, through the matching condition.

- The three-body couplings in the pion system D_1, D_2 (the three-body force). On the lattice, they can be determined from the fit to the three-body spectrum.

- The couplings G_1, G_2 that describe the weak decays of charged kaons into three pions.

[5] In the manifestly covariant framework we are using here, one has $p_\perp^\mu \doteq p^\mu - v^\mu (v \cdot p) = O(\delta)$ instead.

7.2.2 The Lagrangian in the Particle-Dimer Picture

In the particle-dimer picture, the most general Lagrangian at the leading order reads as[6]

$$\begin{aligned}\tilde{\mathcal{L}} = &\sum_{i_3} \pi^\dagger_{i_3} 2w_v \left(i(v\partial) - w_v\right) \pi_{i_3} + \sum_{I,I_3} \sigma_I T^\dagger_{II_3} T_{II_3} + \tilde{\mathcal{L}}_2 + \tilde{\mathcal{L}}_3 \\ &+ K^\dagger_+ 2W_v \left(i(v\partial) - W_v\right) K_+ + \tilde{\mathcal{L}}_K \,,\end{aligned} \tag{7.5}$$

Here $\sigma_I = \pm 1$, depending on the sign of the two-body scattering length. Furthermore, $i_3 = -1, 0, 1$ and $I_3 = -I, \ldots, I$ denote the isospin projection of the pions and isospin-I S-wave dimer field T_{II_3}, respectively. As two pions can couple to $I = 0, 1, 2$, all dimers with different isospins decouple and can be neglected. Furthermore, due to Bose-symmetry two pions can not be in an $I = 1$ state in the S-wave. Therefore, at the leading order, the $I = 1$ dimer does not contribute, and the two-body interaction is described by the Lagrangian

$$\tilde{\mathcal{L}}_2 = \sum_{I,I_3} \left(T^\dagger_{II_3} O_{II_3} + \text{h.c.} \right) , \quad I = 0, 2 \,, \tag{7.6}$$

where the dimer operator is given by a sum over two pion field operators with pertinent Clebsh-Gordan coefficients:

$$O_{II_3} = \sum_{i_3, i_3'} \frac{1}{2} f_I \, \langle 1, i_3; 1, i_3' | I, I_3 \rangle \, \pi_{i_3} \pi_{i_3'} \,. \tag{7.7}$$

Note also that $O_{1I_3} = 0$ for all $I_3 = -1, 0, 1$ follows due to Bose-symmetry. Furthermore, the couplings f_I describe the decay of a dimer into two pions and can be expressed through the S-wave $\pi\pi$ scattering lengths through the matching condition.

The construction of the three-body Lagrangian proceeds by defining particle-dimer operators in the channels with a different total isospin J:

$$O^{(J,I)}_{J_3} = \sum_{I_3, i_3} \langle I, I_3; 1, i_3 | J, J_3 \rangle \, \pi_{i_3} T_{II_3} \,. \tag{7.8}$$

In the channels with the total isospin $J = 2$ and $J = 3$, there is only a single set of operators with the dimers having $I = 2$. For isospin $J = 1$, there are two independent operators, where the dimer has $I = 0$ and $I = 2$ respectively. The most general Lagrangian is thus given by:

$$\tilde{\mathcal{L}}_3 = \sum_{J,J_3} \sum_{I,I'} h^{(I,I')}_J \left(O^{(J,I)}_{J_3} \right)^\dagger O^{(J,I')}_{J_3} \,, \tag{7.9}$$

where, due to hermiticity, $h^{(I,I')}_J = h^{(I',I)}_J$ (Note that $h^{(I,I')}_J$ are real due to the T-invariance.). In the $J = 2$ and $J = 3$ channels, there is a single coupling, $h^{(2,2)}_2$ and $h^{(2,2)}_3$, respectively. For the channel with $J = 1$, there are three couplings $h^{(0,0)}_1$, $h^{(2,2)}_1$ and $h^{(2,0)}_1 = h^{(0,2)}_1$.

Finally, $\tilde{\mathcal{L}}_K$ describes the weak kaon decay. Due to charge conservation, the positively charged

[6] More details about particle-dimer formalism can be found, e.g., in Refs. [71, 81, 101, 134, 214, 299].

Figure 7.1: Full dimer propagator, obtained by summing up self-energy insertions to all orders. The blue double, gray double and black single lines denote the full dimer propagator, the free dimer propagator given by $-\sigma_I^{-1}\delta_{II'}\delta_{I_3I_3'}$, and the particle propagator. The blue dots represent the insertion of the vertex converting a dimer into particles.

kaon can only couple to the operators with $J_3 = 1$:

$$\tilde{\mathcal{L}}_K = \sum_{J,I} g^{(J,I)} \left(K_+^\dagger O_1^{(J,I)} + \text{h.c.} \right) . \tag{7.10}$$

Hence, in the particle-dimer picture, we have the following parameters in the lowest-order Lagrangian

- Two-particle-dimer couplings f_0, f_2. These correspond to the couplings C_i in the three-particle picture.
- Three-body force in the particle-dimer picture, described by the couplings $h_1^{(0,0)}$, $h_1^{(2,2)}$, $h_1^{(2,0)}$, $h_2^{(2,2)}$ and $h_3^{(2,2)}$. These correspond to the couplings D_1, D_2 in the three-particle picture.
- The weak couplings $g^{(1,0)}, g^{(1,2)}, g^{(3,2)}$, corresponding to the parameters G_1, G_2 in the three-particle picture.

Despite the fact that the number of the couplings in different formalisms differ, these formalisms are equivalent. This equivalence is, however, a rather subtle issue, and is discussed in the remaining part of this section.

7.2.3 Matching in the Two-Body Sector

The couplings f_I can be matched to the two-body S-wave scattering length in the $I = 0$ and $I = 2$ isospin channels. Due to isospin symmetry, the dimer propagator is diagonal in the isospin space:

$$i\langle 0|T[T_{II_3}(x)T^\dagger_{I'I_3'}(y)]|0\rangle = \delta_{II'}\delta_{I_3I_3'} \int \frac{d^4P}{(2\pi)^4}\, e^{-iP(x-y)}\, S_I(P^2) . \tag{7.11}$$

Summing up the self-energy insertions (see Fig. 7.1), for $I = 0, 2$ we find

$$S_I(P^2) = \frac{f_I^{-2}}{-\sigma_I f_I^{-2} - \frac{1}{2} I(s)} , \quad s = P^2 , \tag{7.12}$$

where, for $s \geq 4M_\pi^2$,

$$I(s) = \frac{\sigma(s)}{16\pi^2} \ln \frac{\sigma(s)-1}{\sigma(s)+1} = J(s) + \frac{i\sigma(s)}{16\pi} , \quad \sigma(s) = \left(1 - \frac{4M_\pi^2}{s+i\varepsilon}\right)^{1/2} , \tag{7.13}$$

while for $I = 1$ trivially $S_1(P^2) = -\sigma_1^{-1}$.

The two-particle scattering amplitude $\pi_{i_3'}(p_1) + \pi_{j_3'}(p_2) \to \pi_{i_3}(p_3) + \pi_{j_3}(p_4)$ is obtained from the dimer propagator by attaching the vertices that convert a dimer into a particle-pair. The isospin $I = 0, 2$ the amplitudes are given by:

$$T_I(p_1, p_2; p_3, p_4) = f_I^2 \, S_I(P^2) = \frac{16\pi\sqrt{s}}{16\pi\sqrt{s}[-\sigma_I f_I^{-2} - \frac{1}{2}J(s)] - ip(s)}\,, \tag{7.14}$$

where $P^2 = (p_1 + p_2)^2 = (p_3 + p_4)^2$ and $s = P^2 = 4(M_\pi^2 + p^2(s))$. Due to unitarity,

$$16\pi\sqrt{s}[-\sigma_I f_I^{-2} - \frac{1}{2}J(s)] = p(s)\cot\delta_I(s)\,. \tag{7.15}$$

Therefore, for $I = 0, 2$, the matching to the scattering length a_I reads as:

$$\sigma_I^{-1} f_I^2 = 32\pi M_\pi a_I\,. \tag{7.16}$$

As discussed in appendix A.4, integrating out the dimer fields at tree level merely amounts to the replacement

$$T_{II_3} \to -\sigma_I^{-1} O_{II_3}\,. \tag{7.17}$$

The matching condition to the two-particle Lagrangian in the particle picture yields:

$$\begin{aligned}
C_1 &= -\frac{1}{6}\left(\sigma_0^{-1} f_0^2 + 2\sigma_2^{-1} f_2^2\right) = -16\pi M_\pi \frac{1}{3}(a_0 + 2a_2)\,,\\
C_2 &= -\frac{1}{4}\sigma_2^{-1} f_2^2 = -16\pi M_\pi \frac{1}{2}\, a_2\,,\\
C_3 &= -\frac{1}{6}\left(\sigma_2^{-1} f_2^2 - \sigma_0^{-1} f_0^2\right) = -16\pi M_\pi \frac{1}{3}\,(a_2 - a_0)\\
C_4 &= -\frac{1}{12}\left(2\sigma_0^{-1} f_0^2 + \sigma_2^{-1} f_2^2\right) = -16\pi M_\pi \frac{1}{6}\,(2a_0 + a_2)\,,\\
C_5 &= -\frac{1}{2}\,\sigma_2^{-1} f_2^2 = -16\pi M_\pi\, a_2\,.
\end{aligned} \tag{7.18}$$

This result agrees with [206].[7]

[7] Note a different sign convention is used in Ref. [206], namely, $p\cot\delta = 1/a_I + \ldots$ instead of $p\cot\delta = -1/a_I + \ldots$.

7.2.4 Matching of the Three-Body and Decay Lagrangians

At tree level, carrying out the the replacement (7.17) in the particle-dimer operators, one straightforwardly gets:

$$\begin{aligned}
O_{J_3}^{(1,0)} &\to -\frac{\sigma_0^{-1} f_0}{2\sqrt{3}} (2\pi_+\pi_- - \pi_0\pi_0)\pi_{J_3}\,, \\
O_{J_3}^{(1,2)} &\to -\frac{\sigma_2^{-1} f_2}{\sqrt{15}} (2\pi_+\pi_- - \pi_0\pi_0)\pi_{J_3}\,, \\
O_{J_3}^{(2,2)} &\to 0\,, \\
O_{\pm 3}^{(3,2)} &\to -\frac{\sigma_2^{-1} f_2}{2} \pi_\pm\pi_\pm\pi_\pm\,, \\
O_{\pm 2}^{(3,2)} &\to -\frac{\sigma_2^{-1} f_2\sqrt{3}}{2} \pi_\pm\pi_\pm\pi_0\,, \\
O_{\pm 1}^{(3,2)} &\to -\frac{\sigma_2^{-1} f_2\sqrt{3}}{2\sqrt{5}} \left(\pi_\pm\pi_\pm\pi_\mp + 2\pi_\pm\pi_0\pi_0\right)\,, \\
O_{0}^{(3,2)} &\to -\frac{\sigma_2^{-1} f_2}{\sqrt{10}} \left(3\pi_+\pi_-\pi_0 + \pi_0\pi_0\pi_0\right)\,.
\end{aligned} \tag{7.19}$$

Furthermore, performing this replacement in the particle-dimer Lagrangian, one can identify the couplings D_1, D_2 from Eq. (7.3):

$$\begin{aligned}
\sum_{J,J_3}\sum_{I,I'} h_J^{(I,I')} \left(O_{J_3}^{(J,I)}\right)^\dagger O_{J_3}^{(J,I')} &\to D_1 \left(\pi_+^\dagger\pi_+ + \pi_0^\dagger\pi_0 + \pi_-^\dagger\pi_-\right)^3 \\
&+ D_2 \left(2\pi_+^\dagger\pi_-^\dagger - \pi_0^\dagger\pi_0^\dagger\right)\left(\pi_+^\dagger\pi_+ + \pi_0^\dagger\pi_0 + \pi_-^\dagger\pi_-\right)\left(2\pi_+\pi_- - \pi_0\pi_0\right),
\end{aligned} \tag{7.20}$$

with

$$\begin{aligned}
D_1 &= \frac{f_2^2}{4} h_3^{(2,2)}\,, \\
D_2 &= \frac{f_0^2}{12} h_1^{(0,0)} + \frac{\sigma_0^{-1} f_0 \sigma_2^{-1} f_2}{3\sqrt{5}} h_1^{(2,0)} + \frac{f_2^2}{15} h_1^{(2,2)} - \frac{3 f_2^2}{20} h_3^{(2,2)}\,.
\end{aligned} \tag{7.21}$$

Using the same replacement in the Lagrangian that describes the weak decays of kaons (7.4), one could read off the couplings G_1, G_2:

$$\sum_{J,I} g^{(J,I)} \left(K_+^\dagger O_1^{(J,I)} + \text{h.c.}\right) \to G_1 \left(K_+^\dagger\pi_+\pi_+\pi_- + \text{h.c.}\right) + G_2 \left(K_+^\dagger\pi_+\pi_0\pi_0 + \text{h.c.}\right)\,, \tag{7.22}$$

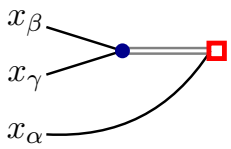

Figure 7.2: Tree level contribution to the decay matrix element. Black solid lines and gray double lines denote a particle propagator and the tree-level dimer propagator, respectively. The blue dot and the empty red square correspond to the particle-dimer conversion vertex and the kaon initial decay coupling, respectively. Furthermore, $(\alpha\beta\gamma)$ stands for some permutation of (123).

with

$$G_1 = -\frac{\sqrt{3}}{\sqrt{5}}\,\sigma_2^{-1} f_2 g^{(3,2)} + \frac{1}{\sqrt{15}}\,\sigma_2^{-1} f_2 g^{(1,2)} + \frac{1}{2\sqrt{3}}\,\sigma_0^{-1} f_0 g^{(1,0)}\,.$$
$$G_2 = -\frac{\sqrt{3}}{2\sqrt{5}}\,\sigma_2^{-1} f_2 g^{(3,2)} - \frac{2}{\sqrt{15}}\,\sigma_2^{-1} f_2 g^{(1,2)} - \frac{1}{\sqrt{3}}\,\sigma_0^{-1} f_0 g^{(1,0)}\,, \tag{7.23}$$

As seen from the above equations (7.21) and (7.23), the number of the couplings in the particle-dimer picture is larger than in the three-particle picture. Namely, one could argue that only two couplings in each set $h_J^{(I,I')}$ and $g^{(J,I)}$ are independent, and others can be chosen freely. Note that establishing the number of the independent couplings is a subtle dynamical issue and is discussed in detail in Ref. [101]. Here, we merely state that in the S-wave $\pi\pi$ scattering no shallow dimers exist that justifies a naive counting presented above. To fix the freedom, we choose $h_1^{(2,0)} = h_1^{(2,2)} = h_2^{(2,2)} = 0$ and $g^{(1,2)} = 3g^{(3,2)}$, $g^{(2,2)} = \sqrt{5}g^{(3,2)}$ (The latter two conditions ensures that, at tree level, the operators $T_{20}\pi_+$ and $T_{21}\pi_0$ are absent in the Lagrangian $\tilde{\mathcal{L}}_K$, which describes the weak decay of a kaon into the particle-dimer pair.).

An important question is, however, whether these redundant couplings, which are absent in the tree-level matching, re-emerge in the loops. We shall address this question in the following section.

7.2.5 Reduction of the Redundant Couplings

Following Eq. (7.19), one can trivially define a linear combination of the operators $O_{J_3}^{(1,0)}$ and $O_{J_3}^{(1,2)}$, which vanishes under the replacement (7.17). One need not display an explicit form of this linear combination here which, together with $O_{J_3}^{(2,2)}$, forms a set of the *irrelevant* operators $\hat{O}_{J_3}^{(a)}$, $a = 1, 2$. The contribution of the irrelevant operators to the physical matrix elements at tree-level vanishes. An orthogonal linear combination of $O_{J_3}^{(1,0)}$ and $O_{J_3}^{(1,2)}$ and $O_{J_3}^{(3,2)}$ form a set of *relevant* operators $O_{J_3}^{(a)}$, $a = 1, 2$. The question which will be addressed below, can be stated as follows: do the irrelevant operators contribute to the physical observables beyond the tree level? We shall demonstrate that this is not the case, and the irrelevant operators can be safely dropped from the beginning.

Let us start from the decay of a kaon into three pions, and consider the following vertex function

$$\hat{G}^{(a)}_{i_1 i_2 i_3}(x_1, x_2, x_3) = \langle 0|T\left[O_{3\pi}^{i_1 i_2 i_3}(x_1, x_2, x_3)\,\left(\hat{O}_1^{(a)}\right)^\dagger(0)\right]|0\rangle\,, \tag{7.24}$$

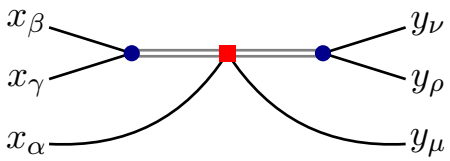

Figure 7.3: The tree-level contribution to the matrix element of the three-pion scattering. Black solid lines and gray double lines denote the particle propagator and the tree-level dimer propagator, respectively. The blue dots and the red rectangle correspond to the particle-dimer conversion vertex and the particle-dimer interaction vertex, respectively. The labels $(\alpha\beta\gamma)$ and $(\mu\nu\rho)$ denote the permutations of (123).

where $O_{3\pi}$ denotes a three-pion operator:

$$O_{3\pi}^{i_1 i_2 i_3}(x_1, x_2, x_3) = \pi_{i_1}(x_1)\pi_{i_2}(x_2)\pi_{i_3}(x_3)\,. \tag{7.25}$$

At tree level, this vertex, shown in Fig. 7.2, vanishes, because of the Bose-symmetry of three pions in the final state. Now, note that the same vertex appears in any loop diagram that describes the kaon decay. It is straightforward to check that these loop diagrams vanish as well, since the tree-level vertex does not depend on the momenta of the final pions – in other words, it does not distinguish between the real an virtual pions. As a result, the contribution of the irrelevant operators to the pion decay amplitude vanishes to all orders in perturbation theory.

A similar argument applies for the three-pion scattering. The tree-level contribution to the quantity

$$\begin{aligned} &V^{(a,b)}_{i_1 i_2 i_3; j_1 j_2 j_3}(x_1, x_2, x_3; y_1, y_2, y_3) \\ =&\langle 0|T\left[O_{3\pi}^{i_1 i_2 i_3}(x_1, x_2, x_3) O_{3\pi}^{j_1 j_2 j_3}(y_1, y_2, y_3)^\dagger \sum_{J_3} \left(O^{(a)}_{J_3}(0)\right)^\dagger \left(\hat{O}^{(b)}_{J_3}(0)\right)\right]|0\rangle \end{aligned} \tag{7.26}$$

is shown in Fig. 7.3. Here, for simplicity, we assume that only one irrelevant operator appears, but the discussion in case of two irrelevant operators follows exactly the same path. The tree-level contribution, where each dimer line is equipped by two-particle lines prior to escaping, obviously vanishes. The question, whether the irrelevant operators contribute in the loops reduces to the question, whether all internal dimer lines end up in the two-pion vertex. There is only one diagram, shown in Fig. 7.4, where this is not the case. However, the tree-level dimer propagator $S_I^{(0)}(x) = -\sigma_I^{-1}\delta^4(x)$ is local in position space. Hence, a closed loop over the non-relativistic pion propagator emerges, which vanishes due to the pole structure of the latter. To summarize, the irrelevant operators contribute neither to the kaon decay amplitudes, nor to the three-pion scattering amplitudes to all orders and, hence, can be safely discarded from the beginning.

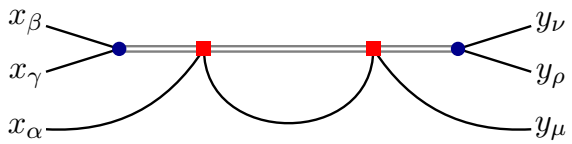

Figure 7.4: The particle-dimer loop diagram that could potentially contribute to the six-pion amplitude. Black solid lines and gray double lines denote a particle propagator and the tree-level dimer propagator, respectively. The blue dots and the red rectangle correspond to the particle-dimer conversion vertex and the particle-dimer interaction vertex, respectively.

7.3 Faddeev Equations and Derivation of the LL Factor

7.3.1 Faddeev Equation for Particle-Dimer Amplitude

We start with writing down the Faddeev equation for the particle-dimer amplitude.[8] There are three isospin channels with $J = 1, 2, 3$ (In the decays of charged kaons, the channel with $J = 0$ is excluded due to charge conservation.). It is important to note that, due to the symmetry properties of the three-pion wave function, the isospin channel $J = 2$ does not contribute to the kaon decay at the leading order. The particle-dimer amplitude $\mathcal{M}_{J;II'}(p, q; P)$ in an arbitrary reference frame defined by a unit vector v^μ obeys the equation

$$\begin{aligned}\mathcal{M}_{J;II'}(p,q;P) &= Z_{J;II'}(p,q;P) \\ &\quad + \sum_{I''} \int^{\Lambda_v} \frac{d^3k_\perp}{(2\pi)^3 2w_v(k)} Z_{J;II''}(p,k;P)\tau_{I''}((P-k)^2)\mathcal{M}_{J;I''I'}(k,q;P)\,. \end{aligned} \tag{7.27}$$

Here, I and I' are the incoming and outgoing dimer isospin indices, p and q represent the on-shell four-momenta of outgoing/incoming particles, respectively, P is the total four-momentum of the three-pion system and $k^\mu_\perp = k^\mu - v^\mu(vk)$ denotes the perpendicular component of any vector k^μ in a frame defined by the unit vector v^μ, see also footnote 5. Furthermore, Λ_v denotes the ultraviolet cutoff which is defined by:

$$\int^{\Lambda_v} \frac{d^3k_\perp}{(2\pi)^3} F(k) = \int \frac{d^4k}{(2\pi)^3}\, \delta^4(k^2 - m^2)\theta(\Lambda^2 + k^2 - (vk)^2)F(k)\,. \tag{7.28}$$

The Faddeev equation is diagrammatically illustrated in Fig. 7.5. Note that, in order to streamline the notations, we have changed the normalization of the amplitude, according to $\mathcal{M}_{J;II'} \to f_I^{-1}\mathcal{M}_{J;II'}f_{I'}^{-1}$. The quantity $Z_{J;II'}$ represents the driving term of the Faddeev equation while τ_I stands for the dimer propagator:

$$\begin{aligned} Z_{J;II'}(p,q;P) &= \frac{c_{J;II'}}{2w_v(P-p-q)(w_v(P-p-q)+w_v(p)+w_v(q)-vP-i\varepsilon)} + \frac{H_{J;II'}(\Lambda)}{\Lambda^2}\,, \\ \tau_I((P-k)^2) &= f_I^2 S_I((P-k)^2)\,. \end{aligned} \tag{7.29}$$

[8] The Faddeev equations in the particle-dimer picture (both the non-relativistic and relativistic cases) has been considered in detail in the following papers [71, 81, 101, 134, 214, 299].

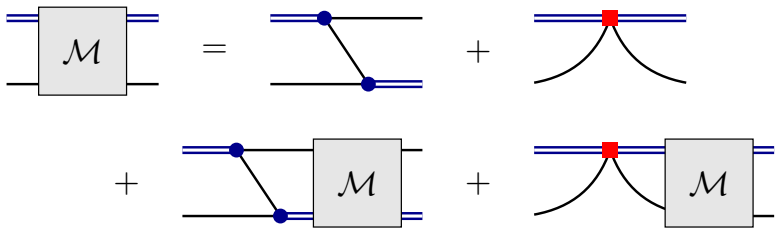

Figure 7.5: Faddeev equation for the particle-dimer scattering amplitude. The double blue line and the solid black line correspond to the full propagator of the dimer field the pion propagator, respectively. The blue circle denotes the vertex, converting the dimer to particles and the red box denotes the dimer-particle contact vertex. Isospin indices are implicit.

The explicit expression for the quantity τ_I, which is directly related to the dimer propagator defined in Eq. (7.12), can be read off from Eq. (7.14). Furthermore, $c_{J;II'}$ are expressed through the Clebsh-Gordan coefficients and emerge after the projection onto the states with total isospin J:

$$c_{1;00} = \frac{1}{3}, \quad c_{1;02} = c_{1;20} = \frac{\sqrt{5}}{3}, \quad c_{1;22} = \frac{1}{6}, \quad c_{2;22} = -\frac{1}{2}, \quad c_{3;22} = 1\,. \tag{7.30}$$

Finally

$$H_{J;II'}(\Lambda) = \Lambda^2 \, f_I^{-1} \, h_J^{(I,I')} \, f_{I'}^{-1}\,. \tag{7.31}$$

According to the choice $h_1^{(2,0)} = h_1^{(2,2)} = h_2^{(2,2)} = 0$, only the couplings $H_{1;00}$ and $H_{3;22}$ are non-zero. Furthermore, as shown in Refs. [134, 214], if one restricts oneself only to the first term in $Z_{J;II'}$ and sets all $H_{J;II'}(\Lambda)$ to zero, the solution of the Faddeev equation is cutoff-dependent and shows oscillatory dependence on Λ. This cutoff-dependence is eliminated by adding the contribution from $H_{J;II'}(\Lambda)$. The Λ-dependence of these couplings is such that it exactly cancels the oscillatory behavior coming from the first term. For our case, two remarks are in order. First, as shown in Ref. [134], since the coefficient in the isospin-two channel, $c_{2;22} = -\frac{1}{2}$, has a negative sign, the amplitude even without the inclusion of $H_{2;22}(\Lambda)$ is cutoff-independent for all momenta $p \ll \Lambda$. Hence, one does not need to introduce the particle-dimer contact term in the $J = 2$ channel altogether. Second there are no physical dimers and hence there is only one independent three-pion amplitude in the $J = 1$ channel. Consequently, in this channel, it is sufficient to match the coupling $H_{1;00}$ only. To summarize, as expected from the beginning, all observable three-pion amplitudes can be made cutoff-independent by matching only two couplings $H_{1;00}$ and $H_{3;22}$, albeit the original particle-dimer Lagrangian contained four independent couplings. This statement does not hold, in general, for the (unobservable) particle-dimer amplitudes (We remind the reader that there are no shallow bound states in our case.).

For matching of $H_{J;II'}(\Lambda)$, we need the three-particle threshold amplitude and, equivalently, the particle-dimer threshold amplitude, which is obtained by setting $\mathbf{p}, \mathbf{q} = 0$ in the CM frame. This amplitude is singular at $E = 3M_\pi$. To get the regular part of this amplitude, we start with evaluating the amplitude slightly below threshold, assuming that $E = 3M_\pi - \varepsilon$, and consider the limit $\varepsilon \to 0$ at the end. Adding loops makes the singularity at $\varepsilon = 0$ weaker, and evaluating the diagrams up to two loops suffices for finding all singularities. Next, the singularities in ε are isolated and subtracted

from the threshold amplitude, in order to obtain the regular part. This process is discussed in detail in Ref. [95] in a purely non-relativistic setting. The singularities in our case are the same and can be easily read off from Ref. [95]:

$$\begin{aligned}\mathcal{S}_{J;II'}(\varepsilon) =& \frac{1}{2M_\pi\varepsilon}c_{J;II'} - \frac{1}{2\sqrt{M_\pi\varepsilon}}\sum_{I''}(c_{J;II''}\, a_{I''}\, c_{J;I''I'}) \\ &+ \frac{\sqrt{3}}{2\pi}\log\frac{\varepsilon}{M_\pi}\sum_{I''}(c_{J;II''}\, a_{I''}^2\, c_{J;I''I'}) \\ &- \frac{2}{3}\log\frac{\varepsilon}{M_\pi}\sum_{I'';I'''}(c_{J;II''}\, a_{I''}\, c_{J;I''I'''}\, a_{I'''}\, c_{J;I'''I'})\,. \end{aligned} \tag{7.32}$$

In an arbitrary frame, the quantity ε should be defined as $\varepsilon = \sqrt{P^2} - 3M_\pi$, whereas $\mathbf{p}, \mathbf{q}$ are replaced by $p_\perp^\mu, q_\perp^\mu$. By subtracting $\mathcal{S}_{J;II'}(\varepsilon)$ from the threshold amplitude $\mathcal{M}_{J;II'}$ and taking the limit $\varepsilon \to 0$, we get the regular particle-dimer threshold amplitude.

The infinite-volume three-particle amplitude[9] is related to the particle-dimer amplitude in the following way:

$$\begin{aligned}T_{J;II'}(\{p\},\{q\};P) = \sum_{\alpha,\beta=1}^{3}\Big[&(2\pi)^3\delta^3(p_{\alpha\perp} - q_{\beta\perp})\delta_{II'}2w_\nu(p_\alpha)\tau_I((P-p_\alpha)^2) \\ &+ \tau_I((P-p_\alpha)^2)\mathcal{M}_{J;II'}(p_\alpha,q_\beta;P)\tau_{I'}((P-q_\beta)^2)\Big]\,. \end{aligned} \tag{7.33}$$

Here, $\{p\}$ represents the set of all four-particle momenta p_α with $\alpha = 1,2,3$. The regular part of the three-particle amplitude can be related to the regular part of the particle-dimer amplitude in an obvious manner.

In a finite volume, the counterpart of the Faddeev equation can be written down as follows

$$\begin{aligned}\mathcal{M}^L_{J;II'}(p,q;P) =& Z_{J;II'}(p,q;P) \\ &+ \sum_{I''}\frac{1}{L^3}\sum_{\mathbf{k}}^{\Lambda_\nu}\frac{1}{2w(\mathbf{k})}Z_{J;II'}(p,k;P)\tau^L_{I''}(P-k)\mathcal{M}^L_{J;I''I'}(k,q;P)\,, \end{aligned} \tag{7.34}$$

where L is the spatial extent of the box and finite-volume quantities are represented by the superscript L. The summation is over the discrete values of momentum $\mathbf{k} = 2\pi\mathbf{n}/L$, $\mathbf{n} \in \mathbb{Z}^3$. The finite-volume propagator is given by

$$\tau_I^L(P) = \frac{16\pi\sqrt{s}}{16\pi\sqrt{s}[-\sigma_I f_I^{-2} - \frac{1}{2}J(s)] - \frac{2}{\sqrt{\pi}L\gamma}Z^{\mathbf{d}}_{00}(1;q_0^2)}\,, \tag{7.35}$$

where $s = P^2$ and the real part of the Chew-Mandelstam function, $J(s)$, is defined in Eq. (7.13).

[9] We would like to stress here that this is not a physical amplitude. The physical states with a given full isospin J can be built up from a pion and a dimer with a isospin I in different ways. in the quantity $T_{J;II'}$, the full isospin J, as well as I, I' are fixed.

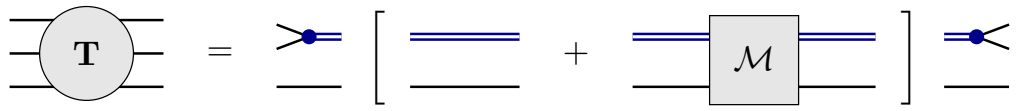

Figure 7.6: The three-particle amplitude in terms of the particle-dimer scattering amplitude. The sum over spectator momenta and the isospin indices are implicit.

Furthermore, the Lüscher zeta-function $Z_{00}^{\mathbf{d}}(1;q_0^2)$ is defined as

$$Z_{00}^{\mathbf{d}}(1;q_0^2) = \frac{1}{\sqrt{4\pi}} \sum_{\mathbf{r}^2 \in P_d} \frac{1}{\mathbf{r}^2 - q_0^2}\,, \tag{7.36}$$

with $\gamma = \dfrac{P_0}{\sqrt{s}}$, $\mathbf{d} = \dfrac{L}{2\pi}\mathbf{P}$, $q_0^2 = \dfrac{L^2}{4\pi^2}\left(\dfrac{s}{4} - m^2\right)$ and

$$P_d = \left\{\mathbf{r} = \mathbb{R}^3 | r_\parallel = \gamma^{-1}\left(n_\parallel - \frac{1}{2}|\mathbf{d}|\right), \mathbf{r}_\perp = \mathbf{n}_\perp, \mathbf{n} \in \mathbb{Z}^3\right\}.$$

The quantization condition, which now explicitly includes different isospin channels, is given by

$$\det(A) = 0\,, \qquad A_{J;II'}(p,q;P) = 2w(\mathbf{k})L^3\delta_{\mathbf{pq}}\delta_{II'}[\tau_I^L(P-k)]^{-1} - Z_{J;II'}(p,q;P)\,. \tag{7.37}$$

The finite-volume spectrum E_n of the three-particle system is determined by the discrete solutions of the quantization condition. The particle-dimer amplitude is factorized near the pole of the quantization condition as follows,

$$\mathcal{M}_{J;II'}^L(p,q;P)\Big|_{E\to E_n} = \frac{\phi_{J;I}^{(n)}(p)\phi_{J;I'}^{(n)}(q)}{P_{n,\parallel} - P_\parallel - i\varepsilon} + \text{regular}\,,$$

where $\phi_{J;I}^{(n)}(p)$ is the finite-volume particle-dimer wave function and it obeys the homogeneous equation:

$$\phi_{J;I}^{(n)}(p) = \sum_{I'} \frac{1}{L^3} \sum_{\mathbf{k}}^{\Lambda_v} \frac{1}{2w(\mathbf{k})} Z_{J;II'}(p,k;P)\tau_{I'}^L(P-k)\phi_{J;I'}^{(n)}(k)\,. \tag{7.38}$$

Note that $Z_{J;II'}(p,k;P)$ and $\tau_I^L(P-k)$ are energy-dependent quantities and hence the wave function is not normalized to unity but rather obeys the following normalization condition

$$\begin{aligned}\sum_{II'} \frac{1}{L^6} \sum_{\mathbf{p},\mathbf{k}}^{\Lambda_v} \phi_{J;I}^{(n)}(p) \frac{\tau_I^L(P-p)}{2w(\mathbf{p})} \frac{dZ_{J;II'}(p,k;P)}{dP_{n,\parallel}} \frac{\tau_{I'}^L(P-k)}{2w(\mathbf{k})} \phi_{J;I'}^{(n)}(k) \\ + \sum_I \frac{1}{L^3} \sum_{\mathbf{p}}^{\Lambda_v} \phi_{J;I}^{(n)}(p) \frac{1}{2w(\mathbf{p})} \frac{d\tau_I^L(P-p)}{dP_{n,\parallel}} \phi_{J;I}^{(n)}(p) = 1\,,\end{aligned} \tag{7.39}$$

where one substitutes $P_\parallel = P_{n,\parallel}$ after differentiation.

7.3.2 Matching of the Three-Pion Coupling

Below, we shall perform the matching of the particle-dimer couplings to the three-pion threshold amplitude. These amplitudes will be evaluated at tree level in perturbation theory.[10] We start from calculating the physical three-particle amplitudes in the particle basis.[11] In order to express these in terms of particle-dimer amplitudes, one has to equip the latter by the full dimer propagators for the outgoing legs and the vertex functions that describe the transition of a dimer into a two-pion pair, see Eq. (7.33). The (connected part of the) threshold amplitude for the scattering of three charged pions is straightforward to obtain, since it contains only the isospin $J = 3$ contribution:

$$T^{\text{conn}}(3\pi^+ \to 3\pi^+) = 9\mathcal{M}_{3;22}(\varepsilon)\tau_2(\varepsilon)^2\,. \tag{7.40}$$

Here, the factor 9 comes after summation over all permutations of the external lines. Similarly, the connected part of the amplitude with three neutral pions is given by

$$\begin{aligned} T^{\text{conn}}(3\pi^0 \to 3\pi^0) = {} & 3\mathcal{M}_{1;00}(\varepsilon)\tau_0^2(\varepsilon) + \frac{12}{\sqrt{5}}\mathcal{M}_{1;02}(\varepsilon)\tau_0(\varepsilon)\tau_2(\varepsilon) \\ & + \frac{12}{5}\mathcal{M}_{1;22}(\varepsilon)\tau_2(\varepsilon)^2 + \frac{18}{5}\mathcal{M}_{3;22}(\varepsilon)\tau_2(\varepsilon)^2\,. \end{aligned} \tag{7.41}$$

The amplitudes entering the above equations are defined as

$$\begin{aligned} \mathcal{M}_{J;II'}(\varepsilon) = \mathcal{M}_{J;II'}(\varepsilon)(\bar{p},\bar{q};\bar{P})\,, \qquad \tau_I(\varepsilon) = \tau_I((\bar{P}-\bar{p})^2)\,, \\ \bar{p} = \bar{q} = (M_\pi, \mathbf{0})\,, \quad \bar{P} = (3M_\pi - \varepsilon, \mathbf{0})\,. \end{aligned} \tag{7.42}$$

Furthermore, according to Eqs. (7.32) and (7.14), the expansion of $\mathcal{M}_{J;II'}(\varepsilon)$ and $\tau_I(\varepsilon)$ in ε takes the following form:

$$\begin{aligned} \mathcal{M}_{J;II'}(\varepsilon) &= \frac{c_{J;II'}}{2M_\pi\varepsilon} + \frac{d_{J;II'}}{2\sqrt{M_\pi\varepsilon}} + e_{J;II'}\log\frac{\varepsilon}{M_\pi} + \bar{\mathcal{M}}_{J;II'} + O(\sqrt{\varepsilon})\,, \\ \tau_I(\varepsilon) &= -32\pi M_\pi a_I\left(1 + a_I\sqrt{M_\pi\varepsilon} + a_I^2 M_\pi\varepsilon - \frac{2a_I\varepsilon}{\pi}\right)\,, \end{aligned} \tag{7.43}$$

where $d_{J;II'}$ and $e_{J;II'}$ are coefficients that are proportional to the powers of the two-body scattering length. Therefore, applying chiral power counting, from Eq. (7.32) it directly follows that

$$c_{J;II'} = O(1)\,, \qquad d_{J;II'} = O(M_\pi^2)\,, \qquad e_{J;II'} = O(M_\pi^4)\,. \tag{7.44}$$

[10] Note that, within the RFT approach, this matching has been carried out at one loop recently [292]. Here, we restrict ourselves to the tree-level calculations. Anyway, it will be demonstrated below that, in the LL factor we are after, there is barely any dependence on the exact value of the threshold tree-body amplitude.

[11] There are only two independent six-pion couplings at lowest order. This means that one can use any two linearly independent physical amplitudes to perform the matching. We use $3\pi^+ \to 3\pi^+$ and $3\pi^0 \to 3\pi^0$ amplitudes for this purpose here.

Taking into account the fact that the tree-level amplitude in ChPT, which will be matched to the six-point amplitudes given in Eqs. (7.40) and (7.41), is of order M_π^2 (see appendix A.5), it follows that, at the accuracy we are working, the regular part of these amplitudes (i.e., the piece that is obtained from the amplitudes after dropping all divergent pieces in ε and performing the limit $\varepsilon \to 0$) is given by

$$\begin{aligned} T_{\text{reg}}^{\text{conn}}(3\pi^+ \to 3\pi^+) &= 9\bar{\mathcal{M}}_{3;22}\bar{\tau}_2^2\,, \\ T_{\text{reg}}^{\text{conn}}(3\pi^0 \to 3\pi^0) &= 3\bar{\mathcal{M}}_{1;00}\bar{\tau}_0^2 + \frac{12}{\sqrt{5}}\bar{\mathcal{M}}_{1;02}\bar{\tau}_0\bar{\tau}_2 + \frac{12}{5}\bar{\mathcal{M}}_{1;22}\bar{\tau}_2^2 + \frac{18}{5}\bar{\mathcal{M}}_{3;22}\bar{\tau}_2^2\,, \end{aligned} \tag{7.45}$$

where $\bar{\tau}_I = 32\pi M_\pi a_I$, and $\bar{\mathcal{M}}_{J;II'}$ denotes the regular part of the particle-dimer scattering amplitude.

These amplitudes can be matched to the ones obtained from ChPT, see the appendix A.5. The result there is given by

$$T_+^\chi = \frac{18M_\pi^2}{F_\pi^4}\,, \qquad T_0^\chi = -\frac{9M_\pi^2}{8F_\pi^4}\,. \tag{7.46}$$

The three-pion couplings $H_{1;00}(\Lambda)$ and $H_{3;22}(\Lambda)$ can be determined by numerically solving the Faddeev equation, extracting the threshold particle-dimer amplitudes $\bar{\mathcal{M}}_{J;II'}$ from these solutions after subtracting the divergent pieces, and then equating the result given in Eq. (7.45), to $T_{+,0}^\chi$.

7.3.3 Derivation of the LL Factor

The LL factor connects the decay amplitudes between the infinite volume and a finite volume. Therefore, in order to obtain the LL factor, we need to calculate the amplitude of $K \to 3\pi$ twice, separately in the infinite volume and in a finite volume.

In the infinite volume, we calculate the decay amplitude in two steps. First, K decays into a dimer and a spectator pion. Then, the dimer further decays into two pions. The final state at threshold can have the total isospin $J = 1, 3$. Assuming, for convenience that $J_3 = 1$, we get

$$\langle \pi^{i_1}(p_1)\pi^{i_2}(p_2)\pi^{i_3}(p_3)|K^+\rangle = \sum_\alpha \sum_I \mathcal{A}(K^+ \to T_{I,(1-i_\alpha)}\pi^{i_\alpha}(p_\alpha))\langle 1, i_\beta; 1, i_\gamma | I, (1-i_\alpha)\rangle\,, \tag{7.47}$$

with $\alpha\beta\gamma = (123), (231), (312)$. The amplitude for K^+ decaying into a dimer and a pion can be expressed as

$$\mathcal{A}(K^+ \to T_{I,(1-i_\alpha)}\pi^{i_\alpha}) = \sum_J \langle I, (1-i_\alpha); 1, i_\alpha | J, 1\rangle \left(g^{(J,I)}\tau_I + \sum_{I'} \tau_I \Phi_{J;II'} g^{(J,I')} \right). \tag{7.48}$$

where the amplitude Φ in the CM frame is defined as

$$\Phi_{J;II'}(\mathbf{p}) = \int^\Lambda \frac{d^3\mathbf{q}}{(2\pi)^3 2w(\mathbf{q})} \mathcal{M}_{J;II'}(\mathbf{p}, \mathbf{q}; E)\tau_{I'}(\mathbf{q}; E)\,, \tag{7.49}$$

where $\tau_{I'}(\mathbf{q}; E)$ stands for $\tau_{I'}((P-q)^2)$ with $P^\mu = (E, \mathbf{0})$ and $q^\mu = (\sqrt{M_\pi^2 + \mathbf{q}^2}, \mathbf{q})$. From the Faddeev equation for the particle-dimer scattering amplitude (7.27), the equation for the amplitude Φ

can be derived:

$$\Phi_{J;II'}(\mathbf{p}) = \sum_{I''} \int^{\Lambda} \frac{d^3\mathbf{q}}{(2\pi)^3 2w(\mathbf{q})} Z_{J;II''}(\mathbf{p},\mathbf{q};E)\tau_{I''}(\mathbf{q};E)\Big(\delta_{I''I'} + \Phi_{J;I''I'}(\mathbf{q})\Big), \tag{7.50}$$

Using Eqs. (7.47), (7.48) and performing the projection onto the S-wave, for the charged ("c") and the neutral ("n") channels we obtain

$$\begin{pmatrix} \langle \pi^+(p_1)\pi^+(p_2)\pi^-(p_3)|K^+\rangle \\ \langle \pi^0(p_1)\pi^0(p_2)\pi^+(p_3)|K^+\rangle \end{pmatrix} = \begin{pmatrix} X_{c0} & X_{c2} \\ X_{n0} & X_{n2} \end{pmatrix} \begin{pmatrix} g^{(1,0)} \\ g^{(3,2)} \end{pmatrix}, \tag{7.51}$$

where we took into account the constraints $g^{(1,2)} = 3g^{(3,2)}$ and $g^{(2,2)} = \sqrt{5}g^{(3,2)}$ already. The entries of the matrix X are:

$$\begin{aligned}
X_{c0} =& \frac{\tau_0(p_1)}{\sqrt{3}}\left[1 + \Phi_{1;00}(p_1)\right] + \frac{\tau_2(p_1)}{2\sqrt{15}}\Phi_{1;20}(p_1) + (p_1 \to p_2) + \frac{3\tau_2(p_3)}{\sqrt{15}}\Phi_{1;20}(p_3), \\
X_{c2} =& \sqrt{3}\tau_0(p_1)\Phi_{1;02}(p_1) + \sqrt{\frac{3}{20}}\tau_2(p_1)\left[\frac{5}{3} + \Phi_{1;22}(p_1) + \frac{2}{3}\Phi_{3;22}(p_1)\right] + (p_1 \to p_2) \\
&+ \sqrt{15}\tau_2(p_3)\left[\frac{2}{3} + \frac{3}{5}\Phi_{1;22}(p_3) + \frac{1}{15}\Phi_{3;22}(p_3)\right], \\
X_{n0} =& -\frac{3\tau_2(p_1)}{2\sqrt{15}}\Phi_{1;20}(p_1) + (p_1 \to p_2) - \frac{\tau_0(p_3)}{\sqrt{3}}\left[1 + \Phi_{1;00}(p_3)\right] + \frac{\tau_2(p_3)}{\sqrt{15}}\Phi_{1;20}(p_3), \\
X_{n2} =& -\sqrt{\frac{27}{20}}\tau_2(p_1)\left[\frac{5}{9} + \Phi_{1;22}(p_1) - \frac{4}{9}\Phi_{3;22}(p_1)\right] + (p_1 \to p_2) \\
&- \sqrt{3}\tau_0(p_3)\Phi_{1;02}(p_3) + \sqrt{\frac{3}{5}}\tau_2(p_3)\left[\frac{5}{3} + \Phi_{1;22}(p_3) + \frac{2}{3}\Phi_{3;22}(p_3)\right].
\end{aligned} \tag{7.52}$$

Note also that we denote $p_i = |\mathbf{p}_i|$.

In a finite volume, our aim is to compute the matrix element $\langle \Gamma n, J|K^+\rangle$. Here, $\langle \Gamma n, J|$ refers to the state on the lattice, carrying total isospin J, total momentum $\mathbf{d}$ (in units of $2\pi/L$), and residing in the irrep Γ, corresponding to the n-th energy level[12] This matrix element can be calculated using the wave function in a finite volume [101]:

$$\langle \Gamma n, J|K^+\rangle = \frac{1}{L^{3/2}} \left(\frac{M_K}{\sqrt{M_K^2 + \left(\frac{2\pi\mathbf{d}}{L}\right)^2}} \right)^{1/2} \sum_I \frac{1}{L^3} \sum_{\mathbf{k}}^{\Lambda_\nu} \frac{1}{2w(\mathbf{k})} \phi^{(n)}_{J;I}(\mathbf{k}) \tau^L_I(\mathbf{k};E) g^{(J,I)}. \tag{7.53}$$

Here, $\phi^{(n)}_{J;I}(\mathbf{k})$ represents the Bethe-Salpeter wave function describing the state $|\Gamma n, J\rangle$, Furthermore,

[12] Here, the size of the lattice is L. This parameter should be adjusted so that the energy E_n exactly equals to M_K. The label n is used for different eigenvalues. In order to avoid the clutter of indices, we have opted for lumping the irrep index Γ, as well as the total momentum $\mathbf{d}$ together with the level index n and hope that this will not lead to a confusion.

$\mathbf{k}$ is the momentum of the spectator, and I is the isospin of the dimer, Λ_v means that cutoff on $\mathbf{k}$ is imposed in a moving system with velocity v [81]. To calculate the wave function $\phi_{JI}^{(n)}(\mathbf{k})$, we first project the Faddeev equation onto irreps Γ, i.e.,

$$\begin{aligned}\mathcal{M}_{J;II'}^{(\Gamma)}(r,r') &= Z_{J;II'}^{(\Gamma)}(r,r') \\ &+ \sum_{I''}\frac{1}{GL^3}\sum_{s}^{\Lambda_v}\left(\frac{\vartheta_s}{2w_s}\right) Z_{J;II'}^{(\Gamma)}(r,s)\tau_{I''}^{L}(s)\mathcal{M}_{J;I''I'}^{(\Gamma)}(s,r')\,. \end{aligned} \tag{7.54}$$

In the projected equation, the momenta of the spectator particles are replaced by shell indices r, r' and s. We use ϑ_s to represent the multiplicity of the shell s, while G denotes the number of elements in the discrete symmetry group that leaves the total three-momentum of the system invariant. The projection of τ and Z is performed, according to the method of Ref. [177]

$$\tau^L(s) = \tau^L(\mathbf{k}_0(s)), \quad Z_{J;II'}^{(\Gamma)}(r,s) = \sum_{g\in\mathcal{G}}\left(T^{(\Gamma)}(g)\right)^{\dagger} Z_{J;II'}(g\mathbf{p}_0(r),\mathbf{k}_0(s)). \tag{7.55}$$

Here $T^{(\Gamma)}(g)$ is the representation matrix and the momenta $\mathbf{p}_0(r)$ and $\mathbf{k}_0(s)$ are the reference vectors of the r-shell and the s-shell, respectively. Based on this, it is not difficult to deduce that the wave function is a solution to the homogeneous equation,

$$\phi_{J;I}^{(n)}(r) = \sum_{I'}\frac{1}{GL^3}\sum_{s}\left(\frac{\vartheta_s}{2w_s}\right) Z_{J;II'}^{(\Gamma)}(r,s)\tau_{I'}^{L}(s)\phi_{J;I'}^{(n)}(s)\,. \tag{7.56}$$

The solutions of the equation should be normalized, according to [101]

$$\begin{aligned}&\sum_{r,s}\sum_{I,I'}\frac{\vartheta_r}{2w_rL^3}\frac{\vartheta_s}{2w_sL^3}\phi_{JI}^{(n)}(r)\tau_I^L(r)\mathbb{P}_{J;II'}(r,s)\tau_{I'}^L(s)\phi_{JI'}^{(n)}(s) \\ &-\sum_{r}\sum_{I}\frac{\vartheta_r}{2w_rL^3}\phi_{JI}^{(n)}(r)\tau_I^L(r)\mathbb{Q}_I(r)\tau_I^L(r)\phi_{JI}^{(n)}(r) = 1. \end{aligned} \tag{7.57}$$

Here

$$\mathbb{P}_{J;II'}(r,s) = \frac{\partial}{\partial P_{\parallel}}Z_{J;II'}^{\Gamma}(r,s)\,, \qquad \mathbb{Q}_I(r) = \frac{\partial}{\partial P_{\parallel}}\left(\tau_I^L(r)\right)^{-1}. \tag{7.58}$$

The time-like component $P_{\parallel}$ is obtained from total four-momentum P^{μ}:

$$P_{\parallel} = v\cdot P = \sqrt{P^2}. \tag{7.59}$$

Similar to the infinite-volume case, we can define the finite-volume amplitude Φ:

$$\Phi_{J;I}^{(n)} = \frac{1}{L^3}\sum_{\mathbf{k}}^{\Lambda_v}\frac{1}{2w(\mathbf{k})}\phi_{J;I}^{(n)}(\mathbf{k})\tau_I^L(\mathbf{k};E) = \frac{1}{L^3}\sum_{r}^{\Lambda_v}\left(\frac{\vartheta_r}{2w_r}\right)\phi_{J;I}^{(n)}(r)\tau_I^L(r)\,. \tag{7.60}$$

Therefore, we have

$$\langle \Gamma n, J|K^+\rangle = \frac{1}{L^{3/2}} \left(\frac{M_K}{\sqrt{M_K^2 + \left(\frac{2\pi \mathbf{d}}{L}\right)^2}} \right)^{1/2} \sum_I \Phi^{(n)}_{J;I} g^{(J,I)} \,. \tag{7.61}$$

Finally, one obtains:

$$\begin{pmatrix} L^{3/2}\langle \Gamma n, 1|K^+\rangle \\ L^{3/2}\langle \Gamma n, 3|K^+\rangle \end{pmatrix} = \begin{pmatrix} A_{10} & A_{12} \\ A_{30} & A_{32} \end{pmatrix} \begin{pmatrix} g^{(1,0)} \\ g^{(3,2)} \end{pmatrix}. \tag{7.62}$$

Here, matrix element A_{JI} is given by

$$A_{JI} = \left(\frac{M_K}{\sqrt{M_K^2 + \left(\frac{2\pi \mathbf{d}}{L}\right)^2}} \right)^{1/2} a_{JI} \Phi^{(n)}_{J;I} \,, \tag{7.63}$$

and the coefficients a_{JI} are

$$a_{10} = 1, \quad a_{12} = 3, \quad a_{30} = 0, \quad a_{32} = 1. \tag{7.64}$$

The decay amplitudes both in a finite and in the infinite volume are expressed through the same couplings $g^{(1,0)}$ and $g^{(3,2)}$, see Eqs. (7.51) and (7.62). Excluding these couplings, we obtain the LL factor for $K \to 3\pi$ which, in this case, is a 2×2 matrix:

$$\begin{pmatrix} \langle \pi^+\pi^+\pi^-|K^+\rangle \\ \langle \pi^0\pi^0\pi^+|K^+\rangle \end{pmatrix} = \begin{pmatrix} \mathbb{L}_{c1} & \mathbb{L}_{c3} \\ \mathbb{L}_{n1} & \mathbb{L}_{n3} \end{pmatrix} \begin{pmatrix} L^{3/2}\langle \Gamma n, 1|K^+\rangle \\ L^{3/2}\langle \Gamma n, 3|K^+\rangle \end{pmatrix}, \tag{7.65}$$

where

$$\begin{pmatrix} \mathbb{L}_{c1} & \mathbb{L}_{c3} \\ \mathbb{L}_{n1} & \mathbb{L}_{n3} \end{pmatrix} = \begin{pmatrix} X_{c0} & X_{c2} \\ X_{n0} & X_{n2} \end{pmatrix} \begin{pmatrix} A_{10} & A_{12} \\ A_{30} & A_{32} \end{pmatrix}^{-1} . \tag{7.66}$$

The explicit expression for the 3-particle LL factor, given by the above formulae, represents one of the main results of the present work.

7.4 Numerical Calculation of LL Factor

7.4.1 Solution of the Faddeev Equation in the Infinite Volume

In order to solve Eq. (7.50) in the infinite volume, we need to first study the analytic properties of the kernel. For simplicity, we restrict ourselves to the CM system and use the notation $p = |\mathbf{p}|$, $q = |\mathbf{q}|$

and $z = \cos\theta$, where θ is the angle between $\mathbf{p}$ and $\mathbf{q}$. It is straightforwardly seen that the singularity of $Z(\mathbf{p}, \mathbf{q}; E)$ is determined by the three-body on-shell condition[13],

$$\sqrt{p^2 + q^2 + 2pqz + M_\pi^2} + \sqrt{p^2 + M_\pi^2} + \sqrt{q^2 + M_\pi^2} = E, \tag{7.67}$$

with $-1 \leq z \leq 1$. As known [80, 239, 300, 301], one can avoid these (logarithmic) singularities by deforming the contour into the complex plane (see Fig. 7.7(a)). In our case, the contour can be chosen as follows,

$$q = \begin{cases} t - i\mu(1 - e^{-t/\sigma})(1 - e^{(t - B_{\max})/\sigma}), & (0 < t < B_{\max}) \\ t, & (B_{\max} < t < \Lambda) \end{cases} \tag{7.68}$$

where the parameters are

$$\delta = 0.5 M_\pi,\ \sigma = M_\pi,\ \mu = 0.1 M_\pi,\ B_{\max} = p_t + \delta. \tag{7.69}$$

Here p_t is the magnitude of the momentum of the spectator, for which the two-body system is exactly at threshold. If $|\mathbf{p}| > p_t$, the two-body system moves below threshold. This gives

$$(E - w(\mathbf{p}))^2 - \mathbf{p}^2 \leq 4M_\pi^2, \tag{7.70}$$

and

$$p \geq \sqrt{\left(\frac{E^2 - 3M_\pi^2}{2E}\right)^2 - M_\pi^2} = p_t. \tag{7.71}$$

The solution of the equation (7.50) proceeds step by step. First, after projecting onto the S-wave, one solves this equation with both the momenta p and q belonging to the contour C:

$$\Phi_{J;II'}(p) = \sum_{I''} \int_C \frac{q^2 dq}{2\pi^2 2w(q)} Z_{J;II''}(p, q; E) \tau_{I''}(q; E) \left(\delta_{I''I'} + \Phi_{J;I''I'}(q)\right). \tag{7.72}$$

The integrand is never singular on the integration contour C. This can be visualized in Fig. 7.7(a), where the shaded area is obtained as follows. The total energy $E = M_K$ is fixed. We first choose the momentum p on the contour and plot the curve for q, obtained by the solution of Eq. (7.67) for $-1 \leq z \leq 1$. Changing then p with a very small step along the contour, we arrive at a new curve. Repeating this procedure many times, we arrive at a shaded area that does not intersect with our integration curve. Hence, for p and q both on the curve, the kernel Z never becomes singular, and the integral equation can be straightforwardly transformed into a set of linear equations by discretizing the integration with the use of the fixed mesh points and weights. We are ultimately interested, however, in the amplitude $\Phi_{J;II'}(p)$ on the real axis, which can be obtained by analytically continuing $\Phi_{J;II'}(p)$, defined by the Eq. (7.72) to the real axis, whereas the argument q, over which the integration is performed, still stays on the the contour C. In doing so, it is important to check that one does not hit the singularities of the kernel Z during this analytic continuation. Below, we shall address this issue

[13] In principle, the dimer propagator τ_L also has singularities, but they are irrelevant to our calculation.

in detail.

Let us define the quantity

$$p_0 \equiv \sqrt{\left(\frac{E - M_\pi}{2}\right)^2 - M_\pi^2} \tag{7.73}$$

It turns out that there are three different regions of p [301, 302]:

1. When $p < p_0$, the singularities of $Z(p, q; E)$ lie just above and below the real axis,[14] see Fig. 7.7(b). Our contour does not intersect with any of these branch cuts and the integration can be safely performed.

2. For $p_0 < p < p_t$, The branch cuts move into the complex plane and start to intersect with the chosen contour, see Fig. 7.7(c). In order to avoid the singularities, one has to deform the integration contour as well. The new contour, C^+, consists of two parts:

   Part 1: Starting from the origin, it follows the positive real axis until the beginning of the branch cut located at the first singularity of the kernel at $q = q_1$, where q_1 is given by

   $$q_1 = \frac{p}{2} - \frac{\varepsilon(p)}{2}\left(1 - \frac{4M_\pi^2}{\varepsilon^2(p) - p^2}\right)^{1/2}, \qquad \varepsilon(p) = E - w(p)\,. \tag{7.74}$$

   After reaching q_1, the contour dives to the second Riemann sheet and goes back to the origin along the real axis. The contribution of this part to the integral is given by

   $$\begin{aligned}
   &\Phi^{(1)}_{J;II'}(p) \\
   &= \sum_{I''}\left(\int_{0+i\varepsilon}^{q_1+i\varepsilon} + \int_{q_1-i\varepsilon}^{0-i\varepsilon}\right)\frac{q^2 dq}{2\pi^2 2w(q)} Z_{J;II''}(p, q; E)\tau_{I''}(q; E)\Big(\delta_{I''I'} + \Phi_{J;I''I'}(q)\Big) \\
   &= \sum_{I''}\int_0^{q_1}\frac{q^2 dq}{2\pi^2 2w(q)}\Big[Z_{J;II''}(p, q; E) - Z^{(\mathrm{II})}_{J;II''}(p, q; E)\Big]\tau_{I''}(q; E)\Big(\delta_{I''I'} + \Phi_{J;I''I'}(q)\Big).
   \end{aligned} \tag{7.75}$$

   The kernel $Z_{J,II'}$, projected on any partial-wave, is expressed through a logarithmic function. Since the discontinuity is caused solely by this logarithm, we conclude that the kernel on the second Riemann sheet, $Z^{(\mathrm{II})}$ is obtained from Z by replacing the $\log z$ with $\log z + 2\pi i$. Furthermore, since $q_1 < p_0$, the function $\Phi(q)$ is known along the real axis and the integral is completely defined.

   Part 2: The second part of the path starts from the origin of the second Riemann sheet, following path C to reach the intersection point q_2 with the branch cut. Returning through q_2 to the first

[14] Remember that the energy E has infinitesimal positive imaginary part.

Riemann sheet, it continues along path C to reach the integration endpoint Λ, that is

$$\begin{aligned}\Phi^{(2)}_{J;II'}(p) &= \sum_{I''}\int_0^{q_2}\frac{q^2dq}{2\pi^2 2w(q)}Z^{(\mathrm{II})}_{J;II''}(p,q;E)\tau_{I''}(q;E)\Big(\delta_{I''I'}+\Phi_{J;I''I'}(q)\Big)\\ &+\sum_{I''}\int_{q_2}^{\Lambda}\frac{q^2dq}{2\pi^2 2w(q)}Z_{J;II''}(p,q;E)\tau_{I''}(q;E)\Big(\delta_{I''I'}+\Phi_{J;I''I'}(q)\Big)\\ &=\sum_{I''}\int_C\frac{q^2dq}{2\pi^2 2w(q)}\tilde{Z}_{J;II''}(p,q;E)\tau_{I''}(q;E)\Big(\delta_{I''I'}+\Phi_{J;I''I'}(q)\Big)\,. \end{aligned}\tag{7.76}$$

The quantity $\tilde{Z}$ is defined in the following way:

$$\tilde{Z}_{J;II'}(p,q;E)=\begin{cases}Z^{(\mathrm{II})}_{J;II'}(p,q;E), & f(p,q;E)<0\\ Z_{J;II'}(p,q;E), & f(p,q;E)\geq 0\end{cases}.\tag{7.77}$$

Here, $f(p,q;E)$ is defined by

$$f(p,q;E)=\Big((\mathrm{Re}q)^2+(\mathrm{Im}q)^2\Big)^2+m^2(d^2(p)-b^2(p))\left(\frac{(\mathrm{Re}q)^2}{d^2(p)}+\frac{(\mathrm{Im}q)^2}{b^2(p)}\right),\tag{7.78}$$

with

$$b(p)=\frac{\varepsilon(p)}{p}\,,\qquad d(p)=\frac{\varepsilon^2(p)-p^2}{2mp}.\tag{7.79}$$

Finally, in the region $p_0<p<p_t$, the full amplitude is given by

$$\Phi_{J;II'}(p)=\Phi^{(1)}_{J;II'}(p)+\Phi^{(2)}_{J;II'}(p).\tag{7.80}$$

3. When $p>p_t$, the branch cuts of the function Z move into the complex plane and do not intersect with our contour C anymore,[15] see Fig. 7.7(d). Therefore, it is again safe to integrate over the initial contour.

By using the techniques described above, we can calculate the amplitudes $\Phi_{1;00}$, $\Phi_{1;02}$, $\Phi_{1;20}$, $\Phi_{1;22}$ and $\Phi_{3;22}$ on the real axis. These solutions are displayed in Fig. 7.9. We choose the cutoff $\Lambda=15M_\pi$ and matched the couplings $H_{1;00}$ and $H_{3;22}$ to the tree-level threshold amplitudes in ChPT as described above. Varying the cutoff, but keeping the threshold amplitude fixed, it can be shown that the three-body couplings exhibit singular behavior that resembles the log-periodic running in the unitary limit, see Fig. 7.8. Note also that the LL factor should be cutoff-independent that will be

[15] In principle, when $p>p_t$ but very close to p_t, the branch cut may still intersect with the contour. Strictly speaking, for any given $p>p_t$, one may choose the parameter μ small enough that there is no intersection. On the contrary, for any fixed finite μ, one may find an interval between p_t and $p_t+\varepsilon'$, when the branch cut and the contour intersect. The quantity ε' depends on μ and tends to zero at $\mu\to 0$. In practical terms, it means that one is not able to determine the solution for $p\in[p_t,p_t+\varepsilon']$ by using the method described here. The length of this interval can be however made arbitrary small with the choice of μ. This does not create problems in actual calculations, while ε' turns out to be extremely small.

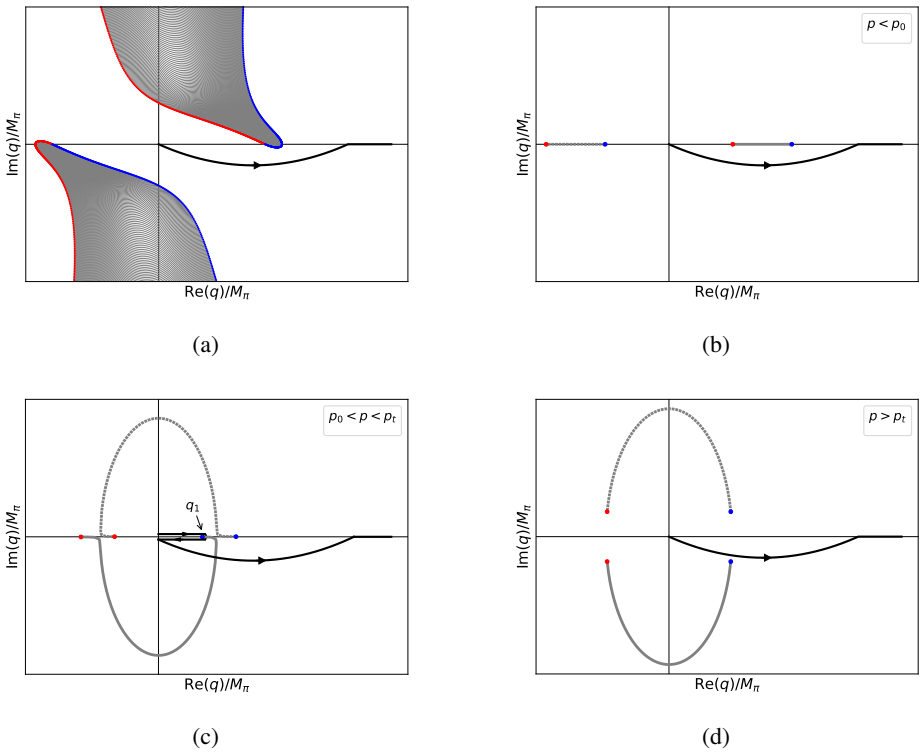

Figure 7.7: In panel (a), the contour and the domain of the singularity of the kernel Z is shown. It is clear that, when both momenta are located on the deformed contour, the kernel does not become singular. In the panels (b,c,d), the choice of the integration contour for the calculation of the amplitude Φ on the real axis is displayed for three different choices, $p < p_0$, $p_0 < p < p_t$, and $p > p_t$, respectively. In the second case, the path should be deformed from the original one, in order to avoid the singularities of the kernel (see the discussion in the text).

explicitly demonstrated below.

Next, in order to estimate the dependence on the kinematical variables, we shall calculate the quantities X_{c0}, X_{c2}, X_{n0} and X_{n2}, defined by Eq. (7.52), which enter the expression of the LL factor. In the CM frame, the total energy is fixed to be the mass of the kaon, i.e., $E = M_K \simeq 3.54 M_\pi$. These quantities depend on the momenta of outgoing pions that can be parameterized by two invariant variables $m_{12}^2 = (p_1 + p_2)^2$ and $m_{23}^2 = (p_2 + p_3)^2$. In Fig. 7.10, we display the Dalitz plots for the quantities X_{c0}, X_{c2}, X_{n0}, X_{n2} that emerge in a result of such calculations.

7.4.2 Finite-Volume Wave Function

In order to calculate Φ in a finite volume, we first need to adjust the lattice size L so that one has the energy level with the energy exactly equal to the kaon mass. Solving the three-body quantization condition in the rest frame and in the different moving frames, we obtain the energy spectrum, see Fig. 7.11 and Fig. 7.12. For demonstration, we choose the moving frame with the total momentum $(0, 0, 1)$ (in units of $2\pi/L$). In the channels with the total isospin $J = 1$ and $J = 3$, respectively, the

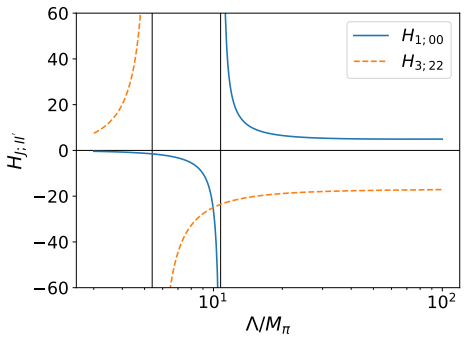

Figure 7.8: The running of the three-body couplings $H_{1;00}$ and $H_{3;22}$ with respect to the cutoff Λ.

adjusted lattice size is given by

$$J = 1: \quad L = 3.55 M_\pi^{-1}; \tag{7.81}$$

$$J = 3: \quad L = 4.09 M_\pi^{-1}. \tag{7.82}$$

Once the lattice size is determined, we proceed to solve the Eq. (7.56) in order to obtain the (properly normalized) wave function in a finite volume. In its turn, this wave function will be substituted into Eq. (7.60) to find the amplitudes $\Phi_{J;I}^{(n)}$ that enter the expression of the LL factor, see Eq. (7.63).

7.4.3 The LL Factor

Putting pieces together, in this section we present the results of the calculation of the LL factor, check its cutoff-dependence and the sensitivity to the input two-body scattering lengths and the three-particle amplitudes. To this end, we shall carry out calculations for three different values of the cutoff. Furthermore, the LL factor depends on the momenta of the final pions. We carry our calculations at an arbitrary chosen point near the center of the Dalitz plot $m_{12}^2 = m_{23}^2 = 5M_\pi^2$.

The Fig. 7.13 summarizes our findings. First, Fig. 7.13(a) shows the calculated LL factor for different values of the cutoff $\Lambda = 15M_\pi, 20M_\pi, 25M_\pi$. The difference is hardly seen by a bare eye, confirming our expectations. Next, in Fig. 7.13(b), we show the results of calculations for varying three-particle threshold amplitudes by 300%, namely, for pairs (T_+^χ, T_0^χ), and $(T_+^\chi \pm 3\times T_+^\chi, T_0^\chi \pm 3\times T_0^\chi)$. The cutoff is fixed at $\Lambda = 15M_\pi$. Again, the differences are small. Finally, in Fig. 7.13(c), we show the result of variation of scattering lengths by 30% only, for the pairs (a_0, a_2) and $(a_0 \pm 0.3\times a_0, a_2 \pm 0.3\times a_2)$, with the three-body input (T_+^χ, T_0^χ) and the cutoff $\Lambda = 15M_\pi$ fixed. Now, the changes are sizable (despite the fact that the changes in the scattering lengths are factor 10 smaller than the changes in the three-body amplitudes), proving that the LL factor is much more sensitive to the two-body input than the three-body threshold amplitudes. This result constitutes the major finding of the present chapter.

It is extremely important to understand the reason of such a behavior. Naively, according to the NREFT counting introduced in Sect. 7.2.1, the exchange term in the kernel Z and the particle-dimer coupling count as $O(\delta^{-2})$ and $O(1)$, respectively. This counting, however, is known not to be valid non-perturbatively [134, 214]. Namely, the particle-dimer coupling should be promoted to the leading order to cope with the singular dependence of the solutions on the cutoff. Hence, the power-counting

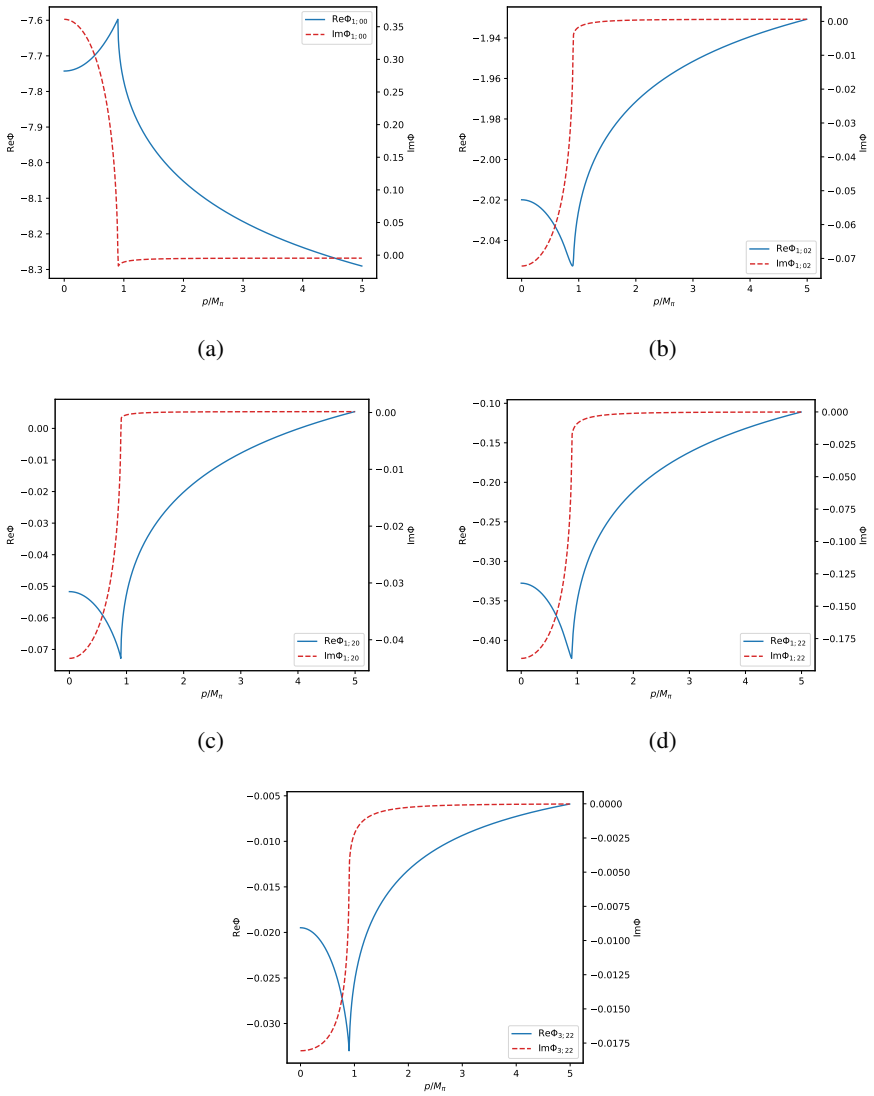

Figure 7.9: The solutions of Eq. (7.50), $\Phi_{1;00}$, $\Phi_{1;02}$, $\Phi_{1;20}$, $\Phi_{1;22}$ and $\Phi_{3;22}$. The blue solid line and the red dashed line represent the real and imaginary parts, respectively. The cutoff $\Lambda = 15M_\pi$ was chosen.

arguments cannot directly explain a very little sensitivity of the calculated LL factor on the three-body input. In order to study this problem in more detail, we have carried out calculations for many different values of the cutoff Λ and noticed an interesting pattern: as soon as Λ came close to the critical values where the particle-dimer coupling becomes critical and flips the sign, the dependence on the three-body input grows and becomes comparable with the dependence on the values of the two-body scattering lengths, whereas away from the critical cutoffs, the dependence on the three-body input was negligible. On the basis of this observation one may argue that the formal promotion of the particle-dimer coupling to the leading order is essential in the vicinity of critical cutoffs, whereas for

other values of the cutoff the arguments based on the naive counting still apply, for what concerns the numerical estimate of the relative size of different contributions. This observation also shows the importance of a proper choice of cutoff in the calculations (away from singularities), albeit the results are formally cutoff-independent.

7.4.4 The Weak Hamiltonian

Up to now, in the derivation of the LL factor, we did not concentrate on the weak input in the $K \to 3\pi$ decays. In other words, the couplings G_1 and G_2 are taken to be completely arbitrary. In Nature, however, these couplings are subject to further restrictions. Namely, at the lowest order in the Fermi-constant G_F, the weak decays are described by the effective weak Hamiltonian that contains $\Delta I = 1/2$ and $\Delta I = 3/2$ pieces, see e.g., [303]. Assuming conservation of isospin in strong interaction, one immediately arrives at the conclusion that the total isospin $J = 3$ decay amplitude should vanish (in real world, it is strongly suppressed by one power of G_F or isospin-breaking parameters: the fine structure constant α or $m_d - m_u$).

In order to see the consequences of this fact on the relative size of the couplings G_1 and G_2, let us explicitly write down the vectors $|J, J_3\rangle$ with $J = 1, 2, 3$ and $J_3 = 1$ in the three-pion space:

$$
\begin{aligned}
|1,1\rangle^{(1)} &= \frac{1}{2}\left(|\pi^+\pi^0\pi^0\rangle - |\pi^0\pi^+\pi^0\rangle - |\pi^+\pi^-\pi^+\rangle + |\pi^-\pi^+\pi^+\rangle\right), \\
|1,1\rangle^{(2)} &= \frac{1}{\sqrt{3}}\left(|\pi^+\pi^-\pi^+\rangle - |\pi^0\pi^0\pi^+\rangle + |\pi^-\pi^+\pi^+\rangle\right), \\
|1,1\rangle^{(3)} &= \frac{2}{\sqrt{15}}\left(6|\pi^+\pi^+\pi^-\rangle + |\pi^+\pi^-\pi^+\rangle + |\pi^-\pi^+\pi^+\rangle\right. \\
&\quad \left. -3|\pi^0\pi^0\pi^+\rangle - 3|\pi^+\pi^0\pi^0\rangle + 2|\pi^0\pi^+\pi^0\rangle\right), \\
|2,1\rangle^{(1)} &= \frac{1}{2}\left(|\pi^+\pi^0\pi^0\rangle - |\pi^0\pi^+\pi^0\rangle + |\pi^+\pi^-\pi^+\rangle - |\pi^-\pi^+\pi^+\rangle\right), \\
|2,1\rangle^{(2)} &= \frac{1}{2\sqrt{3}}\left(2|\pi^+\pi^+\pi^-\rangle - |\pi^+\pi^-\pi^+\rangle - |\pi^-\pi^+\pi^+\rangle\right. \\
&\quad \left. -2|\pi^0\pi^0\pi^+\rangle + |\pi^+\pi^0\pi^0\rangle + |\pi^0\pi^+\pi^0\rangle\right), \\
|3,1\rangle &= \frac{1}{\sqrt{15}}\left(|\pi^+\pi^+\pi^-\rangle + |\pi^+\pi^-\pi^+\rangle + |\pi^-\pi^+\pi^+\rangle\right. \\
&\quad \left. +2|\pi^0\pi^0\pi^+\rangle + 2|\pi^+\pi^0\pi^0\rangle + 2|\pi^0\pi^+\pi^0\rangle\right).
\end{aligned}
\tag{7.83}
$$

At threshold, when momenta of all particles exactly vanish, the positions of the pions in the vectors can be exchanged.[16] This leads to the fact that the vectors which are antisymmetric with respect to the exchange of any pair of pions, namely, $|1,1\rangle^{(1)}$, $|2,1\rangle^{(1)}$ and $|2,1\rangle^{(2)}$, vanish at threshold. From this, one can immediately conclude that the $J = 2$ amplitude does not contribute at threshold. Furthermore, it is straightforward to check that, at threshold, $|1,1\rangle^{(2)} = \frac{\sqrt{5}}{2}|1,1\rangle^{(3)}$. Reverting now Eq. (7.83), expressing the physical states $|\pi^0\pi^0\pi^+\rangle$ and $|\pi^+\pi^+\pi^-\rangle$ through the eigenstates of the total isospin and

[16] The threshold cannot be reached in physical decay process. However, one arrives at the same conclusion at the center of the Dalitz plot $m_{12}^2 = m_{23}^2 = m_{31}^2$.

dropping the contributions from $J = 2, 3$, we finally arrive at a simple relation at threshold:[17]

$$|\pi^+\pi^+\pi^-\rangle = -2|\pi^0\pi^0\pi^+\rangle\,. \tag{7.84}$$

Consequently, $G_2 = -2G_1$ at leading order.

It should be pointed out that our result is in agreement with the explicit calculation of this decay amplitude at next-to-leading order in ChPT [304]. As seen from Eq. (37) of that paper, our relation exactly holds (modulo the overall sign) for the amplitudes evaluated at the center of the Dalitz plot. Furthermore, the latest fit to the experimental data by NA48 collaboration yields the value $A_+ = 1.925 \pm 0.015$ for this ratio (see Ref. [218], Eqs. (3,4)), which is quite close to our value $A_+ = 2$ (the overall sign is undefined in this analysis). The small deviation is due to the contribution of the higher-order terms in the NREFT power counting. Note finally that the difference in sign is due to the use of a particular convention for the basis states in the irreducible representations of the isospin. We consistently use Condon-Shortley phase convention in our calculations.[18]

In conclusion, we wish to point out that the additional restriction $G_2 = -2G_1$ does not affect our calculations of the LL factor since the latter, by definition, does not depend on the weak interactions that lead to the decay. The restriction simply means that only two linear combinations of $\mathbb{L}_{c1}, \mathbb{L}_{c3}, \mathbb{L}_{n1}, \mathbb{L}_{n3}$ will be needed in the final result.

7.5 Conclusions

Below, the results of our findings are briefly summarized:

i) We have performed an explicit calculation of the LL factor in the $K \to 3\pi$ decays at the leading order. Albeit the general framework has been already set up [101, 102], an explicit numerical implementation of this framework is still a non-trivial exercise and represents a very useful endeavor on the way of the actual use of this framework in the analysis of the lattice QCD data. The message that we want to convey with this article, is clear: the framework for the calculation of the $K \to 3\pi$ decay amplitudes on the lattice is now ready. Moreover, higher-order terms can be systematically included in the expressions, when the accuracy of lattice data renders this inclusion necessary.

ii) From the problems to be addressed we would like to single out the issue of the renormalization of the solutions of the Faddeev equations and the matching to the threshold three-pion amplitudes. At the first glance, the number of independent couplings that are needed to render all particle-dimer scattering amplitudes cutoff-independent, exceeds the number of three-particle threshold amplitudes at our disposal. However, as shown, the particle-dimer amplitudes that may (potentially) still have the singular cutoff dependence, do not contribute to the physical decay processes and are therefore harmless.

iii) The main finding of the present chapter is the fact that the calculated LL factor has a very weak dependence on the input three-body threshold amplitudes, even if the latter change by a factor

[17] This relation directly follows from the last line in Eq. (7.83) and the symmetry of the states at threshold with respect to the permutation of the particles 1,2,3.

[18] Here it should be pointed out that in Eq. (2.7) of Ref. [305], which is consistent with [304], a convention different from the Condon-Shortley phase convention is used for the definition of the isospin eigenstates.

of 3 or so. This fact has a crucial importance for the future application of this framework in the studies of kaon decays on the lattice. Namely, one may, at the first stage, avoid extracting the three-pion coupling from lattice data and use instead the rough estimate, obtained from ChPT. From our findings we conclude that even an error of 100% in the threshold amplitudes does not lead to a significant effect in the calculated LL factor, provided the cutoff Λ is chosen away from the critical values.

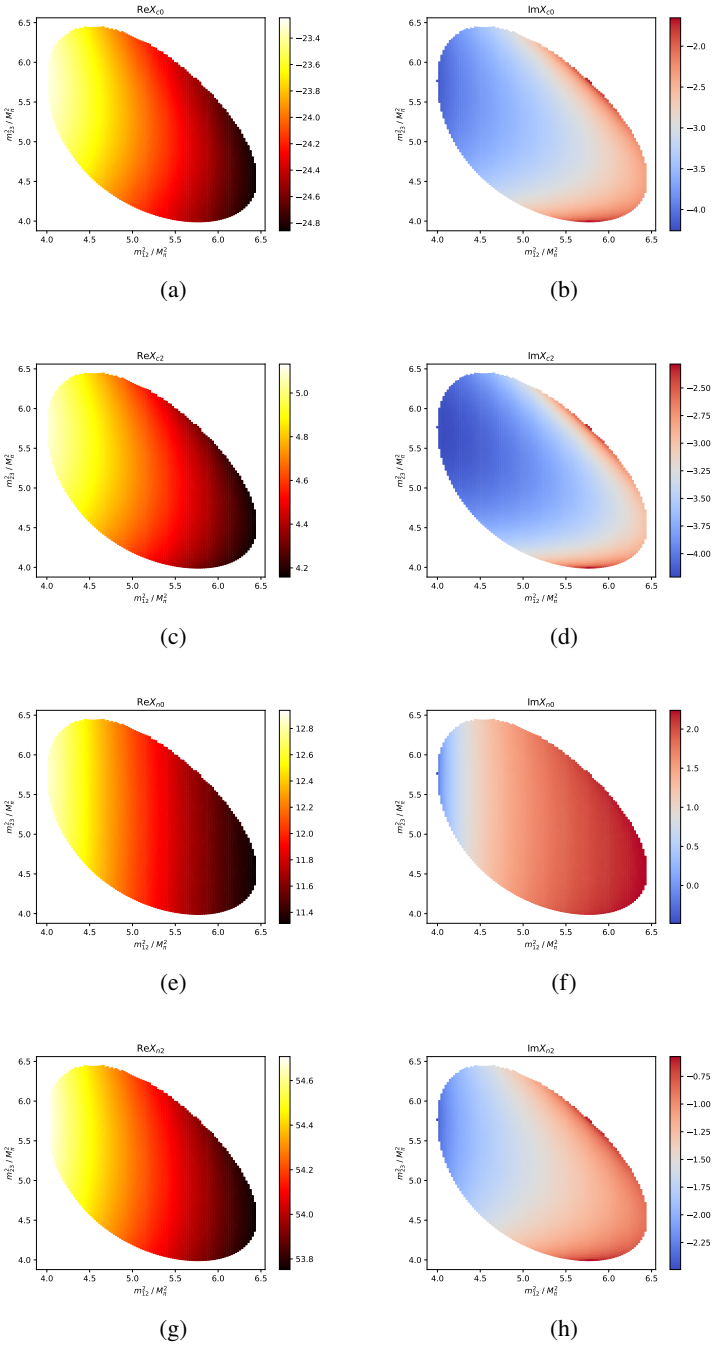

(a) (b)

(c) (d)

(e) (f)

(g) (h)

Figure 7.10: The real and imaginary parts of the quantities X_{c0}, X_{c2}, X_{n0} and X_{n2} in the m_{12}^2, m_{23}^2-plane. The cutoff $\Lambda = 15M_\pi$ is chosen.

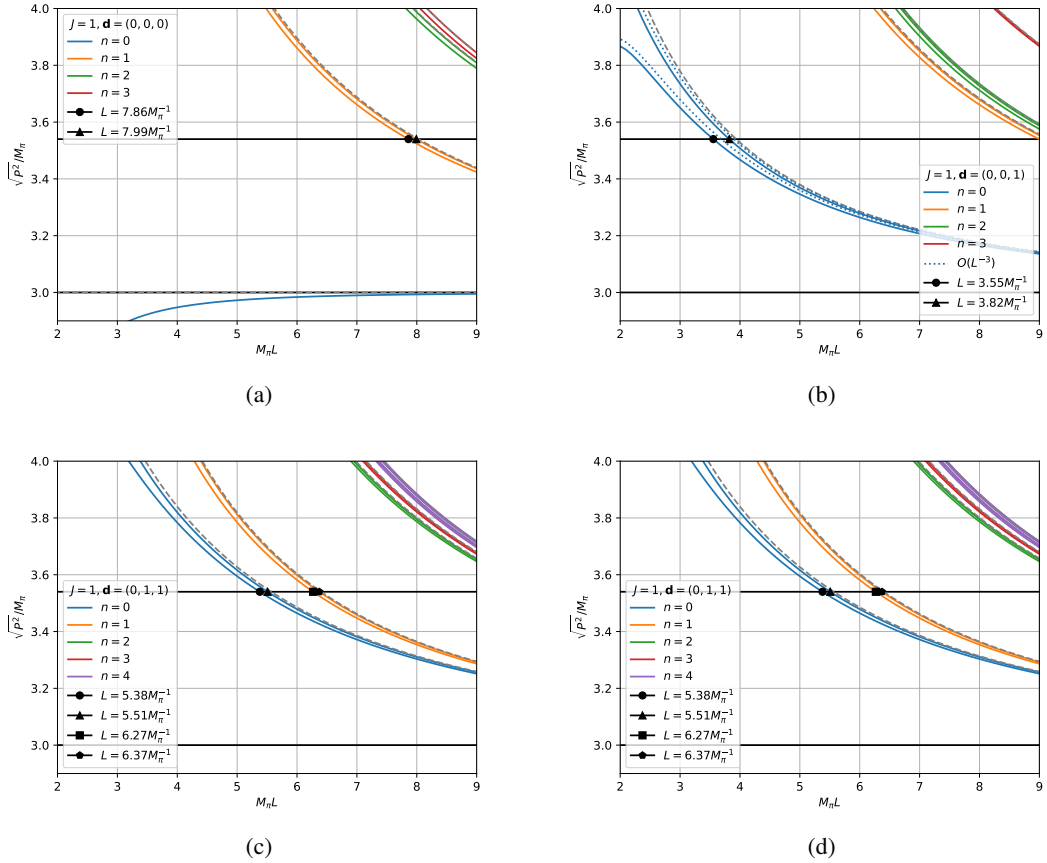

Figure 7.11: Finite-volume spectra of the 3π system with the total isospin $J = 3$. a) is obtained in the rest frame, irrep $\Gamma = A_1^-$. b), c), d) show the spectra in the moving frame $\mathbf{d} = (0, 0, 1)$, $\mathbf{d} = (0, 1, 1)$ and $\mathbf{d} = (1, 1, 1)$, respectively, in the irrep $\Gamma = A_2$ (the naming scheme of the irreps from Ref. [36] is used here). To compute the LL factor, we determine values of the lattice size L for which the invariant mass $\sqrt{P^2} = M_K$ (denoted by the solid black line around $\sqrt{P^2}/M_\pi \simeq 3.54$). In the subfigure b), we show perturbative energy shifts at $O(L^{-3})$ (see Eq. (A.68)). These are denoted by blue dotted lines and give a clear understanding of the fine structure of the spectrum, namely, the splitting of the unperturbed level into two levels, when the interactions are switched on.

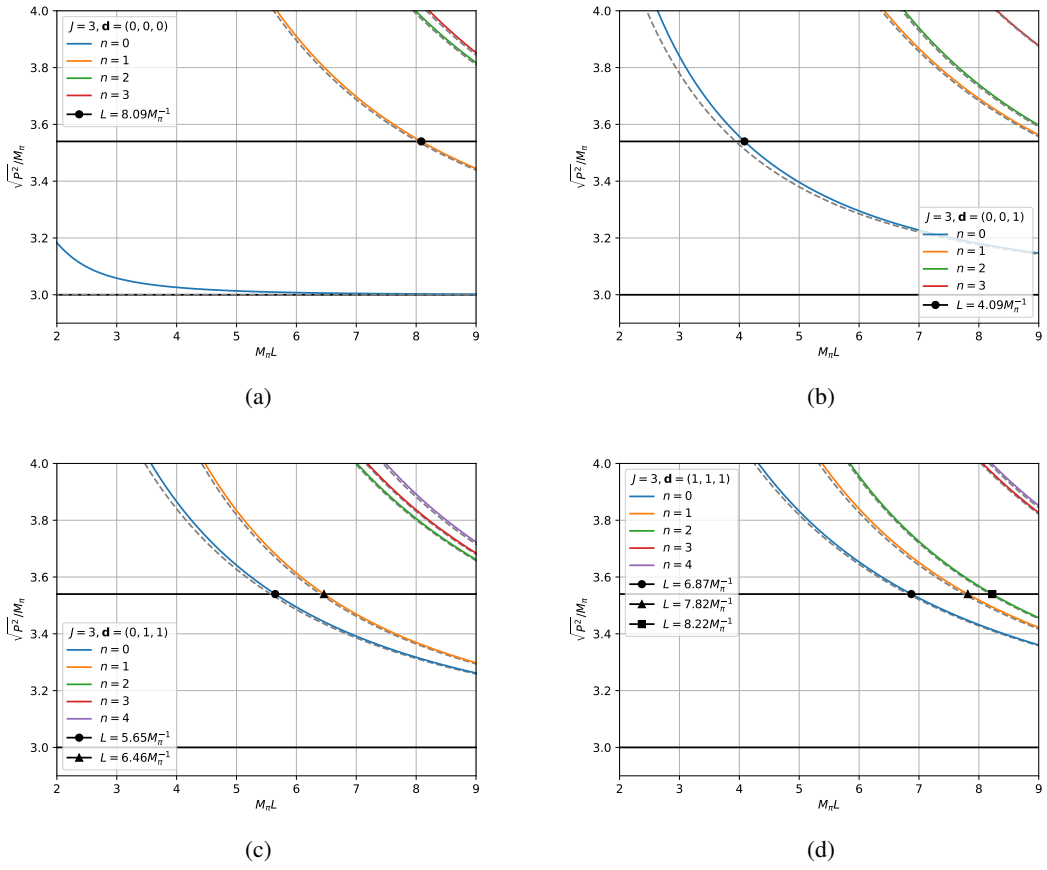

(a) (b)

(c) (d)

Figure 7.12: The same as in Fig. 7.11, but for the total isospin $J = 3$.

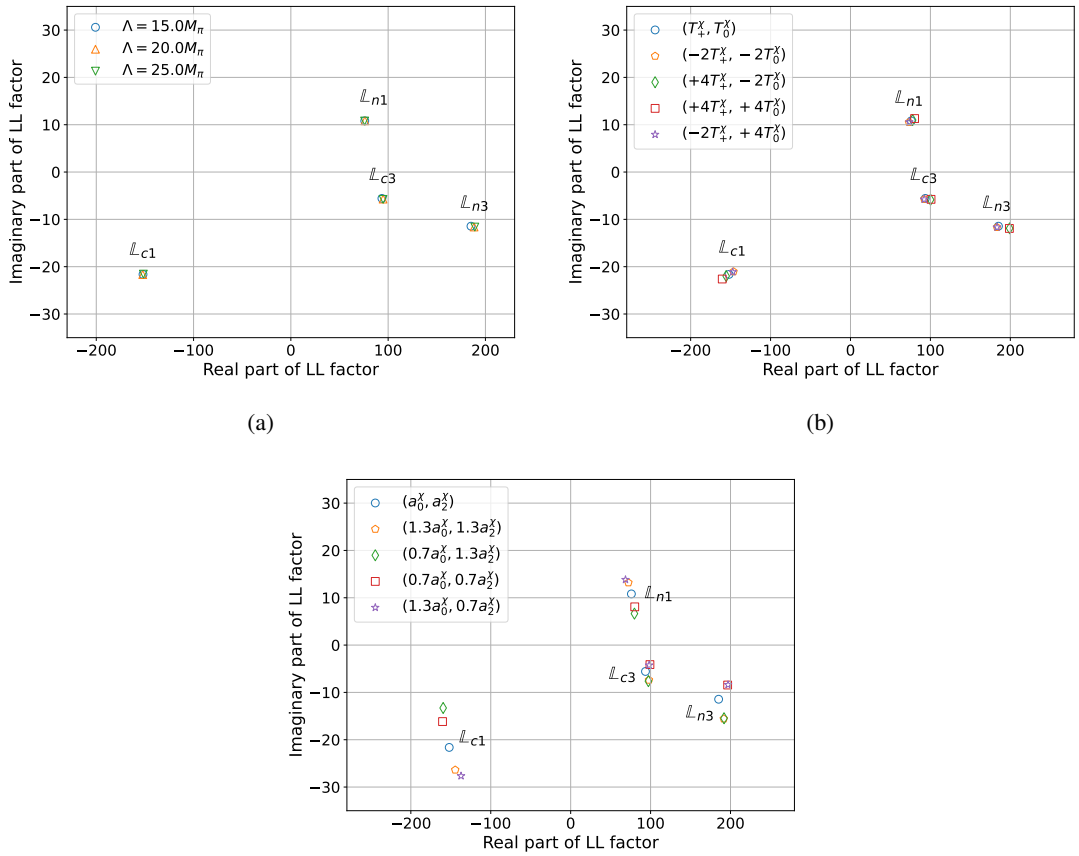

Figure 7.13: a) The cutoff independence of the LL factor. Here, the physical two-body scattering lengths are used and the three-body threshold amplitudes are fixed at (T_+^χ, T_0^χ). The quantities $\mathbb{L}_{c1}$, $\mathbb{L}_{c3}$, $\mathbb{L}_{n1}$ and $\mathbb{L}_{n3}$ are obtained for three different cutoff values: $\Lambda = 15M_\pi, 20M_\pi, 25M_\pi$, represented by blue circles, brown triangles, and green inverted triangles, respectively. In b) and c), the dependence of the LL factor on the three-pion threshold amplitude and two-pion scattering lengths are illustrated.

CHAPTER 8

Summary and Outlook

Quantum Chromodynamics provides one with a fundamental theory for studying strong interactions of hadrons and other particles. However, due to the non-perturbative nature of the strong interaction coupling constant at low energies, a non-perturbative approach needs to be employed. The most successful and popular among these is Lattice QCD, which provides an ab-initio method for solving QCD in this non-perturbative regime. Simulations are performed on a finite-volume lattice and physical observables are then extracted from the energy spectra obtained from these simulations. Over the years many formalism have been developed for extraction of observables from the lattice data. Even though a perturbative analysis of the finite-volume energy spectrum can yield S-matrix observables, such an approach fails to converge in the presence of bound states and resonances. Since these are important features of the hadronic spectra, a more general approach was developed by Lüscher. This method, termed as Lüscher's approach has become the go-to approach when it comes to extracting two-body scattering parameters from the lattice data.

However, with the increase in computation power available to lattice practitioners focus has shifted to more complicated two-body systems. The Lüscher equation is only applicable in the case of short-range interactions due to the constraints under which the equation is derived. Recently, systems such as the NN- and DD^*- systems have come under scrutiny. These system, in addition to the short-range interaction, involve long-range interaction due to the exchange of a light-particle. This leads to the partial-wave projected scattering amplitude developing a t-channel or a left-hand cut very close to the threshold. Analysis of energy levels in a finite volume in this region is not possible with the original Lüscher equation. Moreover, the presence of the long-range force results in a slow convergence of the partial-wave expansion. All of these issues have been discussed in literature and alternative approaches have been proposed.

One of the aims of this research project was to propose a modified Lüscher equation capable of analyzing the finite-volume energy levels in the t-channel cut region. This modified Lüscher equation was derived in Chap. 4. In the case considered here the effective-range expansion shows poor convergence and hence the modified effective-range expansion proposed in Ref. [64] was used. The MERE was recast into the language of NREFT both in the infinite volume and finite volume and a modified quantization condition was derived. This modified Lüscher equation contains the modified effective-range function which is a low-energy polynomial and can be expressed via the couplings of the short-range potential. Moreover, this quantization condition also contains the modified Lüscher function which only depends on the long-range potential. The essence of this approach lies in the fact

that the long-range potential is a well-known function and its parameters can be fit separately. Instead, one can separate out the effects of the long-range potential in the modified effective-range expansion in terms of explicitly calculable functions. With this, lattice data can be used to fit the parameters of the short-range potential.

Furthermore, this research project was also aimed at developing an efficient and accurate numerical algorithm to evaluate the modified Lüscher function and to solve the modified Lüscher equation. This numerical algorithm was detailed in Chap. 5. The modified Lüscher function is divergent and hence a renormalization prescription has to be imposed on it for numerical evaluation. Even though, one is free to choose any prescription as the final result should be independent of such choices, Pauli-Villars and cut-off regularization lead to numerical difficulties for higher partial-wave. Dimensional regularization was shown to be a good choice of renormalization prescription from a numerical point of view. Further the quantization condition was rewritten in a form suitable for numerical evaluation. Solving the quantization condition numerically, the energy levels obtained were verified by comparison to the exact finite-volume spectrum of the Hamiltonian. The loop function was also evaluated in the infinite volume employing dimensional regularization and the VEGAS algorithm. The modified effective-range function was shown to be real even below the t-channel cut making it applicable for extraction of scattering parameters even in this region. The two most important aspect of this numerical implementation are as follows. First, the convergence of the partial-wave expansion is very good in the case of the modified Lüscher equation as only the short-range potential is expanded in partial-waves. Second, exponentially suppressed corrections are small in the case of the modified Lüscher equation as the result matches very well with the finite-volume spectrum of the Hamiltonian. One of the main assumptions in the above formalism was that the long-range potential is perturbative and does not lead to bound states or resonances. The case where these conditions are not satisfied need to be investigated further. Moreover, moving frames and particle with spin should be considered in future works.

With the short-range interactions well understood in the two-body sector on lattice, a lot of progress has also been made in the three-body sector. Even though, perturbative calculation of finite-volume energy levels have been well known for quite some time their application was limited to the spin-zero identical particle case. Recently, this method was applied to the three-pion system [98]. One of the aim of this research project was to extended the application of the perturbative approach to three-fermion system, with special focus on the three-nucleon system. This was carried out in Ref. [99] and the results of this calculation were presented in Chap. 6. The three-nucleon ground state energy shift was presented up to and including $O(L^{-6})$. This formula provides a way for determining the three-particle threshold amplitude by fitting to the measured ground state energy level. An important point to note is that this formula was derived under the assumption that the scattering lengths are of natural size. Even though, this not true in the case of physical nucleons, this method could still be applicable away from physical quark masses where the scattering lengths might become of natural size. Moreover, the derived formula can be applied to other three-fermion systems.

Physical nucleon scattering lengths were substituted in the derived formula (up to $O(L^{-5})$) to get a rough estimate of box size L needed for the perturbative series to converge. The required L turns out to be too large for practical application with the current computational power. Even though, perturbative calculation offer a simple and effective way to fit energy level obtained on the lattice to physical observables, the series fails to converge in case of presence of bound states or resonances. Hence a three-body quantization condition, analogous to the Lüscher equation in the two-body sector, is needed for a more general analysis of three-body lattice data. Three such equivalent formalism have

been developed known as RFT, NREFT and FVU approaches. Due to the presence of shallow bound state in the case of nucleons, a full-fledged three-fermion quantization condition is highly desirable. Such an equation was recently derived in Ref. [87] in RFT framework. A three-fermion quantization condition should also be pursed in the NREFT framework in future works.

With rising computational power and better algorithms, the study of three-body decays has become a real prospect on the lattice. In a finite volume, two-body decays are studied via the Lellouch-Lüscher factor. The three-body equivalent of the LL factor was recently derived in the NREFT framework in Ref. [100], with further generalization to moving frames in Ref. [101]. One of the aim of this research project was to apply this formalism to the decay of kaon into three-pions. This was carried out in Chap. 7. Several technical aspect were discussed in this chapter such as contribution of different isospin channel to this decay, minimal set of independent coupling and solving the Faddeev equation in the infinite volume. One such important technical consideration is regarding the kernel appearing in the Faddeev equation which contains logarithmic singularities. To solve the Faddeev equation the integration contour has to be deformed. An efficient method suitable for numerical calculation was discussed in detail in this chapter.

One of the most computationally expensive part of studying three-particle decay on the lattice would be extraction of the three-particle coupling from the lattice. Hence an important part of this project was to study the dependence of the LL factor on the three-body amplitude. After calculating the LL factor numerically, the three-pion amplitude obtained from Chiral Perturbation Theory calculation was varied in a wide range. It was explicitly shown that the LL factor varies negligibly with the change of the three-pion amplitude. This leads to the important result that one does not need to extract this three-particle amplitude from lattice simulations, rather one can simply use a rough estimate from ChPT calculations. Hence, kaon decay into three pions can be readily studied on the lattice.

This research project has contributed in further understanding of both two-body and three-body sector in a finite volume. In the two-body sector, the modified Lüscher equation, a formalism for extracting physical observables in the presence of long-range interaction was derived for the first time in the NREFT framework. Further more, an efficient numerical routine was developed and implemented for carrying out such an extraction. In the three-body sector, the three-nucleon ground state energy shift was calculated using a perturbative approach for the first time. Lastly, the LL factor for the decay of kaon to three pions was numerically evaluated and its dependence on the three-pion amplitude was probed.

At the next step one should would work towards the following goals:

- Inclusion of electromagnetic interaction in the two- and three-body sector.
- Inclusion of long-range NN force in the three-nucleon quantization condition.
- Apply NREFT formalism for the study of Roper resonance (for a preliminary study see Ref. [291]).

APPENDIX A

Appendix

A.1 Calculating the Green Function

The Green function in the coordinate space can be expressed through the Møller operator

$$\langle \mathbf{r}|G_L(q_0^2+i\varepsilon)|\mathbf{w}\rangle = \int \frac{d^3\mathbf{p}}{(2\pi)^3}\,\langle \mathbf{r}|\Omega(q_0^2+i\varepsilon)|\mathbf{p}\rangle \frac{e^{-i\mathbf{p}\mathbf{w}}}{\mathbf{p}^2-q_0^2-i\varepsilon}\,. \tag{A.1}$$

In Ref. [306], Fuda and Whiting defined the off-shell scattering wave function (cf. with Eq. (4.19)):

$$\langle \mathbf{r}|\Omega(q_0^2+i\varepsilon)|\mathbf{p}\rangle = 4\pi \sum_{\ell m} Y_{\ell m}(\hat{r}) i^\ell \frac{\phi_\ell(q_0,p,r)}{pr} Y^*_{\ell m}(\hat{p})\,. \tag{A.2}$$

This scattering wave function obeys the equation

$$\left(q_0^2+\frac{d^2}{dr^2}-\frac{\ell(\ell+1)}{r^2}-V_L(r)\right)\phi_\ell(q_0,p,r) = (q_0^2-p^2)u_\ell(pr)\,, \tag{A.3}$$

where

$$u_\ell(z)=zj_\ell(z)\,,\qquad v_\ell(z)=zn_\ell(z)\,,\qquad w_\ell^{(\pm)}(z)=zh^{(\pm)}(z)=-v_\ell(z)\pm iu_\ell(z) \tag{A.4}$$

are expressed through the spherical Bessel, Neumann and Hankel functions, respectively. The familiar on-shell wave function is given by $\phi_\ell(p,r)\doteq\phi_\ell(p,p,r)$.

Using the expansion of the plane wave into spherical functions in Eq. (A.1), we obtain

$$G_L^\ell(r,w;q_0^2+i\varepsilon) = 4\pi\int_0^\infty \frac{p^2dp}{(2\pi)^3}\,\frac{\phi_\ell(q_0,p,r)}{pr^{\ell+1}}\,\frac{j_\ell(pw)}{w^\ell}\,\frac{1}{p^2-q_0^2-i\varepsilon}\,. \tag{A.5}$$

Performing the limit $w\to 0$, one gets:

$$G_L^\ell(r,0;q_0^2+i\varepsilon) = \frac{4\pi}{(2\ell+1)!!}\,\frac{(2i)^\ell\ell!}{(2\ell+1)!}\int_0^\infty \frac{pdp}{(2\pi)^3}\,\frac{D^{2\ell+1}\phi_\ell(q_0,p,r)}{p^2-q_0^2-i\varepsilon}\,, \tag{A.6}$$

where

$$D^{2\ell+1}\phi_\ell(q_0,p,r) \doteq \left(\frac{-ip}{2}\right)^\ell \frac{1}{\ell!}\frac{d^{2\ell+1}}{dr^{2\ell+1}} r^\ell \phi_\ell(q_0,p,r)\,. \tag{A.7}$$

Note that the same definition of the operator $D^{2\ell+1}$ is used, if ϕ_ℓ is replaced by an arbitrary function.

In order to perform the integral over p, we rewrite the wave function ϕ_ℓ in terms of the off-shell functions f_ℓ [306]:

$$\begin{aligned}\phi_\ell(q_0,p,r) &= -\frac{\pi p}{2}\left(\frac{q_0}{p}\right)^\ell \frac{f_\ell(q_0,p)-f_\ell(q_0,-p)}{i\pi p f_\ell(q_0)}\, e^{-i\ell\pi/2} f_\ell(q_0,r) \\ &+ \frac{1}{2i}\left(e^{-i\ell\pi/2} f_\ell(q_0,p,r) - e^{i\ell\pi/2} f_\ell(q_0,-p,r)\right)\,,\end{aligned} \tag{A.8}$$

where $f_\ell(q_0,r) \doteq f_\ell(q_0,q_0,r)$. Here, the function f_ℓ obeys the equation

$$\left(q_0^2 + \frac{d^2}{dr^2} - \frac{\ell(\ell+1)}{r^2} - V_L(r)\right) f_\ell(q_0,p,r) = (q_0^2-p^2) e^{i\ell\pi/2} w_\ell^{(+)}(pr)\,, \tag{A.9}$$

and has the asymptotic normalization

$$f_\ell(q_0,p,r) \sim e^{ipr}\,, \qquad \text{as } r\to\infty\,. \tag{A.10}$$

The off-shell Jost functions are defined as

$$f_\ell(q_0,p) = \frac{p^\ell e^{-i\ell\pi/2}(2\ell+1)}{(2\ell+1)!!}\lim_{r\to 0} r^\ell f_\ell(q_0,p,r)\,, \tag{A.11}$$

and the usual Jost functions are obtained from the off-shell Jost functions according to $f_\ell(q_0) = f_\ell(q_0,q_0)$.

Substituting Eq. (A.8) into Eq. (A.6), it is seen that the integration can be extended from $-\infty$ to $+\infty$, owing to the symmetry of the integrand:

$$\begin{aligned}G_L^\ell(r,0;q_0^2+i\varepsilon) &= \frac{1}{(2\ell+1)!!}\frac{(2i)^\ell \ell!}{(2\ell+1)!}\, 2\pi i e^{-i\ell\pi/2}\int_{-\infty}^{\infty}\frac{p\,dp}{(2\pi)^3(p^2-q_0^2-i\varepsilon)} \\ &\times \left(\frac{f_\ell(q_0,p)}{f_\ell(q_0)} D^{2\ell+1} f_\ell(q_0,r) - D^{2\ell+1} f_\ell(q_0,p,r)\right)\,.\end{aligned} \tag{A.12}$$

Note that the factor $\left(q_0/p\right)^\ell$ has disappeared, since $D^{2\ell+1} f_\ell(q_0,r)$ contains the factor q_0^ℓ instead of p^ℓ, cf. Eq. (A.7).

In order to perform the integral by using Cauchy's theorem, it is important to show that the Jost solutions do not have singularities in the upper complex plane of the variable p. To this end, we define

the functions

$$\begin{aligned} g_\ell(q_0,p,r) &= \frac{e^{-i\ell\pi/2}(2\ell+1)}{(2\ell+1)!!}\,(pr)^\ell f_\ell(q_0,p,r)\,, \\ z_\ell(pr) &= \frac{(2\ell+1)}{(2\ell+1)!!}\,(pr)^\ell w^{(+)}(pr)\,. \end{aligned} \tag{A.13}$$

Using Eq. (A.9) and the asymptotic condition, it can be shown that the function g_ℓ obeys the following integral equation

$$\begin{aligned} g_\ell(q_0,p,r) &= z_\ell(pr) - \frac{1}{q_0}\int_0^\infty dw\theta(w-r)\left(\frac{r}{w}\right)^\ell \left(u_\ell(q_0r)v_\ell(q_0w) - v_\ell(q_0r)u_\ell(q_0w)\right) \\ &\times\ V_L(w)g_\ell(q_0,p,w)\,. \end{aligned} \tag{A.14}$$

Solving this equation iteratively, one arrives at

$$g_\ell(q_0,p,r) = z_\ell(pr) + \int_0^\infty dwK_\ell(r,w;q_0)z_\ell(pw)\,. \tag{A.15}$$

An exact form of the kernel K_ℓ is not important. It suffices to know that the kernel does not depend on p and vanishes at $w < r$. Furthermore, assuming $r \to 0$, we get

$$f_\ell(q_0,p) = z_\ell(0) + \int_0^\infty dwK_\ell(0,w;q_0)z_\ell(pw)\ , \qquad z_\ell(0) = \frac{(2\ell+1)!}{l!2^\ell(2\ell+1)!!}\,. \tag{A.16}$$

Acting now with the operator $D^{2\ell+1}$ on Eq. (A.15) and taking the limit $r \to 0$, one gets:

$$\lim_{r\to 0} D^{2\ell+1}f_\ell(q_0,p,r) = p^{2\ell+1}\tilde{z}_\ell(0) + p^\ell\int_0^\infty dw\tilde{K}_\ell(0,w;q_0)z_\ell(pw)\,. \tag{A.17}$$

Again, $\tilde{z}_\ell$, $\tilde{K}_\ell$ are independent of p. Performing now Cauchy integrals, one gets:

$$\begin{aligned} \int_{-\infty}^\infty \frac{pdp}{2\pi i}\,\frac{f_\ell(q_0,p)}{p^2-q_0^2-i\varepsilon} &= z_\ell(0)\int_{-\infty}^\infty \frac{pdp}{2\pi i}\,\frac{1}{p^2-q_0^2-i\varepsilon} + \frac{1}{2}\int_0^\infty K_\ell(0,w;q_0)z_\ell(q_0w) \\ &= -\frac{1}{2}\,z_\ell(0) + \frac{1}{2}\,f_\ell(q_0)\,. \end{aligned} \tag{A.18}$$

Here, one has used the fact that the integral, multiplying $z_\ell(0)$, vanishes in the symmetric boundaries.

Furthermore

$$\begin{aligned}
&\lim_{r\to 0}\int_{-\infty}^{\infty}\frac{pdp}{2\pi i}\,\frac{D^{2\ell+1}f_\ell(q_0,p,r)}{p^2-q_0^2-i\varepsilon}\\
&= \tilde{z}_\ell(0)\int_{-\infty}^{\infty}\frac{pdp}{2\pi i}\,\frac{p^{2\ell+1}}{p^2-q_0^2-i\varepsilon}+\frac{q_0^\ell}{2}\int_0^\infty dw\tilde{K}_\ell(0,w;q_0)z_\ell(q_0w)\\
&= \tilde{z}_\ell(0)\int_{-\infty}^{\infty}\frac{dp(p^{2\ell+2}-q_0^{2\ell+2})}{p^2-q_0^2+i\varepsilon}+\frac{1}{2}\lim_{r\to 0}D^{2\ell+1}f_\ell(q_0,r)\\
&= \tilde{z}_\ell(0)X_\ell(q_0^2)+\frac{1}{2}\lim_{r\to 0}D^{2\ell+1}f_\ell(q_0,r)\,. \qquad \text{(A.19)}
\end{aligned}$$

Here, $X_\ell(q_0^2)$ denotes a polynomial of order ℓ in the variable q_0^2. The coefficients of this polynomial are ultraviolet-divergent and can be regularized, e.g., introducing a momentum cutoff on the integration momenta, $|p|\le\Lambda$.

Collecting all factors together, we obtain

$$\langle G_L^\ell(q_0)\rangle = \frac{1}{4\pi\left((2\ell+1)!!\right)^2}M_\ell(q_0)+\text{real polynomial in } q_0^2\,, \qquad \text{(A.20)}$$

where $M_\ell(q_0)$ is given by Eq. (4.4).

One more remark is in order. It should be pointed out that the final result crucially depends on the validity of Eqs. (A.18) and (A.19). Using Cauchy's theorem straightforwardly is not allowed, since the integrand does not vanish sufficiently fast at the infinity. The result given above corresponds to the choice of symmetric boundary conditions $-\Lambda\le p\le\Lambda$ and $\Lambda\to\infty$, which follows from extending the initial integration area by using the fact that the integrand is even under the interchange $p\leftrightarrow -p$. The terms containing the potential are vanishing exponentially on a large semicircle in the complex plane, and so Cauchy's theorem can be used there without further ado.

A.2 Cancellation of the Poles

Using Eq. (4.17), it is straightforward to see that the full Green function $G=G_0+G_0TG_0$ can be espressed as

$$G(q_0^2)=G_L(q_0^2)+G_L(q_0^2)T_S(q_0^2)G_L(q_0^2)\,. \qquad \text{(A.21)}$$

Our aim is to show that the poles of $G_L(q_0^2)$ will cancel in $G(q_0^2)$. Note that our reasoning will be valid both in a finite as well as in the infinite volume.

Owing to the spectral representation written down in Eq. (4.53), in the vicinity of an isolated pole at $q_0^2=q_n^2$, the Green function G_L has the following representation:

$$G_L(q_0^2)=\frac{|\psi_n\rangle\langle\psi_n|}{q_n^2-q_0^2}+\tilde{G}_L(q_0^2)\,, \qquad \text{(A.22)}$$

where $\tilde{G}_L(q_0^2)$ is regular at $q_0^2 = q_n^2$. Furthermore, defining the quantity

$$\tilde{T}_S(q_0^2) = V_S + V_S \tilde{G}_L(q_0^2) \tilde{T}_S(q_0^2)\,, \tag{A.23}$$

which is apparenly regular at $q_0^2 = q_n^2$, we obtain

$$T_S(q_0^2) = \tilde{T}_S(q_0^2) + \frac{\tilde{T}_S(q_0^2)|\psi_n\rangle\langle\psi_n|\tilde{T}_S(q_0^2)}{q_n^2 - q_0^2 - \langle\psi_n|\tilde{T}_S(q_0^2)|\psi_n\rangle}\,. \tag{A.24}$$

It is explicitly seen that this expression does not contain a pole at $q_0^2 = q_n^2$, if the matrix element in the denominator does not accidentally vanish. Moreover, using Eqs. (A.22) and (A.24) in Eq. (A.21), after a simple algebra one obtains:

$$G = \tilde{G}_L + \tilde{G}_L \tilde{T}_S \tilde{G}_L + \frac{(1 + \tilde{G}_L \tilde{T}_S)|\psi_n\rangle\langle\psi_n|(\tilde{T}_S \tilde{G}_L + 1)}{q_n^2 - q_0^2 - \langle\psi_n|\tilde{T}_S(q_0^2)|\psi_n\rangle}\,. \tag{A.25}$$

Again, the poles that emerge from G_L, have canceled in the final result.

A.3 Partial-Wave Contributions to the Energy Shift of a Given State

In this appendix, we give a qualitative explanation for the uneven convergence of the partial-wave expansion, which is observed in Fig. 5.5. We shall namely argue that the pattern of the convergence in different excited states can be understood solely on the basis of a symmetry argument.

In the beginning, let us note that the energy shifts from the unperturbed states are generally small, so first-order perturbation theory captures the bulk of the effect. These unperturbed states represent the finite-volume momentum eigenstates $|\boldsymbol{n}\rangle$ that satisfy the completeness condition

$$\sum_{\boldsymbol{n}\in\mathbb{Z}^3} |\boldsymbol{n}\rangle\langle\boldsymbol{n}| = \mathbb{1}. \tag{A.26}$$

Let us now introduce the *shells* – sets of vectors generated from a given vector $|\boldsymbol{n}\rangle$ by the action of all elements of the octahedral group O_h. We label these shells by index r. It is clear that the matrix representations of O_h can be realized in the linear space spanned by all vectors belonging to a given shell. These representations are in general reducible, and can be decomposed into the different irreps. There are seven fundamental types of shells (see, e.g. [56, 177, 307]), classified according to how many components of the three-momentum share the same magnitude. The decomposition of the

representations of the group O_h for these shells are given by

$$\begin{aligned}
(0,0,0) &: \quad A_1^+ \,, \\
(0,0,c) &: \quad A_1^+ \oplus E^+ \oplus T_1^- \,, \\
(0,b,b) &: \quad A_1^+ \oplus E^+ \oplus T_1^- \oplus T_2^+ \oplus T_2^- \,, \\
(0,b,c) &: \quad A_1^+ \oplus A_2^+ \oplus 2E^+ \oplus T_1^+ \oplus 2T_1^- \oplus T_2^+ \oplus 2T_2^- \,, \\
(a,a,a) &: \quad A_1^+ \oplus A_2^- \oplus T_1^- \oplus T_2^+ \,, \\
(a,a,c) &: \quad A_1^+ \oplus A_2^- \oplus E^+ \oplus E^- \oplus T_1^+ \oplus 2T_1^- \oplus 2T_2^+ \oplus T_2^- \,, \\
(a,b,c) &: \quad A_1^+ \oplus A_1^- \oplus A_2^+ \oplus A_2^- \oplus 2E^+ \oplus 2E^- \oplus 3T_1^+ \oplus 3T_1^- \oplus 3T_2^+ \oplus 3T_2^- \,.
\end{aligned} \tag{A.27}$$

We denote the basis vectors for each irrep by $|\Gamma t, \alpha; r\rangle$. Here Γ labels the irrep of O_h, α distinguishes the basis vectors within that irrep, r labels shells and t enumerates the multiplicity of the irrep Γ [307].

Let us now evaluate the finite-volume energy shift of an unperturbed state $|\boldsymbol{n}\rangle$. When the interaction is switched on, the level splitting occurs, and the states belonging to the different irreps are shifted differently. For a given interaction potential V, the leading-order perturbative energy shift of a state transforming in the irrep Γ is obtained by diagonalization of the following matrix in the space of indices t, t':

$$V_{tt'}^{(\Gamma)}(r) = \langle \Gamma t, \alpha; r | V | \Gamma t', \alpha; r \rangle . \tag{A.28}$$

Here α is arbitrary due to the Wigner-Eckart theorem.

Furthermore, the interaction potential can be expanded in partial-waves:

$$\langle \boldsymbol{n}_1 | V | \boldsymbol{n}_2 \rangle = 4\pi \sum_{\ell m} Y_{\ell m}(\hat{\boldsymbol{n}}_1) V_\ell(p_1, p_2) Y_{\ell m}^*(\hat{\boldsymbol{n}}_2), \tag{A.29}$$

where $p_i = \dfrac{2\pi}{L}|\boldsymbol{n}_i|$. Therefore, the matrix element in Eq. (A.28) is given by

$$\begin{aligned}
V_{tt'}^{(\Gamma)}(r) &= \sum_{\boldsymbol{n}_1, \boldsymbol{n}_2 \in \text{shell-}r} \langle \Gamma t, \alpha; r | \boldsymbol{n}_1 \rangle \langle \boldsymbol{n}_1 | V | \boldsymbol{n}_2 \rangle \langle \boldsymbol{n}_2 | \Gamma t', \alpha; r \rangle \\
&= 4\pi \sum_{\ell m} V_\ell(p_1, p_2) \sum_{\boldsymbol{n}_1, \boldsymbol{n}_2 \in \text{shell-}r} \langle \Gamma t, \alpha; r | \boldsymbol{n}_1 \rangle Y_{\ell m}(\hat{\boldsymbol{n}}_1) Y_{\ell m}^*(\hat{\boldsymbol{n}}_2) \langle \boldsymbol{n}_2 | \Gamma t', \alpha; r \rangle \,.
\end{aligned} \tag{A.30}$$

Note that since $\boldsymbol{n}_1$ and $\boldsymbol{n}_2$ both belong to the shell-r, $p_1 = p_2$ is the magnitude of the three-momentum in the shell-r.

Next, we introduce the finite-volume partial-wave states $|\ell, m; r\rangle$, defined through projecting the plane-wave basis onto the spherical harmonics [307]

$$|\ell, m; r\rangle = \sum_{\boldsymbol{n} \in \text{shell-}r} \sqrt{4\pi}\, Y_{\ell m}(\hat{\boldsymbol{n}})\, |\boldsymbol{n}\rangle \,, \tag{A.31}$$

and define

$$|\Gamma t \ell, \alpha; r\rangle = \sum_m c_{\ell m}^{\Gamma \alpha t} |\ell, m; r\rangle \,, \tag{A.32}$$

where $c_{\ell m}^{\Gamma \alpha t}$ denotes the pertinent Clebsh-Gordan coefficient, see, e.g., Eq. (5.9). Since the transformation between $|\ell, m; r\rangle$ and $|\Gamma t \ell, \alpha; r\rangle$ is unitary, we have

$$\sum_m |\ell, m; r\rangle\langle \ell, m; r| = \sum_{\Gamma t \alpha} |\Gamma t \ell, \alpha; r\rangle\langle \Gamma t \ell, \alpha; r| \,. \tag{A.33}$$

This means that

$$\begin{aligned} V_{tt'}^{(\Gamma)}(r) &= 4\pi \sum_{\ell m} V_\ell(p,p) \sum_{\boldsymbol{n}_1, \boldsymbol{n}_2 \in \text{shell-}r} \langle \Gamma t, \alpha; r|\boldsymbol{n}_1\rangle Y_{\ell m}(\hat{\boldsymbol{n}}_1) Y_{\ell m}^*(\hat{\boldsymbol{n}}_2) \langle \boldsymbol{n}_2|\Gamma t', \alpha; r\rangle \\ &= \sum_{\ell m} V_\ell(p,p) \langle \Gamma t, \alpha; r|\ell, m; r\rangle\langle \ell, m; r|\Gamma t', \alpha; r\rangle \\ &= \sum_{\ell} V_\ell(p,p) \sum_{\Gamma' t'' \beta} \langle \Gamma t, \alpha; r|\Gamma' t'' \ell, \beta; r\rangle\langle \Gamma' t'' \ell, \beta; r|\Gamma t', \alpha; r\rangle \\ &= \sum_{\ell} V_\ell(p,p) \sum_{t''} \langle \Gamma t, \alpha; r|\Gamma t'' \ell, \alpha; r\rangle\langle \Gamma t'' \ell, \alpha; r|\Gamma t', \alpha; r\rangle. \end{aligned} \tag{A.34}$$

Now let us define

$$G_{\ell, tt'}^{(\Gamma)}(r) = \sum_{t''} \langle \Gamma t, \alpha; r|\Gamma t'' \ell, \alpha; r\rangle\langle \Gamma t'' \ell, \alpha; r|\Gamma t', \alpha; r\rangle. \tag{A.35}$$

The quantity G was calculated in Ref. [307]. In order to understand the result presented in Fig. 5.5, we restrict ourselves to the irrep $\Gamma = A_1^+$ and truncate the partial-wave expansion, keeping only $\ell = 0, 4$. In this case, the multiplicities t, t', t'' and the label of the basis vector, α, all take a single value. For simplicity, we shall ignore these indices in the following. The leading-order energy shift then reduces to

$$\Delta E^{(A_1^+)}(r) = V^{(A_1^+)}(r) = G_0^{(A_1^+)}(r) V_0(p,p) + G_4^{(A_1^+)}(r) V_4(p,p) + \cdots \,. \tag{A.36}$$

The quantity G is given by

$$G_\ell^{(A_1^+)}(r) = |\langle A_1^+; r|A_1^+ \ell; r\rangle|^2. \tag{A.37}$$

This quantity can be evaluated directly, resulting in

$$\begin{aligned} (000) &: \quad G_0^{(A_1^+)} = 1\,, \quad G_4^{(A_1^+)} = 0\,, \\ (001) &: \quad G_0^{(A_1^+)} = 6\,, \quad G_4^{(A_1^+)} = 31.5\,, \\ (011) &: \quad G_0^{(A_1^+)} = 12\,, \quad G_4^{(A_1^+)} = 3.94\,, \\ (012) &: \quad G_0^{(A_1^+)} = 24\,, \quad G_4^{(A_1^+)} = 5.04\,, \\ (111) &: \quad G_0^{(A_1^+)} = 8\,, \quad G_4^{(A_1^+)} = 18.67\,, \\ (112) &: \quad G_0^{(A_1^+)} = 24\,, \quad G_4^{(A_1^+)} = 7.88\,, \\ (123) &: \quad G_0^{(A_1^+)} = 48\,, \quad G_4^{(A_1^+)} = 15.75\,. \end{aligned} \tag{A.38}$$

The seven cases above correspond to the seven types of the momentum shells. Relatively large $G_4^{(A_1^+)}$

factors associated with the shells (001) and (111) are responsible for sizable G-wave contributions to the first and third excited states. And, *vice versa,* much smaller $G_4^{(A_1^+)}$ factors for (011), (012) and (112) shells explain, why the G-wave corrections are negligible in the second, fifth, and sixth excited states, see Fig. 5.5.

A.4 Integrating Out the Dimer Fields

In order to integrate out the dimer fields, note that the dimer Lagrangian can be conveniently written as

$$\begin{aligned}\tilde{\mathcal{L}}_d = &\sum_{I,I_3} \sigma_I \, T^\dagger_{II_3} T_{II_3} + \sum_{I,I_3} \left(T^\dagger_{II_3} O_{II_3} + \text{h.c.} \right) \\ &+ \sum_{I,I_3,i_3} \sum_{I',I_3',i_3'} T^\dagger_{II_3} \pi^\dagger_{i_3} \, h_{II_3 i_3; I' I_3' i_3'} \, \pi_{i_3'} T_{I' I_3'} \\ &+ \sum_{I,I_3,i_3} \left(g_{II_3 i_3} K_+^\dagger T_{II_3} \pi_{i_3} + \text{h.c.} \right) , \end{aligned} \tag{A.39}$$

where the coefficients $h_{II_3 i_3; I' I_3' i_3'}$ and $g_{II_3 i_3}$ can be read off from Eq. (7.9) and Eq. (7.10) respectively – they are linear combinations of the couplings $h_J^{(I,I')}$ and $g^{(J,I)}$. Defining

$$\tilde{T}_{II_3} = \tilde{T}_{II_3} + \sum_{I' I_3'} A^{-1}_{II_3; I' I_3'} B_{I' I_3'} , \tag{A.40}$$

where

$$A_{II_3; I' I_3'} = \sigma_I \delta_{II'} \delta_{I_3 I_3'} + \sum_{i_3, i_3'} \pi^\dagger_{i_3} \, h_{II_3 i_3; I' I_3' i_3'} \, \pi_{i_3'} , \tag{A.41}$$

and

$$B_{II_3} = O_{II_3} + \sum_{i_3} g_{II_3 i_3} \pi^\dagger_{i_3} K_+ , \tag{A.42}$$

the dimer Lagrangian can be brought into a quadratic form:

$$\tilde{\mathcal{L}}_d = \sum_{I,I_3} \sum_{I',I_3'} \tilde{T}^\dagger_{II_3} \, A_{II_3; I' I_3'} \, \tilde{T}_{I' I_3'} - \sum_{I,I_3} \sum_{I',I_3'} B^\dagger_{II_3} \, A^{-1}_{II_3; I' I_3'} \, B_{I' I_3'} . \tag{A.43}$$

The dimer can then be integrated out in the path integral formalism in a standard way. The second term on the right-hand side thus should be matched to the Lagrangian in the particle picture at tree level. Noting that

$$A^{-1}_{II_3; I' I_3'} = \sigma_I^{-1} \delta_{II'} \delta_{I_3 I_3'} - \sigma_I^{-1} \pi^\dagger_{i_3} \, h_{II_3 i_3; I' I_3' i_3'} \, \pi_{i_3'} \sigma_{I'}^{-1} + \dots , \tag{A.44}$$

where the ellipsis contains at least four pion fields, the second term on the right hand side of Eq. (A.43) can be written as

$$
\begin{aligned}
-\sum_{I,I_3}\sum_{I',I_3'} B^\dagger_{II_3}\, A^{-1}_{II_3;I'I_3'}\, B_{I'I_3'} = &\sum_{I,I_3}(-\sigma_I^{-1}O^\dagger_{II_3}O_{II_3}) \\
&+\sum_{I,I_3,i_3}\sum_{I',I_3',i_3'}(-\sigma_I^{-1}O^\dagger_{II_3})\pi^\dagger_{i_3}\, h_{II_3i_3;I'I_3'i_3'}\,\pi_{i_3'}(-\sigma_{I'}^{-1}O_{I'I_3'}) \\
&+\sum_{I,I_3,i_3}\left(g_{II_3i_3}K^\dagger_+(-\sigma_I^{-1}O_{II_3})\pi_{i_3}+\text{h.c.}\right)+\dots\,,
\end{aligned}
\tag{A.45}
$$

where the ellipsis contains at least eight pion- or two kaon fields. These terms do not contribute to the three-body sector. We can conclude that, integrating out the dimer fields, one merely has to replace $T_{II_3}\to-\sigma_I^{-1}O_{II_3}$.

Calculating the Green function

$$
G^{II_3i_3}_{i_1'i_2'i_3'}(x_1,x_2,x_3)=\langle 0|T\left[O^{i_1'i_2'i_3'}_{3\pi}(x_1,x_2x_3)T^\dagger_{II_3}(0)\pi^\dagger_{i_3}(0)\right]|0\rangle
\tag{A.46}
$$

in the particle-dimer picture at tree level, one performs the functional integral

$$
\begin{aligned}
&\int \mathcal{D}T\mathcal{D}T^\dagger\, T^\dagger_{II_3}(0)\,\exp\left\{-i\int d^4x\,\tilde{\mathcal{L}}_d\right\} \\
&=-\sum_{I'I_3'}A^{-1}_{II_3;I'I_3'}B_{I'I_3'}\exp\left\{i\int d^4x\sum_{I',I_3'}\sum_{I'',I_3''}B^\dagger_{I'I_3'}\,A^{-1}_{I'I_3';I''I_3''}\,B_{I''I_3''}\right\}\,.
\end{aligned}
\tag{A.47}
$$

The remaining functional integration is over the pion and kaon fields. At tree level, only $A^{-1}_{II_3;I'I_3'}=\sigma_I^{-1}\delta_{II'}\delta_{I_3I_3'}$ contributes and the term containing the kaon can be dropped from $B_{I'I_3'}$ in the term $A^{-1}_{II_3;I'I_3'}B_{I'I_3'}$ in front of the exponential. Thus, one may conclude that, at tree level, the above Green function in the particle picture corresponds to

$$
G^{II_3i_3}_{i_1'i_2'i_3'}(x_1,x_2,x_3)=\langle 0|T\left[O^{i_1'i_2'i_3'}_{3\pi}(x_1,x_2x_3)(-\sigma_I^{-1}O^\dagger_{II_3}(0))\pi^\dagger_{i_3}(0)\right]|0\rangle\,,
\tag{A.48}
$$

such that again the replacement $T_{II_3}\to-\sigma_I^{-1}O_{II_3}$ is justified.

Similarly, the vertex function

$$
\begin{aligned}
V^{II_3i_3;JJ_3j_3}_{i_1'i_2'i_3';j_1'j_2'j_3'}(x_1,x_2,x_3;y_1,y_2,y_3)=\langle 0|T\Big[&O^{i_1'i_2'i_3'}_{3\pi}(x_1,x_2,x_3)\left(O^{j_1'j_2'j_3'}_{3\pi}(y_1,y_2,y_3)\right)^\dagger \\
&\times T^\dagger_{II_3}(0)\pi^\dagger_{i_3}(0)\pi_{j_3}(0)T_{JJ_3}(0)\Big]|0\rangle\,,
\end{aligned}
\tag{A.49}
$$

can be evaluated in the particle picture by integrating out the dimer fields. At tree level, this gives

$$V^{II_3i_3;JJ_3j_3}_{i_1'i_2'i_3';j_1'j_2'j_3'}(x_1,x_2,x_3;y_1,y_2,y_3) = \langle 0|T\Big[O^{i_1'i_2'i_3'}_{3\pi}(x_1,x_2,x_3)\left(O^{j_1'j_2'j_3'}_{3\pi}(y_1,y_2,y_3)\right)^\dagger \\ \times(-\sigma_I^{-1}O^\dagger_{II_3}(0))\pi^\dagger_{i_3}(0)\pi_{j_3}(0)(-\sigma_J^{-1}O^\dagger_{JJ_3}(0))\Big]|0\rangle\,. \tag{A.50}$$

Note that, in both cases, we implicitly discard disconnected pieces in the Green functions, calculated in the particle picture.

A.5 Three-Pion Amplitude in Chiral Perturbation Theory

For the matching of the particle-dimer coupling, we need to calculate the three-pion threshold amplitude in ChPT. Here, we give only a brief sketch of this calculation, carried out at tree level, which follows the pattern outlined in Ref. [292]. In general, there are only two types of contributions, shown in Fig. A.1: The contact term, which emerges from the six-pion Lagrangian, Fig. A.1(a), and the exchange term that features a single pion propagator (all possible permutations of external lines in *in*- and *out*-states), Fig. A.1(b). We are interested in the processes $3\pi^+ \to 3\pi^+$ and $3\pi^0 \to 3\pi^0$. The contact contributions to these processes at threshold are given by

$$T^\chi_{\text{cont}}(3\pi^+ \to 3\pi^+) = -\frac{18M_\pi^2}{F_\pi^4}\,,$$
$$T^\chi_{\text{cont}}(3\pi^0 \to 3\pi^0) = \frac{27M_\pi^2}{F_\pi^4}\,. \tag{A.51}$$

Symbolically, the exchange contribution can be written down as follows

$$T^\chi_{\text{ex}}(3\pi \to 3\pi) = \sum_{\text{permutations}} \mathcal{M}(2\pi \to 2\pi)\frac{1}{M_\pi^2 - k^2}\mathcal{M}(2\pi \to 2\pi)\,, \tag{A.52}$$

where k denotes the four-momentum of the exchanged pion. Furthermore, the two-body amplitudes at leading order are linear functions of the pertinent Mandelstam variables s, t, u and M_π^2:

$$\mathcal{M}(2\pi \to 2\pi) = \frac{\alpha s + \beta t + \gamma u + \delta M_\pi^2}{F_\pi^2}\,. \tag{A.53}$$

Here, $\alpha, \beta, \gamma, \delta$ stand for some numerical coefficients. Furthermore, one can always choose these variables so that, say, s and t depend only on the external momenta (which are, by definition, on shell). Then, one could use the relation $s + t + u = 3M_\pi^2 + k^2$ and rewrite the expression for the two-body amplitude as

$$\mathcal{M}(2\pi \to 2\pi) = \frac{\alpha s + \beta t + \gamma(4M_\pi^2 - s - t) + \gamma(k^2 - M_\pi^2) + \delta M_\pi^2}{F_\pi^2}\,. \tag{A.54}$$

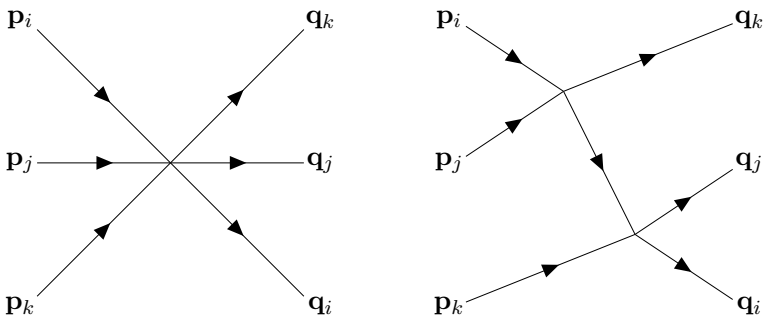

(a) Three-pion contact diagram (b) One-pion exchange diagram

Figure A.1: Two kinds of diagrams that contribute to the three-pion scattering amplitude at leading order in ChPT. Diagram (b) is singular at threshold, whereas diagram (a) is finite.

The part of the amplitude that is proportional to $k^2 - M_\pi^2$ will cancel with the propagator and will contribute to the regular part of the threshold amplitude. Separating the pole terms from the non-pole ones in all diagrams by using Eq. (A.53), in a result one gets for the regular part:

$$\begin{aligned} T^{\mathcal{K}}_{\text{ex,reg}}(3\pi^+ \to 3\pi^+) &= \frac{36M_\pi^2}{F_\pi^4}\,, \\ T^{\mathcal{K}}_{\text{ex,reg}}(3\pi^0 \to 3\pi^0) &= -\frac{225M_\pi^2}{8F_\pi^4}\,. \end{aligned} \tag{A.55}$$

Adding up these two contributions, we finally get

$$\begin{aligned} T^{\mathcal{K}}_{\text{reg}}(3\pi^+ \to 3\pi^+) &\doteq T^{\mathcal{K}}_{+} = \frac{18M_\pi^2}{F_\pi^4}\,, \\ T^{\mathcal{K}}_{\text{reg}}(3\pi^0 \to 3\pi^0) &\doteq T^{\mathcal{K}}_{0} = -\frac{9M_\pi^2}{8F_\pi^4}\,. \end{aligned} \tag{A.56}$$

A.6 Leading-Order Energy Shift of the $n = 1$ State

In this appendix, we shall evaluate the energy shift of the states with the lowest energy in different moving frames as well as in the rest frame. In particular, our aim will be to demonstrate that the level splitting, which we observe in a result of the solution of the quantization condition, can be interpreted with the use of the perturbation theory as well.

We start from the states with total isospin $J = 1$ and choose $J_3 = 1$. One can define three orthogonal

states with these quantum numbers [98]:

$$
\begin{aligned}
|f_1\rangle &= \frac{1}{\sqrt{15}}\left(2|\pi^+\pi^+\pi^-\rangle + 2|\pi^+\pi^-\pi^+\rangle + 2|\pi^-\pi^+\pi^+\rangle\right. \\
&\qquad \left. - |\pi^0\pi^0\pi^+\rangle - |\pi^0\pi^+\pi^0\rangle - |\pi^+\pi^0\pi^0\rangle\right), \\
|f_2\rangle &= \frac{1}{2\sqrt{3}}\left(2|\pi^+\pi^+\pi^-\rangle - |\pi^+\pi^-\pi^+\rangle - |\pi^-\pi^+\pi^+\rangle\right. \\
&\qquad \left. + 2|\pi^0\pi^0\pi^+\rangle - |\pi^0\pi^+\pi^0\rangle - |\pi^+\pi^0\pi^0\rangle\right), \\
|f_3\rangle &= \frac{1}{2}\left(|\pi^+\pi^0\pi^0\rangle - |\pi^0\pi^+\pi^0\rangle - |\pi^+\pi^-\pi^+\rangle + |\pi^-\pi^+\pi^+\rangle\right).
\end{aligned} \tag{A.57}
$$

We consider moving frames with the total three-momentum $\mathbf{P} = 2\pi\mathbf{d}/L$, where $\mathbf{d} = (0,0,1), (1,1,0), (1,1,1)$. For these values of $\mathbf{d}$, the states with the lowest energy are given by

$$
|\mathbf{p}_1, \mathbf{p}_2, \mathbf{p}_3\rangle \in \{|\mathbf{P},\mathbf{0},\mathbf{0}\rangle\,,\ |\mathbf{0},\mathbf{P},\mathbf{0}\rangle\,,\ |\mathbf{0},\mathbf{0},\mathbf{P}\rangle\}\,. \tag{A.58}
$$

From these we construct the total wave functions of the three-pion system denoted by

$$
|f_i;\mathbf{p}_1,\mathbf{p}_2,\mathbf{p}_3\rangle\,, \tag{A.59}
$$

where the momenta $\mathbf{p}_1$, $\mathbf{p}_2$ and $\mathbf{p}_3$ are assigned to the first, second and third pion in the isospin wave function $|f_i\rangle$ respectively. Naively, in the non-interacting case there would be nine degenerate states with energy

$$
E_0 = 2m + \sqrt{m^2 + \left(\frac{2\pi\mathbf{d}}{L}\right)^2}\,. \tag{A.60}
$$

On the other hand, not all states are independent. Using Bose-symmetry we find that:

$$
\begin{aligned}
&|f_1;\mathbf{0},\mathbf{P},\mathbf{0}\rangle = |f_1;\mathbf{P},\mathbf{0},\mathbf{0}\rangle\,, && |f_1;\mathbf{0},\mathbf{0},\mathbf{P}\rangle = |f_1;\mathbf{P},\mathbf{0},\mathbf{0}\rangle\,, \\
&|f_2;\mathbf{0},\mathbf{P},\mathbf{0}\rangle = |f_2;\mathbf{P},\mathbf{0},\mathbf{0}\rangle\,, && |f_2;\mathbf{0},\mathbf{0},\mathbf{P}\rangle = -2\,|f_2;\mathbf{P},\mathbf{0},\mathbf{0}\rangle\,, \\
&|f_3;\mathbf{0},\mathbf{P},\mathbf{0}\rangle = -|f_3;\mathbf{P},\mathbf{0},\mathbf{0}\rangle\,, && |f_3;\mathbf{0},\mathbf{0},\mathbf{P}\rangle = 0\,, \\
&|f_3;\mathbf{P},\mathbf{0},\mathbf{0}\rangle = -\sqrt{3}\,|f_2;\mathbf{P},\mathbf{0},\mathbf{0}\rangle\,.
\end{aligned} \tag{A.61}
$$

Defining the states

$$
\begin{aligned}
|X;\mathbf{P},\mathbf{0},\mathbf{0}\rangle &= -\frac{1}{2}\,|f_2;\mathbf{P},\mathbf{0},\mathbf{0}\rangle + \frac{\sqrt{3}}{2}\,|f_3;\mathbf{P},\mathbf{0},\mathbf{0}\rangle\,, \\
|Y;\mathbf{P},\mathbf{0},\mathbf{0}\rangle &= \frac{\sqrt{3}}{2}\,|f_2;\mathbf{P},\mathbf{0},\mathbf{0}\rangle + \frac{1}{2}\,|f_3;\mathbf{P},\mathbf{0},\mathbf{0}\rangle = 0\,,
\end{aligned} \tag{A.62}
$$

it can be seen that the lowest energy level in the frame $\mathbf{d} \neq \mathbf{0}$ with $J = 1$ is twofold degenerate, corresponding to the states $|f_1;\mathbf{P},\mathbf{0},\mathbf{0}\rangle$ and $|X;\mathbf{P},\mathbf{0},\mathbf{0}\rangle$.

The energy shift is calculated in the degenerate perturbation theory, where the potentials are obtained from the non-relativistic effective field theory. Contrary to [98], here we will use the covariant

formulation. In this setup, the normalized one-particle states are given by:

$$|\pi_i(\mathbf{p})\rangle = L^{-3/2}\,(2w(\mathbf{p}))^{-1/2}\,a_i^\dagger(\mathbf{p})\,|0\rangle\,. \tag{A.63}$$

and the creation and annihilation operators obey the commutation relation

$$[a_i(\mathbf{p}), a_j^\dagger(\mathbf{q})] = \delta_{ij}\,2w(\mathbf{p})L^3\,\delta_{\mathbf{p},\mathbf{q}}\,. \tag{A.64}$$

At the leading order, the energy shift $\Delta E_{\mathbf{d}\neq\mathbf{0}}^{J=1}$ is given by the eigenvalues of the potential

$$V = \frac{1}{3!}\begin{pmatrix}\langle f_1;\mathbf{P},\mathbf{0},\mathbf{0}|H_I|f_1;\mathbf{P},\mathbf{0},\mathbf{0}\rangle & \langle f_1;\mathbf{P},\mathbf{0},\mathbf{0}|H_I|X;\mathbf{P},\mathbf{0},\mathbf{0}\rangle \\ \langle X;\mathbf{P},\mathbf{0},\mathbf{0}|H_I|f_1;\mathbf{P},\mathbf{0},\mathbf{0}\rangle & \langle X;\mathbf{P},\mathbf{0},\mathbf{0}|H_I|X;\mathbf{P},\mathbf{0},\mathbf{0}\rangle\end{pmatrix}, \tag{A.65}$$

where H_I denotes the interaction Hamiltonian

$$H_I = -\int d^3\mathbf{x}\,\mathcal{L}_2\,. \tag{A.66}$$

Here $\mathcal{L}_2$ is the two-body Lagrangian in the particle picture, as in Eq. (7.2). The couplings C_i are matched to the $I = 0, 2$ scattering lengths a_I, according to Eq. (7.16) and Eq. (7.18).

Up to $O(L^{-3})$, the potential is given by:

$$V = \frac{4\pi}{27mL^3}\begin{pmatrix}5(5a_0+4a_2) & 2\sqrt{5}(a_0-a_2) \\ 2\sqrt{5}(a_0-a_2) & 2(4a_0+5a_2)\end{pmatrix}, \tag{A.67}$$

leading to an energy shift

$$\Delta E_{\mathbf{d}\neq\mathbf{0}}^{J=1} = \frac{2\pi}{9mL^3}\left(11a_0+10a_2 \pm \sqrt{41a_0^2+20a_0a_2+20a_2^2}\right), \tag{A.68}$$

and lifting the degeneracy of the non-interacting energy level.

Note that the same result is obtained in the non-covariant approach. The only difference in the covariant and non-covariant potentials, besides the use of different couplings C_i, is the normalization of states: instead of the factor

$$\delta_{\mathbf{p}_i,\mathbf{q}_l}\,\delta_{\mathbf{p}_j+\mathbf{p}_k,\mathbf{q}_m+\mathbf{q}_n} \tag{A.69}$$

which appears in Eqs. (31) and (32) of Ref. [98] for the potentials, sandwiched between the three-pion states that carry the momenta $\mathbf{p}_1, \mathbf{p}_2, \mathbf{p}_3$ and $\mathbf{q}_1, \mathbf{q}_2, \mathbf{q}_3$ respectively, in the covariant approach the following factor emerges

$$\begin{aligned}\Big(2w(\mathbf{p}_j)2w(\mathbf{p}_k)2w(\mathbf{q}_m)2w(\mathbf{q}_n)\Big)^{-1/2}&\delta_{\mathbf{p}_i,\mathbf{q}_l}\,\delta_{\mathbf{p}_j+\mathbf{p}_k,\mathbf{q}_m+\mathbf{q}_n} \\ &= \frac{1}{4m^2}\delta_{\mathbf{p}_i,\mathbf{q}_l}\,\delta_{\mathbf{p}_j+\mathbf{p}_k,\mathbf{q}_m+\mathbf{q}_n}+\cdots\,.\end{aligned} \tag{A.70}$$

Here the multiplicative factors $2w(\mathbf{k}_i)$ account for the different normalization of the one-particle states in the relativistic and non-relativistic framework, see Eq. (A.63). For the same reason, these factors

also arise in the matching condition in the non-covariant framework, while in the covariant matching condition they are absent. Therefore the results after expressing everything in terms of the scattering lengths are identical.

Next, note that, for $J = 3$, there is only a single state with the lowest energy. One can, for example, choose $J_3 = 3$ and consider the state $|\pi^+\pi^+\pi^+; \mathbf{P}, \mathbf{0}, \mathbf{0}\rangle$. The energy shift at the leading order can be calculated in the non-degenerate perturbation theory and is given by

$$\Delta E^{J=3}_{\mathbf{d}\neq\mathbf{0}} = \frac{1}{3!}\langle \pi_+\pi_+\pi_+; \mathbf{P}, \mathbf{0}, \mathbf{0}|H_I|\pi_+\pi_+\pi_+; \mathbf{P}, \mathbf{0}, \mathbf{0}\rangle = \frac{20\pi}{3mL^3}\, a_2\,. \tag{A.71}$$

Finally, note that for the ground state $\mathbf{d} = \mathbf{0}$, the energy shifts corresponding to the total isospin $J = 1$ and $J = 3$ can be obtained in the non-degenerate perturbation theory again. For $J = 1$ and $J_3 = 1$, only the state $|f_1; \mathbf{0}, \mathbf{0}, \mathbf{0}\rangle$ yields the non-vanishing ground state wave function due to Bose-symmetry. The energy shift is then given by:

$$\Delta E^{J=1}_{\mathbf{d}=\mathbf{0}} = \frac{4\pi}{3mL^3}\left(5a_0 + 4a_2\right)\,. \tag{A.72}$$

For $J = 3$ and $J_3 = 3$, the ground state wave function is given by $|\pi_+\pi_+\pi_+; \mathbf{0}, \mathbf{0}, \mathbf{0}\rangle$. At the leading order, the energy shift of this state is equal to

$$\Delta E^{J=3}_{\mathbf{d}=\mathbf{0}} = \frac{12\pi}{mL^3}\, a_2\,. \tag{A.73}$$

Bibliography

[1] E. Rutherford,
LXXIX. The scattering of α and β particles by matter and the structure of the atom,
The London, Edinburgh, and Dublin Philosophical Magazine and Journal of Science **21** (1911) 669, eprint: https://doi.org/10.1080/14786440508637080,
URL: https://doi.org/10.1080/14786440508637080 (cit. on p. 1).

[2] J. Chadwick, *The Existence of a Neutron*, Proceedings of the Royal Society of London. Series A, Containing Papers of a Mathematical and Physical Character **136** (1932) 692,
ISSN: 09501207, URL: http://www.jstor.org/stable/95816 (visited on 20/05/2025) (cit. on p. 1).

[3] W. Heisenberg, *On the structure of atomic nuclei*, Z. Phys. **77** (1932) 1 (cit. on p. 1).

[4] H. Yukawa, *On the Interaction of Elementary Particles. I*,
Progress of Theoretical Physics Supplement **1** (1955) 1, ISSN: 0375-9687,
eprint: https://academic.oup.com/ptps/article-pdf/doi/10.1143/PTPS.1.1/5310694/1-1.pdf,
URL: https://doi.org/10.1143/PTPS.1.1 (cit. on p. 1).

[5] Y. Ne'eman, *Derivation of strong interactions from a gauge invariance*,
Nucl. Phys. **26** (1961) 222, ed. by R. Ruffini and Y. Verbin (cit. on p. 1).

[6] M. Gell-Mann, *Symmetries of Baryons and Mesons*, Phys. Rev. **125** (3 1962) 1067,
URL: https://link.aps.org/doi/10.1103/PhysRev.125.1067 (cit. on p. 1).

[7] S. Okubo, *Note on Unitary Symmetry in Strong Interactions*,
Progress of Theoretical Physics **27** (1962) 949, ISSN: 0033-068X, eprint: https://academic.oup.com/ptp/article-pdf/27/5/949/5400949/27-5-949.pdf,
URL: https://doi.org/10.1143/PTP.27.949 (cit. on p. 1).

[8] V. E. Barnes et al., *Observation of a Hyperon with Strangeness Minus Three*,
Phys. Rev. Lett. **12** (8 1964) 204,
URL: https://link.aps.org/doi/10.1103/PhysRevLett.12.204 (cit. on p. 1).

[9] M. Gell-Mann, *A Schematic Model of Baryons and Mesons*, Phys. Lett. **8** (1964) 214 (cit. on p. 1).

[10] G. Zweig, *An SU(3) model for strong interaction symmetry and its breaking. Version 1*, (1964) (cit. on p. 1).

[11] N. N. Bogolubov, B. V. Struminsky and A. N. Tavkhelidze,
On composite models in the theory of elementary particles, (1965) (cit. on p. 1).

[12] M. Y. Han and Y. Nambu, *Three Triplet Model with Double SU(3) Symmetry*,
Phys. Rev. **139** (1965) B1006, ed. by T. Eguchi (cit. on p. 1).

[13] Y. Miyamoto, *Three Kinds of Triplet Model*,
Progress of Theoretical Physics Supplement **E65** (1965) 187, ISSN: 0375-9687,
eprint: https://academic.oup.com/ptps/article-pdf/doi/10.1143/PTPS.E65.187/5235296/E65-187.pdf,
URL: https://doi.org/10.1143/PTPS.E65.187 (cit. on p. 1).

[14] J. D. Bjorken, *Asymptotic Sum Rules at Infinite Momentum*, Phys. Rev. **179** (5 1969) 1547,
URL: https://link.aps.org/doi/10.1103/PhysRev.179.1547 (cit. on p. 1).

[15] J. I. Friedman, H. W. Kendall and R. E. Taylor, *Nobel lectures in physics 1990*, (1990)
(cit. on p. 2).

[16] E. M. Riordan et al.,
Extraction of $R = \frac{\sigma_L}{\sigma_T}$ from Deep Inelastic $e - p$ and $e - d$ Cross Sections,
Phys. Rev. Lett. **33** (9 1974) 561,
URL: https://link.aps.org/doi/10.1103/PhysRevLett.33.561 (cit. on p. 2).

[17] M. Haguenauer, ""Gargamelle" Experiment",
17th International Conference on High-Energy Physics, 1974 IV.95 (cit. on p. 2).

[18] J. Kuti and V. F. Weisskopf, *Inelastic Lepton-Nucleon Scattering and Lepton Pair Production in the Relativistic Quark-Parton Model*, Phys. Rev. D **4** (11 1971) 3418,
URL: https://link.aps.org/doi/10.1103/PhysRevD.4.3418 (cit. on p. 2).

[19] D. J. Gross and F. Wilczek, *Ultraviolet Behavior of Non-Abelian Gauge Theories*,
Phys. Rev. Lett. **30** (26 1973) 1343,
URL: https://link.aps.org/doi/10.1103/PhysRevLett.30.1343 (cit. on p. 2).

[20] H. D. Politzer, *Reliable Perturbative Results for Strong Interactions?*,
Phys. Rev. Lett. **30** (26 1973) 1346,
URL: https://link.aps.org/doi/10.1103/PhysRevLett.30.1346 (cit. on p. 2).

[21] H. Fritzsch, M. Gell-Mann and H. Leutwyler, *Advantages of the color octet gluon picture*,
Physics Letters B **47** (1973) 365, ISSN: 0370-2693,
URL: https://www.sciencedirect.com/science/article/pii/0370269373906254
(cit. on p. 2).

[22] G. Altarelli, *Experimental tests of perturbative QCD*,
Annu. Rev. Nucl. Part. Sci. **39** (1989) 357, URL: https://cds.cern.ch/record/197024
(cit. on p. 2).

[23] K. G. Wilson, *Confinement of Quarks*, Phys. Rev. D **10** (1974) 2445, ed. by J. C. Taylor
(cit. on p. 2).

[24] N. Metropolis, A. W. Rosenbluth, M. N. Rosenbluth, A. H. Teller and E. Teller,
Equation of state calculations by fast computing machines,
The journal of chemical physics **21** (1953) 1087 (cit. on pp. 2, 15).

[25] M. Creutz, L. Jacobs and C. Rebbi, *Experiments with a Gauge Invariant Ising System*, Phys. Rev. Lett. **42** (1979) 1390 (cit. on p. 2).

[26] K. G. Wilson, *MONTE CARLO CALCULATIONS FOR THE LATTICE GAUGE THEORY*, NATO Sci. Ser. B **59** (1980) 363, ed. by G. 't Hooft et al. (cit. on p. 2).

[27] D. Weingarten, *Monte Carlo Evaluation of Hadron Masses in Lattice Gauge Theories with Fermions*, Phys. Lett. B **109** (1982) 57, ed. by J. Julve and M. Ramón-Medrano (cit. on p. 2).

[28] H. Hamber and G. Parisi, *Numerical Estimates of Hadronic Masses in a Pure SU(3) Gauge Theory*, Phys. Rev. Lett. **47** (1981) 1792, ed. by J. Julve and M. Ramón-Medrano (cit. on p. 2).

[29] M. Fischer, B. Kostrzewa, L. Liu, F. Romero-López, M. Ueding and C. Urbach, *Scattering of two and three physical pions at maximal isospin from lattice QCD*, Eur. Phys. J. C **81** (2021) 436, arXiv: 2008.03035 [hep-lat] (cit. on pp. 3, 4, 132).

[30] A. Alexandru et al., *Finite-volume energy spectrum of the $K^-K^-K^-$ system*, Phys. Rev. D **102** (2020) 114523, arXiv: 2009.12358 [hep-lat] (cit. on pp. 3, 4, 132).

[31] L. Maiani and M. Testa, *Final state interactions from Euclidean correlation functions*, Physics Letters B **245** (1990) 585 (cit. on pp. 3, 18).

[32] M. Luscher, *Volume Dependence of the Energy Spectrum in Massive Quantum Field Theories. 2. Scattering States*, Commun. Math. Phys. **105** (1986) 153 (cit. on pp. 3, 18, 19, 25).

[33] M. Lüscher, *Two-particle states on a torus and their relation to the scattering matrix*, Nuclear Physics B **354** (1991) 531, ISSN: 0550-3213, URL: https://www.sciencedirect.com/science/article/pii/0550321391903666 (cit. on pp. 3, 19, 80, 103, 106).

[34] K. Rummukainen and S. A. Gottlieb, *Resonance scattering phase shifts on a nonrest frame lattice*, Nucl. Phys. B **450** (1995) 397, arXiv: hep-lat/9503028 (cit. on pp. 3, 80).

[35] C. h. Kim, C. T. Sachrajda and S. R. Sharpe, *Finite-volume effects for two-hadron states in moving frames*, Nucl. Phys. B **727** (2005) 218, arXiv: hep-lat/0507006 (cit. on pp. 3, 80).

[36] M. Gockeler et al., *Scattering phases for meson and baryon resonances on general moving-frame lattices*, Phys. Rev. D **86** (2012) 094513, arXiv: 1206.4141 [hep-lat] (cit. on pp. 3, 22, 23, 80, 106, 161).

[37] R. A. Briceño, *Two-particle multichannel systems in a finite volume with arbitrary spin*, Phys. Rev. D **89** (7 2014) 074507, URL: https://link.aps.org/doi/10.1103/PhysRevD.89.074507 (cit. on pp. 3, 20).

[38] F. Romero-López, A. Rusetsky and C. Urbach, *Vector particle scattering on the lattice*, Phys. Rev. D **98** (2018) 014503, arXiv: 1802.03458 [hep-lat] (cit. on p. 3).

[39] S. He, X. Feng and C. Liu, *Two particle states and the S-matrix elements in multi-channel scattering*, JHEP **07** (2005) 011, arXiv: hep-lat/0504019 (cit. on pp. 3, 20, 80).

[40] M. Lage, U.-G. Meißner and A. Rusetsky,
A method to measure the antikaon–nucleon scattering length in lattice QCD,
Physics Letters B **681** (2009) 439, ISSN: 0370-2693, URL:
https://www.sciencedirect.com/science/article/pii/S0370269309012520
(cit. on pp. 3, 20).

[41] M. T. Hansen and S. R. Sharpe, *Multiple-channel generalization of Lellouch-Lüscher formula*,
Phys. Rev. D **86** (1 2012) 016007,
URL: https://link.aps.org/doi/10.1103/PhysRevD.86.016007
(cit. on pp. 3, 20, 80, 133).

[42] R. A. Briceño and Z. Davoudi,
Moving multichannel systems in a finite volume with application to proton-proton fusion,
Phys. Rev. D **88** (9 2013) 094507,
URL: https://link.aps.org/doi/10.1103/PhysRevD.88.094507
(cit. on pp. 3, 20, 80).

[43] L. Lellouch and M. Luscher,
Weak transition matrix elements from finite volume correlation functions,
Commun. Math. Phys. **219** (2001) 31, arXiv: hep-lat/0003023 (cit. on pp. 3, 26, 133).

[44] N. H. Christ, C. Kim and T. Yamazaki,
Finite volume corrections to the two-particle decay of states with non-zero momentum,
Phys. Rev. D **72** (2005) 114506, arXiv: hep-lat/0507009 (cit. on p. 3).

[45] R. A. Briceño, M. T. Hansen and A. Walker-Loud,
Multichannel $1 \to 2$ transition amplitudes in a finite volume, Phys. Rev. D **91** (2015) 034501,
arXiv: 1406.5965 [hep-lat] (cit. on p. 3).

[46] R. A. Briceño and M. T. Hansen,
Relativistic, model-independent, multichannel $2 \to 2$ transition amplitudes in a finite volume,
Phys. Rev. D **94** (2016) 013008, arXiv: 1509.08507 [hep-lat] (cit. on p. 3).

[47] W. Detmold and M. J. Savage,
Electroweak matrix elements in the two-nucleon sector from lattice QCD,
Nuclear Physics A **743** (2004) 170, ISSN: 0375-9474, URL:
https://www.sciencedirect.com/science/article/pii/S0375947404008152
(cit. on p. 3).

[48] V. Bernard, D. Hoja, U. G. Meissner and A. Rusetsky, *Matrix elements of unstable states*,
JHEP **09** (2012) 023, arXiv: 1205.4642 [hep-lat] (cit. on pp. 3, 41, 43, 133).

[49] A. Agadjanov, V. Bernard, U. G. Meißner and A. Rusetsky,
A framework for the calculation of the $\Delta N\gamma^*$ transition form factors on the lattice,
Nucl. Phys. B **886** (2014) 1199, arXiv: 1405.3476 [hep-lat] (cit. on p. 3).

[50] A. Baroni, R. A. Briceño, M. T. Hansen and F. G. Ortega-Gama,
Form factors of two-hadron states from a covariant finite-volume formalism,
Phys. Rev. D **100** (3 2019) 034511,
URL: https://link.aps.org/doi/10.1103/PhysRevD.100.034511 (cit. on p. 3).

[51] J. Lozano, U.-G. Meißner, F. Romero-López, A. Rusetsky and G. Schierholz, *Resonance form factors from finite-volume correlation functions with the external field method*, JHEP **10** (2022) 106, arXiv: 2205.11316 [hep-lat] (cit. on p. 3).

[52] K. H. Sherman, F. G. Ortega-Gama, R. A. Briceño and A. W. Jackura, *Two-current transition amplitudes with two-body final states*, Phys. Rev. D **105** (11 2022) 114510, URL: https://link.aps.org/doi/10.1103/PhysRevD.105.114510 (cit. on p. 3).

[53] R. A. Briceno, J. J. Dudek and R. D. Young, *Scattering processes and resonances from lattice QCD*, Rev. Mod. Phys. **90** (2018) 025001, arXiv: 1706.06223 [hep-lat] (cit. on p. 3).

[54] M. Mai, U.-G. Meißner and C. Urbach, *Towards a theory of hadron resonances*, Phys. Rept. **1001** (2023) 1, arXiv: 2206.01477 [hep-ph] (cit. on p. 3).

[55] J. R. Green, A. D. Hanlon, P. M. Junnarkar and H. Wittig, *Weakly bound H dibaryon from SU(3)-flavor-symmetric QCD*, Phys. Rev. Lett. **127** (2021) 242003, arXiv: 2103.01054 [hep-lat] (cit. on pp. 3, 81, 98, 102).

[56] L. Meng and E. Epelbaum, *Two-particle scattering from finite-volume quantization conditions using the plane wave basis*, JHEP **10** (2021) 051, arXiv: 2108.02709 [hep-lat] (cit. on pp. 3, 31, 80, 81, 98–100, 102, 103, 173).

[57] L. Meng, V. Baru, E. Epelbaum, A. A. Filin and A. M. Gasparyan, *Solving the left-hand cut problem in lattice QCD: $T_{cc}(3875)^+$ from finite volume energy levels*, Phys. Rev. D **109** (2024) L071506, arXiv: 2312.01930 [hep-lat] (cit. on pp. 3, 31, 80, 81, 99, 102).

[58] M.-L. Du et al., *Role of Left-Hand Cut Contributions on Pole Extractions from Lattice Data: Case Study for $T_{cc}(3875)^+$*, Phys. Rev. Lett. **131** (13 2023) 131903, URL: https://link.aps.org/doi/10.1103/PhysRevLett.131.131903 (cit. on pp. 3, 31, 81, 99).

[59] A. B. Raposo and M. T. Hansen, *The Lüscher scattering formalism on the t-channel cut*, PoS **LATTICE2022** (2023) 051, arXiv: 2301.03981 [hep-lat] (cit. on pp. 3, 31, 32, 81).

[60] A. B. Raposo and M. T. Hansen, *Finite-volume scattering on the left-hand cut*, JHEP **08** (2024) 075, arXiv: 2311.18793 [hep-lat] (cit. on pp. 3, 31, 32, 80, 81, 97–100, 102, 103).

[61] M. T. Hansen, F. Romero-López and S. R. Sharpe, *Incorporating $DD\pi$ effects and left-hand cuts in lattice QCD studies of the $T_{cc}(3875)^+$*, JHEP **06** (2024) 051, arXiv: 2401.06609 [hep-lat] (cit. on pp. 3, 31, 80, 81, 99, 100, 102, 103).

[62] S. M. Dawid, F. Romero-López and S. R. Sharpe, *Finite- and infinite-volume study of $DD\pi$ scattering*, JHEP **01** (2025) 060, arXiv: 2409.17059 [hep-lat] (cit. on pp. 3, 80, 102, 103).

[63] S. M. Dawid, F. Romero-López and S. R. Sharpe,
Comparison of integral equations used to study T_{cc}^+, (2025), arXiv: 2505.05466 [nucl-th]
(cit. on pp. 3, 31, 102, 103).

[64] H. van Haeringen and L. P. Kok, *Modified effective-range function*,
Phys. Rev. A **26** (3 1982) 1218,
URL: https://link.aps.org/doi/10.1103/PhysRevA.26.1218
(cit. on pp. 3, 21, 29, 79, 82–84, 89, 90, 92, 100, 103, 165).

[65] K. Polejaeva and A. Rusetsky, *Three particles in a finite volume*, Eur. Phys. J. A **48** (2012) 67,
arXiv: 1203.1241 [hep-lat] (cit. on pp. 3, 28, 132).

[66] R. A. Briceño and Z. Davoudi,
Three-particle scattering amplitudes from a finite volume formalism,
Phys. Rev. D **87** (9 2013) 094507,
URL: https://link.aps.org/doi/10.1103/PhysRevD.87.094507 (cit. on pp. 3, 132).

[67] M. T. Hansen and S. R. Sharpe,
Relativistic, model-independent, three-particle quantization condition,
Phys. Rev. D **90** (11 2014) 116003,
URL: https://link.aps.org/doi/10.1103/PhysRevD.90.116003
(cit. on pp. 3, 28, 81, 132).

[68] M. T. Hansen and S. R. Sharpe, *Expressing the three-particle finite-volume spectrum in terms of the three-to-three scattering amplitude*, Phys. Rev. D **92** (11 2015) 114509,
URL: https://link.aps.org/doi/10.1103/PhysRevD.92.114509
(cit. on pp. 3, 28, 81, 132).

[69] M. Mai and M. Döring, *Three-body Unitarity in the Finite Volume*,
Eur. Phys. J. A **53** (2017) 240, arXiv: 1709.08222 [hep-lat] (cit. on pp. 3, 28, 81, 132).

[70] H.-W. Hammer, J.-Y. Pang and A. Rusetsky,
Three-particle quantization condition in a finite volume: 1. The role of the three-particle force,
JHEP **09** (2017) 109, arXiv: 1706.07700 [hep-lat] (cit. on pp. 3, 28, 53, 58, 81, 132).

[71] H.-W. Hammer, J.-Y. Pang and A. Rusetsky, *Three particle quantization condition in a finite volume: 2. general formalism and the analysis of data*, JHEP **10** (2017) 115,
arXiv: 1707.02176 [hep-lat] (cit. on pp. 3, 28, 53, 58, 59, 81, 132, 136, 142).

[72] M. T. Hansen and S. R. Sharpe, *Lattice QCD and Three-particle Decays of Resonances*,
Ann. Rev. Nucl. Part. Sci. **69** (2019) 65, arXiv: 1901.00483 [hep-lat] (cit. on pp. 3, 132).

[73] T. D. Blanton and S. R. Sharpe,
Equivalence of relativistic three-particle quantization conditions,
Phys. Rev. D **102** (5 2020) 054515,
URL: https://link.aps.org/doi/10.1103/PhysRevD.102.054515
(cit. on pp. 3, 132).

[74] A. W. Jackura et al., *Equivalence of three-particle scattering formalisms*,
Phys. Rev. D **100** (2019) 034508, arXiv: 1905.12007 [hep-ph] (cit. on pp. 3, 132).

[75] T. D. Blanton, F. Romero-López and S. R. Sharpe,
$I = 3$ Three-Pion Scattering Amplitude from Lattice QCD,
Phys. Rev. Lett. **124** (3 2020) 032001,
URL: https://link.aps.org/doi/10.1103/PhysRevLett.124.032001
(cit. on pp. 4, 132).

[76] Z. T. Draper, A. D. Hanlon, B. Hörz, C. Morningstar, F. Romero-López and S. R. Sharpe,
Interactions of πK, $\pi\pi K$ and $KK\pi$ systems at maximal isospin from lattice QCD,
JHEP **05** (2023) 137, arXiv: 2302.13587 [hep-lat] (cit. on p. 4).

[77] R. Brett, C. Culver, M. Mai, A. Alexandru, M. Döring and F. X. Lee,
Three-body interactions from the finite-volume QCD spectrum,
Phys. Rev. D **104** (2021) 014501, arXiv: 2101.06144 [hep-lat] (cit. on pp. 4, 132).

[78] M. Mai et al., *Three-Body Dynamics of the $a_1(1260)$ Resonance from Lattice QCD*,
Phys. Rev. Lett. **127** (2021) 222001, arXiv: 2107.03973 [hep-lat] (cit. on pp. 4, 132).

[79] H. Yan et al., *ω Meson from Lattice QCD*, Phys. Rev. Lett. **133** (2024) 211906,
arXiv: 2407.16659 [hep-lat] (cit. on p. 4).

[80] M. Garofalo, M. Mai, F. Romero-López, A. Rusetsky and C. Urbach,
Three-body resonances in the φ^4 theory, JHEP **02** (2023) 252,
arXiv: 2211.05605 [hep-lat] (cit. on pp. 4, 151).

[81] F. Müller, J.-Y. Pang, A. Rusetsky and J.-J. Wu,
Relativistic-invariant formulation of the NREFT three-particle quantization condition,
JHEP **02** (2022) 158, arXiv: 2110.09351 [hep-lat]
(cit. on pp. 4, 53, 55, 56, 58, 62, 65, 69, 132, 136, 142, 149).

[82] R. A. Briceño, M. T. Hansen and S. R. Sharpe, *Relating the finite-volume spectrum and the two-and-three-particle S matrix for relativistic systems of identical scalar particles*,
Phys. Rev. D **95** (2017) 074510, arXiv: 1701.07465 [hep-lat] (cit. on pp. 4, 132).

[83] R. A. Briceño, M. T. Hansen and S. R. Sharpe,
Three-particle systems with resonant subprocesses in a finite volume,
Phys. Rev. D **99** (2019) 014516, arXiv: 1810.01429 [hep-lat] (cit. on pp. 4, 132).

[84] M. T. Hansen, F. Romero-López and S. R. Sharpe,
Generalizing the relativistic quantization condition to include all three-pion isospin channels,
JHEP **07** (2020) 047, [Erratum: JHEP 02, 014 (2021)], arXiv: 2003.10974 [hep-lat]
(cit. on pp. 4, 132).

[85] T. D. Blanton and S. R. Sharpe,
Relativistic three-particle quantization condition for nondegenerate scalars,
Phys. Rev. D **103** (2021) 054503, arXiv: 2011.05520 [hep-lat] (cit. on pp. 4, 132).

[86] T. D. Blanton and S. R. Sharpe,
Three-particle finite-volume formalism for $\pi^+\pi^+K^+$ and related systems,
Phys. Rev. D **104** (2021) 034509, arXiv: 2105.12094 [hep-lat] (cit. on pp. 4, 132).

[87] Z. T. Draper, M. T. Hansen, F. Romero-López and S. R. Sharpe,
Three relativistic neutrons in a finite volume, JHEP **07** (2023) 226,
arXiv: 2303.10219 [hep-lat] (cit. on pp. 4, 129, 132, 167).

[88] K. Huang and C. N. Yang,
Quantum-Mechanical Many-Body Problem with Hard-Sphere Interaction,
Phys. Rev. **105** (3 1957) 767,
URL: https://link.aps.org/doi/10.1103/PhysRev.105.767 (cit. on pp. 4, 19, 28).

[89] T. T. Wu, *Ground State of a Bose System of Hard Spheres*, Phys. Rev. **115** (6 1959) 1390,
URL: https://link.aps.org/doi/10.1103/PhysRev.115.1390 (cit. on p. 4).

[90] T. D. Lee, K. Huang and C. N. Yang, *Eigenvalues and Eigenfunctions of a Bose System of Hard Spheres and Its Low-Temperature Properties*, Phys. Rev. **106** (6 1957) 1135,
URL: https://link.aps.org/doi/10.1103/PhysRev.106.1135 (cit. on pp. 4, 19, 28).

[91] S. R. Beane, W. Detmold and M. J. Savage,
n-Boson Energies at Finite Volume and Three-Boson Interactions,
Phys. Rev. D **76** (2007) 074507, arXiv: 0707.1670 [hep-lat]
(cit. on pp. 4, 26, 28, 49, 126–128).

[92] M. T. Hansen and S. R. Sharpe,
Perturbative results for two and three particle threshold energies in finite volume,
Phys. Rev. D **93** (2016) 014506, arXiv: 1509.07929 [hep-lat] (cit. on pp. 4, 26, 132).

[93] S. Tan,
Three-boson problem at low energy and implications for dilute Bose-Einstein condensates,
Phys. Rev. A **78** (2008) 013636, arXiv: 0709.2530 [cond-mat.stat-mech] (cit. on p. 4).

[94] W. Detmold and M. J. Savage,
*The Energy of n Identical Bosons in a Finite Volume at O(L**-7)*,
Phys. Rev. D **77** (2008) 057502, arXiv: 0801.0763 [hep-lat] (cit. on pp. 4, 28, 49).

[95] J.-Y. Pang, J.-J. Wu, H.-W. Hammer, U.-G. Meißner and A. Rusetsky,
Energy shift of the three-particle system in a finite volume, Phys. Rev. D **99** (2019) 074513,
arXiv: 1902.01111 [hep-lat] (cit. on pp. 4, 132, 144).

[96] M. T. Hansen and S. R. Sharpe,
Threshold expansion of the three-particle quantization condition,
Phys. Rev. D **93** (2016) 096006, [Erratum: Phys.Rev.D 96, 039901 (2017)],
arXiv: 1602.00324 [hep-lat] (cit. on pp. 4, 26, 132).

[97] F. Romero-López, A. Rusetsky, N. Schlage and C. Urbach,
Relativistic N-particle energy shift in finite volume, JHEP **02** (2021) 060,
arXiv: 2010.11715 [hep-lat] (cit. on pp. 4, 28, 44, 48, 49, 125–127, 132).

[98] F. Müller, T. Yu and A. Rusetsky, *Finite-volume energy shift of the three-pion ground state*,
Phys. Rev. D **103** (2021) 054506, arXiv: 2011.14178 [hep-lat]
(cit. on pp. 4, 28, 49, 126, 127, 132, 166, 180, 181).

[99] R. Bubna, F. Müller and A. Rusetsky,
Finite-volume energy shift of the three-nucleon ground state, Phys. Rev. D **108** (2023) 014518,
arXiv: 2304.13635 [hep-lat] (cit. on pp. 4, 28, 49, 125, 132, 166).

[100] F. Müller and A. Rusetsky, *On the three-particle analog of the Lellouch-Lüscher formula*,
JHEP **03** (2021) 152, arXiv: 2012.13957 [hep-lat] (cit. on pp. 4, 29, 69, 132, 133, 167).

[101] F. Müller, J.-Y. Pang, A. Rusetsky and J.-J. Wu,
Three-particle Lellouch-Lüscher formalism in moving frames, JHEP **02** (2023) 214,
arXiv: 2211.10126 [hep-lat]
(cit. on pp. 4, 29, 69, 70, 72, 76, 131–133, 136, 140, 142, 148, 149, 158, 167).

[102] M. T. Hansen, F. Romero-López and S. R. Sharpe,
Decay amplitudes to three hadrons from finite-volume matrix elements, JHEP **04** (2021) 113,
arXiv: 2101.10246 [hep-lat] (cit. on pp. 4, 29, 69, 76, 132–134, 158).

[103] U.-G. Meißner and A. Rusetsky, *Effective Field Theories*, Cambridge University Press, 2022,
ISBN: 978-1-108-68903-8 (cit. on pp. 5, 26, 34, 41, 49, 51, 52).

[104] S. Weinberg, *Phenomenological Lagrangians*,
Physica A: Statistical Mechanics and its Applications **96** (1979) 327, ISSN: 0378-4371,
URL: https://www.sciencedirect.com/science/article/pii/0378437179902231
(cit. on p. 5).

[105] J. Gasser and H. Leutwyler, *Chiral perturbation theory to one loop*,
Annals of Physics **158** (1984) 142, ISSN: 0003-4916,
URL: https://www.sciencedirect.com/science/article/pii/0003491684902422
(cit. on p. 5).

[106] J. Gasser and H. Leutwyler,
Chiral perturbation theory: Expansions in the mass of the strange quark,
Nuclear Physics B **250** (1985) 465, ISSN: 0550-3213,
URL: https://www.sciencedirect.com/science/article/pii/0550321385904924
(cit. on p. 5).

[107] C. Vafa and E. Witten, *Restrictions on symmetry breaking in vector-like gauge theories*,
Nuclear Physics B **234** (1984) 173, ISSN: 0550-3213,
URL: https://www.sciencedirect.com/science/article/pii/055032138490230X
(cit. on p. 5).

[108] J. Goldstone, *Field Theories with Superconductor Solutions*, Nuovo Cim. **19** (1961) 154
(cit. on p. 5).

[109] J. Goldstone, A. Salam and S. Weinberg, *Broken Symmetries*, Phys. Rev. **127** (3 1962) 965,
URL: https://link.aps.org/doi/10.1103/PhysRev.127.965 (cit. on p. 5).

[110] M. Gell-Mann, R. J. Oakes and B. Renner,
Behavior of Current Divergences under $SU_3 \times SU_3$, Phys. Rev. **175** (5 1968) 2195,
URL: https://link.aps.org/doi/10.1103/PhysRev.175.2195 (cit. on p. 5).

[111] S. Coleman, J. Wess and B. Zumino, *Structure of Phenomenological Lagrangians. I*,
Phys. Rev. **177** (5 1969) 2239,
URL: https://link.aps.org/doi/10.1103/PhysRev.177.2239 (cit. on p. 5).

[112] C. G. Callan, S. Coleman, J. Wess and B. Zumino,
Structure of Phenomenological Lagrangians. II, Phys. Rev. **177** (5 1969) 2247,
URL: https://link.aps.org/doi/10.1103/PhysRev.177.2247 (cit. on p. 5).

[113] T. Becher and H. Leutwyler,
Baryon chiral perturbation theory in manifestly Lorentz invariant form,
Eur. Phys. J. **9** (1999) 643, arXiv: hep-ph/9901384 (cit. on p. 5).

[114] J. Gegelia and G. Japaridze, *Matching heavy particle approach to relativistic theory*,
Phys. Rev. D **60** (1999) 114038, arXiv: hep-ph/9908377 (cit. on p. 5).

[115] T. Fuchs, J. Gegelia, G. Japaridze and S. Scherer,
Renormalization of relativistic baryon chiral perturbation theory and power counting,
Phys. Rev. D **68** (2003) 056005, arXiv: hep-ph/0302117 (cit. on p. 5).

[116] E. Jenkins and A. V. Manohar,
Baryon chiral perturbation theory using a heavy fermion lagrangian,
Physics Letters B **255** (1991) 558, ISSN: 0370-2693,
URL: https://www.sciencedirect.com/science/article/pii/037026939190266S
(cit. on p. 5).

[117] V. Bernard, N. Kaiser, J. Kambor and U.-G. Meißner, *Chiral structure of the nucleon*,
Nuclear Physics B **388** (1992) 315, ISSN: 0550-3213,
URL: https://www.sciencedirect.com/science/article/pii/055032139290615I
(cit. on pp. 5, 34).

[118] S. Myint and C. Rebbi, *Chiral perturbation theory on the lattice: Strong coupling expansion*,
Nuclear Physics B **421** (1994) 241, ISSN: 0550-3213,
URL: https://www.sciencedirect.com/science/article/pii/055032139490233X
(cit. on p. 5).

[119] S. Sharpe and R. Singleton, *Spontaneous flavor and parity breaking with Wilson fermions*,
Phys. Rev. D **58** (7 1998) 074501,
URL: https://link.aps.org/doi/10.1103/PhysRevD.58.074501 (cit. on p. 5).

[120] W. Lee and S. R. Sharpe, *Partial flavor symmetry restoration for chiral staggered fermions*,
Phys. Rev. D **60** (11 1999) 114503,
URL: https://link.aps.org/doi/10.1103/PhysRevD.60.114503 (cit. on p. 5).

[121] J. Gasser and H. Leutwyler, *Light quarks at low temperatures*,
Physics Letters B **184** (1987) 83, ISSN: 0370-2693,
URL: https://www.sciencedirect.com/science/article/pii/0370269387904928
(cit. on p. 5).

[122] H. Leutwyler, *Energy levels of light quarks confined to a box*,
Physics Letters B **189** (1987) 197, ISSN: 0370-2693,
URL: https://www.sciencedirect.com/science/article/pii/0370269387912962
(cit. on p. 5).

[123] J. Gasser and H. Leutwyler,
Spontaneously broken symmetries: Effective lagrangians at finite volume,
Nuclear Physics B **307** (1988) 763, ISSN: 0550-3213,
URL: https://www.sciencedirect.com/science/article/pii/0550321388901071
(cit. on p. 5).

[124] Y. Aoki et al., *FLAG Review 2021*, Eur. Phys. J. C **82** (2022) 869,
arXiv: 2111.09849 [hep-lat] (cit. on p. 5).

[125] W. E. Caswell and G. P. Lepage,
Effective Lagrangians for Bound State Problems in QED, QCD, and Other Field Theories,
Phys. Lett. B **167** (1986) 437 (cit. on p. 5).

[126] G. T. Bodwin, E. Braaten and G. P. Lepage,
Rigorous QCD analysis of inclusive annihilation and production of heavy quarkonium,
Phys. Rev. D **51** (1995) 1125, [Erratum: Phys.Rev.D 55, 5853 (1997)],
arXiv: hep-ph/9407339 (cit. on p. 5).

[127] A. Gall, J. Gasser, V. E. Lyubovitskij and A. Rusetsky, *On the lifetime of the $\pi^+\pi^-$ atom*,
Phys. Lett. B **462** (1999) 335, arXiv: hep-ph/9905309 (cit. on p. 5).

[128] D. B. Kaplan, M. J. Savage and M. B. Wise,
Nucleon-nucleon scattering from effective field theory, Nuclear Physics B **478** (1996) 629,
ISSN: 0550-3213,
URL: https://www.sciencedirect.com/science/article/pii/0550321396003574
(cit. on p. 5).

[129] D. B. Kaplan, *More effective field theory for non-relativistic scattering*,
Nuclear Physics B **494** (1997) 471, ISSN: 0550-3213, URL:
https://www.sciencedirect.com/science/article/pii/S0550321397001788
(cit. on p. 5).

[130] D. B. Kaplan, M. J. Savage and M. B. Wise,
A New expansion for nucleon-nucleon interactions, Phys. Lett. B **424** (1998) 390,
arXiv: nucl-th/9801034 (cit. on p. 5).

[131] S. Weinberg, *Nuclear forces from chiral lagrangians*, Physics Letters B **251** (1990) 288,
ISSN: 0370-2693,
URL: https://www.sciencedirect.com/science/article/pii/0370269390909383
(cit. on p. 5).

[132] U. van Kolck, *Few-nucleon forces from chiral Lagrangians*, Phys. Rev. C **49** (6 1994) 2932,
URL: https://link.aps.org/doi/10.1103/PhysRevC.49.2932 (cit. on p. 5).

[133] P. Bedaque and U. van Kolck, *Nucleon-deuteron scattering from an effective field theory*,
Physics Letters B **428** (1998) 221, ISSN: 0370-2693, URL:
https://www.sciencedirect.com/science/article/pii/S0370269398004304
(cit. on p. 6).

[134] P. F. Bedaque, H. W. Hammer and U. van Kolck,
The Three boson system with short range interactions, Nucl. Phys. A **646** (1999) 444,
arXiv: nucl-th/9811046 (cit. on pp. 6, 56, 134, 136, 142, 143, 155).

[135] E. Epelbaum, H.-W. Hammer and U.-G. Meissner, *Modern Theory of Nuclear Forces*,
Rev. Mod. Phys. **81** (2009) 1773, arXiv: 0811.1338 [nucl-th] (cit. on p. 6).

[136] P. F. Bedaque, H. W. Hammer and U. van Kolck, *Effective theory of the triton*,
Nucl. Phys. A **676** (2000) 357, arXiv: nucl-th/9906032 (cit. on pp. 6, 125, 126).

[137] S. Kreuzer and H.-W. Hammer, *Efimov physics in a finite volume*, Physics Letters B **673** (2009) 260, ISSN: 0370-2693, URL: https://www.sciencedirect.com/science/article/pii/S0370269309002135 (cit. on pp. 6, 132).

[138] S. Kreuzer and H.-W. Hammer, *On the modification of the Efimov spectrum in a finite cubic box*, Eur. Phys. J. A **43** (2010) 229, arXiv: 0910.2191 [nucl-th] (cit. on pp. 6, 132).

[139] S. Kreuzer and H.-W. Hammer, *The Triton in a finite volume*, Phys. Lett. B **694** (2011) 424, arXiv: 1008.4499 [hep-lat] (cit. on pp. 6, 132).

[140] S. Kreuzer and H. W. Grießhammer, *Three particles in a finite volume: The breakdown of spherical symmetry*, Eur. Phys. J. A **48** (2012) 93, arXiv: 1205.0277 [nucl-th] (cit. on pp. 6, 132).

[141] J. Gasser, V. E. Lyubovitskij and A. Rusetsky, *Hadronic atoms in QCD + QED*, Phys. Rept. **456** (2008) 167, arXiv: 0711.3522 [hep-ph] (cit. on p. 6).

[142] S. Navas et al., *Review of Particle Physics*, Phys. Rev. D **110** (3 2024) 030001, URL: https://link.aps.org/doi/10.1103/PhysRevD.110.030001 (cit. on p. 8).

[143] C. Gattringer and C. B. Lang, *Quantum chromodynamics on the lattice*, vol. 788, Berlin: Springer, 2010, ISBN: 978-3-642-01849-7, 978-3-642-01850-3 (cit. on pp. 10, 18).

[144] K. Osterwalder and R. Schrader, *AXIOMS FOR EUCLIDEAN GREEN'S FUNCTIONS*, Commun. Math. Phys. **31** (1973) 83 (cit. on p. 10).

[145] K. Osterwalder and R. Schrader, *Axioms for Euclidean Green's Functions. 2.*, Commun. Math. Phys. **42** (1975) 281 (cit. on p. 10).

[146] H. B. Nielsen and M. Ninomiya, *Absence of Neutrinos on a Lattice. 1. Proof by Homotopy Theory*, Nucl. Phys. B **185** (1981) 20, ed. by J. Julve and M. Ramón-Medrano, [Erratum: Nucl.Phys.B 195, 541 (1982)] (cit. on p. 13).

[147] K. G. Wilson, *Confinement of quarks*, Phys. Rev. D **10** (8 1974) 2445, URL: https://link.aps.org/doi/10.1103/PhysRevD.10.2445 (cit. on p. 13).

[148] J. Kogut and L. Susskind, *Hamiltonian formulation of Wilson's lattice gauge theories*, Phys. Rev. D **11** (2 1975) 395, URL: https://link.aps.org/doi/10.1103/PhysRevD.11.395 (cit. on p. 13).

[149] L. Susskind, *Lattice fermions*, Phys. Rev. D **16** (10 1977) 3031, URL: https://link.aps.org/doi/10.1103/PhysRevD.16.3031 (cit. on p. 13).

[150] H. Neuberger, *Exactly massless quarks on the lattice*, Phys. Lett. B **417** (1998) 141, arXiv: hep-lat/9707022 (cit. on p. 14).

[151] H. Neuberger, *More about exactly massless quarks on the lattice*, Phys. Lett. B **427** (1998) 353, arXiv: hep-lat/9801031 (cit. on p. 14).

[152] D. B. Kaplan, *A Method for simulating chiral fermions on the lattice*, Phys. Lett. B **288** (1992) 342, arXiv: hep-lat/9206013 (cit. on p. 14).

[153] V. Furman and Y. Shamir, *Axial symmetries in lattice QCD with Kaplan fermions*, Nucl. Phys. B **439** (1995) 54, arXiv: hep-lat/9405004 (cit. on p. 14).

[154] M. Luscher, *Exact chiral symmetry on the lattice and the Ginsparg-Wilson relation*, Phys. Lett. B **428** (1998) 342, arXiv: hep-lat/9802011 (cit. on p. 14).

[155] K. Symanzik, *Continuum limit and improved action in lattice theories: (I). Principles and φ^4 theory*, Nuclear Physics B **226** (1983) 187, ISSN: 0550-3213, URL: https://www.sciencedirect.com/science/article/pii/0550321383904686 (cit. on p. 14).

[156] K. Symanzik, *Continuum limit and improved action in lattice theories: (II). O(N) non-linear sigma model in perturbation theory*, Nuclear Physics B **226** (1983) 205, ISSN: 0550-3213, URL: https://www.sciencedirect.com/science/article/pii/0550321383904698 (cit. on p. 14).

[157] B. Sheikholeslami and R. Wohlert, *Improved continuum limit lattice action for QCD with wilson fermions*, Nuclear Physics B **259** (1985) 572, ISSN: 0550-3213, URL: https://www.sciencedirect.com/science/article/pii/0550321385900021 (cit. on p. 14).

[158] M. Luscher, S. Sint, R. Sommer and P. Weisz, *Chiral symmetry and O(a) improvement in lattice QCD*, Nucl. Phys. B **478** (1996) 365, arXiv: hep-lat/9605038 (cit. on p. 14).

[159] M. Luscher, S. Sint, R. Sommer, P. Weisz and U. Wolff, *Nonperturbative O(a) improvement of lattice QCD*, Nucl. Phys. B **491** (1997) 323, arXiv: hep-lat/9609035 (cit. on p. 14).

[160] K. Jansen and R. Sommer, *O(a) improvement of lattice QCD with two flavors of Wilson quarks*, Nucl. Phys. B **530** (1998) 185, [Erratum: Nucl.Phys.B 643, 517–518 (2002)], arXiv: hep-lat/9803017 (cit. on p. 14).

[161] P. Weisz, *Continuum limit improved lattice action for pure Yang-Mills theory (I)*, Nuclear Physics B **212** (1983) 1, ISSN: 0550-3213, URL: https://www.sciencedirect.com/science/article/pii/0550321383905953 (cit. on p. 14).

[162] P. Weisz and R. Wohlert, *Continuum Limit Improved Lattice Action for Pure Yang-Mills Theory. 2.*, Nucl. Phys. B **236** (1984) 397, [Erratum: Nucl.Phys.B 247, 544 (1984)] (cit. on p. 14).

[163] M. Luscher and P. Weisz, *On-shell improved lattice gauge theories*, Commun. Math. Phys. **98** (1985) 433, [Erratum: Commun.Math.Phys. 98, 433 (1985)] (cit. on p. 14).

[164] T. Takaishi, *Heavy quark potential and effective actions on blocked configurations*, Phys. Rev. D **54** (1 1996) 1050, URL: https://link.aps.org/doi/10.1103/PhysRevD.54.1050 (cit. on p. 14).

[165] S. Duane, A. Kennedy, B. J. Pendleton and D. Roweth, *Hybrid Monte Carlo*, Physics Letters B **195** (1987) 216, ISSN: 0370-2693, URL: https://www.sciencedirect.com/science/article/pii/037026938791197X (cit. on p. 15).

[166] W. K. Hastings, *Monte Carlo sampling methods using Markov chains and their applications*, Biometrika **57** (1970) 97, ISSN: 0006-3444, eprint: https://academic.oup.com/biomet/article-pdf/57/1/97/23940249/57-1-97.pdf, URL: https://doi.org/10.1093/biomet/57.1.97 (cit. on p. 15).

[167] S. Durr et al., *Ab-Initio Determination of Light Hadron Masses*, Science **322** (2008) 1224, arXiv: 0906.3599 [hep-lat] (cit. on pp. 17, 18).

[168] M. Creutz, *Gauge fixing, the transfer matrix, and confinement on a lattice*, Phys. Rev. D **15** (4 1977) 1128, URL: https://link.aps.org/doi/10.1103/PhysRevD.15.1128 (cit. on p. 18).

[169] S. Güsken, U. Löw, K.-H. Mütter, R. Sommer, A. Patel and K. Schilling, *Non-singlet axial vector couplings of the baryon octet in lattice QCD*, Physics Letters B **227** (1989) 266, ISSN: 0370-2693, URL: https://www.sciencedirect.com/science/article/pii/S0370269389800346 (cit. on p. 18).

[170] C. Alexandrou, F. Jegerlehner, S. Güsken, K. Schilling and R. Sommer, *B-meson properties from lattice QCD*, Physics Letters B **256** (1991) 60, ISSN: 0370-2693, URL: https://www.sciencedirect.com/science/article/pii/037026939190219G (cit. on p. 18).

[171] C. R. Allton et al., *Gauge invariant smearing and matrix correlators using Wilson fermions at Beta = 6.2*, Phys. Rev. D **47** (1993) 5128, arXiv: hep-lat/9303009 (cit. on p. 18).

[172] M. Albanese et al., *Glueball masses and string tension in lattice QCD*, Physics Letters B **192** (1987) 163, ISSN: 0370-2693, URL: https://www.sciencedirect.com/science/article/pii/0370269387911609 (cit. on p. 18).

[173] A. Hasenfratz and F. Knechtli, *Flavor symmetry and the static potential with hypercubic blocking*, Phys. Rev. D **64** (2001) 034504, arXiv: hep-lat/0103029 (cit. on p. 18).

[174] C. Morningstar and M. J. Peardon, *Analytic smearing of SU(3) link variables in lattice QCD*, Phys. Rev. D **69** (2004) 054501, arXiv: hep-lat/0311018 (cit. on p. 18).

[175] M. Luscher and U. Wolff, *How to Calculate the Elastic Scattering Matrix in Two-dimensional Quantum Field Theories by Numerical Simulation*, Nucl. Phys. B **339** (1990) 222 (cit. on p. 18).

[176] H. A. Bethe, *Theory of the Effective Range in Nuclear Scattering*, Phys. Rev. **76** (1 1949) 38, URL: https://link.aps.org/doi/10.1103/PhysRev.76.38 (cit. on pp. 20, 120, 121).

[177] M. Döring, H. .-. Hammer, M. Mai, J. .-. Pang, §. A. Rusetsky and J. Wu,
Three-body spectrum in a finite volume: the role of cubic symmetry,
Phys. Rev. D **97** (2018) 114508, arXiv: 1802.03362 [hep-lat]
(cit. on pp. 21, 69, 149, 173).

[178] F. Lee, A. Alexandru and R. Brett,
Higher order quantization conditions for two spinless particles,
PoS **LATTICE2021** (2022) 235, arXiv: 2110.03750 [hep-lat] (cit. on pp. 21, 23).

[179] V. Bernard, M. Lage, U.-G. Meissner and A. Rusetsky,
Resonance properties from the finite-volume energy spectrum, JHEP **08** (2008) 024,
arXiv: 0806.4495 [hep-lat] (cit. on pp. 22, 23, 37, 106).

[180] F.-K. Guo, C. Hanhart, U.-G. Meißner, Q. Wang, Q. Zhao and B.-S. Zou, *Hadronic molecules*,
Rev. Mod. Phys. **90** (2018) 015004, [Erratum: Rev.Mod.Phys. 94, 029901 (2022)],
arXiv: 1705.00141 [hep-ph] (cit. on p. 24).

[181] U.-J. Wiese, *Identification of resonance parameters from the finite volume energy spectrum*,
Nuclear Physics B - Proceedings Supplements **9** (1989) 609, ISSN: 0920-5632,
URL: https://www.sciencedirect.com/science/article/pii/0920563289901710
(cit. on p. 25).

[182] C. Culver, M. Mai, A. Alexandru, M. Döring and F. X. Lee,
Pion scattering in the isospin $I = 2$ channel from elongated lattices,
Phys. Rev. D **100** (2019) 034509, arXiv: 1905.10202 [hep-lat] (cit. on p. 25).

[183] F. Müller, *A Non-Relativistic Effective Field Theory Approach*,
PhD thesis: U. Bonn (main), 2024 (cit. on pp. 25, 26).

[184] Z. Bai et al., *Standard Model Prediction for Direct CP Violation in $K \to \pi\pi$ Decay*,
Phys. Rev. Lett. **115** (2015) 212001, arXiv: 1505.07863 [hep-lat] (cit. on p. 26).

[185] R. Abbott et al.,
Direct CP violation and the $\Delta I = 1/2$ rule in $K \to \pi\pi$ decay from the standard model,
Phys. Rev. D **102** (2020) 054509, arXiv: 2004.09440 [hep-lat] (cit. on p. 26).

[186] T. Blum et al., *ΔI=3/2 and ΔI=1/2 channels of $K \to \pi\pi$ decay at the physical point with periodic boundary conditions*, Phys. Rev. D **108** (2023) 094517,
arXiv: 2306.06781 [hep-lat] (cit. on p. 26).

[187] S. R. Beane et al., *Charged multihadron systems in lattice QCD+QED*,
Phys. Rev. D **103** (2021) 054504, arXiv: 2003.12130 [hep-lat] (cit. on pp. 28, 49).

[188] G. Breit, E. U. Condon and R. D. Present, *Theory of Scattering of Protons by Protons*,
Phys. Rev. **50** (9 1936) 825,
URL: https://link.aps.org/doi/10.1103/PhysRev.50.825 (cit. on p. 29).

[189] G. Breit, H. M. Thaxton and L. Eisenbud,
Analysis of Experiments on the Scattering of Protons by Protons,
Phys. Rev. **55** (11 1939) 1018,
URL: https://link.aps.org/doi/10.1103/PhysRev.55.1018 (cit. on p. 29).

[190] J. D. Jackson and J. M. Blatt, *The Interpretation of Low Energy Proton-Proton Scattering*, Rev. Mod. Phys. **22** (1 1950) 77, URL: https://link.aps.org/doi/10.1103/RevModPhys.22.77 (cit. on p. 29).

[191] G. F. Chew and M. L. Goldberger, *On the Analysis of Nucleon-Nucleon Scattering Experiments*, Phys. Rev. **75** (11 1949) 1637, URL: https://link.aps.org/doi/10.1103/PhysRev.75.1637 (cit. on pp. 29, 120, 121).

[192] T. Teichmann, *On the Interpretation of Resonance Levels and Their Widths in Terms of the Scattering Length and the Effective Range*, Phys. Rev. **83** (1 1951) 141, URL: https://link.aps.org/doi/10.1103/PhysRev.83.141 (cit. on p. 29).

[193] T. Trueman, *Energy level shifts in atomic states of strongly-interacting particles*, Nuclear Physics **26** (1961) 57, ISSN: 0029-5582, URL: https://www.sciencedirect.com/science/article/pii/0029558261901158 (cit. on p. 29).

[194] L. D. Landau and J. Smorodinski, *On the Theory of Scattering of Protons by Protons*, J. Phys. (USSR) **8** (1944), ed. by D. ter Haar (cit. on p. 29).

[195] B. R. Levy and J. B. Keller, *Low-Energy Expansion of Scattering Phase Shifts for Long-Range Potentials*, Journal of Mathematical Physics **4** (1963) 54, ISSN: 0022-2488, eprint: https://pubs.aip.org/aip/jmp/article-pdf/4/1/54/19171221/54_1_online.pdf, URL: https://doi.org/10.1063/1.1703889 (cit. on p. 29).

[196] L. Spruch, T. F. O'Malley and L. Rosenberg, *Modification of Effective-Range Theory in the Presence of a Long-Range Potential*, Phys. Rev. Lett. **5** (8 1960) 375, URL: https://link.aps.org/doi/10.1103/PhysRevLett.5.375 (cit. on p. 29).

[197] T. F. O'Malley, L. Spruch and L. Rosenberg, *Modification of Effective-Range Theory in the Presence of a Long-Range (r-4) Potential*, Journal of Mathematical Physics **2** (1961) 491, ISSN: 0022-2488, eprint: https://pubs.aip.org/aip/jmp/article-pdf/2/4/491/19219774/491_1_online.pdf, URL: https://doi.org/10.1063/1.1703735 (cit. on p. 29).

[198] T. F. O'Malley, *Effect of Long-Range Final-State Forces on the Negative-Ion Photodetachment Cross Section near Threshold*, Phys. Rev. **137** (6A 1965) A1668, URL: https://link.aps.org/doi/10.1103/PhysRev.137.A1668 (cit. on p. 29).

[199] Y. Mentkovsky, *Analytical properties of partial scattering amplitudes of charged particles*, Nuclear Physics **65** (1965) 673, ISSN: 0029-5582, URL: https://www.sciencedirect.com/science/article/pii/0029558265903342 (cit. on p. 29).

[200] N. Holzwarth, *Mathieu function solutions to the radial Schrödinger equation for the- f^2/r^4 interaction*, Journal of Mathematical Physics **14** (1973) 191 (cit. on p. 29).

[201] Vishwamittar, *Theory of low-energy scattering by a long-range potential*, Journal of Physics B: Atomic and Molecular Physics **11** (1978) 2313, URL: https://dx.doi.org/10.1088/0022-3700/11/13/015 (cit. on p. 29).

[202] A. Badalyan, L. Kok, M. Polikarpov and Y. Simonov, *Resonances in coupled channels in nuclear and particle physics*, Physics Reports **82** (1982) 31, ISSN: 0370-1573, URL: https://www.sciencedirect.com/science/article/pii/037015738290014X (cit. on pp. 31, 79, 83).

[203] L. L. Foldy and S. A. Wouthuysen, *On the Dirac Theory of Spin 1/2 Particles and Its Non-Relativistic Limit*, Phys. Rev. **78** (1 1950) 29, URL: https://link.aps.org/doi/10.1103/PhysRev.78.29 (cit. on p. 33).

[204] M. E. Luke and A. V. Manohar, *Reparametrization invariance constraints on heavy particle effective field theories*, Phys. Lett. B **286** (1992) 348, arXiv: hep-ph/9205228 (cit. on p. 34).

[205] G. Colangelo, J. Gasser, B. Kubis and A. Rusetsky, *Cusps in $K \to 3\pi$ decays*, Phys. Lett. B **638** (2006) 187, arXiv: hep-ph/0604084 (cit. on pp. 37, 72, 133).

[206] J. Gasser, B. Kubis and A. Rusetsky, *Cusps in $K \to 3\pi$ decays: a theoretical framework*, Nucl. Phys. B **850** (2011) 96, arXiv: 1103.4273 [hep-ph] (cit. on pp. 37, 72, 133, 135, 138).

[207] R. Haag, *On quantum field theories*, Kong. Dan. Vid. Sel. Mat. Fys. Med. **29N12** (1955) 1 (cit. on p. 37).

[208] J. Chisholm, *Change of variables in quantum field theories*, Nuclear Physics **26** (1961) 469, ISSN: 0029-5582, URL: https://www.sciencedirect.com/science/article/pii/0029558261901067 (cit. on p. 37).

[209] S. Kamefuchi, L. O'Raifeartaigh and A. Salam, *Change of variables and equivalence theorems in quantum field theories*, Nuclear Physics **28** (1961) 529, ISSN: 0029-5582, URL: https://www.sciencedirect.com/science/article/pii/0029558261900566 (cit. on p. 37).

[210] A. V. Manohar, *Introduction to Effective Field Theories*, (2018), ed. by S. Davidson, P. Gambino, M. Laine, M. Neubert and C. Salomon, arXiv: 1804.05863 [hep-ph] (cit. on p. 37).

[211] M. Beneke and V. Smirnov, *Asymptotic expansion of Feynman integrals near threshold*, Nuclear Physics B **522** (1998) 321, ISSN: 0550-3213, URL: https://www.sciencedirect.com/science/article/pii/S0550321398001382 (cit. on p. 37).

[212] T. D. Blanton, F. Romero-López and S. R. Sharpe, *Implementing the three-particle quantization condition including higher partial waves*, JHEP **03** (2019) 106, arXiv: 1901.07095 [hep-lat] (cit. on pp. 53, 61, 132).

[213] P. F. Bedaque, G. Rupak, H. W. Griesshammer and H.-W. Hammer,
Low-energy expansion in the three-body system to all orders and the triton channel,
Nucl. Phys. A **714** (2003) 589, arXiv: nucl-th/0207034 (cit. on p. 55).

[214] P. F. Bedaque, H. W. Hammer and U. van Kolck,
Renormalization of the three-body system with short range interactions,
Phys. Rev. Lett. **82** (1999) 463, arXiv: nucl-th/9809025
(cit. on pp. 56, 134, 136, 142, 143, 155).

[215] L. D. Faddeev, *Scattering Theory for a Three-Particle System*,
Sov. Phys. JETP **12** (1961) 1014 (cit. on p. 65).

[216] Ebert, M., Hammer, H.-W. and Rusetsky, A.,
An alternative scheme for effective range corrections in pionless EFT,
Eur. Phys. J. A **57** (2021) 332, arXiv: 2109.11982 [hep-ph] (cit. on pp. 68, 133).

[217] J.-Y. Pang, M. Ebert, H.-W. Hammer, F. Müller, A. Rusetsky and J.-J. Wu,
Spurious poles in a finite volume, JHEP **07** (2022) 019, arXiv: 2204.04807 [hep-lat]
(cit. on pp. 68, 133).

[218] J. R. Batley et al.,
Determination of the S-wave $\pi\pi$ scattering lengths from a study of $K^{\pm} \to \pi^{\pm}\pi^0\pi^0$ decays,
Eur. Phys. J. C **64** (2009) 589, arXiv: 0912.2165 [hep-ex] (cit. on pp. 70, 158).

[219] V. Agrawala, J. Belinfante and G. Renninger, *On the cutkosky-leon normalization conditions*,
Il Nuovo Cimento A (1965-1970) **44** (1966) 740 (cit. on p. 74).

[220] Sebastian König, *Effective quantum theories with short- and long-range forces*,
PhD thesis: Rheinische Friedrich-Wilhelms-Universität Bonn, 2013,
URL: https://hdl.handle.net/20.500.11811/5783 (cit. on p. 74).

[221] R. Bubna, H.-W. Hammer, F. Müller, J.-Y. Pang, A. Rusetsky and J.-J. Wu,
Lüscher equation with long-range forces, JHEP **05** (2024) 168,
arXiv: 2402.12985 [hep-lat] (cit. on pp. 79, 102–105, 122).

[222] X. Kong and F. Ravndal, *Coulomb effects in low-energy proton proton scattering*,
Nucl. Phys. A **665** (2000) 137, arXiv: hep-ph/9903523 (cit. on pp. 79, 82, 84).

[223] M. Lage, U.-G. Meißner and A. Rusetsky,
A Method to measure the antikaon-nucleon scattering length in lattice QCD,
Phys. Lett. B **681** (2009) 439, arXiv: 0905.0069 [hep-lat] (cit. on p. 80).

[224] V. Bernard, M. Lage, U.-G. Meißner and A. Rusetsky, *Scalar mesons in a finite volume*,
JHEP **01** (2011) 019, arXiv: 1010.6018 [hep-lat] (cit. on p. 80).

[225] C. Liu, X. Feng and S. He,
Two particle states in a box and the S-matrix in multi-channel scattering,
Int. J. Mod. Phys. A **21** (2006) 847, ed. by K.-T. Chao, X.-D. Ji and C. Liu,
arXiv: hep-lat/0508022 (cit. on p. 80).

[226] N. Li and C. Liu, *Generalized Lüscher formula in multichannel baryon-meson scattering*,
Phys. Rev. D **87** (2013) 014502, arXiv: 1209.2201 [hep-lat] (cit. on p. 80).

[227] P. Guo, J. Dudek, R. Edwards and A. P. Szczepaniak, *Coupled-channel scattering on a torus*,
Phys. Rev. D **88** (2013) 014501, arXiv: 1211.0929 [hep-lat] (cit. on p. 80).

[228] L. Leskovec and S. Prelovsek, *Scattering phase shifts for two particles of different mass and non-zero total momentum in lattice QCD*, Phys. Rev. D **85** (2012) 114507, arXiv: 1202.2145 [hep-lat] (cit. on p. 80).

[229] V. Baru, E. Epelbaum, A. A. Filin and J. Gegelia, *Low-energy theorems for nucleon-nucleon scattering at unphysical pion masses*, Phys. Rev. C **92** (2015) 014001, arXiv: 1504.07852 [nucl-th] (cit. on p. 81).

[230] V. Baru, E. Epelbaum and A. A. Filin, *Low-energy theorems for nucleon-nucleon scattering at $M_\pi = 450$ MeV*, Phys. Rev. C **94** (2016) 014001, arXiv: 1604.02551 [nucl-th] (cit. on p. 81).

[231] M. Mai and M. Döring, *Finite-Volume Spectrum of $\pi^+\pi^+$ and $\pi^+\pi^+\pi^+$ Systems*, Phys. Rev. Lett. **122** (2019) 062503 (cit. on pp. 81, 132).

[232] S. R. Beane and M. J. Savage, *Two-Particle Elastic Scattering in a Finite Volume Including QED*, Phys. Rev. D **90** (2014) 074511, arXiv: 1407.4846 [hep-lat] (cit. on pp. 81, 84, 100).

[233] Y. Cai and Z. Davoudi, *QED-corrected Lellouch-Luescher formula for $K \to \pi\pi$ decay*, PoS **LATTICE2018** (2018) 280, arXiv: 1812.11015 [hep-lat] (cit. on pp. 81, 100).

[234] N. Christ, X. Feng, J. Karpie and T. Nguyen, *π-π scattering, QED, and finite-volume quantization*, Phys. Rev. D **106** (2022) 014508, arXiv: 2111.04668 [hep-lat] (cit. on pp. 81, 100).

[235] M. L. Goldberger and K. M. Watson, *Collision Theory*, Dover Publications, 2004, ISBN: 978-0486435077 (cit. on p. 83).

[236] M. C. Birse, J. A. McGovern and K. G. Richardson, *A Renormalization group treatment of two-body scattering*, Phys. Lett. B **464** (1999) 169, arXiv: hep-ph/9807302 (cit. on p. 84).

[237] J. V. Steele and R. J. Furnstahl, *Removing pions from two nucleon effective field theory*, Nucl. Phys. A **645** (1999) 439, arXiv: nucl-th/9808022 (cit. on p. 84).

[238] M. Döring, C. Hanhart, F. Huang, S. Krewald and U.-G. Meißner, *The Role of the background in the extraction of resonance contributions from meson-baryon scattering*, Phys. Lett. B **681** (2009) 26, arXiv: 0903.1781 [nucl-th] (cit. on p. 92).

[239] S. M. Dawid, M. H. E. Islam and R. A. Briceño, *Analytic continuation of the relativistic three-particle scattering amplitudes*, Phys. Rev. D **108** (2023) 034016, arXiv: 2303.04394 [nucl-th] (cit. on pp. 99, 151).

[240] Z. Davoudi, J. Harrison, A. Jüttner, A. Portelli and M. J. Savage, *Theoretical aspects of quantum electrodynamics in a finite volume with periodic boundary conditions*, Phys. Rev. D **99** (2019) 034510, arXiv: 1810.05923 [hep-lat] (cit. on p. 100).

[241] M. G. Endres, A. Shindler, B. C. Tiburzi and A. Walker-Loud, *Massive photons: an infrared regularization scheme for lattice QCD+QED*, Phys. Rev. Lett. **117** (2016) 072002, arXiv: 1507.08916 [hep-lat] (cit. on p. 100).

[242] R. Bubna, H.-W. Hammer, B.-L. Hoid, J.-Y. Pang, A. Rusetsky and J.-J. Wu, *Modified Lüscher zeta-function and the modified effective range expansion in the presence of a long-range force*, JHEP **10** (2025) 197, arXiv: 2507.18399 [hep-lat] (cit. on p. 101).

[243] A. B. Raposo, R. A. Briceño, M. T. Hansen and A. W. Jackura, *Extracting scattering amplitudes for arbitrary two-particle systems with one-particle left-hand cuts via lattice QCD*, JHEP **06** (2025) 186, arXiv: 2502.19375 [hep-lat] (cit. on pp. 102, 103).

[244] S. M. Dawid, A. W. Jackura and A. P. Szczepaniak, *Finite-volume quantization condition from the N/D representation*, Phys. Lett. B **864** (2025) 139442, arXiv: 2411.15730 [hep-lat] (cit. on pp. 102, 103).

[245] M. Abolnikov, V. Baru, E. Epelbaum, A. A. Filin, C. Hanhart and L. Meng, *Internal structure of the $T_{cc}(3875)^+$ from its light-quark mass dependence*, Phys. Lett. B **860** (2025) 139188, arXiv: 2407.04649 [hep-ph] (cit. on p. 102).

[246] M.-L. Du, F.-K. Guo and B. Wu, "Effective range expansion with the left-hand cut and its application to the $T_{cc}(3875)$", *11th International Workshop on Chiral Dynamics*, 2025, arXiv: 2502.19774 [hep-ph] (cit. on p. 102).

[247] K. Yu, G.-J. Wang, J.-J. Wu and Z. Yang, *Finite volume Hamiltonian method for two-particle systems containing long-range potential on the lattice*, JHEP **04** (2025) 108, arXiv: 2502.05789 [hep-lat] (cit. on p. 102).

[248] T. Whyte, D. J. Wilson and C. E. Thomas, *Near-threshold states in coupled $DD^* - D^*D^*$ scattering from lattice QCD*, Phys. Rev. D **111** (2025) 034511, arXiv: 2405.15741 [hep-lat] (cit. on p. 102).

[249] S. Collins, A. Nefediev, M. Padmanath and S. Prelovsek, *Toward the quark mass dependence of T_{cc}^+ from lattice QCD*, Phys. Rev. D **109** (2024) 094509, arXiv: 2402.14715 [hep-lat] (cit. on pp. 102, 112).

[250] S. Prelovsek, E. Ortiz-Pacheco, S. Collins, L. Leskovec, M. Padmanath and I. Vujmilovic, *Doubly heavy tetraquarks from lattice QCD: Incorporating diquark-antidiquark operators and the left-hand cut*, Phys. Rev. D **112** (2025) 014507, arXiv: 2504.03473 [hep-lat] (cit. on p. 102).

[251] L. Meng, E. Ortiz-Pacheco, V. Baru, E. Epelbaum, M. Padmanath and S. Prelovsek, *Doubly charm tetraquark channel with isospin 1 from lattice QCD*, Phys. Rev. D **111** (2025) 034509, arXiv: 2411.06266 [hep-lat] (cit. on p. 102).

[252] S. Amarasinghe et al., *Variational study of two-nucleon systems with lattice QCD*, Phys. Rev. D **107** (2023) 094508, [Erratum: Phys.Rev.D 110, 119904 (2024)], arXiv: 2108.10835 [hep-lat] (cit. on p. 102).

[253] J. R. Green, "Status of two-baryon scattering in lattice QCD", *11th International Workshop on Chiral Dynamics*, 2025, arXiv: 2502.15546 [hep-lat] (cit. on p. 102).

[254] S. Aoki and T. Doi, *Lattice QCD and baryon-baryon interactions: HAL QCD method*, Front. in Phys. **8** (2020) 307, arXiv: 2003.10730 [hep-lat] (cit. on pp. 102, 103).

[255] Y. Lyu, S. Aoki, T. Doi, T. Hatsuda, Y. Ikeda and J. Meng, *Doubly Charmed Tetraquark T_{cc}^+ from Lattice QCD near Physical Point*, Phys. Rev. Lett. **131** (2023) 161901, arXiv: 2302.04505 [hep-lat] (cit. on pp. 102, 103).

[256] S. Aoki, T. Doi and Y. Lyu, *Left-hand cut and the HAL QCD method*, PoS **LATTICE2024** (2025) 089, arXiv: 2501.16804 [hep-lat] (cit. on pp. 102, 103).

[257] D. Minossi et al., *Modified effective range expansion for nucleon-nucleon scattering*, EPJ Web Conf. **3** (2010) 05018 (cit. on p. 113).

[258] G. P. Lepage, *A New Algorithm for Adaptive Multidimensional Integration*, J. Comput. Phys. **27** (1978) 192 (cit. on p. 119).

[259] G. P. Lepage, *Adaptive multidimensional integration: VEGAS enhanced*, J. Comput. Phys. **439** (2021) 110386, arXiv: 2009.05112 [physics.comp-ph] (cit. on p. 119).

[260] J. A. Oller and D. R. Entem, *The exact discontinuity of a partial wave along the left-hand cut and the exact N/D method in non-relativistic scattering*, Annals Phys. **411** (2019) 167965, arXiv: 1810.12242 [hep-ph] (cit. on p. 121).

[261] J.-W. Chen, G. Rupak and M. J. Savage, *Nucleon-nucleon effective field theory without pions*, Nucl. Phys. A **653** (1999) 386, arXiv: nucl-th/9902056 (cit. on pp. 125, 126).

[262] R. W. Hackenburg, *Neutron-proton effective range parameters and zero-energy shape dependence*, Phys. Rev. C **73** (4 2006) 044002, URL: https://link.aps.org/doi/10.1103/PhysRevC.73.044002 (cit. on p. 127).

[263] J.-Y. Pang, R. Bubna, F. Müller, A. Rusetsky and J.-J. Wu, *Lellouch-Lüscher factor for the $K \to 3\pi$ decays*, JHEP **05** (2024) 269, arXiv: 2312.04391 [hep-lat] (cit. on p. 131).

[264] M. Jansen, H.-W. Hammer and Y. Jia, *Finite volume corrections to the binding energy of the X(3872)*, Phys. Rev. D **92** (11 2015) 114031, URL: https://link.aps.org/doi/10.1103/PhysRevD.92.114031 (cit. on p. 132).

[265] P. Guo, *One spatial dimensional finite volume three-body interaction for a short-range potential*, Phys. Rev. **D95** (2017) 054508 (cit. on p. 132).

[266] S. R. Sharpe, *Testing the threshold expansion for three-particle energies at fourth order in ϕ^4 theory*, Phys. Rev. **D96** (2017) 054515 (cit. on p. 132).

[267] P. Guo and V. Gasparian, *Numerical approach for finite volume three-body interaction*, Phys. Rev. D **97** (2018) 014504 (cit. on p. 132).

[268] P. Guo and V. Gasparian, *A solvable three-body model in finite volume*, Phys. Lett. B **774** (2017) 441, arXiv: 1701.00438 [hep-lat] (cit. on p. 132).

[269] Y. Meng, C. Liu, U.-G. Meißner and A. Rusetsky, *Three-particle bound states in a finite volume: unequal masses and higher partial waves*, Phys. Rev. D **98** (2018) 014508 (cit. on p. 132).

[270] P. Guo, M. Döring and A. P. Szczepaniak, *Variational approach to N-body interactions in finite volume*, Phys. Rev. **D98** (2018) 094502 (cit. on p. 132).

[271] P. Guo and T. Morris, *Multiple-particle interaction in (1+1)-dimensional lattice model*, Phys. Rev. D **99** (2019) 014501 (cit. on p. 132).

[272] P. Klos, S. König, H. W. Hammer, J. E. Lynn and A. Schwenk, *Signatures of few-body resonances in finite volume*, Phys. Rev. **C98** (2018) 034004 (cit. on p. 132).

[273] R. A. Briceño, M. T. Hansen and S. R. Sharpe, *Numerical study of the relativistic three-body quantization condition in the isotropic approximation*, Phys. Rev. **D98** (2018) 014506 (cit. on p. 132).

[274] M. Mai, M. Döring, C. Culver and A. Alexandru, *Three-body unitarity versus finite-volume $\pi^+\pi^+\pi^+$ spectrum from lattice QCD*, Phys. Rev. D **101** (2020) 054510 (cit. on p. 132).

[275] P. Guo and M. Döring, *Lattice model of heavy-light three-body system*, Phys. Rev. D **101** (2020) 034501 (cit. on p. 132).

[276] P. Guo, *Modeling few-body resonances in finite volume*, Phys. Rev. D **102** (2020) 054514 (cit. on p. 132).

[277] R. A. Briceño, M. T. Hansen, S. R. Sharpe and A. P. Szczepaniak, *Unitarity of the infinite-volume three-particle scattering amplitude arising from a finite-volume formalism*, Phys. Rev. **D100** (2019) 054508 (cit. on p. 132).

[278] F. Romero-López, S. R. Sharpe, T. D. Blanton, R. A. Briceño and M. T. Hansen, *Numerical exploration of three relativistic particles in a finite volume including two-particle resonances and bound states*, JHEP **10** (2019) 007 (cit. on p. 132).

[279] S. König, *Few-body bound states and resonances in finite volume*, Few Body Syst. **61** (2020) 20 (cit. on p. 132).

[280] T. D. Blanton and S. R. Sharpe, *Alternative derivation of the relativistic three-particle quantization condition*, Phys. Rev. D **102** (2020) 054520 (cit. on p. 132).

[281] J.-Y. Pang, J.-J. Wu and L.-S. Geng, *DDK system in finite volume*, Phys. Rev. D **102** (2020) 114515 (cit. on p. 132).

[282] M. T. Hansen, R. A. Briceño, R. G. Edwards, C. E. Thomas and D. J. Wilson, *Energy-Dependent $\pi^+\pi^+\pi^+$ Scattering Amplitude from QCD*, Phys. Rev. Lett. **126** (2021) 012001 (cit. on p. 132).

[283] S. R. Beane, W. Detmold, T. C. Luu, K. Orginos, M. J. Savage and A. Torok, *Multi-Pion Systems in Lattice QCD and the Three-Pion Interaction*, Phys. Rev. Lett. **100** (2008) 082004 (cit. on p. 132).

[284] W. Detmold et al., *Multi-Pion States in Lattice QCD and the Charged-Pion Condensate*, Phys. Rev. **D78** (2008) 014507 (cit. on p. 132).

[285] W. Detmold, K. Orginos, M. J. Savage and A. Walker-Loud, *Kaon Condensation with Lattice QCD*, Phys. Rev. D **78** (2008) 054514 (cit. on p. 132).

[286] B. Hörz and A. Hanlon, *Two- and three-pion finite-volume spectra at maximal isospin from lattice QCD*, Phys. Rev. Lett. **123** (2019) 142002 (cit. on p. 132).

[287] C. Culver, M. Mai, R. Brett, A. Alexandru and M. Döring,
Three pion spectrum in the $I = 3$ channel from lattice QCD, Phys. Rev. D **101** (2020) 114507 (cit. on p. 132).

[288] F. Romero-López, A. Rusetsky and C. Urbach,
Two- and three-body interactions in φ^4 theory from lattice simulations,
Eur. Phys. J. **C78** (2018) 846 (cit. on p. 132).

[289] T. D. Blanton, A. D. Hanlon, B. Hörz, C. Morningstar, F. Romero-López and S. R. Sharpe,
Interactions of two and three mesons including higher partial waves from lattice QCD,
JHEP **10** (2021) 023 (cit. on p. 132).

[290] T. D. Blanton, F. Romero-López and S. R. Sharpe,
Implementing the three-particle quantization condition for $\pi^+\pi^+K^+$ and related systems,
JHEP **02** (2022) 098 (cit. on p. 132).

[291] D. Severt, M. Mai and U.-G. Meißner,
Particle-dimer approach for the Roper resonance in a finite volume, JHEP **04** (2023) 100,
arXiv: 2212.02171 [hep-lat] (cit. on pp. 132, 167).

[292] J. Baeza-Ballesteros, J. Bijnens, T. Husek, F. Romero-López, S. R. Sharpe and M. Sjö,
The isospin-3 three-particle K-matrix at NLO in ChPT, JHEP **05** (2023) 187,
arXiv: 2303.13206 [hep-ph] (cit. on pp. 132, 146, 178).

[293] M. Mai, M. Döring and A. Rusetsky,
Multi-particle systems on the lattice and chiral extrapolations: a brief review,
Eur. Phys. J. ST **230** (2021) 1623 (cit. on p. 132).

[294] T. Peterken and M. T. Hansen,
Higher partial wave contamination in finite-volume 1-to-2 transitions, (2023),
arXiv: 2304.14259 [hep-lat] (cit. on p. 133).

[295] H. B. Meyer, *Lattice QCD and the Timelike Pion Form Factor*,
Phys. Rev. Lett. **107** (2011) 072002, arXiv: 1105.1892 [hep-lat] (cit. on p. 133).

[296] V. Cirigliano, G. Ecker, H. Neufeld, A. Pich and J. Portoles,
Kaon Decays in the Standard Model, Rev. Mod. Phys. **84** (2012) 399,
arXiv: 1107.6001 [hep-ph] (cit. on p. 133).

[297] J. R. Batley et al., *Search for direct CP violating charge asymmetries in $K^\pm \to \pi^\pm\pi^+\pi^-$ and $K^\pm \to \pi^\pm\pi^0\pi^0$ decays*, Eur. Phys. J. C **52** (2007) 875, arXiv: 0707.0697 [hep-ex]
(cit. on p. 133).

[298] M. Ebert, H.-W. Hammer and A. Rusetsky,
An Alternative Scheme for Pionless EFT: Neutron-Deuteron Scattering in the Doublet S-Wave,
Few Body Syst. **64** (2023) 87, arXiv: 2308.09545 [nucl-th] (cit. on p. 133).

[299] P. F. Bedaque, H. W. Hammer and U. van Kolck,
Effective theory for neutron deuteron scattering: Energy dependence,
Phys. Rev. C **58** (1998) R641, arXiv: nucl-th/9802057 (cit. on pp. 136, 142).

[300] W. Glockle, *S-matrix pole trajectory in a three-neutron model*, Phys. Rev. C **18** (1978) 564
(cit. on p. 151).

[301] R. T. Cahill and I. H. Sloan, *Theory of neutron-deuteron break-up at 14.4 MeV*, Nucl. Phys. A **165** (1971) 161, [Erratum: Nucl.Phys.A 196, 632–632 (1972)] (cit. on pp. 151, 152).

[302] E. W. Schmid and H. Ziegelmann, *Quantum Mechanical Three-body Problem*, Vieweg, 1974, ISBN: 978-0080182407 (cit. on p. 152).

[303] G. Buchalla, A. J. Buras and M. E. Lautenbacher, *Weak decays beyond leading logarithms*, Rev. Mod. Phys. **68** (1996) 1125, arXiv: hep-ph/9512380 (cit. on p. 157).

[304] J. Bijnens, P. Dhonte and F. Borg, *$K \to 3\pi$ decays in chiral perturbation theory*, Nucl. Phys. B **648** (2003) 317, arXiv: hep-ph/0205341 (cit. on p. 158).

[305] C. Zemah, *Three-pion decays of unstable particles*, Phys. Rev. B **133** (1964) 1201 (cit. on p. 158).

[306] M. G. Fuda and J. S. Whiting, *Generalization of the Jost Function and Its Application to Off-Shell Scattering*, Phys. Rev. C **8** (1973) 1255 (cit. on pp. 169, 170).

[307] Y. Li, J.-J. Wu, C. D. Abell, D. B. Leinweber and A. W. Thomas, *Partial Wave Mixing in Hamiltonian Effective Field Theory*, Phys. Rev. D **101** (2020) 114501, arXiv: 1910.04973 [hep-lat] (cit. on pp. 173–175).

List of Figures

List of Tables

Acknowledgements

I would like to first express my deepest gratitude to Akaki Rusetsky for being a wonderful supervisor and guiding me throughout my time at HISKP. It is only with his enormous support that I have been able to complete this journey. He was always available to answer my doubts, engage in discussions, and provide me with interesting scientific questions to tackle. Working with him has been a pleasure. I would also like to thank Ulf-G. Meißner and Bernard Metsch for interesting discussions and for making my time at HISKP wonderful.

Next, I would like to extend my gratitude to Fabian Müller, Jia-Jun Wu, Jin-Yi Pang, Hans-Werner Hammer, and Bai-Long Hoid for guiding me and helping me throughout the various projects on which we worked together. Working together with them made every problem seem less intimidating. Moreover, I would like to thank Maxim Mai, Helen Meyer, and Ajay S. Sakthivasan for the lovely discussions on topics related and unrelated to physics. The time spent at Mensa with them has led to many memorable moments for me. I would also like to thank Christa Börsch, Heike Frömbgen-Penkert, Lara Lagemann, and Nesrin Mercan for the great amount of help with all organizational matters.

I would like to thank my parents and my sister for their never-ending support over the years and their faith in me. Lastly, I would also like to thank Shravani for always being there for me.